Fish-mediated functions on coral reefs.

Nina Schiettekatte

PSL
UNIVERSITÉ PARIS

THÈSE DE DOCTORAT
DE L'UNIVERSITÉ PSL

Préparée à l'École Pratique des Hautes Études

Fonctions écosystémiques des poissons des récifs coralliens

Fish-mediated functions on coral reefs

Soutenue par
Nina M. D. SCHIETTEKATTE
Le 30 juin 2021

École doctorale n° 472
École doctorale de l'École Pratique des Hautes Études

Spécialité
67 - Biologie des populations et écologie

Composition du jury :

Stéphanie MANEL Directeur d'Etudes, EPHE	*Président, Examinateur*
Maria DORNELAS Reader, University of St Andrews	*Rapporteur*
Sean R. CONNOLLY Prof., Smithsonian Tropical Research Institute	*Rapporteur*
Isabelle COTÉ Prof., Simon Fraser University	*Examinateur*
Valeriano PARRAVICINI Directeur d'Etudes, EPHE	*Directeur de thèse*
Sébastien VILLÉGER Chargé de recherche, CNRS	Co-*directeur de thèse*

École Pratique des Hautes Études | PSL

"It's a crazy world out there. Be curious."

— Stephen Hawking

Acknowledgements

First and foremost, I thank my supervisor, Valeriano Parravicini for providing countless opportunities, continuous guidance, and intellectual support throughout the years of my degree. I have a hard time finding the right words to express how lucky I feel to work with him. His tremendous generosity, advice, and endless patience were invaluable. I particularly thank him for trusting me and believing in my abilities even at times when I did not. On top of the scientific guidance, I am grateful for the informal walking meetings with his loyal lab assistants Pumbaa and Juno. I am also very grateful to my co-supervisor, Sébastien Villéger, for his guidance, scientific rigorousness, and immediate presence whenever I needed his help. In particular, the many discussions on nutrient cycling and the role of fish feces brought important insights for my work.

Additionally, I would like to thank the unofficial advisors and wonderful human beings who were an essential part of the scientific development of my work. I thank Jordan Casey for transferring her impeccable organization and field planning skills, giving excellent advice for every doubt I had, providing valuable guidance on English writing, and being a badass female scientist role model. I further thank Simon Brandl for the many brainstorm sessions that shaped much of my work, patiently teaching me about fish identification, and providing stellar comments on every piece of writing. Finally, I am very grateful to have had the chance to learn from Diego Barneche, who introduced me to the good practices of R package development, metabolic theory, the world of Bayesian magic, and reproducible work flows. My work would not have been the same without the help and guidance of these three magnificent scientists.

Furthermore, I would like to thank all other collaborators who have contributed to this thesis in one way or another. This includes: Nick Graham, Tommy Norin, Deron Burkepile, Jacob Allgeier, Jesús Arias-Gonzaléz, Graham Edgar, Carlos Ferreira, Sergio Floeter, Alan Friedlander, Alison Green, Michel Kulbicki, Yves Letourneur, Osmar Luiz, Katrina Munsterman, Enrico Rezende, Fabian Rodríguez-Zaragoza, Rick Stuart-Smith, Laurent Vigliola, Chloé Pozas-Schacre, Mireille Harmelin-Vivien, Giovanni Strona, Jérémy Carlot, Jérémy Wicquart, Jacey Van Wert, Beverly French, and Christopher Fulton. I further thank Sophie Schiettekatte for providing comments on several pieces of writing included in my thesis, Nina Prasil-Delaval, Jérémy Carlot, and Marion Chapeau for kindly proofreading sections of this thesis, and Jérémy Wicquart for helping me with latex-related issues.

I also want to thank everyone who has helped me during field and lab work: Alexandre Mercière, Jordan Casey, Simon Brandl, Fabien Morat, Benoit Espiau, Sam Degregori, Titouan Roncin, Jérémy Carlot, Beverly French, Gabrielle Martineau, Niké Dekkers, Kailey Bissel, Kim Eustache, Camille Gache, Ana Guerra, Daphne Cortese, Hendrikje Jorissen, Yann Lacube, Marc Besson, Marie Derrien, Gonzalo Pérez-Rosales Blanch, Anne Van Domburg, Sam Manning, Jonathan Grimond, Calvin Quigley, Francesca Conte, and the entire staff of CRIOBE in Mo'orea. I am particularly grateful for the support of Alex, his technical advice, and field support, Fabien Morat for teaching me all about fish dissections and otolith extraction, Francesca Conte for her big contribution through video analysis, and the fishy A team for making the countless hours of dissection surprisingly pleasurable.

Moreover, I want to thank the entire R community. The completion of this thesis would not have been possible without the many innovative open source R packages, the wide array of accessible tutorials and blogs, and the help of the R community for debugging pieces of code whenever I got stuck.

Further, I want to thank everybody who has helped me with administrative and technical issues I encountered, namely Nathalie Tolou, Céline Alcaces, and Peter Esteve, Marie-Louise Brassier, Aurelie Mariotti, and Fabien Morat.

Additionally, I thank all friends and colleagues who brightened my days throughout this journey inside and outside the workspace. A special thanks to Jordan Casey and Simon Brandl for their constant support, encouragement, and friendship. I also owe a big thanks to Jérémy Carlot for being such a loyal and generous friend, house mate, and supporter in all circumstances. I further thank Charlotte Sève for the emotional support, Victor for the philosophical discussions, Charles Loiseau for keeping things entertaining, Jason Vii for his positive energy, Claire Peyran for the supportive coffee breaks, Celine Tardy for the occasional dance sessions, Nina Junior for her permanent smiling, Daphne Cortese for her calm positivity, Gonzalo Pérez-Rozales Blanch for his contagious laugh, Jérémy Wicquart for being geeky with me, Beverly French for spreading love, and many more for being awesome. I will forever treasure the friends and colleagues with whom I shared unforgettable moments in Perpignan and French Polynesia.

Finally, I would like to express my immense gratitude to my family. The love of my parents, grandparents, and siblings, and their unconditional believe in me have pushed me towards where I am today. I especially thank my parents, Aarnaud Schiettekatte and Annick de Jaeger, who supported all my educational endeavors with love and patience and have always worked hard to allow me to pursue my dreams. I thank my sister, Sophie Schiettekatte, for being a listening ear and generously providing good advice in all circumstances, my brother, Simon Schiettekatte, for looking out for me and being a devoted family man, and my little sister, Emma Schiettekatte, for already being an inspiring young woman and making me proud. Finally, I thank Marion Chapeau for being an inexhaustible source of radiant energy, patiently listening to my every thought, and always making me smile.

Abstract

Preserving coral reef functioning is a critical challenge of the 21st century. As fishes represent a high proportion of consumer biomass on coral reefs, they govern a large part of the storage and flux of nutrients and energy – functions. In light of ongoing global anthropogenic threats to fish communities, it is urgent to increase our understanding on functions mediated by fishes. However, the data and tools to appropriately quantify them are sparse, and assessments of ecosystem functioning in coral reefs are largely based on proxies such as biomass. Therefore, in this thesis, I aim to develop methods to better quantify fish-mediated functions to ultimately disentangle the drivers and vulnerabilities of multiple functions.

First, focusing on the individual level I developed a novel framework relying on bioenergetics and mass balance theory to estimate how fishes partition carbon, nitrogen, and phosphorus into main fish functions/processes such as growth, excretion, respiration, excretion and egestion. The main novelty is that the approach takes into account the potential of nitrogen and phosphorus limitation alongside the more traditionally used carbon limitation, which is particularly useful for fishes feeding on low-nutrient diets. Additionally, the model framework is accompanied by an R package called 'fishflux' to increase the applicability.

Second, I scaled up the quantification of functions to the community level for reefs worldwide. To do so, I first predicted trophic guilds and all parameters needed to apply the bioenergetic model to global reef fish species using a combination of empirical data and phylogenetic regression models. Then, I quantified five key functions—

nitrogen and phosphorus cycling, biomass production, herbivory, and piscivory—mediated by reef fish communities across the world's tropical oceans. This quantification demonstrates that functions exhibit critical trade-offs driven by diverging community structures, such that no reef can holistically maximize functioning. Further, functions are locally dominated by few species, but worldwide, the identity of dominant species varies greatly. These findings highlight the need for a nuanced approach to coral reef conservation that considers variable processes beyond the effect of standing stock biomass. Third, while the important role of fish excretion has been increasingly studied in recent years, fish egestion has received little attention even though it may play an important trophic role through coprophagy. Therefore, I estimated the quality and quantity of fish feces, and compared the nutrient flow in excretion and egestion for 51 coral reef fish species in Mo'orea, French Polynesia. This analysis sheds light on a remarkably low assimilation of carbon, nitrogen, and phosphorus in coral reef fishes. As a result, feces can have relatively high nutritional value, hinting on a relevant role of coprophagy. Further, modeled rates of egestion and excretion demonstrate the unrecognized importance of fish feces as a vector of nutrients in coral reef communities.

Lastly, organismal metabolic rates are the basis of energy and nutrient fluxes through ecosystems. However, the metabolic demand of fishes in the wild is poorly documented. I therefore introduce a novel approach to estimating field metabolic rates by combining laboratory-based respirometry and field-based stereo-video systems, and demonstrate the approach with a case study of seven reef fish species. As a non-destructive, widely applicable technique, this approach can improve our ability to estimate elemental fluxes mediated by fishes. In conclusion, this thesis contributes to a better understanding of fish-driven functions on coral reefs and will help quantifying the functional impacts of human stressors to improve conservation of coral reefs.

Résumé

La conservation du fonctionnement des récifs coralliens est un défi pour le 21ème siècle. Comme les poissons représentent une proportion élevée de la biomasse des consommateurs dans les récifs coralliens, ils régissent une grande partie du stockage et des flux de nutriments et d'énergie, c'est-à-dire les fonctions. Dans le contexte de l'impact grandissant de l'homme, il est urgent de mieux comprendre les fonctions assurées par les poissons. Cependant, nous manquons de données et de méthodes pour les quantifier de manière précises, et les évaluations du fonctionnement des récifs coralliens sont souvent basées sur des proxies, tels que la biomasse. Lors de cette thèse, j'ai développé des méthodes pour mieux quantifier les fonctions assurées par les poissons afin de identifier les déterminants et les vulnérabilités de ces multiples fonctions.

Tout d'abord, j'ai développé un nouveau modèle individuel basé sur la bioénergétique et la théorie du bilan de matière pour estimer les flux de carbone, de l'azote et de phosphore dans la croissance, l'excrétion, et la respiration de chaque individu. La principale nouveauté de cette approche est l'intégration de la limitation en azote et en phosphore en plus de la limitation en carbone plus traditionnellement utilisée. De plus, j'ai développé le package R "fishflux" afin de faciliter l'utilisation du modèle.

Deuxièmement, j'ai quantifié des fonctions à l'échelle des communautés pour les récifs du monde entier. Dans ce but, j'ai d'abord prédit les guildes trophiques ainsi que tous les paramètres nécessaires pour appliquer mon modèle bioénergétique aux espèces de poissons récifaux à l'échelle mondiale. Ensuite, j'ai quantifié cinq fonc-

tions - l'excrétion d'azote et de phosphore, la production de biomasse, l'herbivorie et la piscivorie - assurées par les communautés de poissons récifaux. J'ai ainsi mis en évidence des compromis critiques entre les fonctions induites par des structures communautaires divergentes, de sorte qu'aucun récif ne peut maximiser son fonctionnement de manière complète. En outre, les fonctions sont localement dominées par peu d'espèces clés, mais à l'échelle mondiale, l'identité des espèces clés varie fortement. Ces résultats soulignent la nécessité d'une approche nuancée de la conservation des récifs coralliens, basée sur plusieurs fonctions clés et pas seulement sur l'effet de la biomasse.

Troisièmement, contrairement à l'excrétion de nutriments dissous, l'égestion de matière organique par les poissons est peu étudiée. Pour combler ce manque, j'ai quantifié la qualité et la quantité des fèces de poissons et comparé les flux de nutriments via l'excrétion et l'égestion pour 51 espèces de poissons récifaux à Mo'orea, en Polynésie française. Cette analyse met en avant une assimilation faible des éléments nutritifs par ces espèces. Par conséquent, les fèces peuvent avoir une valeur nutritive élevée, ce qui laisse supposer un rôle trophique non négligeable de la coprophagie. De plus, la comparaison des taux d'excrétion et d'égestion démontre l'importance méconnue des fèces de poissons comme vecteur de nutriments au sein des récifs coralliens.

Finalement, les taux métaboliques des organismes impactent les flux d'éléments dans les écosystèmes. Cependant, le taux métabolique des poissons dans la nature est encore peu documenté. J'ai donc proposé une nouvelle approche pour estimer les taux métaboliques sur le terrain en intégrant la respirométrie et les systèmes stéréo-vidéo in situ. J'ai démontré le potentiel de cette approche pour sept espèces de poissons. Etant une technique non-destructive, cette approche améliore donc notre capacité à estimer les fonctions assurées par les poissons. En conclusion, cette thèse contribue à une meilleure compréhension des fonctions assurées par les poissons dans les récifs coralliens et permettra de quantifier les impacts des activités anthropiques sur le fonctionnement des récifs coralliens afin d'améliorer la conservation de ces écosystèmes.

Table of Contents

List of Tables

List of Figures

Chapter 1

General introduction

The fluxes of elements through biological communities fuel all life on Earth. Over the last century, scientists increasingly recognized that human impact is drastically interfering with this functioning of ecosystems around the world (Steffen *et al.* 2011). Consequently, preserving these fluxes (i.e., functions) has become a major contemporary conservation goal (Bridgewater *et al.* 2014). However, for many functions, we lack the tools or knowledge to appropriately monitor them. While many studies have successfully quantified functions of plant communities, few studies have quantified functions mediated by animal communities (Duffy *et al.* 2017). This thesis contributes to filling this gap in the context of a unique ecosystem, coral reefs.

Coral reefs are known as the rainforests of the ocean because of their high diversity and productivity. Simultaneously, they represent a key example of an ecosystem that is heavily affected by climate change and other human pressures, which adds urgency to increase our understanding of how these systems work. Since coral reef fishes represent the highest biomass of animal consumers in this system, it is crucial to increase our knowledge concerning fish-mediated functions on coral reefs (Bellwood *et al.* 2019). However, while the topic of function has rightfully gained much interest in coral reef studies over the past decades, methodological challenges have thus far

limited the precise quantification of functions (Brandl *et al.* 2019a). In this thesis, I seek to advance our understanding by developing and applying a series of tools that allow the quantification of fish-mediated functions at the organismal and community level.

In this first chapter, I will introduce the core concepts that formed the basis and motivation of my thesis. First, I start with an introduction on ecosystem functioning and the essential role of consumers (1.1). I then introduce coral reefs, the focal ecosystem of this thesis, underlining the urgency of studying their functioning in light of anthropogenic stressors (1.2), followed by briefly discussing the functioning of coral reefs (1.3). Furthermore, I introduce the functions related to coral reef fishes, and discuss what has been done and what is lacking in terms of their quantification (1.4). Finally, I conclude this chapter by detailing the key objectives of my thesis (1.5).

1.1 Ecosystem functioning and the role of consumers

This thesis situates itself in the branch of marine science that deals with functional ecology. Ecology is "the entire science of the relations of the organism to the surrounding exterior world, to which we can count in the broader sense all the conditions of existence. These are partly organic, partly of inorganic nature" (Haeckel 1866). Since then, many definitions have followed, but all of them put the relationships between organisms and their environments at the center of the discipline (Friederichs (1958)). If ecology describes interactions, functional ecology is a relatively younger branch that describes these relationships among organisms and between organisms and their environment as a flow of material and energy (Calow 1987; Keddy 1992).

Within the field of functional ecology, the terms function and functioning have

become prominent concepts in ecology, yet, are often used with different meanings depending on the author (Jax 2005). For the purpose of clarity and situating the thesis within the functional ecology literature, I will briefly explain the different ways in which these concepts are used and specify the definitions that will be used in this thesis. First, 'function' may refer to the flux of energy or material within an ecosystem. Therefore, 'functioning' of a complex system of interactions can be defined as the sum of processes or functions that sustain the system (Jax 2005). Alternatively, the term function is often used to describe a role or purpose for organisms in the ecosystem. In the context of ecological traits, for example, organisms are classified into functional groups based on their role or morphological characteristics that may relate to functions (Wilson 1999; Violle *et al.* 2007). Finally, the word function has also been used to denote a role or service of an entire system to human beings, effectively talking about an ecosystem service (Millennium Ecosystem Assessment 2005). In this thesis, I apply the first and most commonly accepted use of the word function to define a flux of matter mediated by an organism or an entire community (e.g., flux of nitrogen or biomass production). I further use the term ecosystem functioning as a broad concept to describe the 'performance' of the ecosystem with reference to multiple functions.

Consumers play an essential role in ecosystem functioning. They influence community structure through consumption (top-down) and primary production through nutrient cycling (bottom-up) (Duffy 2002). Primary consumers (e.g., herbivores) are major determinants of standing plant biomass, community composition, physical vegetation structure, primary production, and decomposition rates (Lubchenco & Gaines 1981; Duffy 2002). Similarly, secondary consumers (i.e., animals feeding on other animals) control the populations of their prey, and can indirectly influence ecosystems through cascade effects that propagate through the food web (Sih *et al.* 1998). Indeed, several authors find that strong top-down effects are common and may have critical indirect effects on ecological structure and function (Duffy 2002). Direct and indirect effects of consumers can thus be assessed by investigating the topology of

food webs (i.e., who eats whom) as well as the interaction strengths (i.e., how much does a consumer group feed on a prey group) (Duffy 2002).

Beyond their top-down effects, consumers play an important role in biogeochemical cycles through processes of nutrient supply (i.e., excretion and egestion) (Sterner & Elser 2002; Allgeier *et al.* 2017). This role becomes even more influential in oligotrophic systems, where excretion and egestion supply limiting nutrients to the system and fuel primary production. Most research on consumer-mediated nutrient dynamics has focused on terrestrial ecosystems, rivers, and lakes (Allgeier *et al.* 2017). In the marine realm, a well-known example can be found in the open ocean, where zooplankton is involved in the recycling of limiting nutrients (Nugraha *et al.* 2010). Importantly, nutrient regeneration by zooplankton can account for up to 23% of the total requirement of phytoplankton primary production (Hernández-León *et al.* 2008). Moreover, migrating animals such as schooling fishes and whales are responsible for a huge translocation of nutrients (Meyer *et al.* 1983; Roman & McCarthy 2010). More recently, the focus of consumer-mediated nutrient dynamics research has found its way to coastal ecosystems, such as oligotrophic coral reefs, the focal ecosystem of this thesis (Allgeier *et al.* 2017).

Functions are challenging to measure directly, and especially the functions performed by communities of large and/or mobile organisms. Therefore, major efforts have been made to link easily measurable ecological traits and functions (Lavorel & Garnier 2002). Some evidence on the relationship between traits and functions is documented in the literature. For example, the primary production can be predicted by the traits of plant communities (Lavorel & Garnier 2002; Violle *et al.* 2007). Further, there is a growing consensus that trait diversity and composition, rather than species diversity, determine ecosystem functioning of plant communities (Díaz & Cabido 2001). Therefore, functional richness (i.e., number of species with a unique set of traits) is often used as proxy for ecosystem functioning (Flynn *et al.* 2011). Particularly in highly diverse systems, the use of functional groups is an attractive approach to decompose complexity and to quantify functional metrics such as func-

tional richness and functional redundancy (Halpern *et al.* 2008; e.g., Belmaker *et al.* 2013; Brandl *et al.* 2016). Considering functional richness as a proxy for ecosystem functioning rests on the broad assumption that traits describe the ecological niche of species and that functionally diverse communities have a higher functioning due to niche complementarity as resources are used more effectively (Loreau *et al.* 2001). This link has been demonstrated for plant communities (Díaz & Cabido 2001; Loreau *et al.* 2001). However, evidence for consumer communities is restricted to few experiments on terrestrial communities (Duffy *et al.* 2017), while direct investigation is lacking for many other animal groups, even for well studied taxa such as coral reef fishes (Brandl *et al.* 2019a). The scarcity of studies quantifying functions of consumer communities compared to plant communities thus impedes the general use of trait diversity as a proxy for functioning. It is therefore necessary to develop ways to effectively quantify animal-mediated functions, which this thesis contributes to.

1.2 Coral reefs in the Anthropocene

Contemporary ecosystems and their functioning are threatened by the harmful dominance of humans. However, the pervasive influence of humans on ecosystems is not a recent phenomenon. Human populations have shaped animal and plant communities across the globe since the late Pleistocene (Western 2001). Throughout history, we see that both increased human populations and technological developments have triggered an ecological crisis (Holdren & Ehrlich 1974). Over the last century, scientists increasingly recognized that the human footprint on the global environment is reaching massive proportions, rivaling with some of the great forces of nature in its impact on the functioning of the Earth system (Steffen *et al.* 2011). In 2000, Crutzen and Stoermer coined the term 'Anthropocene' to define the era in which humans have altered the global biogeochemistry of the planet while challenging the survival of many of its inhabitants (Crutzen & Stoermer 2000). Today, 25% of all species on earth are at risk of extinction (Webb & Mindel 2015). Many studies reported that our modern

society has initiated a mass extinction episode, unprecedented in human history and threatening the functioning of the planet's ecosystems (Ceballos *et al.* 2015).

The ongoing biodiversity crisis and dramatic defaunation of our planet has prompted several international conservation initiatives (Johnson *et al.* 2017). In 1992, the convention on biological diversity was created to halt biodiversity loss and signed by 196 nations (CBD; www.cbd.int). Loss of species and degradation of ecosystems are likely to further accelerate in the coming years. Our understanding of this crisis is now clear, and world leaders have pledged to avert it. Nonetheless, global goals to reduce the rate of biodiversity loss have mostly not been achieved. In 2002, leaders across the globe pledged through the CBD "to achieve by 2010 a significant reduction of the current rate of biodiversity loss." Alongside biological diversity, the goal of conserving functioning has increasingly found its place in environmental law texts and policy under the form of the concept of biological integrity (Bridgewater *et al.* 2014). Unlike diversity, which refers to a number of entities - these can include genes, species, or landscapes - integrity refers to a system's wholeness, including presence of all appropriate elements and occurrence of all processes regulating the flow of energy and materials at appropriate rates (Angermeier & Karr 1994). As such, the "Aichi Biodiversity targets" (successor of the CBD 2010 targets) also include a more complex plan to safeguard ecosystem services. However, the concept of biological integrity as a conservation goal is vague, open to interpretation, and unachievable because the 'untouched' natural world arguably does not even exist anymore. So far, none of the major international biodiversity targets were reached, the continuing decline of global biodiversity is undeniable, and our ability to monitor certain targets is weak (Johnson *et al.* 2017). We urgently need to improve our capacity of monitoring ecosystem functioning.

This thesis intends to contribute to our understanding of the functioning of the coral reef ecosystems in particular. Coral reefs represent a prime example of an ecosystem that is severely impacted by anthropogenic threats including warming, acidification, nutrient enrichment, habitat destruction, intensive fishing pressure, and

sedimentation (Gardner *et al.* 2003; Wolanski *et al.* 2009; Edwards *et al.* 2013; D'Angelo & Wiedenmann 2014; Hughes *et al.* 2017). At the same time, millions of people depend on them, as they provide multiple ecosystem services to human populations such as shoreline protection (Moberg & Folke 1999; Harris *et al.* 2018), and 10% of the world's fisheries (Knowlton *et al.* 2010). Thus, coral reefs are simultaneously very vulnerable to increasing human stressors and very important for human wellbeing. Below, I discuss some of the major threats of coral reefs in more detail.

Global climate change is one of the most imminent threats to coral reef ecosystems (Hughes *et al.* 2017; Bruno *et al.* 2019). Corals are particularly sensitive to warming and acidification and are being struck by increasingly frequent mass bleaching episodes (Hughes *et al.* 2017). In fact, a recent estimation suggests that 60% of global coral reefs may be lost by 2030 (Wilkinson 2008), setting the stage for the loss of critical habitat for associated reef fishes and other biota. Following events of mass coral mortality, some reefs show signs of recovery, but maintain an altered functional structure with less functional diversity (McWilliam *et al.* 2020). Reefs that do not recover, may remain in degraded states dominated by algae, that may be difficult to reverse (Folke *et al.* 2004; Graham *et al.* 2015).

As corals are the engineers that produce the typical three-dimensional structure of the habitat, dying corals followed by biological and physical erosion transform complex reefs into rubble fields with low structural complexity (Hughes *et al.* 2017) (figure 1.1). Degradation and homogenization of the reefs and the associated loss of structural complexity have serious consequences for overall reef diversity, ecosystem functions and services (Alvarez-Filip *et al.* 2009). Decreasing complexity alters abundance, biomass, diversity and trophic structure of fishes (Friedlander *et al.* 2003; Graham & McClanahan 2013; Darling & D'agata 2017). Moreover, reductions in structural complexity and habitat diversity can result in local extinctions (Graham *et al.* 2006; Newman *et al.* 2015), and declining fisheries productivity (Rogers *et al.* 2014). Both obligate and facultative coral feeders are affected by the loss of live corals in a direct way and appear the most susceptible to acute coral loss (Pratchett *et al.* 2008). Fur-

ther, decreasing topographic complexity particularly affects small fishes (Graham *et al.* 2011). Thus, both the loss of live coral and the decline of structural complexity may trigger local extinctions and compromise ecosystem functioning (Pratchett *et al.* 2011).

Figure 1.1: Coral reef in a healthy (left), bleaching (middle), and dead (right) state. American Samoa. credit: THE OCEAN AGENCY

Another major threat to coral reef communities is the over-exploitation of fisheries (Pauly *et al.* 2002; Newton *et al.* 2007). Many coastal fisheries throughout the world are unsustainable or already overexploited (Pauly *et al.* 2002), and coral reef fisheries have collapsed in many tropical island countries (Newton *et al.* 2007). Moreover, destructive fishing practices have greatly increased the impact of human populations on the reef habitat (Mcmanus *et al.* 1997). Importantly, habitat degradation and fishing affect different sides of the fish community. Fisheries typically target larger fishes often occupying a high trophic level (Pauly *et al.* 1998), while habitat degradation and coral loss have more effect on small or corallivorous fishes (Wilson *et al.* 2009; Graham *et al.* 2011). Nevertheless, intensive fishing and habitat degradation often co-occur, leading to strong overall declines in the biomass and abundance of fishes, especially in heavily populated regions of the world (Wilson *et al.* 2009; Graham *et al.* 2011).

While coral reef fishes are vulnerable to extinction due to both climate change and fishing (Cheung *et al.* 2005; Graham *et al.* 2011), extinctions are more likely to occur locally than globally (Hughes *et al.* 2014). The species that have gone locally extinct or drastically declined tend to be highly dependent on live corals (Wilson *et al.* 2006) or heavily targeted by local fisheries (Bellwood *et al.* 2003). The relevance of these losses to ecosystem functioning will ultimately depend on their contributions to functions (Pratchett *et al.* 2011). Drastic declines in abundance and biomass of a local key species may have profound impact on ecosystem functioning representing ecological extinctions, where a species is unable to maintain key functions because the species has become too rare (Bellwood *et al.* 2019). While maintaining diversity may provide an ecological insurance, it is important to investigate the role of species identity because the most abundant species within a community or functional group often contribute the most to ecosystem functioning (Gaston & Fuller 2008; Topor *et al.* 2019).

The drastic declines of both corals and fishes, and shifting communities in coral reefs have evoked serious concerns about their persistence, functioning, and ability to

provide valuable services (Bellwood *et al.* 2019; Williams *et al.* 2019). The ongoing coral reef crisis has forced scientists to rethink coral reef conservation and even to use the concept of 'novel ecosystem,' which has been coined to define agro-ecosystems with no analog in the natural world (Bellwood *et al.* 2019; Graham *et al.* 2020). Marine protected areas have shown to effectively increase the biomass of fishes such as targeted herbivores. Protecting herbivores with the goal of boosting the resilience of the entire system has been put forward as a key local solution to save corals. However, it is becoming increasingly clear, local protection does not provide clear benefits for the reef benthos after major bleaching events, and reserve effects cannot protect all the species that participate to local biodiversity (Graham *et al.* 2020). While marine reserves have important roles for the conservation of coral reefs in the face of climate change, they do not provide equal benefits for all species and functional groups and thus can also produce communities that are far from 'natural' coral reefs. With the increasing frequency and severity of heating events, the effect of climate change seems too strong for marine protected areas alone to save the day (Côté & Darling 2010; Graham *et al.* 2020).

There is an urgent need to better understand the processes that underlie the functioning of coral reefs to identify functional changes we may expect in the Antropocene, and to reform conservation efforts to address both specific local issues and larger-scale threats (Bellwood *et al.* 2019). It is now clear that we cannot conserve nor restore the integrity of coral reefs as they were before humans touched them (Bellwood *et al.* 2019). Moving forward, scientists are stressing the need to embrace transition and guide coral reefs through the Anthropocene in a way where the loss of function is mitigated (Bellwood *et al.* 2004; Graham *et al.* 2014; Bellwood *et al.* 2019; Williams *et al.* 2019). To appropriately advise policy makers on how to achieve this goal, scientists need to increase the understanding of coral reef functioning - we need to be able to quantify functions before we can think about managing them (Bellwood *et al.* 2019; Brandl 2019).

1.3 Functioning of coral reefs

This thesis will contribute to our understanding of coral reef functioning. The mystery of coral reef functioning and the quest to understand and describe them dates centuries back. In 1832, for example, Charles Darwin sailed across the Pacific Ocean and explored coral reef ecosystems. He observed that coral reefs were able to flourish in nutrient-poor waters and under constant pressure of powerful waves (Darwin 1839): "The ocean throwing its waters over the broad reef appears an invincible, all-powerful enemy; yet we see it resisted, and even conquered, by means which at first seem most weak and inefficient." He compared stumbling upon coral reef ecosystems in the middle of an ocean with encountering a swarming oasis in the middle of a desert. This phenomenon later became known as Darwin's paradox. Without fully understanding the mechanisms, Darwin recognized the uniqueness of coral reefs in terms of biodiversity and productivity in remarkably nutrient-poor waters.

Centuries later, Darwin's paradox continues to puzzle scientists, and both pelagic subsidies and efficient internal cycling have been put forward as potential drivers. Coral reefs depend on pelagic subsidies for their productivity through for example input of seabird guano (McCauley *et al.* 2012), upwelling (Gove *et al.* 2016), and fish larvae subsidies (Brandl *et al.* 2019b). In some windward reefs, pelagic subsidies can even account for almost half of fish productivity (Morais & Bellwood 2019a). On the other hand, the productivity of coral reefs is also driven by internal cycling of nutrients governed by animals such as sponges (De Goeij *et al.* 2013), invertebrates (Williams & Carpenter R. C. 1988), or fishes (Burkepile *et al.* 2013). Coral reef fishes alone contribute to a large proportion of the animal biomass, and therefore have an important impact on functioning of coral reefs (Newman *et al.* 2006). For example, aggregations of resting nocturnal fish in coral reefs can create concentrated nutrient hotspots and increase coral growth up to 70% (Meyer *et al.* 1983; Shantz *et al.* 2015). Another example at small spatial scales is the interaction between corals and small planktivorous damselfishes - corals that shelter damselfishes can grow 50%

faster than those without fishes. Finally, on a larger scale, fish-mediated nutrient excretion stabilizes stoichiometry on coral reefs (Allgeier *et al.* 2014), matching ideal growth conditions of corals (Atkinson *et al.* 1995; Ferrier-Pages *et al.* 2000). Thus, fishes play an important role in providing nutrients and enhancing the productivity of corals.

In line with its multiple general uses (see 1.1), the term 'function' has produced considerable confusion and debates in the context of coral reefs (Bellwood *et al.* 2019). The definition of ecosystem function - flow of energy or material within an ecosystem - implies that the terms 'ecosystem function,' 'ecosystem process,' and 'ecosystem flux' can be used interchangeably. Functions should thus ideally be expressed as a rate of energy, nutrients or mass. On the other hand, the term 'function' is often used to describe a purpose or a role (Bellwood *et al.* 2019). For example, the defined role or purpose of a fish may be to eat certain algae in a specific habitat. This second use of the term 'function' is thus related to its ecological niche. However, the two definitions are closely related since the complementarity of ecological niches can imply higher community-level rates of functioning.

Brandl et al. (2019) proposes a framework with a focus on eight reciprocal process-based ecosystem functions: calcium carbonate production and bioerosion, primary production and herbivory, secondary production and predation, and nutrient uptake and nutrient release. Quantifying these ecosystem functions is a key step to increase our understanding of how reefs work and disentangle the role of diversity and individual species in ensuring functions (Brandl *et al.* 2019a). My thesis is in line with this proposed process-based approach.

1.4 Fish-mediated functions on coral reefs

Coral reef fishes play an essential role in coral reef functioning which is why I will focus on fish-mediated functions. Indeed, coral reef fishes contribute to a high propor-

tion of consumer biomass and therefore represent essential vectors of fluxes of carbon, nitrogen and phosphorus through storage and recycling (McIntyre *et al.* 2008; Allgeier *et al.* 2014; Barneche *et al.* 2014). Broad ecosystem functions mediated by coral reef fishes include nutrient cycling, biomass production, herbivory (primary consumption), and piscivory (secondary consumption) (Brandl *et al.* 2019a). Individual-level processes contribute to ecosystem functions through multiple pathways (figure 1.2). First, depending on their diet, fishes can contribute to essential functions such as predation and herbivory, and thus perform top-down control on primary producers or animal prey. Secondly, growing fish contribute to secondary production, and thus may serve as food for other animals including humans. Biomass production has received most attention since the production of edible biomass is correlated to food provision, an important ecosystem service with clear benefits to humans. Third, a proportion of the food that fishes consume is released back into the environment under the form of excretion or egestion. The released nitrogen and phosphorus then contribute to the system-wide nutrient cycles.

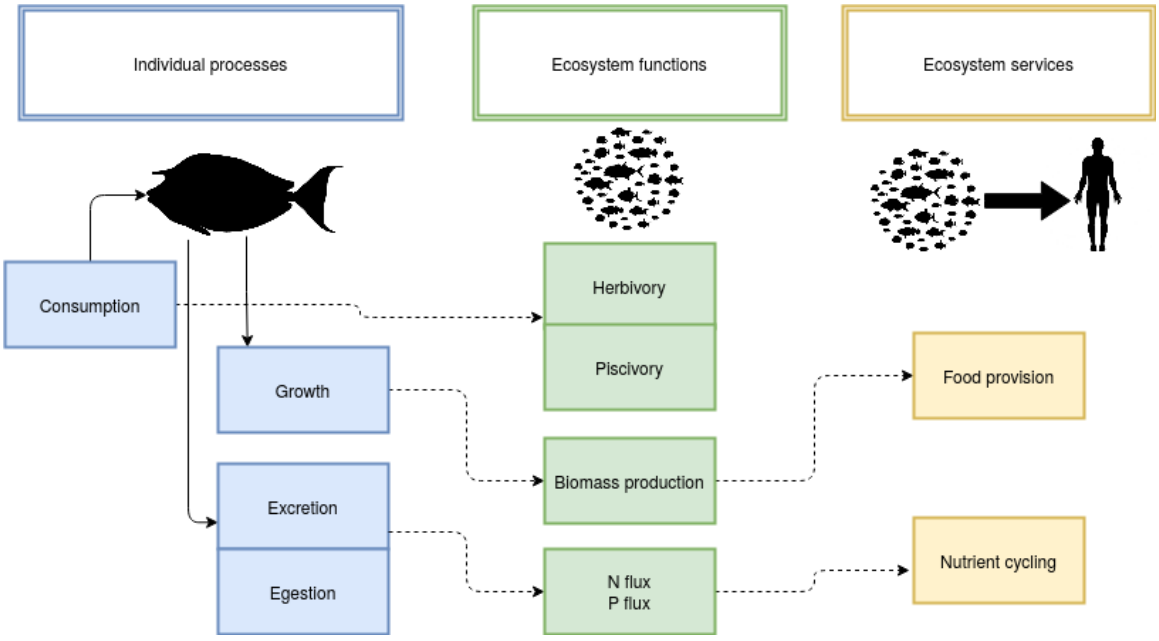

Figure 1.2: Diagram showing the links between individual processes, ecosystem functions and ecosystem services.

While the high diversity of coral reef fishes has inspired many studies with a focus on ecosystem functioning, only a handful of studies have attempted to quantify functions as continuous fluxes (Brandl *et al.* 2019a). Rather, ecosystem functioning is often defined with the use of proxies such as trait diversity or total biomass (Mora & Sale 2011; e.g., Mouillot *et al.* 2014). In fact, most studies on coral reef fishes that mention functioning rely on proxies (Brandl *et al.* 2019a). Further, studies that do quantify functions are mostly focused on biomass production (e.g., Morais & Bellwood 2019b) or fish excretion (e.g., Francis & Côté 2018). I will briefly discuss the use of proxies for functioning in previous studies. Then, I will describe what has been done and what is lacking in terms of quantifying process-based functions, which lays the foundation of how my work will fill important knowledge gaps.

1.4.1 Proxies of functioning

Studies using trait-based metrics have shed light on the mismatch between species richness, functional richness, and the functional vulnerability of coral reef fish communities. Species richness does not necessarily correlate with functional richness (Stuart-Smith *et al.* 2013; Parravicini *et al.* 2014). As a result, even coral reefs with a high diversity of reef fishes can be vulnerable since some functional groups are represented by a limited number of species (Halpern *et al.* 2008; Mouillot *et al.* 2014). Further, human stressors including fishing and climate change critically impact functional diversity. Functional diversity declines disproportionally with human density, revealing the potential loss of functional groups in reefs that are close to humans (D'agata *et al.* 2014; Cinner *et al.* 2020). Furthermore, when coral reefs shift to an algal-dominated state after bleaching events, the functional structure of reef fishes shifts substantially (Graham *et al.* 2015). While coarse-scale trait-based approaches have provided interesting insights, it is crucial to empirically verify the link between traits and function (Bellwood *et al.* 2019). Otherwise, concepts such as functional redundancy and vulnerability, as commonly measured by trait-based

approaches, have little significance in terms of insurance or vulnerability of ecosystem functioning. A direct investigation of processes performed by coral reef fishes, however, is lacking, which impedes our understanding of trait-function relationships (Brandl *et al.* 2019a).

Another largely used proxy for ecosystem functioning is standing stock biomass (Mora & Sale 2011; Micheli *et al.* 2014; MacNeil *et al.* 2015). Specifically, several studies have used biomass as a proxy for secondary production to show a positive relationship with diversity measures (Mora & Sale 2011; Micheli *et al.* 2014). Further, biomass of functional groups has been used as a proxy for key functions such as herbivory or predation (MacNeil *et al.* 2015). The positive correlation between biomass and function is intuitive - more fishes yield higher function. However, this relationship is likely to be non-linear following metabolic theory (Brown *et al.* 2004). Further, biomass may not be sufficient to represent function, because community structure may have a large impact. For example, small species tend to grow faster (Morais & Bellwood 2018). Therefore, biomass production will depend both on standing stock biomass and the size structure of the community. Thus, while it is evident that biomass is an important driver of function, the exact relationship should be investigated alongside other aspects of the fish community.

Finally, much work has been done to approximate herbivory and biorerosion, as these are important functions for sustaining coral survival and recovery after disturbance (Hughes *et al.* 2003; Hughes *et al.* 2007; Burkepile & Hay 2008; Graham *et al.* 2015). A popular approach to approximate herbivory is the use of algal bioessays where herbivory is quantified as the percent mass of algae removed (Topor *et al.* 2019). Another proxy is bite rate multiplied by a fish's biomass (e.g., Lefcheck *et al.* 2019). For key herbivore and bioeroder species, detailed individual-level information has been collected yielding rates of volume removed per area (e.g., Fox & Bellwood 2007). These studies have brought insights on algal removal and a positive effect of herbivore diversity on algal removal (Rasher *et al.* 2013; Topor *et al.* 2019). However, the direct link between these measures and the mass of algae removed by individual

species as well as entire communities (i.e., process based function) remains largely unexplored.

1.4.2 Process-based functions

Only a handful of studies have quantified processes to define reef ecosystem functions, and to my knowledge there are currently no studies that have attempted to quantify an array of key functions mediated by coral reefs simultaneously. Recent advances integrating empirical data, extrapolation, and community surveys have allowed the quantification of nutrient cycling rates and biomass production on the community level. A major goal of contemporary coral reef conservation is to maintain functioning under human stressors (Bellwood *et al.* 2004). Studies quantifying functions at the community level allow the direct investigation of the effect of human impact on function (Allgeier *et al.* 2016; eg Morais & Bellwood 2019b; Morais *et al.* 2020b). Most work related to process-based functions has focused on somatic growth (i.e., biomass production) and nutrient cycling (i.e., excretion).

Somatic growth is a central element in fisheries stock assessments. Yet, few studies have attempted to quantify fish growth at the community level, and the growth of tropical fishes has been relatively understudied (Pauly 1980). Nevertheless, recent work has compiled data to design a standardized framework to predict growth rate parameters of reef fishes on a global scale (Morais & Bellwood 2018). Fish growth rates decrease with body size and increase with temperature, consistent with metabolic theory (Brown *et al.* 2004; Morais & Bellwood 2018). This conceptual framework helps to investigate community growth patterns, allowing timely insights into biomass production on coral reefs under undergoing stressors (Morais & Bellwood 2018). For example, linking biomass production with human exploitation gradients has revealed that while size-selective fishing depletes fish biomass, it triggers increased production per unit biomass, yielding a 'buffering productivity' in biomass-depleted fish assemblages under high exploitation (Morais & Bellwood 2019b). Further, coral

loss may lead to slower paced reefs (i.e., with a lower biomass turnover rate) due to a community shift with less small fast-growing fish families such as Chaetodontidae, Pomacentridae, Blenniidae, and Gobiidae (Morais *et al.* 2020b). Finally, comparing productivity of tiny cryptobenthic fishes and larger coral reef fishes has underlined the critical role of cryptobenthics in fueling reef trophodynamics (Brandl *et al.* 2019b).

Nutrient-cycling mediated by fishes has a critical impact on coral and algal growth (Burkepile *et al.* 2013; Shantz *et al.* 2015). This increasingly recognized importance of fishes for fueling primary production has yielded several efforts to quantify nutrient cycling rates of reef fish communities by combining empirical measurements with bioenergetic modeling or extrapolation of regression models. Excretion rates of nitrogen and phosphorus of individual fishes can be empirically measured by putting a fish in a certain volume of filtered seawater for a fixed amount of time. Multiple studies have used this technique to quantify nutrient cycling rates for several coral reef fish species (Allgeier *et al.* 2014; Allgeier *et al.* 2015; Francis & Côté 2018). By modeling these rates with biomass and taxonomy, studies have been able to estimate nutrient cycling rates on the community level (Allgeier *et al.* 2015; Allgeier *et al.* 2016, 2017; Francis & Côté 2018). Bioenergetic models provide another way of estimating individual-level cycling rates of all fishes in a community and have been applied in the context of coral reefs (Allgeier *et al.* 2014).
These studies have highlighted how nutrient cycling relates to habitat type, species richness, and community structure (Allgeier *et al.* 2014), fish movement patterns through diurnal migration (Francis & Côté 2018), and intensive fishing (Allgeier *et al.* 2016). Thus, fish biomass, behavior, community structure, and human impact can all affect nutrient cycling on coral reefs.

Aside from biomass production and nutrient cycling through excretion, there are currently no studies that effectively quantified nutrient cycling rates through egestion, nor consumption rates at the community level for coral reef fishes. It is commonly assumed that excretion is the dominant vector of nutrient release by aquatic animals (Atkinson *et al.* 2014), but in fact, egestion has been shown to be an important

overlooked pathway in freshwater settings (Halvorson & Atkinson 2019). In coral reefs, efforts have been made to quantify excretion of nutrients (e.g., Allgeier *et al.* 2014; Francis & Côté 2018), but egestion is largely overlooked. Nevertheless, there are indications that fish feces can be nutrient rich and act as a food source for other fishes. Coprophagy is in fact a common phenomenon among coral reef fishes (Robertson 1982), and some carnivores and planktivores with a nutrient-rich diet have more nutrients in their feces compared to food sources of nominally fishes that feed on algae or detritus (Bailey & Robertson 1982). Thus, fish feces may have an important role in the foodweb, but we currently lack understanding of the quality and flux of coral reef fish egestion.

Mass balance models provide a promising avenue for quantifying multiple functions simultaneously because they can be used to estimate how consumers partition carbon, nitrogen, and phosphorus into nutrient excretion, egestion, and growth (Sterner & Elser 2002). Consumption rates can be approximated by modeling the metabolic requirements of individuals (i.e., bioenergetic models, Kitchell *et al.* 1974; Hanson *et al.* 1997; Kooijman 2010). Modeled consumption rates and the absorption efficiency (i.e., the proportion of elements absorbed in the gastrointestinal tract) then allow for the estimation of egestion rates. Absorbed elements are partitioned into growth, excretion, and respiration. Together, this framework thus allows the quantification of multiple fish-mediated functions.

However, several methodological and empirical knowledge gaps limit the application of bioenergetic models to coral reef fish communities. First, existing bioenergetic models use energy (carbon) as the main currency and rely on the assumption that fishes are limited by energy (Kitchell *et al.* 1974; Hanson *et al.* 1997). However, there is mounting evidence that fishes can be limited by nutrients, rather than energy because their diets contain lower nutrient levels than their needs (Hood *et al.* 2005; Benstead *et al.* 2014; El-Sabaawi *et al.* 2016; Moody *et al.* 2019). This means that these fishes will have a higher consumption rate to compensate for the low levels of nutrients. Particularly in coral reefs that are located in nutrient-poor locations this

mechanism may be important. Moreover, fishes in low trophic levels that feed on low-quality resources often account for a significant proportion of coral reef fish biomass (Graham *et al.* 2017). Applying the traditional bioenergetic models to fish species that are limited by nitrogen or phosphorus normally results in biologically implausible predictions of functions. Further, it is common to use high constants values (~0.8) for absorption efficiencies of carbon, nitrogen, and phosphorus, while in reality they can vary substantially (Czamanski *et al.* (2011)). For coral reef fishes, data on absorption efficiency is scarce, hampering the use of bioenergetic models to quantify egestion rates. Furthermore, physical activity is a major component of the metabolic rate of free-living fishes in their natural habitats (Norin & Clark 2016). The activity scope (i.e., the ratio between field metabolic rate and standard metabolic rate (Chung *et al.* 2019)) is an essential parameter in bioenergetic models to estimate the metabolic requirements of fishes in their natural environment. However, quantification is rare because field metabolic rates are challenging to measure in the aquatic environment and have only been estimated for a small number of fishes (e.g., Lucas *et al.* 2011; Murchie *et al.* 2011; Cruz-Font *et al.* 2016; Chung *et al.* 2019), and none of them are coral reef fishes.

Beyond methodological aspects, quantifying fish-mediated functions at the community level requires key species-specific information for a wide range of fishes (e.g., diet, growth rate, metabolic rate) that may be unreliable or lacking for coral reef fishes. For example, diet of fishes impacts internal processes such as growth, assimilation, and consumption rate (e.g., Morais & Bellwood 2018). In most cases, trophic categories are based on experts, that often disagree among them with particular ambivalence on the resolution at which to define herbivores and invertivores (e.g., Mouillot *et al.* 2014; Stuart-Smith *et al.* 2018). The classification of species into trophic groups has advantages for our understanding of ecological patterns (Mason & Bello 2013; Mouillot *et al.* 2013; Villéger *et al.* 2017). However, the lack of agreement and the limited transparency of trait-based datasets can inhibit the emergence of general patterns. For coral reef fishes, we are still at the brink of knowing what they eat,

let alone what the elemental content of their diet is. We need additional data and reproducible approaches to predict species-level information for a high diversity of fishes, and ultimately estimate fish-mediated functions on the community level. My thesis aims to fill these outlined knowledge gaps to allow a better quantification of process-based fish-mediated functions.

1.5 PhD objectives

The main goal of my thesis is to quantify ecosystem functions mediated by fishes on coral reefs. I aimed to increase our understanding of functions through three main parts: (1) developing a theoretical framework to predict individual processes, (2) scaling up ecosystem functions to the community level for global reefs, and (3) empirically investigating essential and understudied elements that affect individual processes.

First, in part one, I developed a novel bioenergetic model that accounts for nutrient limitation of fishes alongside energy limitation. As many coral reef fishes are herbivorous and likely to be limited by nitrogen or phosphorus rather than energy, the existing methods were not appropriate to use for the diversity of fishes living on coral reefs. Therefore, I developed a novel framework that includes the possibility of nutrient limitation alongside energy limitation (chapter 2). I also made the model accessible to use by developing an R package called 'fishflux.'

Second, I estimate important ecosystem functions on the community level for reefs across the globe by using the framework shown in chapter 2. Applying the bioenergetic model to any species requires specific information. An important element affecting bioenergetic models is diet. Therefore, I predicted trophic guilds for a global species list in a reproducible way that includes uncertainty (chapter 3). Further, the application of the modeling framework (chapter 2) requires a number of additional parameters. Chapter 4 is a methodological chapter that describes how I

estimated these parameters for a global species list using a combination of empirical data and extrapolation methods. Then, using these parameter estimates, I applied bioenergetic models to 9118 reef fish communities across 585 sites worldwide to quantify five community-level reef fish functions (nitrogen excretion, phosphorus excretion, biomass production, herbivory, and piscivory). This application further aids to (1) investigate trade-offs among functions, (2) extract the community- and species-level effects on these functions, and (3) gauge the vulnerability of reef fish functioning in the Anthropocene.

Third, I focused on elements that can heavily affect ecosystem functions, yet are not well known. While a lot of research on nutrient cycling mediated by fishes is focused on the inorganic form of nitrogen and phosphorus (i.e., excretion), the role of fish egestion is less known. In chapter 6, I investigate the importance of egestion by quantifying the quality and quantity of fish egestion. Finally, the activity rate of fishes in the wild affects the metabolic needs of fishes, but has not been quantified for coral reef fishes. In chapter 7, I propose a new approach to estimate the field metabolic rate.

Part I: Quantifying functions on the individual level

Individuals are the building blocks of communities. Ecosystem functions mediated by fish communities are defined by the sum of individual contributions. Therefore, the first part of my thesis focuses on the elemental fluxes in fishes on the individual level. At the beginning, I sought to use existing bioenergetic models to predict the rate of elemental cycling by fishes. However, existing models counter-intuitively predict negative excretion rates for fishes that feed on low-nutrient diets such as algae or detritus. Bioenergetic models typically assume fishes are limited by energy (carbon), but we know that some fishes can be limited by nitrogen or phosphorus instead. Thus, existing models were not appropriate for the wide range of fishes found on coral reefs. In chapter 2, I thus present a new model that integrates estimates of energy requirements with the explicit consideration of carbon, nitrogen, or phosphorus limitation. With empirically measured parameters, the model predicts elemental fluxes through consumption, growth, excretion, respiration, and egestion. Alongside the theoretical model, I developed an R package called 'fishflux' which makes the model user-friendly (See appendix A). This model became the basis for a large part of my thesis.

Chapter 2

Nutrient limitation, bioenergetics, and stoichiometry: a new model to predict elemental fluxes mediated by fishes

This chapter is published in *Functional Ecology*.

Authors: Nina M. D. Schiettekatte, Diego R. Barneche, Sébastien Villéger, Jacob E. Allgeier, Deron E. Burkepile, Simon J. Brandl, Jordan M. Casey, Alexandre Mercière, Katrina S. Munsterman, Fabien Morat & Valeriano Parravicini

Citation: Schiettekatte, NMD, Barneche, DR, Villéger, S, et al. Nutrient limitation, bioenergetics and stoichiometry: A new model to predict elemental fluxes mediated by fishes. Funct Ecol. 2020; 34: 1857– 1869. https://doi.org/10.1111/1365-2435.13618

2.1 Abstract

Energy flow and nutrient cycling dictate the functional role of organisms in ecosystems. Fishes are key vectors of carbon (C), nitrogen (N), and phosphorus (P) in aquatic systems, and the quantification of elemental fluxes is often achieved by coupling bioenergetics and stoichiometry. While nutrient limitation has been accounted for in several stoichiometric models, there is no current implementation that permits its incorporation into a bioenergetics approach to predict consumption rates. This may lead to biased estimates of elemental fluxes. Here, we introduce a theoretical framework that combines stoichiometry and bioenergetics with explicit consideration of elemental limitations. We examine varying elemental limitations across different trophic groups and life stages through a case study of three trophically-distinct reef fishes. Further, we empirically validate our model using an independent database of measured excretion rates. Our model adequately predicts elemental fluxes in the examined species and reveals species- and size-specific limitations of C, N, and P. In line with theoretical predictions, we demonstrate that the herbivore *Zebrasoma scopas* is limited by N and P, and all three fish species are limited by P in early life stages. Further, we show that failing to account for nutrient limitation can result in a greater than two-fold underestimation of ingestion rates, which leads to severely biased excretion rates. Our model improved predictions of ingestion, excretion, and egestion rates across all life stages, especially for fishes with diets low in N and/or P. Due to its broad applicability, its reliance on many parameters that are well defined and widely accessible, and its straightforward implementation via the accompanying R-package `fishflux`, our model provides a user-friendly path toward a better understanding of ecosystem-wide nutrient cycling in the aquatic biome.

2.2 Introduction

Internal biological processes of consumer species, such as growth, respiration, and excretion are important drivers of ecosystem-scale biogeochemical cycles (Barton *et al.* 2013). To survive, individuals need to gather resources from the environment and, in doing so, transfer energy and nutrients within and across ecosystems (Mackenzie *et al.* 1993; Brown *et al.* 2004). Therefore, the quantification of energy and nutrient fluxes in ecosystems is affected by our ability to understand how energy and materials are utilized and transformed at the individual level (Kitchell *et al.* 1974; Sterner & Elser 2002; Allgeier *et al.* 2013).

In many aquatic ecosystems, fishes account for most of the heterotrophic biomass (Odum & Odum 1955; Vanni 2002) and contribute substantially to the storage and flux of carbon (C), nitrogen (N), and phosphorus P (Vanni 2002; McIntyre *et al.* 2008; Burkepile *et al.* 2013; Allgeier *et al.* 2014; Barneche *et al.* 2014). Storage is primarily dictated by food that is assimilated and allocated to growth, which ultimately underpins critical ecosystem services (e.g., finfish fisheries). Fluxes are derived from assimilated (respired carbon and excreted nutrients) and non-assimilated food (egested organic waste) (Schreck & Moyle 1990), and they can have important effects on ecosystem processes, such as primary production (McIntyre *et al.* 2008; Allgeier *et al.* 2013; Capps & Flecker 2013). Disentangling how fishes partition ingested elements into biomass and waste products is therefore key to linking individual-level physiology to ecosystem-level processes, which are of inherent human interest (Hessen *et al.* 2004; Anderson *et al.* 2005; Hou *et al.* 2008; Barneche & Allen 2018).

Ecological stoichiometry provides a theoretical framework to understand how consumers partition C, N, and P (Sterner & Elser 2002). On the basis of the conservation of mass, the material ingested by consumers equals the sum of biomass accumulation and waste products such as respired carbon, excreted nutrients, and egested organic material. Furthermore, stoichiometric theory predicts that the ratio of recycled elements depends on the elemental composition of the consumer body, diet, and the

gross growth efficiency of the limiting element (Sterner 1990; Frost *et al.* 2006). Thus, given known consumption rates, stoichiometric mass balance models allow for the prediction of fish excretion rates (Kraft 1992; Schindler & Eby 1997). Consumption rates can be approximated using empirical relationships with body mass and temperature (e.g., Elliott & Persson 1978; El-Sabaawi *et al.* 2016), but these estimates are highly species-specific, require extensive lab experiments, and may not reflect fish consumption rates in the wild.

Alternatively, consumption rates can be estimated using bioenergetic models. In fact, there is a rich history of bioenergetic modelling approaches to estimate energy allocation in fishes under the assumption that they are limited by energy (C) (e.g., the "Wisconsin model," Kitchell *et al.* (1974); Hanson *et al.* (1997) and the "Dynamic Energy Budget model," Kooijman (2010)). Combined with elemental stoichiometry, bioenergetic models therefore provide a conceptual basis to predict how fishes partition energy and nutrients into growth, metabolism, and waste (Schreck & Moyle 1990; Kraft 1992; Schindler & Eby 1997; Deslauriers *et al.* 2017). This approach has been widely used to estimate consumption rates, given known growth rates in wild fish populations [especially via the Fish Bioenergetics software; Deslauriers *et al.* (2017)]. Nutrient cycling predictions are then made by combining modeled ingestion rates based on energetic needs, assimilation efficiencies, and nutrient stoichiometry of both a fish's body and diet (Kraft 1992; Schindler & Eby 1997; Anderson *et al.* 2005).

Although useful and successfully implemented (Deslauriers *et al.* 2017), this approach is limited in its application to fishes that are limited by C. This can be the case, especially for trophic groups that feed on nutrient-rich prey (e.g., Schindler & Eby 1997); yet, many fish species in low trophic levels may be limited by N or P because their diets contain lower nutrient levels than their body tissues (Schindler & Eby 1997; McIntyre *et al.* 2008). Thus, applying the traditional approach of combining stoichiometry and bioenergetics (Kraft 1992) to fish species that are limited by N or P normally results in biologically implausible predictions of excretion rates. Indeed, there is mounting evidence that fishes can be limited by nutrients, rather

than energy (Hood *et al.* 2005; Benstead *et al.* 2014; El-Sabaawi *et al.* 2016; Moody *et al.* 2019). While, negative predicted excretion rates can provide evidence for nutrient limitation (e.g., Hood *et al.* 2005), they do not aid our understanding and prediction of realistic elemental fluxes in communities where nutrient-limited species are prevalent. Thus, although many stoichiometric models take into account nutrient limitation (e.g., Sterner 1990; El-Sabaawi *et al.* 2016; Guariento *et al.* 2018; Moody *et al.* 2018, 2019), there is presently no solution for integrating nutrient limitation into bioenergetic models that quantify consumption rates. As fishes in low trophic levels often account for a significant proportion of biomass (e.g., Graham *et al.* 2017) and represent important vectors of nutrients, a new approach is needed to accurately predict elemental fluxes in the absence of known consumption rates.

Here, we present a theoretical framework (and a companion R package for its implementation: `fishflux`) to predict elemental fluxes in fishes that combines bioenergetics and ecological stoichiometry while directly accounting for N and P limitation, alongside C limitation. The proposed model framework predicts ingestion rates based on the needs of a fish at a certain size for all three elements and a known growth rate. We test our framework via a case study of three trophically-distinct coral reef fish species: the herbivore *Zebrasoma scopas* (family Acanthuridae), the omnivore *Balistapus undulatus* (family Balistidae), and the carnivore *Epinephelus merra* (family Serranidae). We also validate our model against independent empirical excretion estimates for our three fish species. Furthermore, we test whether fishes in different trophic levels and life stages are limited by different elements and hypothesize that fishes at low trophic levels are limited by N or P rather than C. Finally, we posit that, by building on existing approaches, our framework considerately improves the prediction of key processes such as ingestion and excretion in the case of strong nutrient limitation, as compared to models that only consider C-limitation.

2.3 Materials and Methods

2.3.1 Theoretical framework

Carbon, nitrogen, and phosphorus (CNP, expressed in grams) are the three chemical elements considered in our model. The approach applies a mass-balance framework based on ecological stoichiometry and the metabolic theory of ecology (Sterner & Elser 2002; Brown *et al.* 2004). Further, the approach relies on the growth trajectory of natural fish populations. The proposed model has four main steps (figure 2.1): (1) The minimal required ingestion or minimal supply rate of CNP is defined as the sum of CNP needed for a given growth increment and minimal inorganic flux (i.e., the minimal requirements of CNP needed for metabolism and the maintenance of the body stoichiometry). In this step, we also consider assimilation efficiency, which is defined as the capacity of an organism to assimilate C, N or P (input parameters of the model). (2) Ingestion is estimated based on the limiting element that is defined by the imbalance between the CNP composition of the minimal supply rate and that of the diet. (3) The egestion rate is then quantified according to the ingestion rate and the assimilation efficiencies of each element. (4) The residual CNP are allocated toward the total inorganic flux of CNP (i.e., the waste inorganic CNP that is produced from physiological transformation). For the sake of comparison with existing literature, we note that the inorganic flux of C is generally called total metabolic rate, whereas the inorganic fluxes of N and P are called excretion rates. Materials that are not assimilated are egested as organic waste. An overview of all main variables predicted by the model and input parameters that need to be specified by the user is given in table 2.1, while other parameters mentioned in the text are fixed in the model. In the following sections, we detail each component of the model.

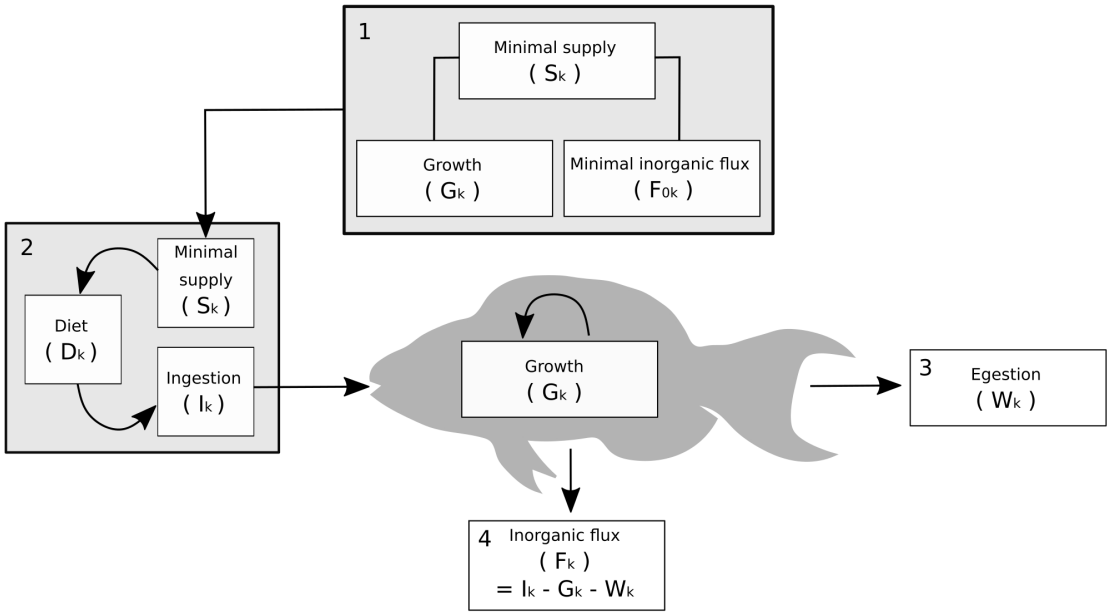

Figure 2.1: Conceptual diagram, explaining different model components. Required ingestion of C, N and P is calculated through the sum of elements needed for growth and minimal inorganic flux, taking into account the element-specific assimilation efficiencies, a_{k} (1). Based on the limiting element (due to the imbalance of food and the required CNP), the ingestion rate can be estimated (2). The ingested material is partitioned into egestion (3) and assimilation (body mass growth and flux (4)). The symbol of each component is indicated in between brackets. The input parameters needed to calculate the different variables are italicised. See table 2.1 for a description of each parameter.

Table 2.1: Overview of model parameters and variables, including input parameters, to be specified by the user of the model, which are indicated with $\times$. Main output variables, predicted by the model are indicated with $\star$. VBGC = von Bertalanffy growth curve.

Symbol	Description	Unit
k	Index for element C, N or P	—
S_{k} $\star$	Element-specific minimal supply rate	g d^{-1}
G_{k} $\star$	Element-specific growth	g d^{-1}
$F_{0\mathrm{k}}$ $\star$	Element-specific minimal inorganic flux	g d^{-1}
a_{k} $\times$	Element-specific assimilation efficiency	—
l_{t} $\times$	Total length of individual at time t	cm
t	Age	yr
l_∞ $\times$	Asymptotic adult length (VBGC)	cm
κ $\times$	Growth rate parameter (VBGC)	yr^{-1}
t_0 $\times$	Age at settlement (VBGC)	yr
lw_a $\times$	Parameter length-weight relationship	g cm^{-1}
lw_b $\times$	Parameter length-weight relationship	—
Q_{k} $\times$	Element-specific body content percentage of dry mass	%
m_{w}	Wet body mass	g
$F_{0\mathrm{Cr}}$	Resting metabolic rate	g d^{-1}
$F_{0\mathrm{Cz}}$	Mass-specific turnover rate of C	g $\mathrm{Cg}^{-1}\mathrm{d}^{-1}$
$F_{0\mathrm{Cs}}$	Rate of C spent in body mass growth	g d^{-1}
f_0 $\times$	Metabolic normalisation constant independent of body mass	g $\mathrm{Cg}^{-\alpha}\mathrm{d}^{-1}$
α $\times$	Mass-scaling exponent	—
$m_{w\infty}$	Asymptotic wet mass of an adult individual	g
ϕ	Cost of growth	g C g^{-1}
θ $\times$	Activity scope	—
v $\times$	Environmental temperature	řC
h $\times$	trophic level	—
r $\times$	Aspect ratio of caudal fin	—
$F_{0\mathrm{Nz}}$ $\times$	Mass-specific turnover rate of N	g $\mathrm{Ng}^{-1}\mathrm{d}^{-1}$
$F_{0\mathrm{Pz}}$ $\times$	Mass-specific turnover rate of P	g $\mathrm{Pg}^{-1}\mathrm{d}^{-1}$
m_{dw}	Ratio of dry mass and wet mass of fish	—
m_{d}	Dry body mass	g
D_{k} $\times$	Element-specific diet content percentage of dry mass	%
I_{k} $\star$	Element-specific ingestion rate	g d^{-1}
W_{k} $\star$	Element-specific egestion rate	g d^{-1}
F_{rk} $\star$	Element-specific residual inorganic flux	g d^{-1}
F_{k} $\star$	Element-specific total inorganic flux	g d^{-1}

Minimal suppy rate

The first step of the model is an estimate of the minimal supply rate of elements (C, N and P) required per day for a given growth increment in an individual of a given size. The required CNP is the sum of the elements needed for body mass growth and overhead metabolic and maintenance costs (i.e., minimal inorganic flux). The minimal supply rate S_{k} (g d^{-1}) of the element k = {C, N, P} can therefore be estimated as

$$S_{\mathrm{k}} = \frac{(G_{\mathrm{k}} + F_{0\mathrm{k}})}{a_{\mathrm{k}}}, \tag{2.1}$$

where G_{k}, $F_{0\mathrm{k}}$ and a_{k} are element-specific growth rate (g d^{-1}), minimal inorganic flux (g d^{-1}), and assimilation efficiency (%), respectively.

Growth

The aim of our model is to predict elemental fluxes of fishes in their natural environment. Therefore, we use growth rates that can be calculated from otolith analysis. In our model, we thus assume that there is enough food available to fulfill the observed growth pattern. We further use the von Bertalanffy growth curve (VBGC) to describe the growth trajectory (Bertalanffy 1957). Empirically, the VBGC is favorable because its parameters are statistically simple to obtain, easy to interpret, and are available for a large number of species (Morais & Bellwood 2018). Body length, l_t (cm in total length, i.e., T.L.), at age t (yr) is

$$l_t = l_\infty \left(1 - e^{-\kappa(t-t_0)}\right), \tag{2.2}$$

where t_0 is age at settlement, l_∞ is the asymptotic adult length (i.e., length when growth rate is 0), and κ is a growth rate parameter (yr^{-1}) (Bertalanffy 1957). With this equation, we can quantify the age of a fish of a certain size. Then, by adding one day to that age, we can also approximate the amount a fish will grow in one day. Using length-weight relationships and wet-to-dry mass conversion constants from the literature and FishBase (Froese & Pauly 2018), we can finally calculate total growth

rate (i.e., G) expressed in dry mass (g d^{-1}). Using element-specific body content percentages, Q_{k}, we calculate element-specific growth as:

$$G_{\mathrm{k}} = \frac{Q_{\mathrm{k}}}{100} G. \tag{2.3}$$

Minimal inorganic flux

Traditionally, the field metabolic rate, $F_{0\mathrm{C}}$, has been studied more intensively than minimal excretion rates for N and P, $F_{0\mathrm{N}}$, and $F_{0\mathrm{P}}$. As a consequence, we currently have a better understanding of how assimilated carbon is partitioned into body mass growth (G_C) and metabolic overhead costs ($F_{0\mathrm{C}}$). For instance, we know that $F_{0\mathrm{C}}$ predictably scales with individual wet body mass, m_w (g) (Hou *et al.* 2008):

$$\begin{aligned} F_{0\mathrm{C}} &= \theta F_{0\mathrm{C}r} = \\ \theta(F_{0\mathrm{C}z} m_w &+ F_{0\mathrm{C}s}) = \\ \theta(f_0 m_{w\infty}^{\alpha-1} m_w &+ \phi G), \end{aligned} \tag{2.4}$$

where $F_{0\mathrm{C}r}$ is the resting metabolic rate (g C d^{-1}), $F_{0\mathrm{C}z}$ is the mass-specific turnover rate (g C g^{-1} d^{-1}), $F_{0\mathrm{C}s}$ is the rate of carbon spent in body mass growth, and f_0 is a metabolic normalization constant that is independent of body mass (g C $g^{-\alpha}$ d^{-1}) and varies among fish taxa, environmental temperature, and trophic level (Barneche & Allen 2018). α is a dimensionless mass-scaling exponent (generally between 0.5 and 1), $m_{w\infty}$ is the asymptotic mass of an individual, and ϕ is the energy expended to produce one unit of body mass (g C g^{-1}; hereafter the "cost of growth"). In equation 2.4, $F_{0\mathrm{C}}$ is defined as the sum of the resting metabolic rate, $F_{0\mathrm{C}r}$, and the active rate that sustains locomotion, feeding, and other activities. We assume that $F_{0\mathrm{C}} = \theta F_{0\mathrm{C}r}$ in the expression above, where θ is a dimensionless parameter referred to as 'activity scope,' which is constrained to be greater than 1 and less than the ratio between maximum metabolic rate and resting metabolic rate (Hou *et al.* 2008; Barneche & Allen 2018).

The cost of growth, ϕ, varies substantially among fishes, and it may increase with environmental temperature, v, trophic level, h, and aspect ratio of caudal fin, r (a proxy for activity level) (Froese & Pauly 2018). Following Barneche & Allen (2018), the cost of growth can be calculated as

$$\ln\phi = \beta_0 + \beta_v v + \beta_h \ln h + \beta_r \ln(r+1), \tag{2.5}$$

where β_0 is a constant, β_v, β_h, and β_r are respectively the model slopes for v, h, and r. We note that h and r are two ecological variables that can be retrieved from FishBase (Froese & Pauly 2018). For the purposes of our bioenergetic model, we use average, across-species estimates for β_0, β_v, β_h, and β_r published in Barneche & Allen (2018).

Aside from inorganic fluxes of C, N and P will also be released at a minimal rate, even when they are limiting (Sterner & Elser 2002; Anderson *et al.* 2005). The minimal inorganic flux of N and P can be experimentally measured as minimal excretion rates during starvation (Mayor *et al.* 2011). We can thus explicitly incorporate N and P turnover rates to estimate minimal inorganic flux of N and P (Anderson *et al.* 2005).

$$F_{0\mathrm{N}} = F_{0\mathrm{N}z}\frac{Q_{\mathrm{N}}}{100}m_d, \text{ and} \tag{2.6}$$

$$F_{0\mathrm{P}} = F_{0\mathrm{P}z}\frac{Q_{\mathrm{P}}}{100}m_d, \tag{2.7}$$

where $F_{0\mathrm{N}z}$ and $F_{0\mathrm{P}z}$ are nutrient-specific dry mass-specific turnover rates for N (g N g $^{-1}$ d^{-1}) and P (g P g^{-1} d^{-1}), respectively, and m_d is the dry mass of the fish (g). Equations 2.6 and 2.7 assume that $F_{0\mathrm{N}z}$ and $F_{0\mathrm{P}z}$ remain constant during ontogeny.

Ingestion

In our model, the quantification of ingestion rate is a two-step process. First, we define the minimal required ingestion of CNP by summing element-specific minimal supply rates S_{k}. Second, we approximate the actual ingestion rates by using ecological

stoichiometric theory (Sterner & Elser 2002). With known elemental stoichiometry of the diet (D_{C}, D_{N}, D_{P}) we can determine the limiting element as follows:

$$\text{limiting element} = \begin{cases} C, & \text{if } \frac{S_{\mathrm{C}}}{S_{\mathrm{N}}} > \frac{D_{\mathrm{C}}}{D_{\mathrm{N}}} \text{ and } \frac{S_{\mathrm{C}}}{S_{\mathrm{P}}} > \frac{D_{\mathrm{C}}}{D_{\mathrm{P}}} \\ N, & \text{if } \frac{S_{\mathrm{N}}}{S_{\mathrm{P}}} > \frac{D_{\mathrm{N}}}{D_{\mathrm{P}}} \text{ and } \frac{S_{\mathrm{C}}}{S_{\mathrm{N}}} < \frac{D_{\mathrm{C}}}{D_{\mathrm{N}}} \\ P, & \text{otherwise} \end{cases} \tag{2.8}$$

The actual ingestion rate is then approximated according to the limiting element, following Liebig's minimum law. To do so, we assume fishes have enough food available to meet their minimal needs (S_{k}). For example, if P is limiting, element-specific ingestion rates, I_{k}, (g d^{-1}) are

$$I_{\mathrm{P}} = S_{\mathrm{P}}, \tag{2.9}$$

$$I_{\mathrm{N}} = I_{\mathrm{P}} \frac{D_{\mathrm{N}}}{D_{\mathrm{P}}}, \tag{2.10}$$

$$I_{\mathrm{C}} = I_{\mathrm{P}} \frac{D_{\mathrm{C}}}{D_{\mathrm{P}}}, \tag{2.11}$$

where D_{k} represents element-specific body content percentage of dietary items. Once ingestion rate is estimated, the partitioning of the ingested matter into various pathways (i.e., egestion, excretion and respiration) can be defined.

Egestion or organic waste production

The rate of organic waste production or egestion rate, W_{k} (g d^{-1}) can be computed using the ingestion rate of each element and element-specific assimilation efficiencies (Schreck & Moyle 1990):

$$W_{\mathrm{k}} = (1 - a_{\mathrm{k}}) I_{\mathrm{k}}. \tag{2.12}$$

Total inorganic flux

The rate of total inorganic waste production or flux (i.e., total respiration and excretion) equals the ingestion rate minus body mass growth rate and egestion rate for each element (Schreck & Moyle 1990; Sterner & Elser 2002). If an element is limiting, the individual is likely to consume other elements in excess in order to meet the target for that limiting element. In such cases, it is often assumed that the exceeding "residual" element will be subject to post-absorptive release via inorganic waste production (i.e., residual flux F_{rk}) to maintain body homeostasis (Anderson *et al.* 2005). When N or P are limiting, for example, a certain residual amount of C, Fr_{C} remains unutilised. However, if C is limiting instead of N or P, excretion rates F_{N} and F_{P} will increase by an overhead residual flux F_{rk}. In the example of C limitation, the residual flux F_{rC} would equal zero. We can thus quantify the total inorganic flux as follows:

$$F_{\mathrm{k}} = F_{0\mathrm{k}} + F_{\mathrm{rk}}, \tag{2.13}$$

where

$$F_{\mathrm{rk}} = I_{\mathrm{k}} - G_{\mathrm{k}} - F_{0\mathrm{k}} - W_{\mathrm{k}}. \tag{2.14}$$

2.3.2 Application

We validate our modelling approach using data from three reef fish species: the herbivore *Zebrasoma scopas* (family Acanthuridae), the omnivore *Balistapus undulatus* (family Balistidae), and the carnivore *Epinephelus merra* (family Serranidae). All parameters were quantified using empirical data augmented with information from the literature when needed (see supplementary methods 2.7). An overview of all parameter estimates is provided in (2.8).

We ran the model using R (R Core Team 2019) and Stan (Stan Development

Team 2018). For an easy application of the presented framework, we developed the R package `fishflux`, which provides a set of user-friendly functions to simulate the model, extract the output variables, and visualize the results (see 2.7). Parameter means and standard deviations are provided, and a Monte Carlo method is applied to randomly draw each parameter assuming normal distributions in each iteration. To account for co-variances among parameters, we used the Stan function `multi_normal_rng()`, which samples each parameter under consideration of the co-variance matrix. We included co-variances for body stoichiometry (Q_{k}), diet stoichiometry (D_{k}), length-weight parameters (ϵ and b), and metabolic parameters (α and f_0). These parameters were sampled from their log-transformed multinormal distribution then back-transformed to natural scale. All other parameters were sampled from truncated normal distributions, where the lower and upper bounds are the possible ranges of each respective parameter. For our case study, we used 5,000 iterations. If the standard deviation of a given parameter is unknown (e.g., r, reported on FishBase), the function automatically fills in the standard deviation with a very low value of 10^{-9} in order to keep the respective parameter approximately constant at each iteration of the simulation.

To compare the predictions of ingestion and excretion rates of our model framework with the case where only C-limitation is considered, we simulated ingestion and excretion rates, based only on the minimal supply rate of C, thus where I_{c} equals S_{c}. Excretion rates or total inorganic flux rates of N and P are then defined as follows:

$$F_{\mathrm{N}} = S_{\mathrm{C}} \frac{D_{\mathrm{N}}}{D_{\mathrm{C}}} - G_{\mathrm{N}} - W_{\mathrm{N}}, \tag{2.15}$$

$$F_{\mathrm{P}} = S_{\mathrm{C}} \frac{D_{\mathrm{P}}}{D_{\mathrm{C}}} - G_{\mathrm{P}} - W_{\mathrm{P}}. \tag{2.16}$$

We compared the predicted excretion rates for N and P with our own independent database of experimental excretion rates. We collected individual fish using barrier nets, dip nets, cast nets, traps, clove oil, and hook and line across different reef habitats around Moorea, French Polynesia during austral winter of 2016 and 2017

(n = 128). We aimed to collect individuals across the size spectrum present in each species. We immediately transported individuals back to shore in an aerated cooler for excretion experiments (see 2.7). Excretion rates were measured within a maximum of 3 hours after capture. The capture and handling of fishes for this project were approved in a protocol from the University of California Santa Barbara's Institutional Animal Care and Use Committee (IACUC #915 2016-2019).

Finally, to illustrate the effect of diet stoichiometry, we simulated the model with varying % of N and P. For this simulation, we used the parameters of *Z. scopas* and ran the simulation for an individual of 10cm. We kept D_{C} constant at 20%. The values of D_{N} and D_{P} varied around the elemental ratio of S_{k}. We used color palettes from the R package fishualize (Schiettekatte *et al.* 2019).

2.4 Results

The application of the developed modeling framework reveals distinct elemental limitations across the three species at different lengths (figure 2.2). *Z. scopas* is limited by either N or P over its full size range, with P being the limiting element early in its ontogeny and N becoming the limiting element after reaching approximately 7 cm TL. Although *B. undulatus* and *E. merra* are also limited by P at an early life stage, they are predominantly limited by C upon maturation.

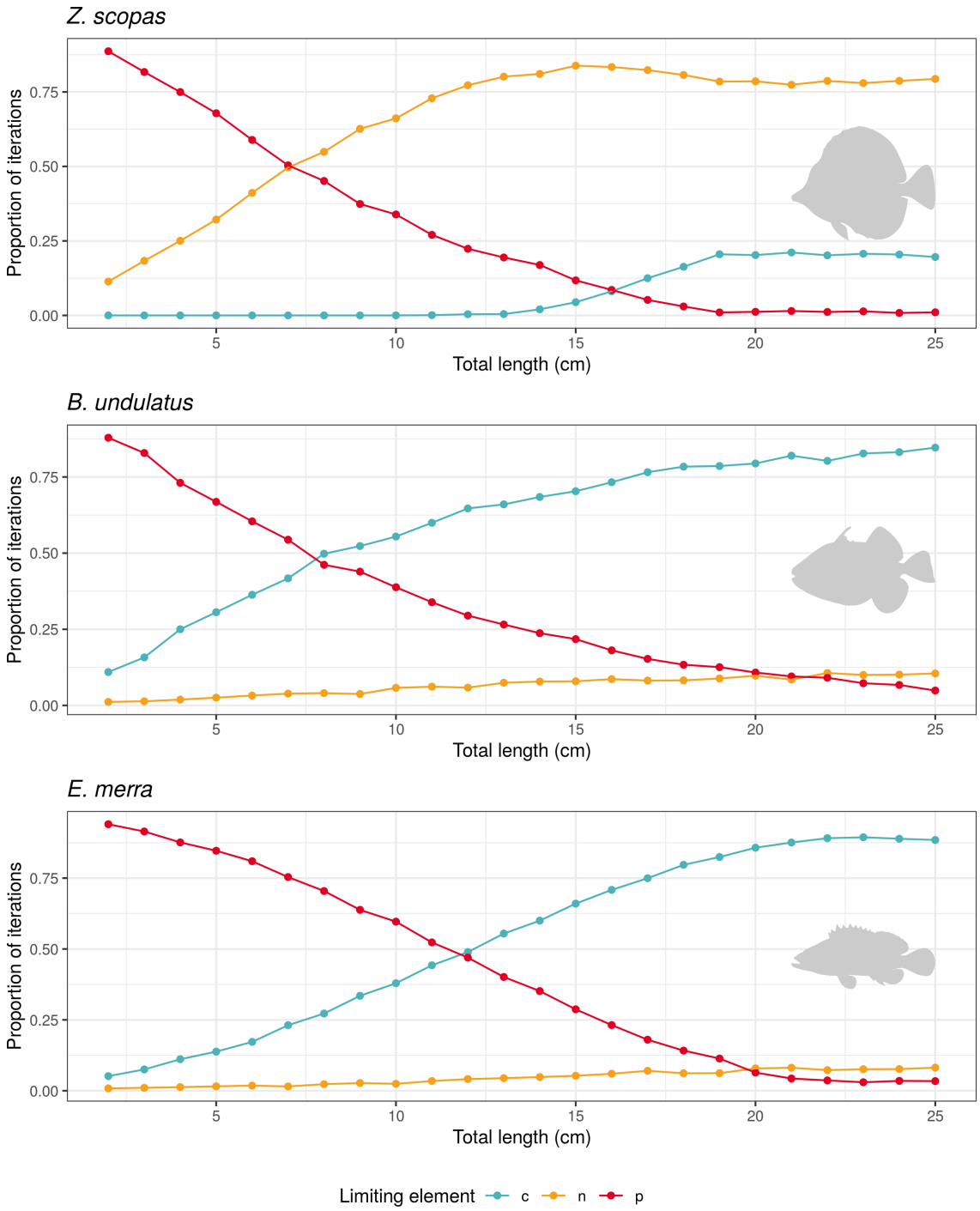

Figure 2.2: Proportion of the simulation iterations that determine C, N and P as the limiting element for *Zebrasoma scopas*, *Balistapus undulatus*, and *Epinephelus merra*.

Our approach demonstrates that defining the limiting element can be critical to predict a species' ingestion rate, which affects all downstream calculations in the model (e.g., excretion rates of N and P) compared to models only considering C limitation (figure 2.3). Specifically, assuming C limitation in *Z. scopas* results in a severe underestimation of ingestion and excretion rates (figure 2.3, A, B and C). In the omnivore *B. undulatus* and the carnivore *E. merra*, the limiting element has less influence on ingestion rates. Still, without incorporation of P limitation, model predictions may result in negative excretion rates of P for growing individuals of *B. undulatus* and *E. merra*. In the case of *E. merra*, C-only models predict negative P excretion rates for more than half of the simulations under a total length of 10 cm (figure 2.3, I). Thus, our framework reveals that nutrient limitations and their consequences for ingestion rate estimations are highly specific to the three study species and their ontogenetic stage.

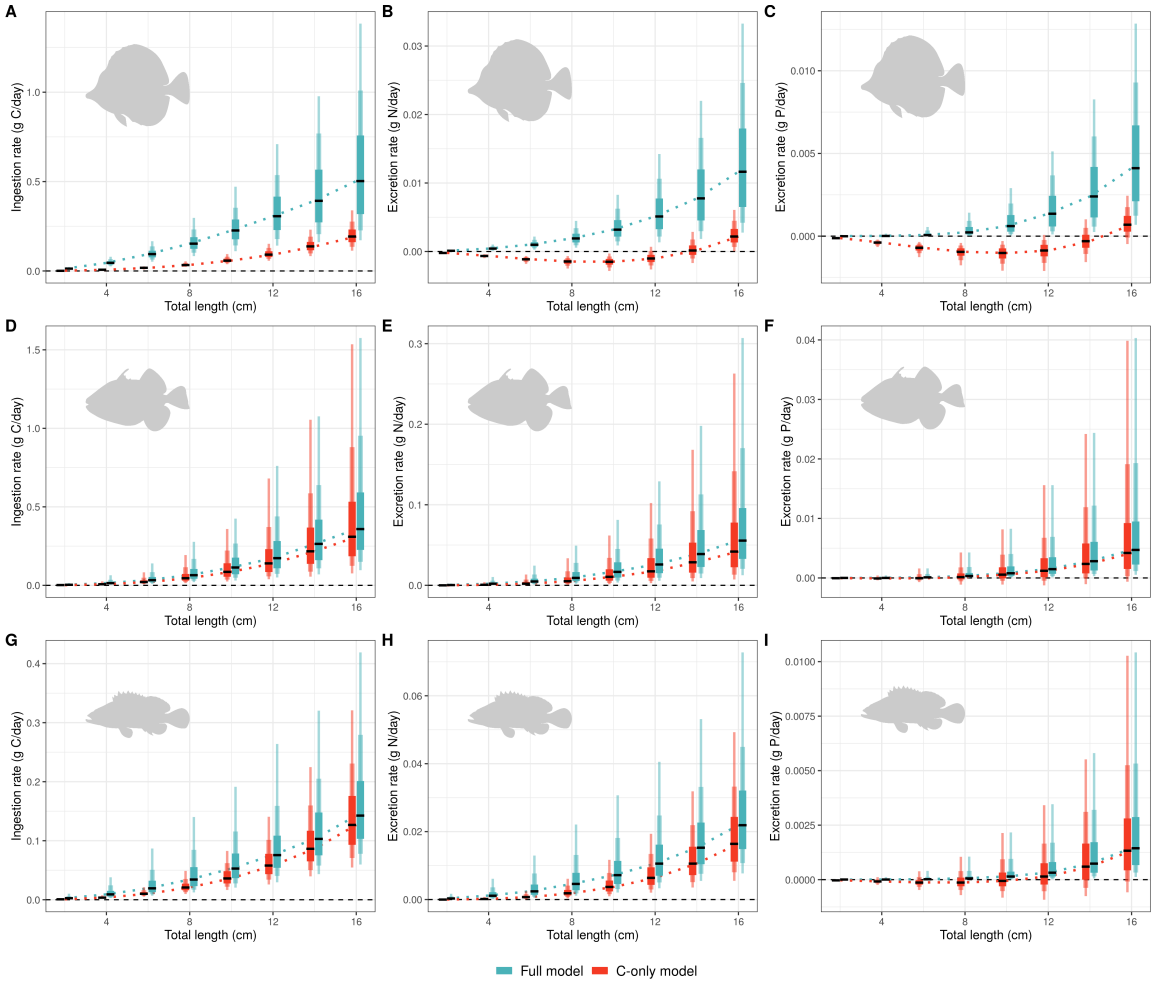

Figure 2.3: Predicted daily ingestion of carbon and excretion rates for the full model, considering nutrient limitation and for a model, only taking into account C-limitation. Horizontal lines show the median values and 95%, 80%, and 50% confidence intervals are illustrated respectively in vertical lines. A. C ingestion rates of *Z. scopas*, B. N excretion rates of *Z. scopas*, C. P excretion rates of *Z. scopas*, D. C ingestion rates of *B. undulatus*, E. N excretion rates of *B. undulatus*, F. P excretion rates of *B. undulatus*, G. C ingestion rates of *E. merra*, H. N excretion rates of *E. merra*, I. P excretion rates of *E. merra*.

Our model predicts ingestion rates for *Z. scopas*, *B. undulatus* and *E. merra* at 15 cm TL to be 28.2 (11.7 – 68.4), 12.9 (3.7 – 56.7), 14.1 (5.5 – 40.1), respectively (in mg dry weight per g wet weight of fish per day, median and 95% confidence interval (C.I.)) (see 2.8). Comparing our predicted excretion rates with empirical data on excretion rates shows that our model adequately predicts excretion rates with almost all experimental data falling inside the predicted 95% confidence interval (figure 2.4). For N excretion, 100%, 97% and 94% of the experimental excretion rates are captured by our predictions for *Z. scopas*, *B. undulatus* and *E. merra*, respectively. For P excretion, we adequately predict 93%, 94%, and 90% of the experimental excretion rates for the three species, respectively. Predictions for *E. merra* are slightly overestimated compared to experimental excretion rates. Groupers feed infrequently, and their stomachs were often found empty, which may have impacted the measured excretion rates.

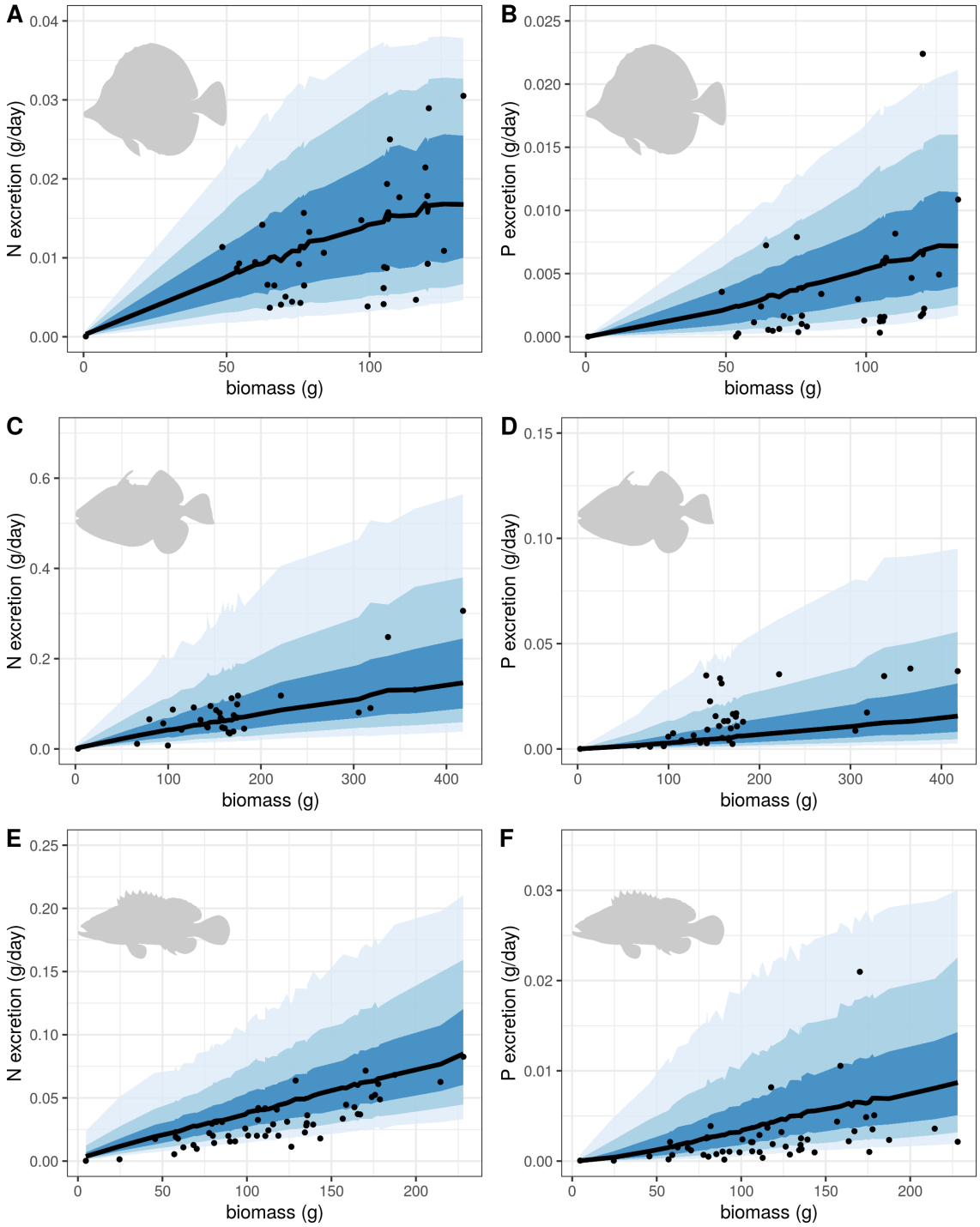

Figure 2.4: Predicted excretion rates for each species of both N and P. The 50%, 80% and 95% confidence intervals are presented around the median. Points show the experimental excretion rates, obtained from an independent database. A. N excretion rates of *Z. scopas*, B. P excretion rates of *Z. scopas*, C. N excretion rates of *B. undulatus*, D. P excretion rates of *B. undulatus*, E. N excretion rates of *E. merra*, F. P excretion rates of *E. merra*.

Predictions are substantially affected by variability in the stoichiometry of dietary sources. To illustrate how the diet stoichiometry affects limitations by different elements and ingestion and excretion rates, we simulated different scenarios by varying the diet percentages of N and P around the stoichiometry of the minimal supply rate of an individual of *Z. scopas* of 10 cm (figure 2.5). When diet stoichiometry differs from this ideal stoichiometry of the minimal supply rate, either C, N or P is the limiting element, which in turn affects all downstream biological processes. For example, when the percent of P in the diet is low, P is the limiting element (figure 2.5, A).This leads to an increased ingestion rate (figure 2.5, B), a minimal excretion rate of P (figure 2.5, C), and a high excretion rate of N (figure 2.5, D).

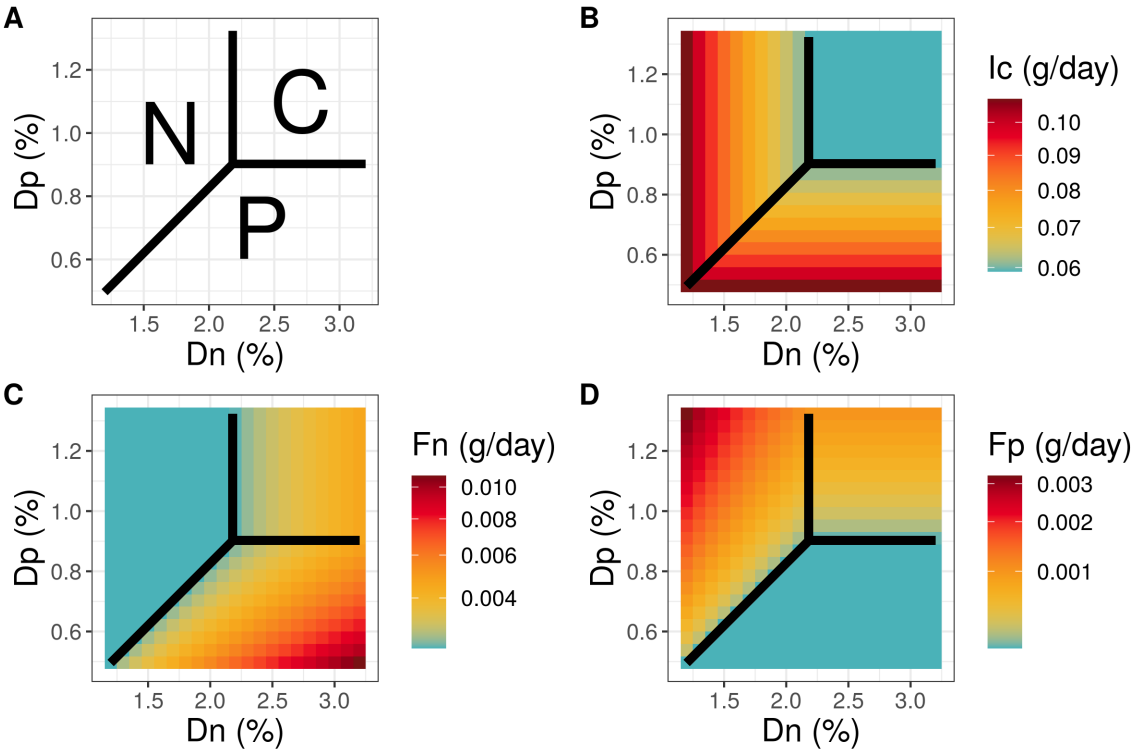

Figure 2.5: Model simulations with varying levels of D_N and D_P. D_C is kept constant. Diet stoichiometry affects the limitation and the rates of multiple processes, such as the ingestion rate and excretion rates. A. The limiting element is indicated for varying levels of diet stoichiometry (D_N and D_P). Lines indicate where one limiting element switches to another. This is equivalent to the threshold elemental ratio, B. I_C or Ingestion rates of C (g/day), C. F_N or Total inorganic flux of N (g/day), D. F_P or Total inorganic flux of P (g/day).

2.5 Discussion

Combining stoichiometry and bioenergetic modeling provides a framework to predict elemental fluxes in consumers and their contribution to key biogeochemical cycles. Here, we introduce a model that incorporates the nutrient requirements of fishes alongside their energetic needs to provide accurate predictions of their ingestion, respiration, excretion, and egestion rates. With our framework, we confirm the existence of nutrient limitation in fishes, specific to the trophic group and life stage, and its effect on multiple processes. We demonstrate the accuracy and applicability of the model to predict ingestion and excretion rates for three tropical reef fish species, while also reflecting the natural variability of these variables. Our framework provides an accurate tool to predict CNP fluxes in fishes across diverse trophic groups and gauge the role of fish consumers in ecosystems worldwide.

There is a growing consensus that many fishes are limited by nutrients (Hood *et al.* 2005; Benstead *et al.* 2014; El-Sabaawi *et al.* 2016; Moody *et al.* 2019). Yet, fish growth and maintenance are often assumed to be limited by energy (C) when applying coupled bioenergetic and stoichiometric models (Kraft 1992; Schindler & Eby 1997; Allgeier *et al.* 2013; Burkepile *et al.* 2013). Our case study confirms that ingestion rates can indeed be determined by N or P limitation rather than C limitation, especially in species with nutrient-poor diets. This finding is expected given the elemental imbalance between the consumer's body and dietary CNP content; however, failing to account for nutrient limitation substantially skews predictions of ingestion rates. For example, assuming only energy limitation for a herbivorous adult *Z. scopas* would result in a greater than two-fold underestimation of its ingestion rate and consequently drastic underestimations of excretion and egestion rates. Given the high densities of species with nutrient-poor diets across a variety of ecosystems (e.g., herbivorous and detritivorous species; Williams & Hatcher (1983); Takeuchi *et al.* (2010); Hood *et al.* (2005)), such underestimates may result in strong misconceptions about ecosystem-scale nutrient and energy fluxes. Our model framework provides

means for the direct incorporation of varying elemental limitation across species.

The developed model predicts ingestion through the integration of metabolic theory and elemental limitation, thus circumventing the difficult task of measuring ingestion rates in natural populations. Therefore, the first step of our framework focuses on quantifying the minimal supply rate for each element (S_{k}) and determining the limiting element. This includes both maintenance rates and element-specific growth rates based on the growth trajectory of natural populations. Then, by comparing the stoichiometry of these minimal supply rates with diet stoichiometry, we can determine the limiting element. This approach is inspired by threshold elemental ratio (TER) theory, which predicts the ratio at which growth limitation switches from one element to another (Urabe & Watanabe 1992; Sterner & Elser 2002). In fishes, it is widely accepted to integrate metabolic rate into the calculation of TERs (Frost *et al.* 2006). We built on this work to account not only for maintenance requirements of C, but also of N and P. Similar to the energy (C) that is needed to sustain the metabolic rate of fishes in the wild, minimal N and P is needed for cell turnover and maintenance of body composition. The specific turnover rate of P ($F_{0\mathrm{Pz}}$) is lower than the turnover rate of N ($F_{0\mathrm{Nz}}$) because bone cells, which contain the majority of P, degrade slowly compared to other cell types (Manolagas 2000; Sterner & Elser 2002). Thus, including minimal requirements for all three elements lowers the TER of C and nutrients of fishes and increases the probability of detecting nutrient limitation.

The inclusion of nutrient limitation ensures that predicted excretion rates (F_{P}, F_{N}) are always higher than zero. This is crucial since N and P will always be released at a minimal rate, even when they are limiting (Sterner & Elser 2002; Anderson *et al.* 2005; Mayor *et al.* 2011). Our approach reveals that all three study species are limited by P in their early life. By explicitly including minimal supply rates in our model, we move beyond simply detecting evidence for nutrient limitation (i.e., negative excretion rates; Hood et al, 2005) towards quantifying its effect on vital processes across species and ontogeny. Bone growth, for example, requires substantial amounts of P and is most rapid during early life-stages (Vanni 2002), and evidence

from freshwater ecosystems shows that P can limit fish growth (Hood *et al.* 2005; Benstead *et al.* 2014). The ontogenetic variation in elemental limitation presented herein confirms the importance of considering P-limitation for growth when predicting elemental fluxes in fishes.

Beyond the incorporation of nutrient limitation, our model framework provides a way to estimate uncertainty of predictions. Empirically-measured excretion rates can considerably vary for similarly sized individuals of the same species (Whiles *et al.* 2011; Allgeier *et al.* 2015; Francis & Côté 2018). Yet, existing models that combine stoichiometry and bioenergetics do not account for this natural variability (e.g., Deslauriers *et al.* 2017), which hampers our ability to gauge the uncertainty of resulting estimates. With the use of MCMC iterations, the R package `fishflux` incorporates the distribution of parameters with their means and standard deviations, resulting in realistic credibility intervals of ingestion and excretion rates, although variability in model output does not necessarily reflect natural variability. The utility of this approach is clear when comparing our predictions to reported ingestion rates. For example, *Z. scopas* reportedly ingests 49 mg of dry mass per gram of wet fish weight (Polunin *et al.* 1995), a value centered within the predicted range of our model (11.7 – 68.4 at 15 cm TL). Similarly, the ingestion rate of juvenile coral trout, *Plectropomus leopardus*, a predatory species in the same family as *E. merra* (family Serranidae), ranges between 9 to 14 mg of dry mass per gram of wet weight (Sun *et al.* 2014), which lies within the 95% prediction for *E. merra* from our model (5.5 – 40.1). Tracing the sensitivity of predictions to uncertainty in specific parameters enables the determination of the main sources of variability that may shift estimates among studies or species.

As all models, our approach relies on several simplifying assumptions. First, our model assumes that fishes maintain homeostasis (Sterner 1990). Since fishes can have flexible body stoichiometry depending on dietary nutrient content (Benstead *et al.* 2014; Dalton *et al.* 2017), this assumption may impose biases when simulating effects of varying diet stoichiometry on elemental fluxes. Yet, empirically measured

relationships between nutrient content of body and diet can easily be incorporated into our model simulations, thus ameliorating the effects of this simplification. Second, similar to most stoichiometric mass balance models, our framework is based on Liebig's minimal rule, which states that growth is strictly limited by the element in shortest supply relative to demand. However, there is emerging evidence that consumers may simultaneously be limited by more than one element (Sperfeld *et al.* 2012). For example, P plays an essential role in fish energy uptake (Xie *et al.* 2011), and the incorporation of interactive co-limitation into stoichiometric models may further improve predictions of elemental fluxes. Finally, we assume that fishes follow a growth trajectory defined by the VBGC curve, and that there is enough food available in the natural environment to meet the growth requirements for each element. The VBGC is fitted on size-at-age data that are mostly acquired via annual otolith readings. In our model, we use this fitted growth function to estimate daily growth rates for each element through integration with length-weight relationships and body stoichiometry. This does not capture, for instance, seasonal variation of food availability. Other stoichiometric models mostly use gross growth efficiencies (GGEs, i.e., growth/ingestion of the limiting element) (Frost *et al.* 2006; McManamay *et al.* 2011; e.g., El-Sabaawi *et al.* 2016; Guariento *et al.* 2018; Moody *et al.* 2019). However, consumer GGEs vary widely, and specific values are poorly understood (McManamay *et al.* 2011). Furthermore, even if element-specific GGEs are quantified, they may not reflect growth observed in natural populations. Therefore, we suggest that the use of otolith-based growth quantification provides a reasonable alternative to model elemental fluxes of natural fish populations.

Beyond model assumptions, the accuracy of our model naturally relies on the accuracy of each parameter estimate. Yet, parameters are often difficult to obtain. We sought to balance the accuracy of predictions and ease of application. Parameters involving growth, length-weight relationships, metabolism, and stoichiometry are increasingly accessible for many species due to predictive modeling and open-access databases (Barneche *et al.* 2014; e.g., Froese *et al.* 2014; Killen *et al.* 2016; Vanni *et*

al. 2017; Froese & Pauly 2018; Morais & Bellwood 2018). Yet, there are a number of parameters that are still sparsely quantified and may limit the applicability of our framework. In particular, data on diet stoichiometry and assimilation efficiencies are rare. In our case study, we used assimilation efficiency constants for C, N and P, that are predominantly based on predatory fishes. In reality, assimilation efficiencies can vary substantially, and, in particular, assimilation efficiency of phosphorus is likely correlated with diet quality (Czamanski *et al.* 2011). Further, N- and P-specific turnover rates are newly introduced parameters and therefore poorly known. As these parameters depend on the cell turnover rates of N- and P-rich tissues (e.g., bone cells for P), we suggest that these parameters may be applicable across species. Nevertheless, further research is needed to gain more insight. While variation in these parameters can impact the model output via the limiting element and ingestion rate, ongoing compilations of databases of poorly known parameters will improve the application of the proposed modeling framework.

In addition, we quantified the activity scope (i.e., field metabolic rate) as the average of maximum metabolic rates (MMR) and standard metabolic rates (SMR) divided by the SMR, assuming that a fish reaches values close to MMR when undertaking activities in the wild (Murchie *et al.* 2011). In reality, activity scope may vary depending on life history traits and behavior (Killen *et al.* 2017), and field metabolic rates can be elevated with the presence of predators, which in turn can affect nutrient cycling (Dalton *et al.* 2018; Guariento *et al.* 2018). Refining established techniques, such as bio-telemetry (Norin & Clark 2016) or otolith chemistry (Chung *et al.* 2019) may improve estimates of field metabolic rates. Similarly, specific dynamic action (SDA), which is the metabolic rate needed to assimilate food (Hou *et al.* 2008) depends on the quality and quantity of food (McCue 2006) and may thus influence ingestion rates, but it is poorly known across most species. Finally, reproduction is not yet incorporated into the model because data on both gonad stoichiometry and reproductive growth is rare. This may underestimate energy and nutrient investment of fishes, thus skewing model predictions. Nonetheless, as new data on reproductive

growth, activity scope, or SDA become available, these elements can be incorporated in the future.

Despite these limitations, our framework provides new avenues for addressing pressing questions in ecology. Data on the daily actions of fishes are difficult to obtain due to the challenges of conducting research in aquatic environments. Novel techniques such as fish gut content DNA metabarcoding (Casey *et al.* 2019) or compound-specific stable isotope analyses (Hopkins & Ferguson 2012) permit improved insights into species-specific ingestion of prey resources. However, no current empirical technique can estimate rates of food ingestion via these linkages across a broad range of species. Combining our model with emerging techniques to quantify species-specific resource use can help us to address long standing questions. How much prey do top predators consume daily? How do rates of algal consumption differ among herbivorous species? How much production by lower trophic levels is needed to fuel the growth of predatory fisheries species? By providing a tool to answer these questions, our model empowers fundamental and applied researchers to tackle some of the most important questions in fish ecology.

Beyond single species and their pairwise interactions, our model provides means to examine community- and ecosystem-scale dynamics. Specifically, based on simple census data of fish communities, our model can help decompose system-wide fluxes (cf. Burkepile *et al.* 2013; Allgeier *et al.* 2014; Francis & Côté 2018). This is particularly important for open ecosystems in which the dominant sources of energy and nutrients are unclear or variable. For example, on coral reefs, debates persist on the importance of external (i.e., pelagic) subsidies versus internal nutrient cycling (e.g., Brandl *et al.* 2019b; Morais & Bellwood 2019b). Our model can help estimate how much pelagic or benthic prey is consumed by reef fishes and how these resources are propagated through food webs, which enables researchers to quantify reef functioning (Brandl *et al.* 2019a). Thus, merging what is eaten (i.e., food web assembly) with how much is eaten (i.e., realistic consumption rates as provided by our model) can significantly augment our understanding of ecosystem functioning, especially in systems where

fishes are the dominant consumers.

Finally, given the heavy exploitation of fish communities for global human consumption, our model offers a tool for understanding and predicting the effect of human-driven changes on ecosystem functioning. Yearly, more than 100 million tons of fishes are caught in marine systems worldwide (Cashion *et al.* 2018). Our model provides a tool to estimate the impact of this disturbance on system-wide biogeochemichal fluxes. In addition, increasing temperatures resulting from climate change can affect primary production in the world's oceans, thus imposing a bottom-up effect on fish communities (Lotze *et al.* 2019), which are likewise affected by rising temperatures (Pinsky *et al.* 2019). Given human-driven alterations in both primary production through climate change and fish community structure through extensive fishing, it is urgent to understand how these changes may impact biogeochemical fluxes. Our model and its implementation provide a path toward rising to this challenge.

2.6 Data accessibility

All data and code to reproduce figures are available online at `https://zenodo.org/record/3894509#.XuysMZZS-V4`. The R package `fishflux`, containing the model can be installed through GitHub: `https://github.com/nschiett/fishflux`.

2.7 Supplementary methods

Here, we provide more information on the quantification of the experimental excretion rates used for model validation in the main text and the parameters needed to run the model.

2.7.1 Fish excretion

We measured excretion estimates in situ following the methodologies of Schaus *et al.* (1997), as modified by Whiles *et al.* (2011). We placed individual fish in an incubation chamber (0.47 – 75 L Ziploc bag) containing a known volume (0.08 to 19.5 L) of pre-filtered seawater ($0.7\mu m$ pore size Gelman GFF) for 30 minutes (Whiles *et al.* 2011; Allgeier *et al.* 2015). We incubated a set of controls (typically n = 6) for the same time period at each sampling event. All incubated fishes and controls were kept at a constant temperature during the excretion trial (25 – 27.5°C). We extracted seawater samples from each bag (filtered with $0.45\mu m$ pore size Whatman nylon membrane filters) and immediately placed them on ice. We analysed samples for ammonium and phosphorous.

Seawater samples extracted from each incubation container (filtered with $0.45\mu m$ pore size Whatman nylon membrane filters) and placed immediately on ice. Within 12 hours, samples were analysed for ammonium using the methodologies of Taylor *et al.* (2007), or frozen for transport to University of California Santa Barbara (UCSB) for soluble reactive phosphorus analyses using the ascorbic acid method and colorimetric analyses (Eaton *et al.* 1995). Excretion rates were converted to g d^{-1} by multiplying hourly estimates by 24.

2.7.2 Turnover rates of N and P

Following equations 6 and 7, we measured F_{N} and F_{P} as minimal excretion rates for N and P. Fish (n = 27) were collected by divers in Moorea in 2018 and placed in a holding tank (1,000 L) with flow-through seawater for 72 hours with no food. Following the starvation period, individuals were placed in incubation containers and nutrient samples were taken using the same methodology as for excretion rates. Water samples were frozen immediately after filtration and analysed in Moorea at CRIOBE using standard methods following Aminot & Kérouel (2007). Here we assume turnover

to be equal to the measured excretion rates of starved fish. As expected, $F_{0\mathrm{Pz}} < F_{0\mathrm{Nz}}$ because bone cells, which contain most P, generally degrade slowly compared to other cell types ()$F_{\mathrm{P}} \approx 0.0003$ g P d^{-1}, 10% per year; Manolagas (2000); Sterner & Elser (2002)). There were no significant differences in minimal excretion rates among the three species, so average across-species values were used.

2.7.3 Metabolism

We used flow-through respirometry to measure standard metabolic rate (SMR) and maximum metabolic rate (MMR), which is defined as the maximum rate of oxygen consumption that a fish can achieve at a given temperature (Norin & Clark 2016) for a wide range of body sizes (see 3.2). Here SMR is considered a synonym of $F_{\mathrm{C}r}$. The parameters α, f_0 and θ were obtained by fitting a Bayesian regression model of SMR and MMR (g C d^{-1}) as a function of body mass (g) using the R package `brms` (see 3.3, Burkner PC 2017). Estimates for the cost of growth, ϕ, were obtained using the model of Barneche & Allen (2018) (equation 5, main text), and values for trophic level and aspect ratio were extracted from FishBase using `fishflux` functions `trophic_level()` and `aspect_ratio()`, respectively.

Fish capture

Fish were caught by divers using nets and clove oil in the lagoon at 1–8 m depth near Opunohu Bay in Moorea, French Polynesia during fall 2018. After capture, fish were transported to the lab and were starved for 24 to 48 h at 27–28°C in large tanks.

Respirometry

Oxygen consumption was measured using intermittent-flow respirometry combined with pyroscience optic fibre, following the methods described by Svendsen *et al.*

(2016). Intermittent-flow respirometry combines short measurement periods in a recirculating, but closed, respirometer with clean water flush periods (Svendsen *et al.* 2016). One complete measurement cycle consists of three timing periods: the flush period where the chamber is open followed by two closed periods, wait and measure. The wait period is required before measuring oxygen consumption to allow all the water in the chamber to mix and the oxygen content to decline linearly (Svendsen *et al.* 2016). The respirometer volume should be chosen depending on the fish's volume and behaviour while still being small enough to result in a readable decline in oxygen concentration. A respirometer:organism volume ratio between 20 and 50 appears to be comfortable for most organisms but is small enough to result in a 10% drop in oxygen concentration (Svendsen *et al.* 2016). Three different volumes of chambers (0.36 L, 0.97270 L and 4.4 L) were used to have a chamber volume-to-fish volume ratio of 61:1–9:1 for *Epinephelus merra*, 358:1–10:1 for *Zebrasoma scopa*, and 241:1–10:1 for *Balistapus undulatus*. When the ratio was too high or too low, the closing time (respirometry cycle) of the chamber was adapted to obtain accurate MO_2 measurements. Respirometry cycles were processed during a 20 h period (12 p.m. to 8 a.m. the following day) while leaving the fish undisturbed in the chamber. For each measurement and each chamber size, a blank chamber was used simultaneously, and a post blank measurement was processed for each chamber at the end of the run to account for microbial respiration. Temperature was kept constant to 28.20 ± 0.35°C, and a light cycle of 12 h was used (6 a.m. to 6 p.m.). SMR was calculated using MO_2 measurement during the entire period. Noisy measurements were removed by checking the R^2 of the drop in oxygen. Then, SMR was defined, using the average of the lowest 10% of the MO_2 values, after removal of the outliers, following recommendations by Chabot *et al.* (2016). At the start of a respirometry run, all fish where chased for 1 min and immediately placed in the chamber to estimate maximum metabolic rates (MMR) by recording the first 30 s of the first respirometry cycle. This seems to be the most efficient way to get the MMR for a wide range of species (Norin & Clark 2016).

Metabolic parameters

To obtain parameters $f0$ and α, we fit linear regression models for each species with the log-transformed SMR (g/day) as the response variable and the log-transformed biomass (g) as the explanatory variable. Models were fit in a Bayesian framework using the R package RStan (Stan Development Team 2018). The body mass-independent metabolic normalisation constant (g C $g^{-\alpha}$ d^{-1}), $f0$ (see eqn 4 in the main text), was obtained by exponentiating the intercept of this log-log regression. The slope of the regression equals α, the a dimensionless mass-scaling exponent in eqn 4. We used weakly informative priors. We assumed the activity scope, θ to equal $(SMR + MMR)/2SMR$. A second linear model was applied, similar to the above mentioned model, but with the log-transformed MMR as the response variable. The slope of each species of this regression did not differ from the slope of the SMR regressions, as their respective 95% credible intervals overlapped substantially. Thus, our data suggests that the intra-specific ratio of mass scaling exponents (SMR and MMR) is 1 on average. Therefore, for each species, we averaged values of θ across all individuals to calculate an overall θ.

2.7.4 Growth

We used otoliths to fit growth curves for each species. Individuals were collected in Moorea, French Polynesia with the use of spearguns, and otoliths were extracted, processed and read for annual growth increments (see 4.1, 4.2). `fishflux` provides the function `oto_growth()` to estimate VBGC parameters from otolith readings, using a Bayesian hierarchical regression model (see 4.3). If original otolith readings are unavailable, VBGC parameters l_∞, k and t_0 can be retrieved from FishBase for many species. The `fishflux` function `growth_params()` returns estimates that are available on FishBase. We note that parameter estimates from otolith analysis are considered better than other methods, and parameters can vary with location due to temperature differences, thus introducing potential biases (Barneche & Allen

2018; Morais & Bellwood 2018). We suggest using the standardised estimates and standard deviations following the fish growth model of Morais & Bellwood (2018) when location-specific otolith data is unavailable.

We convert mass from total length using the length-weight equation $m = \epsilon l^b$, where ϵ (g cm^{-b}) is constant, and b is a dimensionless exponent. Their respective standard deviations were retrieved from FishBase and estimated using a Bayesian model (Froese *et al.* 2014). `fishflux` provides the function `find_lw()` to obtain means and standard deviations of these parameters. Wet-to-dry mass conversion constants were measured from the same specimens that were used for the nutrient content analysis (see 5. Elemental stoichiometry).

Sample collection

A total of 288 specimens belonging to 20 species were collected in March 2016 and November 2018 in Moorea, French Polynesia using spear guns. Total (TL) and standard length (SL) were measured to the nearest millimetre. For each individual, pairs of sagittae were extracted, cleaned with distilled water, dried and transported to Perpignan, France.

Otolith processing and back-calculation

For each species, one or both of the otoliths was cut transversely, using a diamond disc saw (Presi Mecatome T210) to obtain a section of 500 μm. Sections were then fixed on a glass slide with thermoplastic glue, sanded with abrasive discs of decreasing grain size (2 400 and 1 200 grains per 2 cm) to get closer to the nucleus and polished using a 0.25μm diameter diamond suspension. All sections were photographed under Leica DM750 light microscope with a Leica ICC50 HD microscope camera and LAS software (Leica Microsystems). For each species, a reading transect was chosen and distances across annual growth increments were measured using ImageJ (version 1.51j8). This

procedure was repeated twice by two readers in order to limit observer bias on age estimates. The measurements realised by the different readers were averaged for each section. To estimate the fish lengths for previous ages, the back-calculation procedure, proposed by Vigliola & Meekan (2009) was used.

Growth parameters

The von Bertalanffy growth curve (VBGC) was selected to describe the fish growth [eqn 2 in the main text; Bertalanffy (1957)]. The VBGC was fitted on length-at-age data with a hierarchical non-linear regression in a Bayesian framework using stan (Carpenter *et al.* 2017) and (RCore Team 2018). In the model, l_∞ varies among individuals, unlike $t0$. It has been shown that VBGC parameters l_∞ and κ are correlated in a consistent way, where the slope of the log-transformed regression theoretically has an average of -2.31 (Morais & Bellwood 2018). This correlation is explicitly included in the regression model where $\kappa = exp(sl * log(l_\infty) + gp)$, where sl is the slope and gp is the intercept, which is the growth performance index (Morais & Bellwood 2018). Informative priors for sl and gp were specified, using published information (Morais & Bellwood 2018) and a weakly-informative prior was set for l_∞:

$$\begin{aligned} sl &\sim normal(-2.3, 0.22), \\ gp &\sim normal(3, 2), \\ l_\infty &\sim normal(15, 5). \end{aligned} \tag{2.17}$$

Estimates for l_∞ can vary substantially among populations or even individuals (Morais & Bellwood 2018). We standardised κ to the maximum measured total length in Moorea (unpublished data), to avoid individuals reaching the asymptotic length prematurely and growth equalling zero in the application of the bioenergetic model for the case study.

2.7.5 Elemental stoichiometry of fish and diet

Sixteen individuals were collected in 2016 in Moorea, their gut contents were removed, and the whole body was freeze-dried and ground to powder with a Precellys homogeniser. Q_{k} (%) were then measured in the lab using standard methods. Ground samples were analysed for %C and %N content using a CHN Carlo-Erba elemental analyzer (NA1500) for %P using dry oxidation-acid hydrolysis extraction followed by a colorimetric analysis (Allen *et al.* 1974). Elemental content was calculated based on dry mass. Means and standard deviations for C, N and P were obtained through a hierarchical multivariate model with fixed effects per family, genus and species. C, N and P content of diet items were analysed using the same methods as described above.

Values for D_{k} (%) were approximated from published estimates. *Zebrasoma scopas* is known to feed on red algae (Choat *et al.* 2002). We adopted Q_{N} [0.68 %; Lin & Fong (2008)] and Q_{C} [20.9%; Pillans *et al.* (2004)] from *Acanthophora spicifera*, and Q_{P} [0.33%; Suzumura *et al.* (2002)] from another red algae species, *Galaxaura* sp. D_{k} values for *B. undulatus* and *E. merra* were estimated based on a collection of potential diet items of similar families (Allgeier *et al.* 2015). *B. undulatus* feeds on a wide range of plant and animal matter, but the majority of their prey items are in the phylum Arthropoda, followed by Chordata and Mollusca (Casey *et al.* 2019). Therefore, we averaged D_{k} values of molluscs, crustaceans and small fishes (n = 15). Finally, *E. merra* feeds primarily on crabs (Randall & Brock 1960). Thus, we averaged D_{k} values measured from small crabs (n = 5). Stoichiometry of diet items were analysed using similar methods as described above.

2.7.6 Assimilation efficiencies

Element-specific assimilation efficiencies, a_{k}, are needed to estimate the available proportion of matter after ingestion. These parameters were treated as fixed, with

values of 0.8, 0.8 and 0.7 for C, N and P respectively (Deslauriers *et al.* 2017).

2.7.7 R package `fishflux`

`fishflux` makes the application of our theoretical framework user-friendly with the use of the main function `cnp_model_mcmc()`. We devised our model to rely on parameters that are widely available, while accounting for uncertainties. Several parameters for `fishflux` are publicly accessible, and the package provides user-friendly functions to retrieve them. For example, growth parameters for the VBGC are available on FishBase or can be extrapolated with basic traits such as temperature and body size (Morais & Bellwood 2018). Moreover, length-weight parameters have been predicted for all species on FishBase (Froese *et al.* 2014), and metabolic parameters F_0 and α can be extracted from flow-through respirometry experiments. To calculate the energetic cost of growth, we use traits that are likewise available on FishBase (i.e., aspect ratio and trophic level, Barneche & Allen 2018). Equipped with these parameters, the most critical input data is body size, which is frequently collected at the individual level in underwater visual censuses or fisheries catch data (Samoilys & Carlos 2000). As such, our model offers a unique opportunity to infer biogeochemical dynamics from standardized and widely used survey techniques in fish ecology. Furthermore, `fishflux` provides functions to extract specific results (`extract()`), plot output (`cnp_plot()`), extract the limiting element (`limitation()`), and investigate the sensitivity of the predictions due to the uncertainty of input parameters (`sensitivity()`). For details, see the help pages and vignettes of `fishflux`, the website (`https://nschiett.github.io/fishflux/index.html`), and the reference manual (Appendix A).

2.8 Supplementary tables

Table 2.3: Overview of all input parameter values for each species and sources.

	Z. scopas	*B. undulatus*	*E. merra*	Source
Q_{C}	31.85 (4.00)	32.36 (3.83)	35.33 (3.24)	This study
Q_{N}	10.00 (1.00)	9.09 (0.71)	9.64 (0.89)	This study
Q_{P}	5.83 (1.10)	5.41 (1.24)	4.39 (0.82)	This study
D_{C}	22.60 (4.00)	21.60 (7.00)	20.00 (3.60)	Pillans et al. (2004), Allgeier et al. (2015)
D_{N}	0.77 (1.0e-02)	4.50 (1.7e+00)	4.20 (9.0e-01)	Suzumura et al. (2002), Allgeier et al. (2015)
D_{P}	0.35 (1e-02)	0.60 (3e-01)	0.60 (4e-01)	Lin et al. (2008), Allgeier et al. (2015)
a_{C}	0.80 (_)	0.80 (_)	0.80 (_)	Fish Bioenergetics 4.0
a_{N}	0.80 (_)	0.80 (_)	0.80 (_)	Fish Bioenergetics 4.0
a_{P}	0.70 (_)	0.70 (_)	0.70 (_)	Fish Bioenergetics 4.0
l_{∞}	19 (_)	26 (_)	22 (_)	This study
κ	0.69 (6e-02)	0.15 (8e-03)	0.45 (1e-03)	This study
t_0	-2.1e-02 (_)	-3.1e-01 (_)	-6.0e-02 (_)	This study
lw_a	2.5e-02 (2.7e-03)	3.5e-02 (1.2e-02)	1.1e-02 (2.7e-03)	Froese et al. (2013)
lw_b	2.98 (2.6e-02)	3.00 (7.7e-02)	3.06 (5.6e-02)	Froese et al. (2013)
m_{dw}	0.250483293190712 (_)	0.282414512324743 (_)	0.293540629343531 (_)	This study
$F_{0\mathrm{Nz}}$	3.7e-03 (4.6e-03)	3.7e-03 (4.6e-03)	3.7e-03 (4.6e-03)	This study
$F_{0\mathrm{Pz}}$	3.7e-04 (5.1e-04)	3.7e-04 (5.1e-04)	3.7e-04 (5.1e-04)	This study
f_0	4.0e-03 (4.6e-04)	2.0e-03 (6.0e-04)	1.8e-03 (3.2e-04)	This study
α	0.69 (3.0e-02)	0.81 (6.0e-02)	0.80 (4.2e-02)	This study
θ	1.83 (_)	3.15 (_)	2.80 (_)	This study
r	2.00 (_)	1.95 (_)	1.50 (_)	Fishbase
h	2.00 (_)	3.37 (_)	4.10 (_)	Fishbase

Table 2.4: Predicted ingestion rates in dry mass per mass wet weight of the fish. 95% CI are reported for biomass and ingestion rates in between brackets.

Species	TL (cm)	Biomass (g)	Ingestion rate ($g^{-1}d^{-1}$)
Z. scopas	2.00	0.2 (0.2-0.2)	259.4 (129.3-523)
Z. scopas	3.00	0.6 (0.5-0.8)	167.8 (83.3-349.2)
Z. scopas	4.00	1.5 (1.2-2)	122.2 (63.1-246.8)
Z. scopas	5.00	3 (2.2-4)	95.4 (49.2-196.5)
Z. scopas	6.00	5.1 (3.8-6.8)	78.8 (40.5-155)
Z. scopas	7.00	8 (5.9-10.9)	66.7 (34.2-129.8)
Z. scopas	8.00	12 (8.8-16.4)	56.8 (29-110.9)
Z. scopas	9.00	17.1 (12.5-23.5)	50.1 (24.7-97.6)
Z. scopas	10.00	23.2 (17-32.4)	45.1 (22.1-86.6)
Z. scopas	11.00	30.9 (22.3-42.4)	40.8 (19.3-79.1)
Z. scopas	12.00	40.4 (29.5-56.1)	37.1 (17.2-76.1)
Z. scopas	13.00	50.9 (36.9-71.1)	33.5 (14.8-71.8)
Z. scopas	14.00	63.4 (44.6-89.7)	30.9 (13.2-70.6)
Z. scopas	15.00	78.2 (55.9-108.6)	28.2 (11.7-68.4)
Z. scopas	16.00	95.1 (67.6-135.5)	26.4 (11-65.1)
Z. scopas	17.00	113.6 (80.1-159.2)	24.7 (9.3-63.4)
Z. scopas	18.00	134.2 (93.8-191.6)	24.1 (8.4-65.3)
Z. scopas	19.00	156.9 (111.8-226.7)	22.3 (7.3-64)
Z. scopas	20.00	183.8 (129.2-258.9)	21.1 (6.8-57.6)
Z. scopas	21.00	211.2 (148.2-298.3)	21 (6-60.1)
Z. scopas	22.00	245.9 (170.8-347.6)	19.8 (5.3-58.8)
Z. scopas	23.00	278.3 (197.1-403.4)	18.1 (4.9-58.7)
Z. scopas	24.00	317.9 (221.6-457.2)	18.5 (4.3-57.3)
Z. scopas	25.00	356.9 (252.2-518.9)	17.8 (4.2-56.5)
B. undulatus	2.00	0.3 (0.1-0.6)	74.9 (30.3-196.5)
B. undulatus	3.00	0.9 (0.4-2.1)	48.3 (19.2-135.5)

B. undulatus	4.00	2.1 (0.9-5.1)	36.4 (14.2-104.6)
B. undulatus	5.00	4.2 (1.8-10.3)	28.9 (10.4-84.5)
B. undulatus	6.00	7.1 (2.8-17.8)	24.3 (8.4-77.1)
B. undulatus	7.00	11.5 (4.5-29.1)	21.3 (7.5-64.3)
B. undulatus	8.00	17.2 (6.5-45.1)	19 (6.8-65.9)
B. undulatus	9.00	24.9 (9.5-63.6)	17.6 (5.8-61.7)
B. undulatus	10.00	34.3 (12.1-91)	15.5 (5.2-58.1)
B. undulatus	11.00	44.2 (16.7-120.5)	15.5 (4.8-63.1)
B. undulatus	12.00	58.3 (22-157.8)	14.9 (4.8-56.1)
B. undulatus	13.00	72.2 (26.3-202.3)	14 (4.2-60.6)
B. undulatus	14.00	91.7 (33.5-254.7)	13.6 (4.1-61.4)
B. undulatus	15.00	112.4 (41.4-319.3)	12.9 (3.7-56.7)
B. undulatus	16.00	138.7 (47.9-409.7)	12.7 (3.4-59.2)
B. undulatus	17.00	165.4 (56.4-476.2)	12.6 (3.6-60.9)
B. undulatus	18.00	194.1 (66.8-557.5)	12.1 (3.3-58.1)
B. undulatus	19.00	230.6 (79.5-669.9)	12.3 (3.2-59.1)
B. undulatus	20.00	270.3 (91.3-860.1)	11.7 (3.1-59)
B. undulatus	21.00	309.3 (105.3-949.9)	11.8 (2.9-59.7)
B. undulatus	22.00	360.6 (126.6-1042.7)	11.4 (3-59.3)
B. undulatus	23.00	400.2 (137.2-1231)	11.7 (2.8-62.1)
B. undulatus	24.00	477.9 (162.7-1456.8)	11.3 (2.8-57.8)
B. undulatus	25.00	518.2 (174.4-1685.3)	11.3 (2.8-62.3)
E. merra	2.00	0.1 (0.1-0.2)	43.5 (11.2-294.9)
E. merra	3.00	0.3 (0.2-0.5)	30.8 (9.9-188.2)
E. merra	4.00	0.7 (0.4-1.4)	25.8 (8.2-139.2)
E. merra	5.00	1.5 (0.8-2.9)	22.5 (8-109.7)
E. merra	6.00	2.5 (1.3-4.9)	19.7 (7.4-92.9)
E. merra	7.00	4.1 (2.1-7.9)	18.5 (7-76.3)
E. merra	8.00	6.1 (3.1-12.3)	16.9 (6.9-58.7)
E. merra	9.00	8.7 (4.3-17.6)	16.9 (6.4-55.7)

E. merra	10.00	12.1 (5.9-24.3)	15.6 (6.1-48.5)
E. merra	11.00	16.3 (7.9-33.7)	15.4 (6-46.7)
E. merra	12.00	21.6 (10.2-44)	14.6 (5.7-42.7)
E. merra	13.00	27.3 (13.4-57)	14.5 (5.7-42.6)
E. merra	14.00	33.9 (16.4-70.8)	14 (5.7-42.6)
E. merra	15.00	42.4 (19.9-89)	14.1 (5.5-40.1)
E. merra	16.00	51.4 (23.5-111.8)	13.7 (5.2-37.9)
E. merra	17.00	61.7 (29.1-129.5)	13.4 (5.3-38.2)
E. merra	18.00	74 (33.7-161.5)	13.4 (5.2-38.6)
E. merra	19.00	86.5 (40.4-190.8)	13.3 (5.5-37.7)
E. merra	20.00	100.2 (47-231.1)	13.3 (5.1-37.6)
E. merra	21.00	119.2 (53.3-257.1)	12.8 (4.7-35.8)
E. merra	22.00	137.9 (60.2-304.8)	12.8 (4.6-37.5)
E. merra	23.00	156 (72.1-359.6)	13 (4.7-35.8)
E. merra	24.00	179.6 (80.5-396.9)	12.8 (4.6-35.9)
E. merra	25.00	200.9 (89.5-454)	13.1 (4.8-35.8)

Part II: From individual to community

The next step in understanding ecosystem functions mediated by fishes is to scale up individual processes to the community level. I aimed to quantify five key ecosystem functions - biomass production, nitrogen excretion, phosphorus excretion, herbivory and piscivory - by applying the theoretical framework described in chapter 2 to all individuals in global coral reef fish communities. Applying the model to a wide range of fishes required preparatory steps described in methodological chapters 3 and 4.

Functions related to consumption, and nitrogen and phosphorus cycling are highly dependent on the diet of fishes, which is often unknown for coral reef fishes. Moreover, experts tend to disagree on the assignment of trophic guilds. Therefore, the first step towards applying bioenergetic models to a variety of fishes was to find a reproducible and quantitative method to assign trophic guilds to global coral reef fishes. Chapter 3 presents a classification of trophic guilds through network analysis based on data from community-wide gut content analyses of tropical coral reef fishes worldwide. Specifically, I developed a method to extrapolate trophic guilds to a global species list based on phylogeny and body size.

Further, the model framework presented in chapter 2 requires a large number of parameters, that depend on species characteristics and sometimes temperature. To assemble a database of parameters for global reef fish species, I integrated literature

data, novel data collections, and Bayesian models, described in chapter 4. One of the impactful parameters is the growth rate coefficient. I developed an R package called `fishgrowbot` to fit growth models and extract growth parameters from otolith data (appendix B).

Finally, I applied bioenergetic models to a global reef fish community database (chapter 5) to (1) quantify community-level reef fish functions and their trade-offs, (2) extract the community- and species-level effects on these functions, and (3) gauge the vulnerability of reef fish functioning in the Anthropocene.

Chapter 3

Delineating reef fish trophic guilds with global gut content data synthesis and phylogeny

This chapter is published in *Plos Biology*, and was led by Valeriano Parravicini and Jordan M. Casey. My role in the project was to fit Bayesian phylogenetic models, and extrapolate trophic guilds to a global reef fish database.

Authors: Valeriano Parravicini, Jordan M. Casey, Nina M. D. Schiettekatte, Simon J. Brandl, Chloé Pozas-Schacre, Jérémy Carlot, Graham J. Edgar, Nicholas A. J. Graham, Mireille Harmelin-Vivien, Michel Kulbicki, Giovanni Strona & Rick D. Stuart-Smith

Citation: Parravicini V*, Casey JM*, Schiettekatte NMD, Brandl SJ, Pozas-Schacre C, et al. (2020) Delineating reef fish trophic guilds with global gut content data synthesis and phylogeny. PLOS Biology 18(12): e3000702. https://doi.org/10.1371/journal.pbio.3000702

3.1 Abstract

Understanding species' roles in food webs requires an accurate assessment of their trophic niche. However, it is challenging to delineate potential trophic interactions across an ecosystem, and a paucity of empirical information often leads to inconsistent definitions of trophic guilds based on expert opinion, especially when applied to hyperdiverse ecosystems. Using coral reef fishes as a model group, we show that experts disagree on the assignment of broad trophic guilds for more than 20% of species, which hampers comparability across studies. Here, we propose a quantitative, unbiased, and reproducible approach to define trophic guilds and apply recent advances in machine learning to predict probabilities of pairwise trophic interactions with high accuracy. We synthesize data from community-wide gut content analyses of tropical coral reef fishes worldwide, resulting in diet information from 13,961 individuals belonging to 615 reef fish. We then use network analysis to identify 8 trophic guilds and Bayesian phylogenetic modeling to show that trophic guilds can be predicted based on phylogeny and maximum body size. Finally, we use machine learning to test whether pairwise trophic interactions can be predicted with accuracy. Our models achieved a misclassification error of less than 5%, indicating that our approach results in a quantitative and reproducible trophic categorization scheme, as well as high-resolution probabilities of trophic interactions. By applying our framework to the most diverse vertebrate consumer group, we show that it can be applied to other organismal groups to advance reproducibility in trait-based ecology. Our work thus provides a viable approach to account for the complexity of predator–prey interactions in highly diverse ecosystems.

3.2 Introduction

A fundamental goal in ecology is to understand the mechanisms behind the maintenance of biodiversity and ecosystem functioning (Reiss *et al.* 2009; Tilman *et al.* 2014). Understanding the ecological niches of species and their role in ecosystems is central to this endeavor (Whittaker *et al.* 1973; Finke & Snyder 2008). In fact, the degree of niche overlap among species can be a major determinant of relationships among species richness (Levine & HilleRisLambers 2009), ecosystem productivity (Loreau *et al.* 2001; Poisot *et al.* 2013; Terborgh 2015), and vulnerability (Mouillot *et al.* 2013) since limited functional redundancy can make ecosystems more prone to lose entire energetic pathways (Rosenfeld 2002; Wohl *et al.* 2004; Brandl & Bellwood 2014). With growing threats to flora and fauna worldwide, the need to quantify the impact of biodiversity loss has amplified the use of functional groups, which group species (and life history stages) that share common ecological characteristics and are often defined by coarse, categorical descriptors of species traits (McGill *et al.* 2006; Kraft *et al.* 2008; Belmaker *et al.* 2013).

Natural systems are inherently complex, with almost innumerable, non-random linkages across an intricate network of ecological interactions (De Deyn *et al.* 2008). Accounting for such complexity is critical to define energetic pathways and, ultimately, ecosystem functioning (Jordano 2016). However, our understanding of even basic predator–prey interactions is limited for many ecosystems, and expert opinion does not adequately fill this knowledge gap (Gravel *et al.* 2013). To overcome this limitation, scientists have developed methods to infer the probability of ecological interactions based on species' evolutionary history and ecological traits (Dalla Riva & Stouffer 2016; Sander *et al.* 2017; Laigle *et al.* 2018; Pichler *et al.* 2020). However, predicting trophic interactions across the entire spectrum of potential predator–prey interactions often remains unresolved in hyperdiverse ecosystems. In these cases, categorical traits are frequently used as proxy of both ecosystem functioning and trophic structure (Flynn *et al.* 2011).

Delineating the ecological niche with discrete categories has several operational advantages. First, grouping species into categories helps decompose highly complex ecosystems into comprehensible units, while traditional taxonomic analyses may be difficult to interpret. Second, ecological predictions tied to species are restricted to the geographic range of the species, whereas predictions of functional groups can be globally comparable. Third, the use of functional groups enables the quantification of functional metrics (e.g., functional richness and functional redundancy) from a standard community data matrix without complex manipulative experiments (Belmaker *et al.* 2013; Schmera *et al.* 2015; Brandl 2019). The promise of "user-friendly" metrics for functional ecology has encouraged the employment of trait-based data in community ecology; even with a paucity of empirical information, it is often assumed that experts can achieve accurate descriptions of the ecological niche of species (Aubin *et al.* 2013; Schmera *et al.* 2015; Nash *et al.* 2017).

Coral reefs, one of the most diverse ecosystems on Earth, have inspired a plethora of studies that assess ecosystem functioning. However, only few studies have attempted to categorize fluxes on a continuous gradient across an entire food web (Gilarranz *et al.* 2016), and most studies use expert opinion to define simple functional groups. Indeed, recent efforts have compiled trait-based datasets for 2 major components of this ecosystem: corals and fishes (Stuart-Smith *et al.* 2013; Madin *et al.* 2016). For some traits, such as maximum body size in fishes, the compilation process is simple and accurate because unidimensional, quantitative data (e.g., maximum total length) are compiled in publicly accessible databases; however, when it comes to species' diet or behavior, obtaining consensual data is much more difficult. For example, dietary data are multidimensional (i.e., various prey items can be recorded across individuals), influenced by ontogenetic and spatio-temporal variables (i.e., life history, time, and location can incur dietary shifts), and prone to methodological differences and thus observer bias. Therefore, while some exceptions exist (Bascompte *et al.* 2005; Gilarranz *et al.* 2016), our capacity to define coral reef trophic interactions still largely depends on discrete trophic categories defined by expert opinion (Brandl

et al. 2019a).

Although experts sometimes agree on relevant traits to define trophic categories, there is often an implicit disagreement. Across the coral reef literature, the number and resolution of reef fish trophic guilds substantially differs. Studies commonly define 3 (McClanahan 1995) to 8 (Ferreira *et al.* 2004) trophic guilds, with particular ambivalence on the resolution at which to define herbivores and invertivores (Micheli *et al.* 2014; Mouillot *et al.* 2014; Parravicini *et al.* 2014; Stuart-Smith *et al.* 2018). Among all trait classification schemes for reef fishes, only a few are openly accessible (e.g., Stuart-Smith *et al.* (2018), Bejarano *et al.* (2019)). Consequently, different research groups tend to employ proprietary classifications, with little possibility to cross-check and compare assigned traits. The classification of species into functional groups has advantages for our understanding of ecological patterns (Mason & Bello 2013; Mouillot *et al.* 2013). However, the lack of agreement and the limited transparency of trait-based datasets can conjure skepticism and inhibit the emergence of general patterns.

Here, we quantify expert agreement in the definition of coral reef fish trophic guilds and propose a novel, quantitative framework to delineate trophic guilds. Moreover, we test whether machine learning allows us to go beyond the definition of discrete categories, accurately predicting individual trophic interactions in hyperdiverse ecosystems. We compiled all quantitative, community-wide dietary analyses from several locations across the Indo-Pacific and the Caribbean. Then, we used network analysis to quantitatively define modules that correspond to trophic guilds and machine learning to infer pairwise trophic interactions. We then examined phylogenetic niche conservatism between species to predict trophic guilds and probabilities of pairwise trophic interactions for the global pool of coral reef fishes. Our framework is fully reproducible and can be extended and updated as new data become available.

3.3 Materials and methods

3.3.1 Assessment of expert agreement

We systematically searched Google Scholar, including papers since 2000, using the following keywords: "coral reefs" AND "reef fish" AND ("fish community" OR "fish assemblage") AND "diet" AND ("functional group" OR "functional trait" OR "functional entity" OR "trophic guild" OR "trophic group"). The search yielded 856 papers, which were individually assessed. We only kept studies performed at the community level that targeted all trophic levels. Most studies were excluded because they only included specific families or groups, or the data were not provided with the publication. When the data were not provided with the publications, we contacted authors with trophic classifications used widely used across the literature. We often found redundant results, with groups publishing several papers using the same classification scheme. In those cases, only the most recent reference was retained. Of the 856 papers, 163 papers were inaccessible (i.e., non-English language and/or data inaccessibility despite contacting the first author). Thus, 182 studies met the criteria of our initial assessment, which ultimately yielded 33 papers with independent trophic classifications (see 3.6 table S1).

The classifications were not uniform in terms of the number and nature of trophic guilds. In order to compare trophic guilds across publications, we first standardized the schemes by converting the original trophic categories into 5 broad trophic guilds: "herbivores and detritivores," "invertivores," "omnivores," "planktivores," and "piscivores." All classification schemes could be attributed to these categories with the exception of 8 papers that did not include either "omnivores" or "piscivores" as a category. In these cases, the comparison was only made across the 4 comparable guilds.

In order to assess expert agreement, we compared each possible pair of classifications that shared at least 50 species, generated a confusion matrix (also known as an

error matrix; (Stehman 1997)), and measured agreement as the proportion of species with matching trophic guild assignments. We then calculated the average agreement between classification pairs for each trophic guild. Simplifying categories into 5 comparable, broad trophic guilds therefore reduced the number of trophic categories and naturally inflated agreement among authors; thus, our estimates of author agreement are conservative.

3.3.2 Data collection on fish gut contents

To provide a quantitative definition of trophic guilds for reef fishes, we collected gut content data across the literature at the individual or species level for Elasmobranchii (i.e., cartilaginous fishes) and Actinopterygii (i.e., ray-finned fishes). We obtained dietary information from 5 published works: Hiatt and Strasburg (1960) for the Marshall Islands (Hiatt & Strasburg 1960), Randall (1967) for Puerto Rico and the Virgin Islands (Randall & Brock 1960), Hobson (1974) for Hawaii (Hobson 1974), Harmelin-Vivien (1979) for Madagascar (Harmelin-Vivien 1979), and Sano and colleagues (1984) for Okinawa (Sano *et al.* 1984). In addition, we provide hitherto unpublished data on the gut contents of 3,015 individuals of 111 species collected in New Caledonia from 1984 to 2000.

All dietary information was based on visual gut content analysis that reported prey ingestion as a volumetric percentage or frequency. The data were standardized and analyzed as proportions. To our knowledge, the compiled dataset represents the first detailed synthesis of community-wide visual gut content analyses to infer the structure of coral reef food webs across ocean basins. A total of 13,961 non-empty fish guts belonging to 615 species were analyzed, and more than 1,200 different prey items were described across the original datasets.

First, fish species and family names were taxonomically verified and corrected with the R package rfishbase (Boettiger *et al.* 2012). Only species with at least 10 non-

empty guts were kept for further analysis. The taxonomic classification of each prey item was then obtained, and all non-informative and redundant items were discarded (e.g., unidentified fragments; "crustacea fragments" when co-occurring with an item already identified to a lower taxonomic level such as "shrimp"). Prey identification was highly heterogeneous across the 6 datasets, differing in taxonomic level and the use of common or scientific names (e.g., crabs versus Brachyura). In order to make the 6 datasets comparable, prey items were grouped into 38 ecologically informative prey groups (see 3.6 table S2). Items were generally assigned to groups corresponding to their phylum or class. Due to the high diversity and detailed descriptions of crustaceans, they were assigned to the level of order or superorder. Most groups follow official taxonomic classifications except for "detritus," "inorganic," and "zooplankton." In the West Indies dataset (Randall & Brock 1960), items labelled as "Algae & Detritus" were assigned to both of the categories "detritus" and "benthic autotroph," and the percentage was equally divided in 2. The category "zooplankton" includes all eggs and larvae regardless of taxonomy.

3.3.3 Definition of trophic guilds with network analysis

Of the 615 species with dietary information, 516 were present in only 1 location, 66 were collected in 2 locations, 25 in 3 locations, 7 in 4 locations, and only 1 across 5 locations. We tested whether there was a strong dietary difference in species present in more than 1 location by creating a quantitative bipartite network (Barrat *et al.* 2004) where fish species at each location were linked to the 38 prey groups. This network was weighted so that edge weights represent the proportional contribution of each prey group to the diet of a species at a given location.

In order to identify network modules that correspond to reef fish trophic guilds and their ingested prey, we used the maximization of the weighted network modularity based on weighted bipartite networks (Beckett 2016). Due to the high occurrence of accidental predation in reef fishes, we used weighted networks to define modules so

that rare or accidental prey would not drive the definition of trophic guilds.

Since the modularity maximization algorithm has an initial random step, it may converge to different (although similar) suboptimal solutions each time the analysis is performed, which is common across several optimization algorithms, such as simulated annealing (Serafini 1994). To guarantee reproducibility and reduce the risk of basing our analysis on an outlier, we performed the modularity maximization 500 times and retained the medoid solution, which was identified as the solution with the highest similarity to the other 499 modules. Similarity between classifications was assessed as the variation of information, which is an accepted metric to compare multiple clustering results (Meilă 2007). Overall, 68% of the species found in more than 1 location belonged to the same module. Therefore, we considered the regional effect to be minor and performed the analysis on the global network, ignoring regional variability and increasing the number of individuals per species.

3.3.4 Phylogenetic conservatism of trophic guilds

We extracted the phylogenetic position of the 615 species used for the definition of trophic guilds through the Fish Tree of Life (Rabosky *et al.* 2018). A total of 603 out of 615 species were available in the Fish Tree of Life, but only 535 species had verified phylogenetic information. For the taxa available in the Fish Tree of Life without verified phylogenetic information, we retrieved the pseudo-posterior distribution of 100 synthetic stochastically resolved phylogenies where missing taxa were placed according to taxonomy using the function `fishtree_complete_phylogeny()` in the R package fishtree (Chang *et al.* 2019).

We quantified the phylogenetic conservatism of trophic guilds by calculating the phylogenetic statistic δ, which uses a Bayesian approach for discrete variables (Yu *et al.* 2017). The δ statistic can be arbitrarily large with a high level of variation, depending on the number of species and trait levels. To evaluate the significance of

the δ statistic, we applied a bootstrapping approach where we quantified δ 100 times after randomly shuffling the trait values.

We then fitted a multinomial phylogenetic regression to predict fish trophic guild according to phylogeny and body size with the R package brms (Burkner PC 2017). We used a multinomial logit link function. As such, the probability of a particular trophic guild (k) for species (phy) is computed as follows:

$$Pr(k|mu_{phy,1}, mu_{phy,2}, ..., mu_{phy,8}) = \frac{mu_{phy,k}}{\sum_{i=1}^{8} exp(mu_{phy,i})},$$

with $mu_{phy,k}$ defined as

$$mu_{phy,1} = 0, mu_{phy,k|2:8} = \beta_{0k} + \beta_{1k} log(sizemax) + \gamma_{0phy,k},$$

where β_{0k} is the category-specific fixed-effect intercept, β_{1k} is the slope for the natural transformed maximum body size for each category k, and $\gamma_{0phy,k}$ is the random effect coefficient that account for intercept variation based on relatedness as described by the phylogeny for each species phy diet category k. We used uninformative priors and ran the model for 3 chains, each with 6,000 iterations and a warm-up of 1,000 iterations. We visualized the fitted probabilities for each trophic guild with a phylogenetic tree, including the 535 species with verified phylogenetic positions using the R package ggtree (Yu *et al.* 2017). Next, we used our model to predict the most likely trophic guild for the global pool of reef fish species. For the extrapolation, we selected all species within reef fish families with more than 1 representative species (but we also included Zanclus cornutus, which is the only species in the family Zanclidae), which resulted in 50 families. Further, we only selected species with a maximum length greater than 3 cm, which was the maximum size of the smallest fish in our compiled database. This selection process resulted in a list of 4,554 reef fish species.

Currently, no streamlined method exists to predict traits for new species from a phylogenetic regression model. We circumvented this issue by extracting draws of the

phylogenetic effect (γ_{0phyxk}) for each species included in the model. We subsequently predicted the phylogenetic effects for missing species with the help of the function `phyEstimate` from the R package `picante` (Kembel *et al.* 2010). This function uses phylogenetic ancestral state estimation to infer trait values for new species on a phylogenetic tree by re-rooting the tree to the parent edge to predict the node (Garland & Ives 2000). We repeated this inference across 2,000 draws. Per draw, we randomly sampled 1 of the 100 trees. Then, we predicted the probability of each species to be assigned to each diet category by combining the predicted phylogenetic effects with the global intercept and slopes for maximum body size for each draw. Finally, we summarized all diet category probabilities per species by taking the mean and standard deviation across all 2,000 draws.

We quantified the total standard deviation (i.e., the square root of the quadratic sum of the standard deviations in each category) and the negentropy value, a measure of certainty calculated by subtracting 1 from the entropy value (i.e., uncertainty). Thus, the negentropy value lies between 0 and 1, and the higher the value, the higher the certainty for trophic guild assignment (i.e., if a given species has a high probability of assignment to a dietary category, the negentropy value will be high).

Finally, we conducted a cross validation to validate our extrapolation of trophic guilds to the global pool of fish species. Specifically, we repeated the extrapolation approach (as described above) 535 times, each time leaving out 1 species and predicting the trophic guild of that species. We then compared this prediction to the original assigned trophic guild and calculated the accuracy of each of the 8 trophic guild predictions.

3.3.5 Prediction of trophic interactions with machine learning

To complement the assignment of discrete trophic guilds, we also modeled pairwise trophic interactions. In accordance with previous studies that infer trophic interactions by matching species traits or phylogenetic position (Gravel *et al.* 2013; Guénard *et al.* 2013; Morales-Castilla *et al.* 2015; Laigle *et al.* 2018), we predicted the probability of pairwise trophic interactions between the 535 reef fish species and the 38 prey categories in our dataset. Building on Laigle and colleagues (Laigle *et al.* 2018), we developed a new machine learning approach to extract the reef fish phylogenetic tree from the Fish Tree of Life (Rabosky *et al.* 2018) and obtain phylogenetic eigenvector maps for each species, which were used as explanatory variables in our models (Guénard *et al.* 2013). We then predicted the probability of trophic interactions between fish species and prey categories based on phylogenetic position and maximum body size. Specifically, using the R package `h2o` (LeDell *et al.* 2020), we employed an ensemble modeling approach based on 3 models calibrated with 10-fold cross validation: extreme gradient boosting (Chen & Guestrin 2016), boosted regression trees (Elith *et al.* 2008), and random forest (Breiman 2001). A cross-validated general linear model was used as a super-learner to create an optimal weighted average (i.e., an ensemble) of the predictions from the 3 models. The 3 models were implemented using 2,000 regression trees and default settings to reduce overfitting. Model performance was assessed using the area under the receiver operating characteristic curve (AUC) and true skills statistics (TSS) (Allouche *et al.* 2006).

In addition to applying this analysis to our dataset, we also tested whether this technique could reliably predict pairwise trophic interactions for new species and locations. To this aim, we calibrated the models with only 5 locations, excluding the dataset from New Caledonia. We then used the New Caledonia dataset to assess model performance. As detailed above, after cross validation, we used our model to predict probabilities of pairwise trophic interactions between the 4,554 reef fish

species and the 38 prey categories.

3.4 Results

3.4.1 Assessment of expert agreement

We evaluated expert agreement among 33 distinct and independent trophic guild classifications by comparing the classification schemes in pairs. Considering the broadness of the expert-assigned categories, we found low agreement. The median agreement between pairs, expressed as the proportion of species with matching trophic group assignments, was 78% (figure 3.1). For approximately 50% of the pairwise comparisons, at least a quarter of the species were attributed to different trophic groups. In the most severe disagreement, the proportion of mismatched assignments reached 38%. In addition, expert agreement differed depending on the trophic group. Expert disagreement on the classification of "herbivores and detritivores" was low, with an average expert agreement of 95% and pairs of expert disagreement only reaching 20% (figure 3.1 B). In contrast, "omnivores" showed the highest mismatch, with experts agreeing on an average of only 70% of the species and peaks of disagreement between expert pairs reaching 47% (figure 3.1 B).

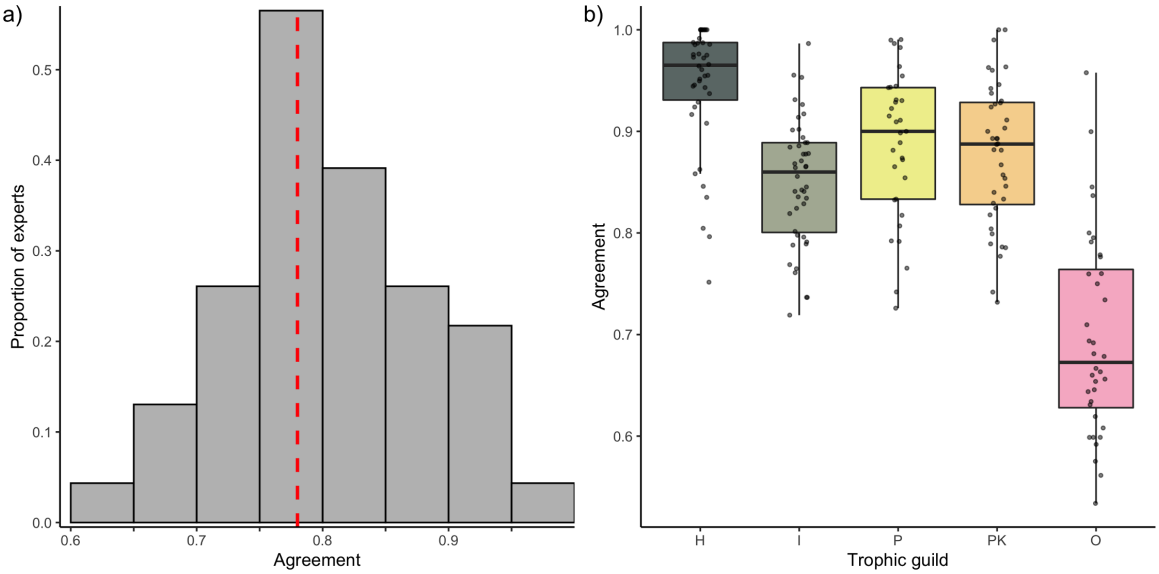

Figure 3.1: Expert agreement on trophic guild assignment. (A) The distribution of the agreement (i.e., proportion of species assigned to the same trophic category) across the 32 comparisons between pairs of experts. The red dotted line represents the median. (B) Agreement between pairs of experts by trophic category. H, herbivores and detritivores; I, invertivores; O, omnivores; P, piscivores; PK, planktivores.

Expert agreement was variable and often homogeneously distributed around the mean for all the trophic categories. Therefore, the high agreement between a few combinations of experts did not necessarily exclude peaks of disagreement (figure 3.1B). The analysis of individual confusion matrices between pairs of experts revealed high heterogeneity (figure 3.2). For example, Morais and Bellwood were generally in agreement with Mouillot and colleagues (Mouillot *et al.* 2014) (across 89% of the 515 species in common), while Mouillot and colleagues (Mouillot *et al.* 2014) agreed with Stuart-Smith and colleagues (Stuart-Smith *et al.* 2013) across only 68% of the 2,211 species in common.

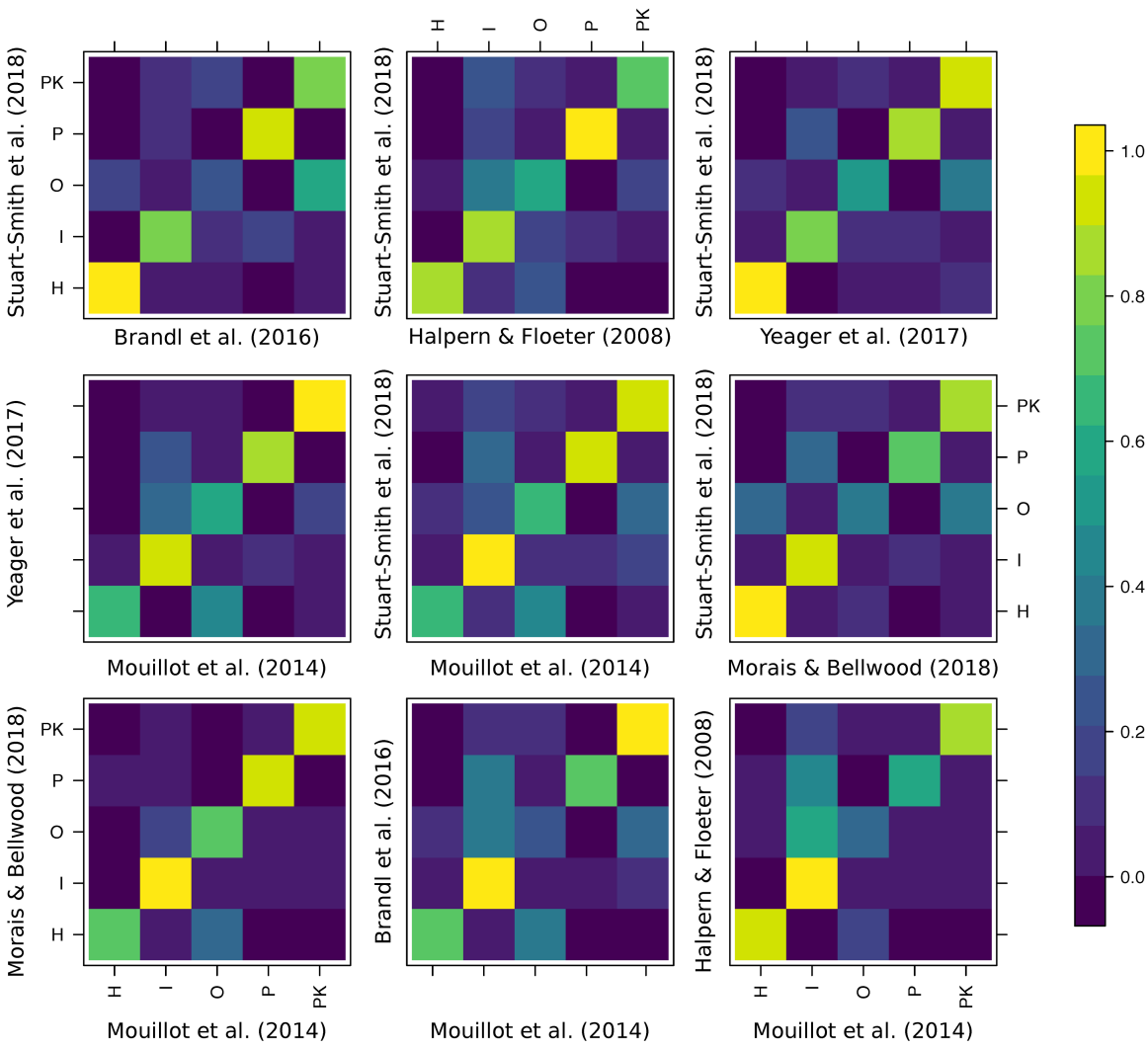

Figure 3.2: Confusion matrices of the agreement between pairs of experts that share at least 200 species in common and define all 5 trophic categories. Colors represent proportions of species in each trophic guild as classified by experts. H, herbivores and detritivores; I, invertivores; O, omnivores; P, piscivores; PK, planktivores.

Surprisingly, there was also a high heterogeneity in groups with high disagreement (i.e., multiple alternative assignments for species not assigned to the same trophic group). Species classified as "invertivores" according to 1 expert were considered "omnivores," "piscivores," or "planktivores" according to other classification schemes (figure 3.2). Similarly, species considered "omnivores" by 1 expert were alternatively considered "invertivores," "herbivores and detritivores," or "planktivores" by another expert.

3.4.2 Definition of trophic guilds with network analysis

We defined trophic guilds by identifying modules (i.e., combinations of predators and prey) that maximize the weighted modularity of the global network (Beckett 2016). Our analysis robustly identified 8 distinct modules that correspond to different trophic guilds (figure 3.3). We identified these trophic guilds as

1. "Sessile invertivores": species predominantly feeding on Asteroidea, Bryozoa, Cirripedia, Holothuroidea, Porifera, and Tunicata;
2. "Herbivores, microvores, and detritivores (HMD)": species primarily feeding on autotrophs, detritus, inorganic material, foraminifera, and phytoplankton;
3. "Corallivores": species predominantly feeding on Anthozoa and Medusozoa;
4. "Piscivores": species primarily feeding on Actinopterygii and Cephalopoda;
5. "Microinvertivores": species primarily feeding on Arachnida, Pycnogonida, small Crustacea (Peracarida), and worms (Annelida, Hemichordata, Nematoda, Nemertea, and Sipuncula);
6. "Macroinvertivores": species primarily feeding on Mollusca (Bivalvia, Gastropoda, Polyplacophora, and Scaphopoda), Echinoidea, and Ophiuroidea;
7. "Crustacivores": species primarily feeding on large Crustacea (Decapoda and Stomatopoda);
8. "Planktivores": species mainly feeding on zooplankton, cyanobacteria and Harpacticoida.

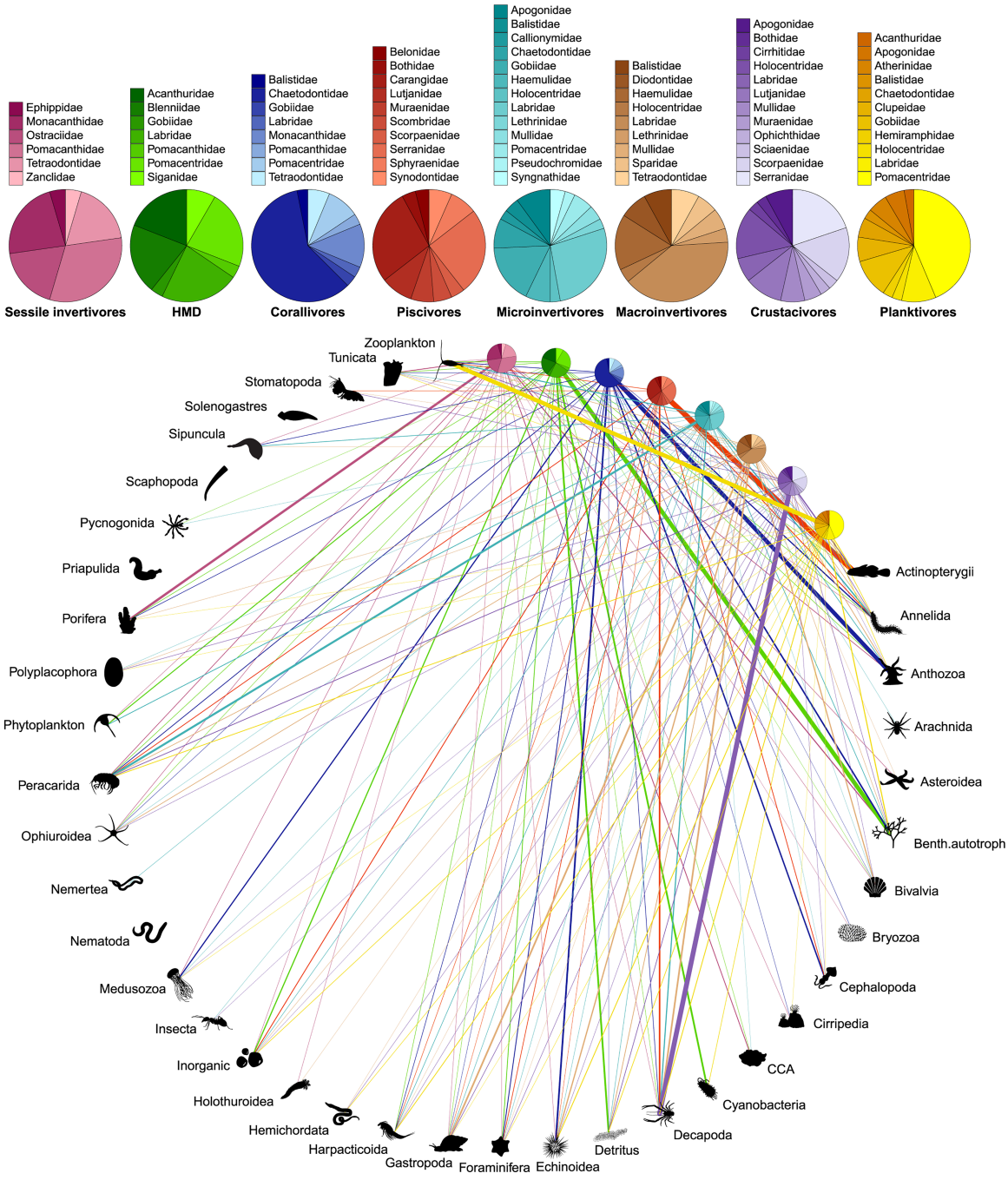

Figure 3.3: Bipartite network including 615 fish species (grouped into 8 trophic guilds) and their prey items (grouped into 38 categories; see table S1). The relative proportion of each prey category consumed by each trophic guild corresponds with the width of each interaction bar. The pie charts show the relative proportion of fish families within each trophic guild.

3.4.3 Phylogenetic conservatism of trophic guilds

To evaluate the significance of the phylogenetic statistic value ($\delta = 9.37$), we applied a bootstrapping approach and quantified δ after randomly shuffling the trait values 100 times. The median δ of these null models was 0.000199 (95% confidence interval [0.000196, 0.000204]), indicating a strong phylogenetic signal associated with the 8 trophic guilds.

Phylogeny and maximum body size were sufficient to correctly predict the trophic guild of 97% of the species in our dataset. For most families, there was strong phylogenetic conservatism, which resulted in the high confidence of these predictions (figure 3.4). Within some families, however, closely related species displayed distinct dietary preferences, as showcased by high negentropy values for families such as Balistidae, Diodontidae, and Labridae.

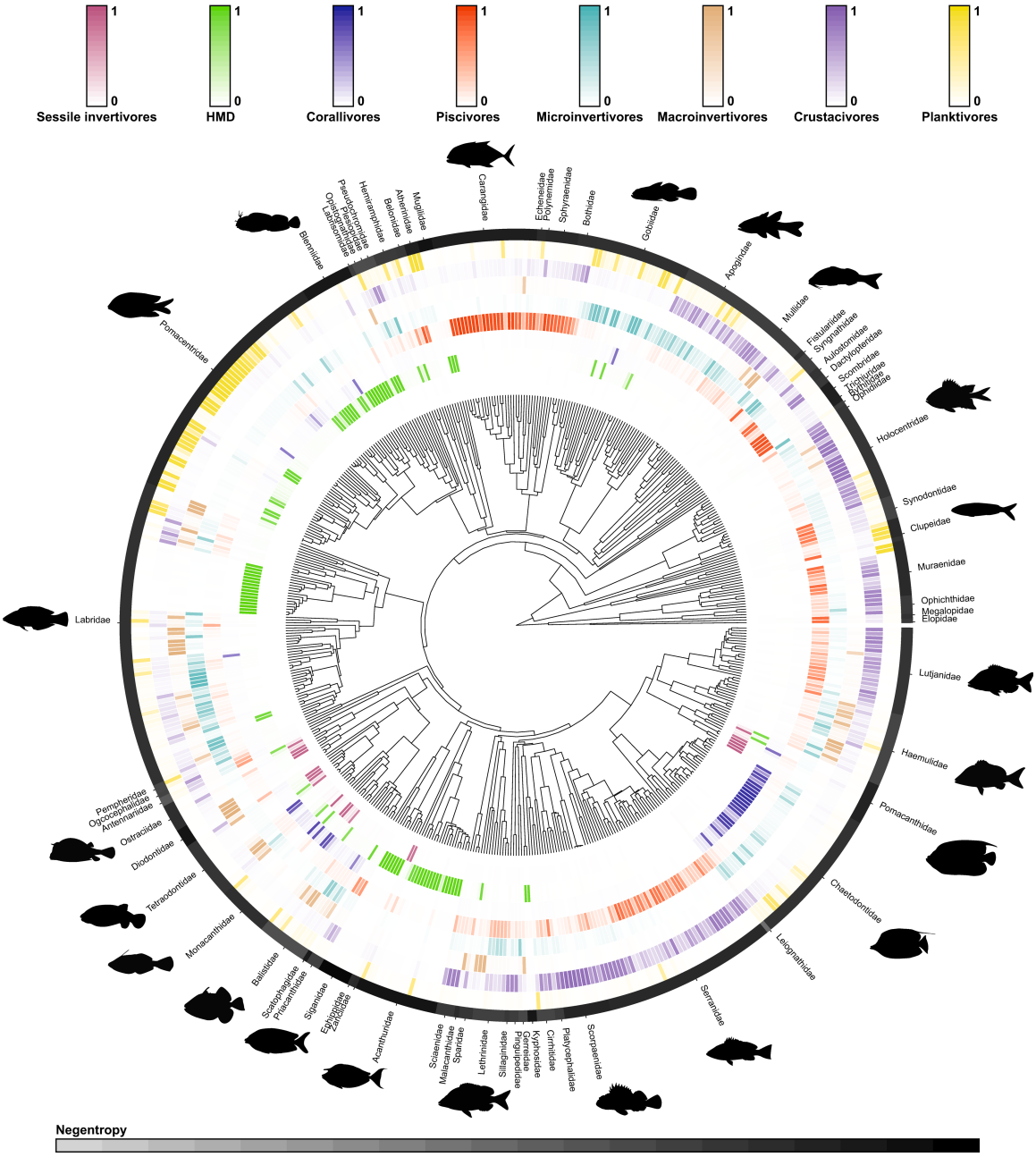

Figure 3.4: Phylogenetic tree of 535 reef fish species with fitted trophic guild assignments based on empirical dietary data. Trophic guild predictions were made with a Bayesian multinomial phylogenetic regression. The probability of trophic guild assignments for each species is visualized with color scales (depicted above the phylogenetic tree), with darker colors indicating a higher probability of assignment. In the outer black ring, each distinct segment represents a fish family (with silhouettes included for the most speciose families). Uncertainty of overarching trophic guild assignment for each fish family is visualized with negentropy values (i.e., reverse entropy); thus, darker shades indicate a higher degree of certainty of trophic guild assignment.

Given its high predictive performance, we used our Bayesian phylogenetic model to extrapolate the probability of all reef fish species belonging to the 8 trophic guilds and assigned the trophic guild with the highest probability (see 3.6 table S3). Using leave-one-out cross validation, the final accuracy of this approach was 65%, which is comparable with other phylogenetically extrapolated traits applications, such as those involving microbial traits (Goberna & Verdú 2016).

By inspecting the confusion matrix of the leave-one-out cross validation, we obtained more detailed information on the accuracy of the trophic guild predictions (figure 3.5). Most categories were well predicted with our extrapolation approach. In particular, the "sessile invertivores," "HMD," and "piscivores" trophic guilds were predicted with high accuracy (77%, 75%, and 73% correct predictions, respectively). The confusion matrix also provided information on incorrectly assigned categories. For example, when "piscivores" were incorrectly assigned, they were mostly classified as "crustacivores." However, the network plot revealed that the fishes classified as "piscivores" also fed on crustaceans (mostly decapods), so this "incorrect assignment" was grounded in ecological reality and reflected uncertainty within the model. Additionally, the "microinvertivores" trophic guild had the highest proportion of inaccurate predictions (52 % correct predictions). Here, species were often misclassified as "crustacivores" or "planktivores."

3.4.4 Prediction of trophic interactions with machine learning

Using machine learning, our model achieved high predictive performance in quantifying probabilities of pairwise trophic interactions (AUC = 0.99; TSS = 0.94). After calibration with 535 fish species and 3,479 trophic interactions, our model accurately identified 3,410 of these interactions, demonstrating an exceptionally low rate of false negative interactions. In addition, the model accurately predicted absent trophic interactions, with a false positive interaction rate of only 3.6%. When the model was

calibrated with only 5 locations, excluding the data from New Caledonia, the model still performed well (AUC = 0.82; TSS = 0.52). The model correctly detected 82% of the trophic interactions in the New Caledonia dataset, with a false positive interaction rate of 27%. Based on the high predictive performance of the model, we used the full model with all 6 locations to predict the probability of pairwise trophic interactions on a continuous spectrum between the 4,554 reef fish species with available phylogenetic information and our 38 prey categories (see 3.6 table S4).

3.5 Discussion

Functional ecology requires standardized and reproducible classification schemes to characterize species' niches (Schneider *et al.* 2019; Weiss & Ray 2019; Gallagher *et al.* 2020). Rather than relying on expert opinion for the assignment of trophic groups, which often results in variable assignments, we demonstrate that the categorization of discrete trophic guilds and pairwise trophic interactions can be achieved with a quantitative, reproducible framework grounded in empirical data across biogeographic regions. We employed network analysis to partition 535 tropical coral reef fish species into 8 trophic guilds based on a synthesis of globally distributed, community-wide fish dietary analyses, and then we applied a Bayesian phylogenetic model that predicts trophic guilds based on phylogeny and body size, attaining a 5% misclassification error. Moreover, using a machine learning approach, we demonstrate that a continuous spectrum of trophic interactions can also be accurately predicted based on phylogeny and body size. Our framework represents the first implementation of a quantifiable classification scheme for coral reef fishes, which form some of the most diverse vertebrate communities worldwide.

Unlike traditional trophic guilds based on expert opinion (Newman *et al.* 2006; Halpern *et al.* 2008; Graham *et al.* 2011; Mouillot *et al.* 2014; Parravicini *et al.* 2014; Brandl *et al.* 2016; Yeager *et al.* 2017; Morais & Bellwood 2018; Stuart-Smith

et al. 2018), our trophic approaches are reproducible, provide uncertainty estimates, and can be updated and improved in the future with additional dietary information. In an effort to encourage new, accessible benchmarks to categorize fish trophic guilds, our classification of discrete trophic guilds and probabilities of pairwise trophic interactions are publicly available with this publication. Given the growing number of trait-based studies that assign trophic guilds to understand and monitor ecosystem functioning in our changing world, it is imperative that we establish comparable and reproducible trophic classification frameworks.

Our findings highlight the discordance of expert opinion in the assignment of trophic guilds and the necessity to develop quantifiable and reproducible classification schemes that are accessible to the wider scientific community (c.f. (Cano-Barbacil *et al.* 2020)). Despite broad similarities between the trophic guilds reported in the literature and the groups identified by our analysis, our classification scheme reveals a higher level of partitioning among invertebrate-feeding fishes as compared to previously proposed trophic guilds. In the past, invertebrate-feeding fishes were generally considered "sessile invertivores," "mobile invertivores," or "omnivores" (e.g., Parravicini *et al.* (2014); Micheli *et al.* (2014); Yeager *et al.* (2017)), but we identify 5 distinct invertebrate-feeding groups: "corallivores," "sessile invertivores," "microinvertivores," "macroinvertivores," and "crustacivores." Given the extreme numerical dominance of invertebrates in coral reef environments (Glynn & Enochs 2011), the collapse of all invertebrate-feeders into 2 or 3 trophic groups was possibly an artefact of expert oversight, and the expansion of invertebrate-feeding trophic guilds to 5 groups stands to improve ecological resolution of fishes feeding on invertebrate prey.

In contrast to the high resolution achieved within invertebrate-feeding groups, our classification achieved limited resolution among the nominally herbivorous species, "HMD." Across the literature, past classification schemes often separate macroalgal feeders, turf algae croppers, and detritivores (e.g., Mouillot *et al.* (2014); Parravicini *et al.* (2014); Bejarano *et al.* (2019); Siqueira *et al.* (2019)). The lack of precision in our framework is rooted in the difficulty in distinguishing algae, microbes, and detritus

within the alimentary tract of fishes, resulting in the pooling of these ingested items during the visual assessment of fish gut contents. Consequently, species classified as "HMD" may have fundamentally different foraging strategies, dietary preferences, and evolutionary histories (Clements *et al.* 2016), which can greatly impact their functional role on coral reefs (e.g., Brandl *et al.* (2016)). Thus, while our identified trophic guilds promise increased resolution for fishes that consume animal prey, our identified groupings may not adequately capture consumer–producer dynamics on coral reefs. Emerging techniques, such as gut content metabarcoding, may provide the additional resolution needed to further discriminate prey items in this group (Casey *et al.* 2019; Brandl *et al.* 2020a). Alternatively, coupling diet categorization with other traits, such as feeding behavior, may help to pinpoint the variety of feeding modes that exist within the "HMD" trophic guild.

While our delineation of trophic guilds is applicable to functional studies that employ discrete categories, the continuous output of trophic interaction probabilities holds promise for a variety of other approaches, such as trophic network analyses. On coral reefs, previous studies have employed network analysis to examine human impacts on coral reef food webs [30,33]. However, these studies only incorporate local fish gut content data, which limits their spatial application. Larger-scale network analyses exist (e.g., Albouy *et al.* (2019)), but they are predominantly based on co-occurrence patterns and solely consider piscivores, thus neglecting a large portion of marine food webs, which are typically dominated by invertebrate-feeders. Therefore, our demonstrated ability to predict trophic interactions based on phylogeny and body size opens new avenues for marine food web research. Moreover, the high performance of the reduced model to predict pairwise trophic interactions in New Caledonia confirms the potential of our approach to predict probabilities of local trophic interactions for entire food webs.

Our findings add to recent evidence that evolutionary history (i.e., phylogenetic relatedness) is essential to evaluate the ecological traits of fishes (c.f. (Westoby 2006; Floeter *et al.* 2018; Siqueira *et al.* 2020)). Recently, taxonomy and body size have

been revealed as important predictors of fish diet composition and size structure (Soler *et al.* 2016b; Soler *et al.* 2016a), and in the highest resolution analyses of coral reef fish diet, taxonomic family was a better predictor of fish diet than broad trophic guilds (Casey *et al.* 2019). Given the exceedingly low rate of misclassification error in our predictions, we posit that phylogeny is a critical variable that should be consistently considered in the assignment of trophic guilds for reef fishes. Across a plethora of organismal groups (e.g., birds (Lovette & Hochachka 2006), reptiles (Knouft *et al.* 2006), fishes (Peres-Neto 2004; Gajdzik *et al.* 2019), insects (Weiblen *et al.* 2006), parasites (Mouillot *et al.* 2006), and plants (Silvertown *et al.* 2006)), phylogenetic niche conservatism has been alternately supported and dismissed. In our case, when examining fish trophic guilds using 38 prey categories, phylogenetic conservatism is readily apparent at a relatively coarse dietary resolution and may allow us to extrapolate trophic assignments to closely related consumer species and potentially extend this framework to fishes inhabiting other habitats. However, with increasing dietary resolution beyond what is detailed in the present study, phylogenetic signals may weaken (Mazel *et al.* 2018) since even closely related species may exhibit dietary specialization (Casey *et al.* 2019; Leray *et al.* 2019). In the future, with the availability of higher resolution of dietary information, phylogenetic niche conservatism can be easily examined within our framework.

With ongoing environmental and ecological change, a firm grasp on shifts in ecosystem functioning will depend on the reliable assignment of organismal traits (McGill *et al.* 2006) and the comparability of trait-based approaches across space, time, and independent studies (Weiss & Ray 2019). Especially in complex, hyperdiverse environments such as coral reefs, it is imperative to standardize how we measure and report these traits to prevent idiosyncratic results based on subjective trait assignments (Bellwood *et al.* 2019; Brandl *et al.* 2019a). Trophic guilds are among the most commonly applied trait to assess ecosystem functioning because they directly relate to energy and nutrient fluxes across trophic levels. Thus, our standardized framework represents a major step forward for coral reef functional ecology, while

heeding the call for openly accessible, reproducible trait databases (Madin *et al.* 2016; Gallagher *et al.* 2020; Jeliazkov *et al.* 2020). As trait-based ecology continues to be used to examine disturbances and implement management strategies, our cohesive and accessible framework can provide key insights into the trajectory of coral reef communities.

Further, our results can serve as the foundation for an online platform that permits researchers to collate, update, and utilize trait-based data on coral reef fishes. Similar to current initiatives across the entire tree of life (Gallagher *et al.* 2020), the creation of an online, user-maintained dietary database will facilitate collaboration and traceability in trait-based reef fish research. One challenge will lie in merging visual fish gut content analysis databases with molecular data, such as gut content DNA metabarcoding (e.g., Casey *et al.* (2019)), and biochemical data, such as stable isotope analysis (e.g., Eurich *et al.* (2018)), and short-chain fatty acid profiles (e.g., Choat *et al.* (2002)), which indicate nutritional assimilation rather than the simple ingestion of prey items (Clements *et al.* 2016). Despite this challenge, accessibility to a large breadth of reef fish dietary information would improve our framework. Our proposed trophic guilds and probabilities of trophic interactions are model predictions, so they are only as reliable as the underlying dietary data. In addition, these predictions may suffer from extrapolation biases; for example, if limited dietary information exists across species within a taxonomic group, extrapolations to closely related species are more likely to be assigned erroneous trophic guilds. Consequently, an ongoing, extensive compilation of dietary traits across coral reef fishes will continuously improve our predicted trophic guild assignments and pairwise trophic interactions.

Finally, our proposed framework is not limited to coral reef fishes; indeed, trophic guild assignments can be quantifiable, reproducible, and transparent, with the inclusion of uncertainty metrics, across many organismal groups. However, the standardization of trophic guilds is sorely lacking across the ecological literature (Cano-Barbacil *et al.* 2020), especially based on quantitative data (e.g., González-Salazar

et al. (2014)). We posit that a similar approach can be readily applied across a multitude of organisms and environments. In fact, given the paucity of dietary information available for coral reef fishes in comparison to other organisms, particularly birds and mammals, building rigorous, global trophic classification schemes for many other organisms should be readily achievable within our framework. With a quantitative, transparent trophic classification scheme that can be augmented over time and is applicable across ecological systems, our framework represents a significant advancement for trait-based ecology and a viable approach to monitor ecosystem dynamics into the future (Gallagher *et al.* 2020).

3.6 Supplementary materials

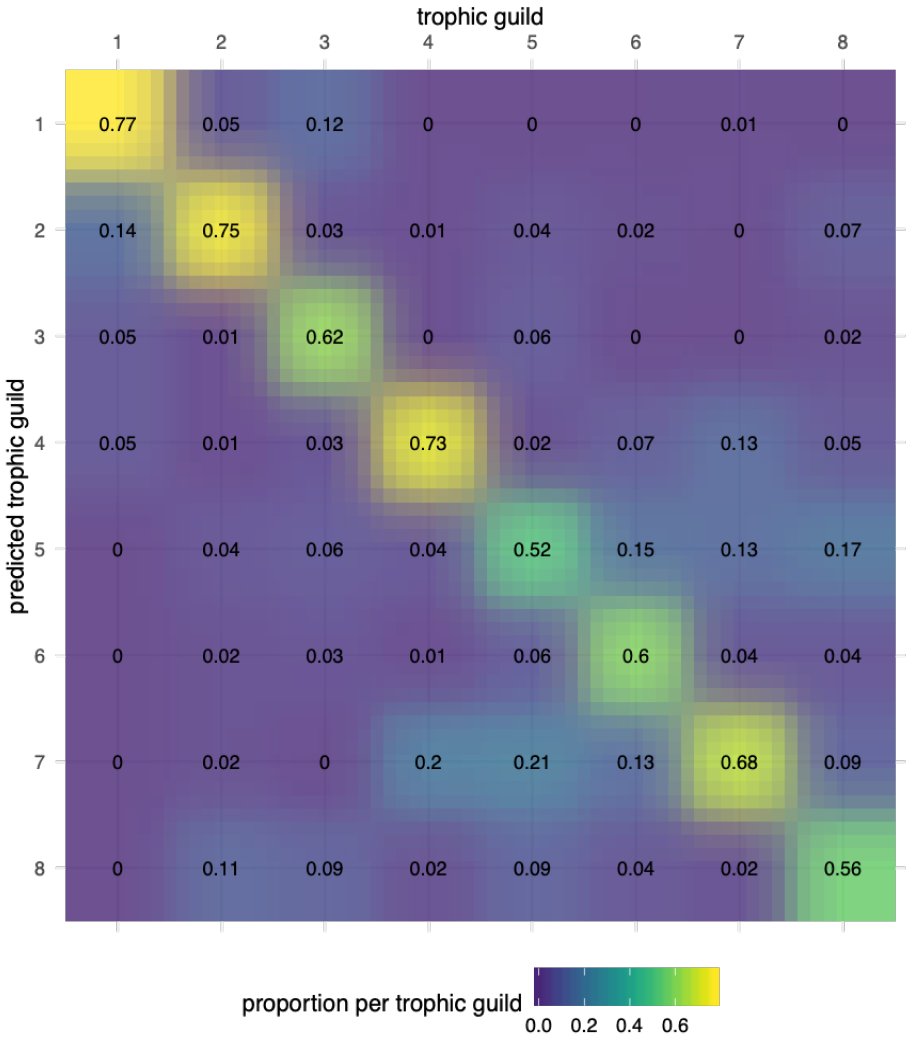

Figure 3.5: Confusion matrix showcasing the accuracy of the 8 trophic guild predictions from the leave-one-out cross validation based on the extrapolation of the Bayesian phylogenetic model. Trophic guilds include (1) sessile invertivores, (2) herbivores, microvores, and detritivores, (3) corallivores, (4) piscivores, (5) microinvertivores, (6) macroinvertivores, (7) crustacivores, and (8) planktivores.

Tables available on-line:

S1 Table. Prey categories used to define the trophic guilds of coral reef fishes. https://doi.org/10.1371/journal.pbio.3000702.s002 (CSV)

S2 Table. Summary of the 33 papers used to evaluate expert agreement on reef fish trophic guilds. The column named "Fishes" refers to the number of fish species included in that study. https://doi.org/10.1371/journal.pbio.3000702.s003 (CSV)

S3 Table. Global extrapolation to infer the probability of each of the 4554 reef fish species to belong to the 8 trophic guilds. The mean and the standard deviation (e.g., p1-8_m, and p1-8_sd) of the posterior probabilities are reported alongside with the mean and standard deviation of the negentropy. https://doi.org/10.1371/journal.pbio.3000702.s004 (CSV)

S4 Table. Probability of trophic interaction between the 4554 reef fish species and the 38 prey categories according to the extrapolation performed by the machine learning approach. https://doi.org/10.1371/journal.pbio.3000702.s005 (CSV)

3.7 Supplementary information

Acknowledgments We thank the Centre de Recherche Insulaires et Observatoire de l'Environnement (CRIOBE) in Perpignan, France and all the researchers who have made their fish gut content data and/or trait-based fish trophic guild assignments publicly available for use by the wider scientific community.

Funding This research was funded by the BNP Paribas Foundation (Reef Services Project) and the French National Agency for Scientific Research (ANR; REEFLUX Project; ANR-17-CE32-0006). This research is product of the SCORE-REEF group funded by the Centre de Synthèse et d'Analyse sur la Biodiversité (CESAB) of the Foundation pour la Recherche sur la Biodiversité (FRB) and the Agence Nationale de la Biodiversité (AFB). VP was supported by the Institut Universitaire de France (IUF), JMC was supported by a Make Our Planet Great Again Postdoctoral Grant (mopga-pdf-0000000144) and JC was supported by the French Polynesian Government (RisqueRecif project). The funders had no role in study design, data collection and analysis, decision to publish, or preparation of the manuscript.

Data availability All methods are described within the paper and its Supporting Information files. The data and the R code are available at the GitHub repository `https://github.com/valerianoparravicini/Trophic_Fish_2020`.

Chapter 4

Quantifying biological parameters of global coral reef fishes

This chapter is methodological and represents the supplementary methods of chapter 5, in revision for *Nature Ecology and Evolution*.

4.1 Introduction

One of the main goals of my thesis was to estimate multiple community-level fish-mediated functions on coral reefs across the globe. To understand the dynamics of community-level functions, we first need to be able to quantitatively estimate them by summing up individual-level processes of each fish in the community. In chapter 2, I presented a novel framework to estimate element-specific elemental fluxes mediated by fishes. Applying this framework to many coral reef fish species across the globe necessitates a number of parameters (see table 2.1). In this methodological chapter, I describe how all required biological parameters were quantified for 1110 coral reef fish species through a combination of existing data, empirical measures, and Bayesian models.

4.2 Species list

I assembled a global species list based on an openly accessible database of reef fish abundances and sizes collected during belt transects by divers (Barneche *et al.* 2019). This database includes sites on the outer reef slope in the Central Indo-Pacific, Central Pacific, Eastern Pacific, Western Indian, Eastern Atlantic, Western Atlantic. Specifically, I selected the species belonging to families for which we had body stoichiometric data, and that were at least 7cm to minimize the bias related to the identification of small individuals. Further, I discarded rare species (i.e., for which less than 20 individuals were ever recorded across all transects). The dataset then included 1110 species that belong to 25 families: Acanthuridae, Balistidae, Bothidae, Chaetodontidae, Cirrhitidae, Fistulariidae, Haemulidae, Holocentridae, Kyphosidae, Labridae, Lethrinidae, Lutjanidae, Monacanthidae, Mugilidae, Mullidae, Ostraciidae, Pempheridae, Pomacanthidae, Pomacentridae, Sciaenidae, Scorpaenidae, Serranidae, Siganidae, Tetraodontidae, Zanclidae.

4.3 Growth parameters

The developed bioenergetic model `fishflux` uses the Von Bertalanffy growth function to calculate daily growth. This growth function relies on three parameters: l_∞, κ, and t_0. For κ, I used a standardized coefficient that describes the potential growth trajectory of an individual if l_∞ were to be equal to its maximum length (i.e., k_{max}, Morais & Bellwood 2018). For simplicity, I kept $t0$ constant at 0 for all species.

4.3.1 Data compilation

I first compiled maximum lengths for all species using Fishbase (Froese & Pauly 2018) and used these lengths for the l_∞. Then, I extracted the available data for k_{max} from Morais & Bellwood (2018), which are essentially κ values from Fishbase, standardized to the maximum length (Morais & Bellwood 2018). I filtered out the species of our species list and only included the k_{max} estimates coming from otolith studies. In total, this selection process resulted in 439 observations of kmax for varying species and temperatures.

Further, I used an openly accessible otolith dataset, including measurements of fishes from five French Polynesian islands, and to which I contributed through data collection and analysis (Morat *et al.* 2020). This dataset includes total length measurements to the nearest millimeter and fish weights to the nearest 0.1 grams. Further, it includes distances between annual growth increments, measured by two independent researchers to prevent biases induced by a single observer. These data can be used to estimate growth rate parameters using a two-step approach: back-calculation to achieve individual-level size-at-age data and hierarchical regression to fit the Von Bertalanffy growth curve (see appendix B).

Specifically, I used the Modified Fry back-calculation model (MF) (Vigliola *et al.* 2000) to estimate fish lengths at previous ages. I adapted the traditional model to

also estimate the uncertainty around the obtained length estimates and allow for the inclusion of missing values using a Bayesian approach (see appendix B for details). Then, I fitted the Von Bertalanffy growth model to all species at each location for which there were at least 3 individuals, using Bayesian hierarchical regression models. Both steps of this procedure were carried out using the developed R package 'fishgrowbot' (appendix A. The package also automatically estimates the parameter k_{max}.

After combining the two data sources, I obtained 496 estimates of k_{max} for 181 species across varying temperatures.

4.3.2 Data analysis and extrapolation

Aside from phylogeny, k_{max} is mostly determined by body size and temperature (Morais & Bellwood 2018). I therefore aimed to predict k_{max} based on body size, temperature, and phylogeny by using a phylogenetic regression model.

I extracted the phylogenetic position of all species included through the Fish Tree of Life (Rabosky *et al.* 2018). I retrieved 100 synthetic stochastically resolved phylogenies where missing taxa were placed according to the highest level of taxonomy using the function `fishtree_complete_phylogeny()` in the R package fishtree (Chang *et al.* 2019). For each tree, I calculated the correlation matrix and then averaged each element across the 100 matrices to get one correlation matrix that could be used in the regression model.

I then fitted a Bayesian phylogenetic regression to predict the growth rate parameter of fishes depending on body size, temperature, and phylogeny with the R package brms (Burkner PC 2017):

$$\ln k_{max} \sim normal(mu, sigma)$$

$$mu = (\beta_0 + \gamma_{0\text{phy}}) + \beta_1 \ln sizemax + \beta_2 sst,$$

where $\ln k_{max}$ represents the natural log-transformed k_{max} value, mu is the predicted average, and sigma is the standard deviation, β_0 is the fixed-effect intercept, $\gamma_{0\text{phy}}$ is a random-effect coefficient for species *phy* that accounts for the residual intercept variation, based on the relatedness as described by the phylogeny, β_1 is the slope for the natural transformed maximum body size, β_2 is the slope for the average ambient sea surface temperature. I used uninformative priors and ran the model for 2000 iterations with a warm-up of 1000 iteration for 4 chains.

The model fit confirmed a negative relationship of $\ln k_{max}$ with maximum body size, and a positive relationship with sea surface temperature (figure 4.1). I verified model convergence and fit by checking the posterior predictive plot, inspecting parameter trace plots, and checking the R statistic. The Bayesian R2 of the model was 0.738 (95%CI: 0.702-0.769).

The phylogenetic heritability (equivalent to Pagel'λ) was estimated as the proportion of total variance, conditioned on the effects attributable to the phylogeny (i.e., $\lambda = \frac{\text{sd}(\gamma_{0\text{phy}})^2}{\text{sd}(\gamma_{0\text{phy}})^2 + \epsilon^2}$). This calculation resulted in a phylogenetic signal of 0.74 (95% CI: 0.70 - 0.77).

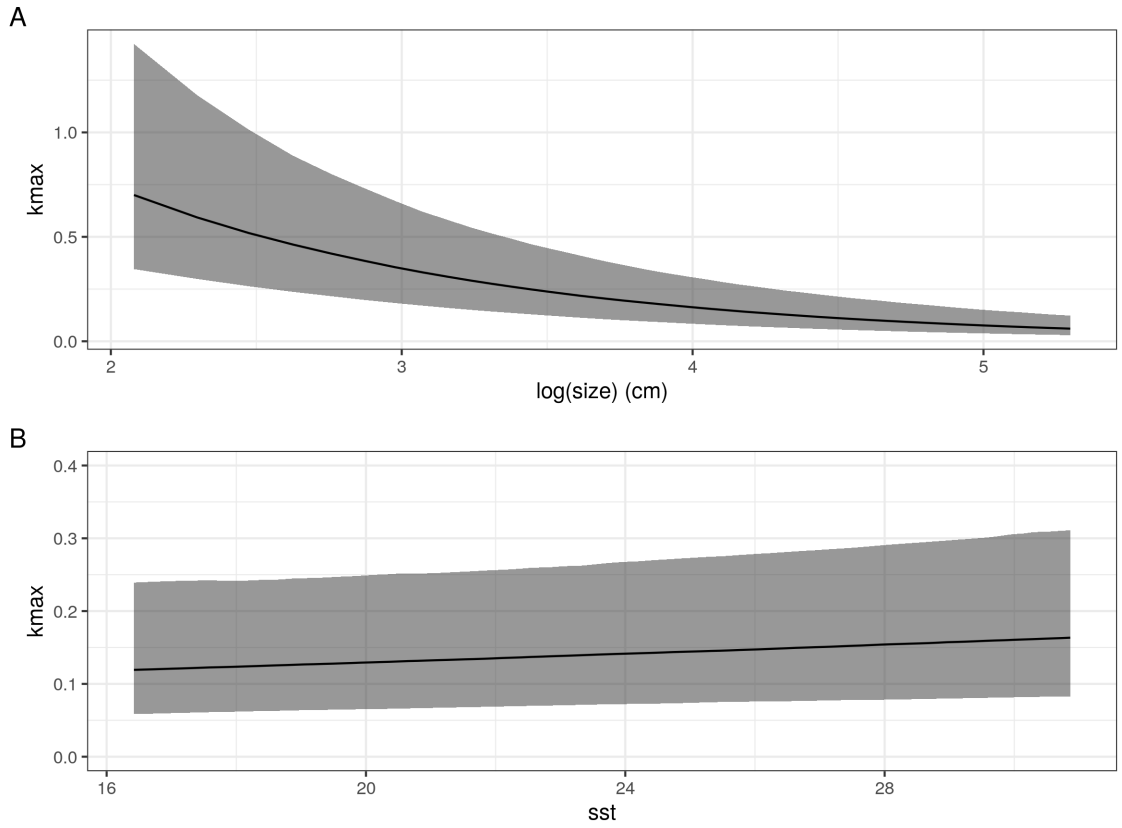

Figure 4.1: Conditional effect plots of dependent variables sea surface temperature and maximum body size. The line represents the mean estimates, and the shaded areas indicate the 95% credible interval.

I extrapolated k_{max} for all species across the full temperature range in which species occur in the uvc database (Barneche & Allen 2018). I rounded temperature to the °C, which results in 4712 unique temperature and species combinations. Similarly to the approach described in chapter 3, I extracted draws of the phylogenetic effect ($\gamma_{0\text{phy}}$) for each species included in the model. I subsequently predicted these phylogenetic effects for missing species with the help of the function phyEstimate in the picante package for R (Kembel *et al.* 2010). This function uses phylogenetic ancestral state estimation to infer trait values for new species on a phylogenetic tree by rerooting the tree to the parent edge for the node to be predicted (Kembel *et al.* 2012). I repeated this for all 100 trees and 1000 draws. Per draw, I averaged the extrapolated values per species across the 100 trees. Then, by combining the

predicted phylogenetic effects with the global intercept and slopes for body size and temperatures for each draw, I predicted k_{max} for each species. Finally, I summarized all k_{max} predictions per sst per species by taking the mean and standard deviation across the 1000 draws.

4.4 Body stoichiometry

4.4.1 Data collection

1633 individuals of 108 species and 25 families were collected between 2015 and 2017 in Mo'orea (Parravicini, unpub.), the Caribbean (Allgeier *et al.* 2020), and Palmyra (Bukepile unpub.). Their gut contents were removed and the whole body was freeze-dried and ground to powder with a Precellys homogenizer. Whole body elemental proportions (Q_{k}) were then measured in the lab using standard methods. Specifically, ground samples were analyzed for %C and %N content using a CHN Carlo-Erba elemental analyzer (NA1500), and for %P using dry oxidation-acid hydrolysis extraction followed by a colorimetric analysis (Allen *et al.* 1974). Elemental content was calculated based on dry mass.

4.4.2 Data analysis and extrapolation

The CNP% content of organisms is known to be highly conserved within families (Allgeier *et al.* 2020). I therefore use phylogeny to extrapolate these values. I fitted C, N and P contents (%) through a hierarchical phylogenetic multivariate normal model with phylogenetic effects and random effects per species.

$$\begin{bmatrix} Y_1 \\ Y_2 \\ Y_3 \end{bmatrix} \sim MVNormal(\begin{bmatrix} mu1 \\ mu2 \\ mu3 \end{bmatrix}, S),$$

$$mu_{\mathrm{n\times k}} = \beta_{0\ \mathrm{k}} + \gamma_{0\mathrm{phy}\times\mathrm{k}} + \gamma_{0\mathrm{sp}\times\mathrm{k}},$$

where Y_1, Y_2 and Y_3 are the % content of C, N, and P respectively, $mu_{\mathrm{n\times k}}$ represents the average % content of element k (C, N, and P) per species, $\beta_{0\ \mathrm{k}}$ is the fixed-effect intercept for each element k, $\gamma_{0\mathrm{phy}\times\mathrm{k}}$ is the random-effect coefficient, based on the relatedness as described by the phylogeny for each species *phy* and element k, $\gamma_{0\mathrm{sp}\times\mathrm{k}}$ is the random-effect coefficient that accounts for the residual species-level intercept variation per element k, and S is a covariance matrix, with three rows and columns, representing the covariance among C, N, and P.

I used uninformative priors and ran the model for 2000 iterations with a warm-up of 1000 iteration for 4 chains. The Bayesian R2 of the model was 0.39 (95%CI: 0.36-0.42), 0.50 (95%CI: 0.48-0.53), and 0.43 (95%CI: 0.40-0.46) for C, N and P respectively. The phylogenetic heritability was 0.41 (95%CI: 0.28-0.55), 0.58 (95%CI: 0.4-0.66), and 0.57 (95%CI: 0.46-0.69) for C, N, and P respectively.

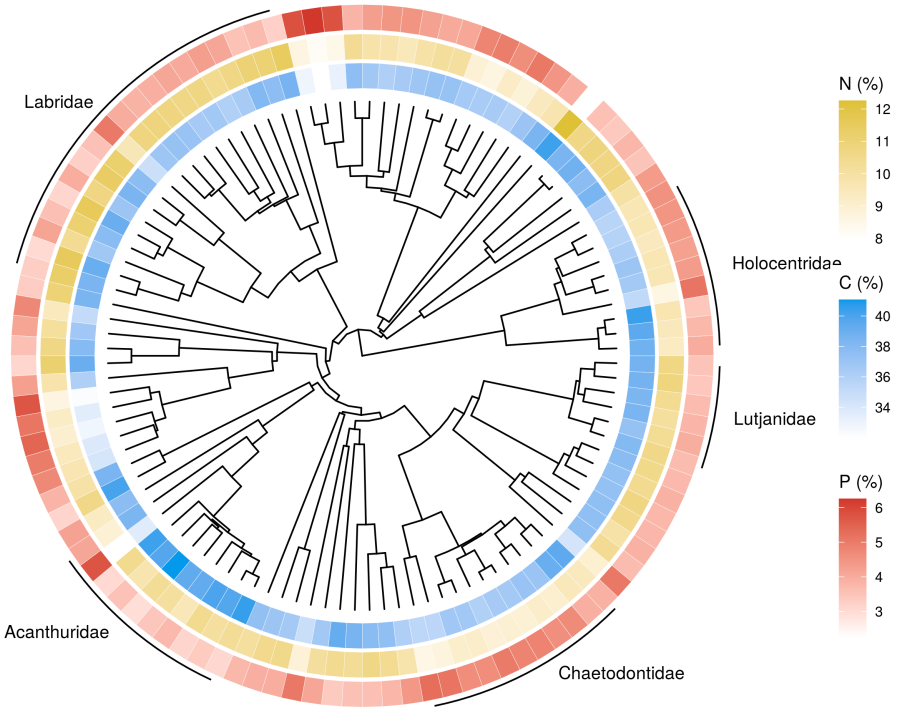

Figure 4.2: Fitted carbon (C), nitrogen (N), and phosphorus (P) concentrations, mapped on the phylogenetic tree.

As before, I used 1000 fitted draws for each species, and 100 phylogenetic trees to extrapolate to all species with unknown body stoichiometry. Specifically, I used the 'phylopars' function from the 'Rphylopars package' (Bruggeman *et al.* 2009). This function uses ancestral state reconstruction and Brownian motion, and takes the correlation between C, N and P into account.

4.5 Diet

4.5.1 Data collection

Together with colleagues, I collected 571 adult individuals of 51 species between 2018 and 2019 in Mo'orea, Tetiaroa, and Mangareva, three French Polynesian islands. I then extracted the stomach content and stored it in a 2ml tube. After freezing the samples, I freeze-dried all samples for at least 24 hours, and ground them to powder. Then, samples were sent to the lab for CNP content analysis using similar methods as for the fish body stoichiometry described above.

4.5.2 Data analysis and extrapolation

Using trophic guilds defined by Parravicini *et al.* (2020) (chapter 3), I fitted a multivariate Bayesian regression model to summarize CNP% content data per trophic guild with random effects at the species level. This model had a median Bayesian R2 of 0.62, 0.62, and 0.48 for C, N and P respectively. Next, I extracted 1000 draws of the predicted CNP% per trophic guild. The model from chapter 3 provides the probability of global reef fish species to be assigned to each of the eight defined trophic guilds (i.e., sessile invertivores; herbivores, microvores, and detrivores; corallivores; piscivores; microinvertivores; macroinvertivores; crustacivores; planktivores). By combining these probabilities with the predicted diet contents per trophic guild, I finally estimated the diet CNP% for each species in our database. I then took the average and standard deviation across all 1000 draws. While there is bias in using diet CNP% estimates based on a dataset in one region, the variability between food categories (e.g., animal material and primary producers) is higher than regional differences within trophic categorizations. Further, as the trophic guild classification includes probabilities of belonging to each group, variation is included when the trophic categorization is not well known. For example, if a species has a 50% probability to be a herbivore and

a 50% probability to be a sessile invertivore this uncertainty will be reflected in the estimation of the diet CNP%.

4.6 Metabolic parameters

4.6.1 Data collection and lab experiments

To quantify standard metabolic rate (SMR) and maximum metabolic rate (MMR), intermittent-closed respirometry experiments were carried out (Steffensen 1989; Clark *et al.* 2013). In the period between 2018 and 2019, 1393 individuals of 61 species and 18 families with a minimum of 3 replicates per species were collected using hand nets and clove oil by scuba divers (Parravicini, Brandl, and Mercière, unpub.). After an acclimatization and fasting period of 48 h in aquaria, the fishes were individually transferred to a water-filled tub at 28°C (ambient sea water temperature) and manually chased by the experimenter until exhausted (Clark *et al.* 2012; S. Butail *et al.* 2013). Then, they were placed in respirometry chambers submersed in an ambient and temperature-controlled tank, where they were left for ~23 h. The intermittent respirometry cycles started immediately after a fish was placed in its respirometry chamber. The cycles consisted of a measurement (sealed) period followed by a flush period during which the respirometry chambers were flushed with fully aerated water from the ambient tank. Because fish were exhausted right before entering the respirometry chambers, it was possible to measure the approximate MMR. Depending on fish size, 8 respirometry chambers ranging in volume (including tubes and pumps) from 0.4 to 4.4 L were run in parallel, and measurement and flush periods lasted between 3 to 15 min and 3 to 5 min, respectively. SMR was calculated as the average of the 10 % lowest values measured during the entire period, after the removal of outliers (Chabot *et al.* 2016). MMR was calculated from the slope of the first measurement period.

4.6.2 Data analysis and extrapolation

To retrieve the parameters f_0 (Metabolic normalisation constant independent of body mass; g $Cg^{-\alpha}d^{-1}$), α (mass-scaling exponent), and θ (factorial activity scope), I fitted a normal Bayesian mixed effect model predicting the log10-transformed metabolic rate with the log10-transformed biomass including random effects of family, species, and mr type (SMR or MMR) on both the species and family intercept effect using brms (Burkner PC 2017). I ran the model for 4000 iterations, with a warm-up of 2000 iterations, and four chains. Further, I used an informative prior for the slope ($\alpha \sim normal(0.8, 0.5)$. The model had a Bayesian R2 of 0.973 (95%CI: 0.972-0.974). I then predicted the family-level α by summing the slope of the model with the effects of the family on the slope of the SMR (figure 4.3). I did this for all iterations and then took the mean and standard deviation. In a similar way, I extracted the family-level intercept for SMR and MMR (figure 4.4), and then quantified mean and standard deviation of f_0 after the back-transformation of all iterations of the intercept (i.e., the intercept for SMR). Finally, I estimated θ as followed, based on the assumption that fishes rest 12h a day and they on average spend the remaining 12 hours at a metabolic rate that is the average of their SMR and MMR:

$$\theta = \frac{3\text{SMR} + \text{MMR}}{4\text{SMR}},$$

where all iterations of the back-transformed family-level intercepts were used for SMR and MMR. I then summarized these predictions by taking the mean and standard deviation. I used the family-level estimates for these parameters for all species in our database. For families that were not represented in our respirometry dataset, I used the average across all families. The parameter $f0$ was adjusted for each temperature in the varying locations of the uvc database, following Barneche *et al.* (2014):

$$f0_{adjusted} = f0(T_{ref})e^{E_r(\frac{1}{\kappa T_ref} - \frac{1}{\kappa T})},$$

where κ is the Boltsmann's constant ($8.62 * 10^{-5} eV K^{-1}$), E_r is the activation energy (0.59 eV, extracted from Barneche *et al.* (2014)), $f0(T_{ref})$ is the value of the metabolic normalization at a fixed reference temperature (301.15 K = 28 + 273.15K), T is the temperature of interest (K).

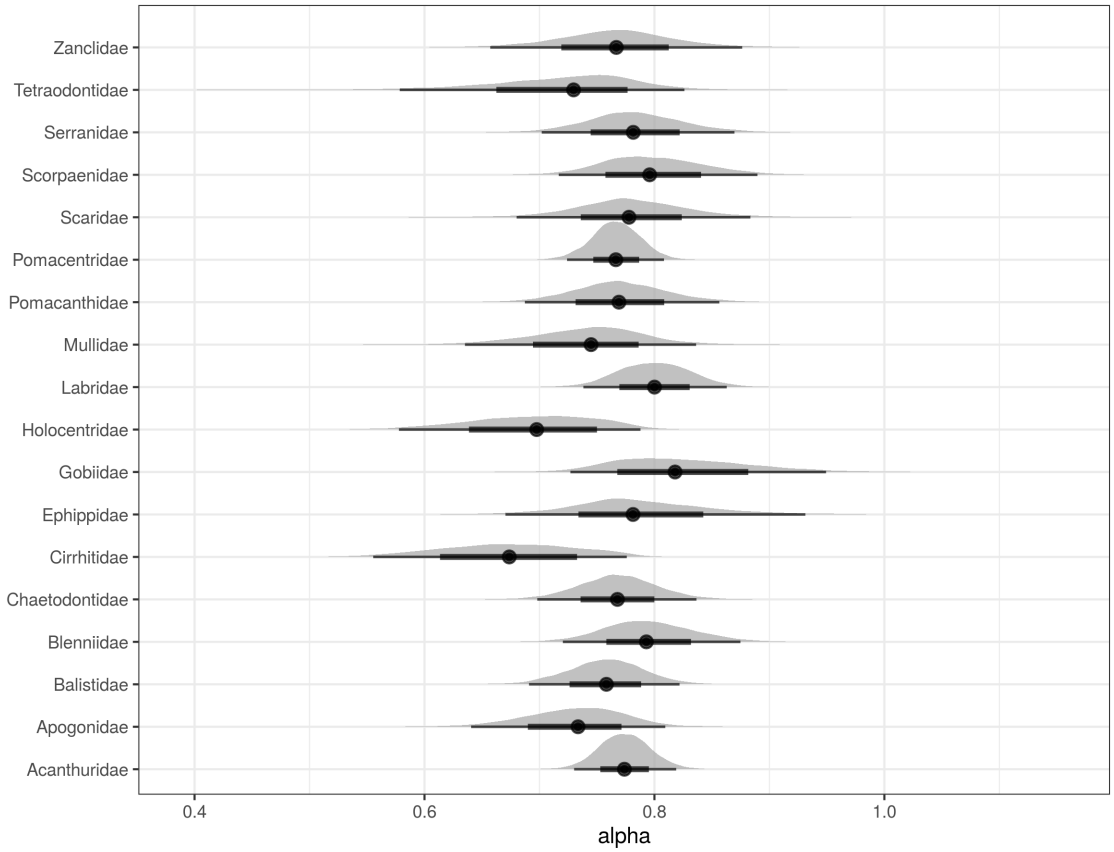

Figure 4.3: Distribution of family-level predictions of parameter alpha. Points indicate the average, lines show the 50% and 95% credible interval. The SMR intercept represents the parameter f0

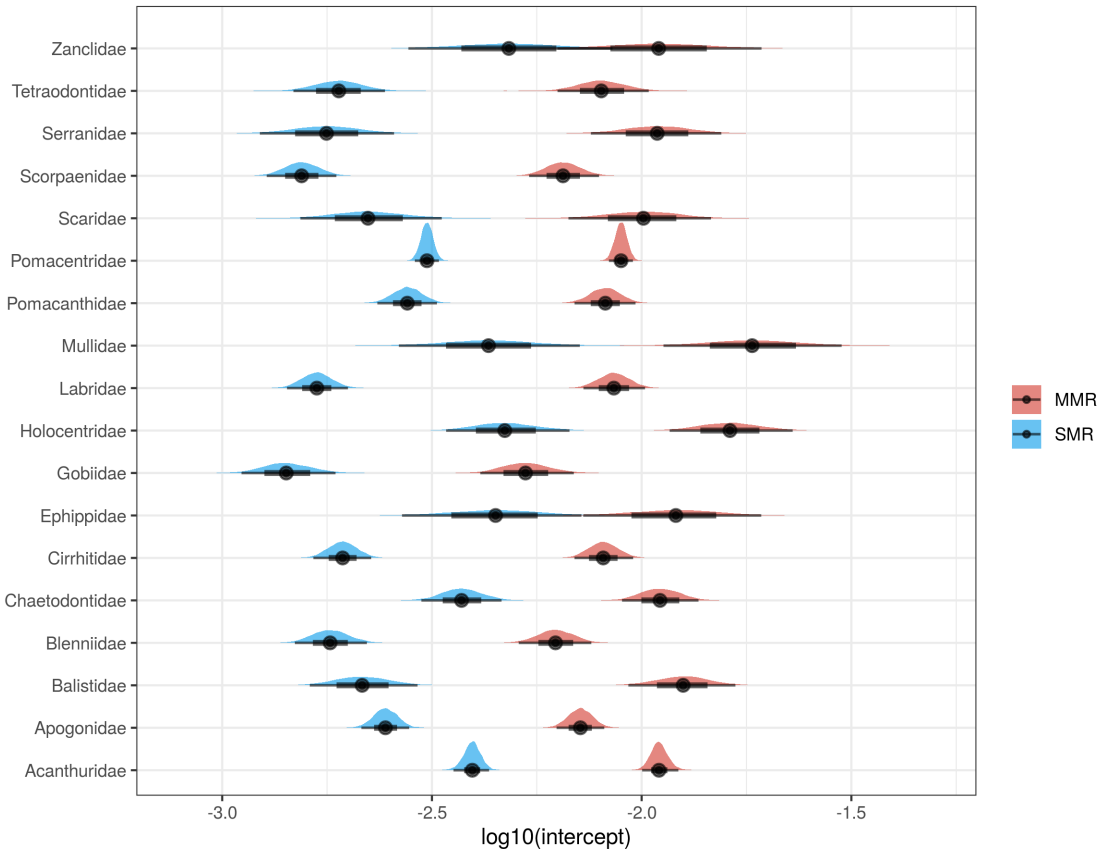

Figure 4.4: Distribution of family-level predictions of parameter the intercept for SMR and MMR. Points indicate the average, lines show the 50% and 95% credible interval.

4.7 Additional parameters

I retrieved the parameters lw_a, lw_b, h, and r from fishbase (Froese & Pauly 2018). For the mass-specific turnover rates for N and P($F_{0\mathrm{Nz}}$; $F_{0\mathrm{Pz}}$), I used the estimates provided in Schiettekatte et al. (2020) (Schiettekatte *et al.* (2020); chapter 2).

Chapter 5

Biological trade-offs underlie coral reef ecosystem functioning

This chapter is currently in revision for *Nature Ecology and Evolution*.

Authors: Nina M. D. Schiettekatte, Simon J. Brandl, Jordan M. Casey, Nicholas A. J. Graham, Diego R. Barneche, Deron E. Burkepile, Jacob E. Allgeier, Jesús E. Arias-Gonzaléz, Graham J. Edgar, Carlos E. L. Ferreira, Sergio R. Floeter, Alan M. Friedlander, Alison L. Green, Michel Kulbicki, Yves Letourneur, Osmar J. Luiz, Alexandre Mercière, Fabien Morat, Katrina S. Munsterman, Enrico L. Rezende, Fabian A. Rodríguez-Zaragoza, Rick D. Stuart-Smith, Laurent Vigliola, Sébastien Villéger, Valeriano Parravicini

5.1 Abstract

Preserving the functioning of coral reefs is a critical challenge of the 21st century. However, a lack of quantitative assessments of multiple functions across large spatial scales has hindered local and regional conservation efforts. We integrate empirically-parametrized bioenergetic models and global community surveys to quantify five key functions mediated by coral reef fishes. We show that functions exhibit critical trade-offs driven by diverging community structures, such that no reef can holistically maximize functioning. Further, functions are locally dominated by few species, but worldwide, the identity of dominant species greatly varies; 70% of the 1,110 species in our dataset are functionally dominant. Our results underline the need for a nuanced approach to coral reef conservation that considers variable processes beyond the effect of standing stock biomass.

5.2 Main text

The flow of elements through biological communities fuels all life on Earth (Barton *et al.* 2013). Preserving these fluxes, often termed ecosystem functions, is critical for the integrity of ecosystems (Barton *et al.* 2013). For millennia, resources have been managed with an economic mindset to maximize desirable functions such as the production of biomass (Weisser *et al.* 2017). Sustaining multiple functions requires both high species richness and a variety of species assemblages across a landscape (Zavaleta *et al.* 2010). However, there can be trade-offs between functions, and efforts to maximize one function can negatively impact another (Zavaleta *et al.* 2010). A deeper understanding of such trade-offs is required to make informed management decisions, but simultaneously quantifying multiple ecosystem functions is challenging. Therefore, trade-offs between functions, their drivers, and their vulnerability remain poorly understood in many ecosystems (Brandl *et al.* 2019a).

Coral reefs are among the most diverse and productive ecosystems on Earth and provide essential ecosystem services (Teh *et al.* 2013). Yet, their integrity is threatened by a plethora of anthropogenic stressors (Hughes *et al.* 2017). Severe declines in habitat quality and fish biomass have brought coral reef functioning to the forefront of scientific discourse (Bellwood *et al.* 2019; Brandl *et al.* 2019a). However, our capacity to evaluate reef functioning typically relies on static proxies of functions, such as live coral cover, standing stock biomass of reef fishes, or the diversity of qualitative traits (e.g., Cinner *et al.* 2020). Conversely, we know comparatively little about actual functions - fluxes of elements and energy - and their drivers (but see Allgeier *et al.* (2016)), which constitutes a severe limitation to efficient management (Brandl *et al.* 2019a).

Here, we integrate biogeochemistry and community ecology to advance our understanding of the elemental fluxes that underpin reef fish functioning. Using empirically-collected species-specific data on basic organismal processes and Bayesian phylogenetic models, we parameterize individual-level bioenergetic models to estimate five

key ecosystem functions: nitrogen (N) excretion, phosphorus (P) excretion, biomass production, herbivory, and piscivory. We apply these bioenergetic models to 9,118 reef fish communities across 585 sites worldwide to: (1) quantify community-level reef fish functions and their trade-offs, (2) extract the community- and species-level effects on these functions, and (3) gauge the vulnerability of reef fish functioning in the Anthropocene.

The five key ecosystem functions performed by fishes across the world's coral reefs exhibit high variability (figure 5.1). Biomass is the most commonly employed indicator of coral reef functioning (Brandl *et al.* 2019a; Cinner *et al.* 2020), and we observed a predictably strong relationship between fish biomass and all five functions (figure 5.5a-e, figure 5.6). However, our analyses demonstrate striking variability after accounting for biomass: in communities with similar biomass, functions may differ by two orders of magnitude or more (figure 5.5a-f). Thus, using biomass as a proxy for functioning masks fundamental differences in critical community-level functions. Further, we demonstrate strong trade-offs among the five functions, independent of biomass (figure 5.1, figure 5.5g). For example, high herbivory rates and nitrogen excretion negatively correlate with rates of phosphorus excretion. Consequently, for a given value of biomass, no reef can yield above average values across all five functions. While many coral reefs may stand out as hotspots for one function, none can holistically maximize functioning (figure 5.1).

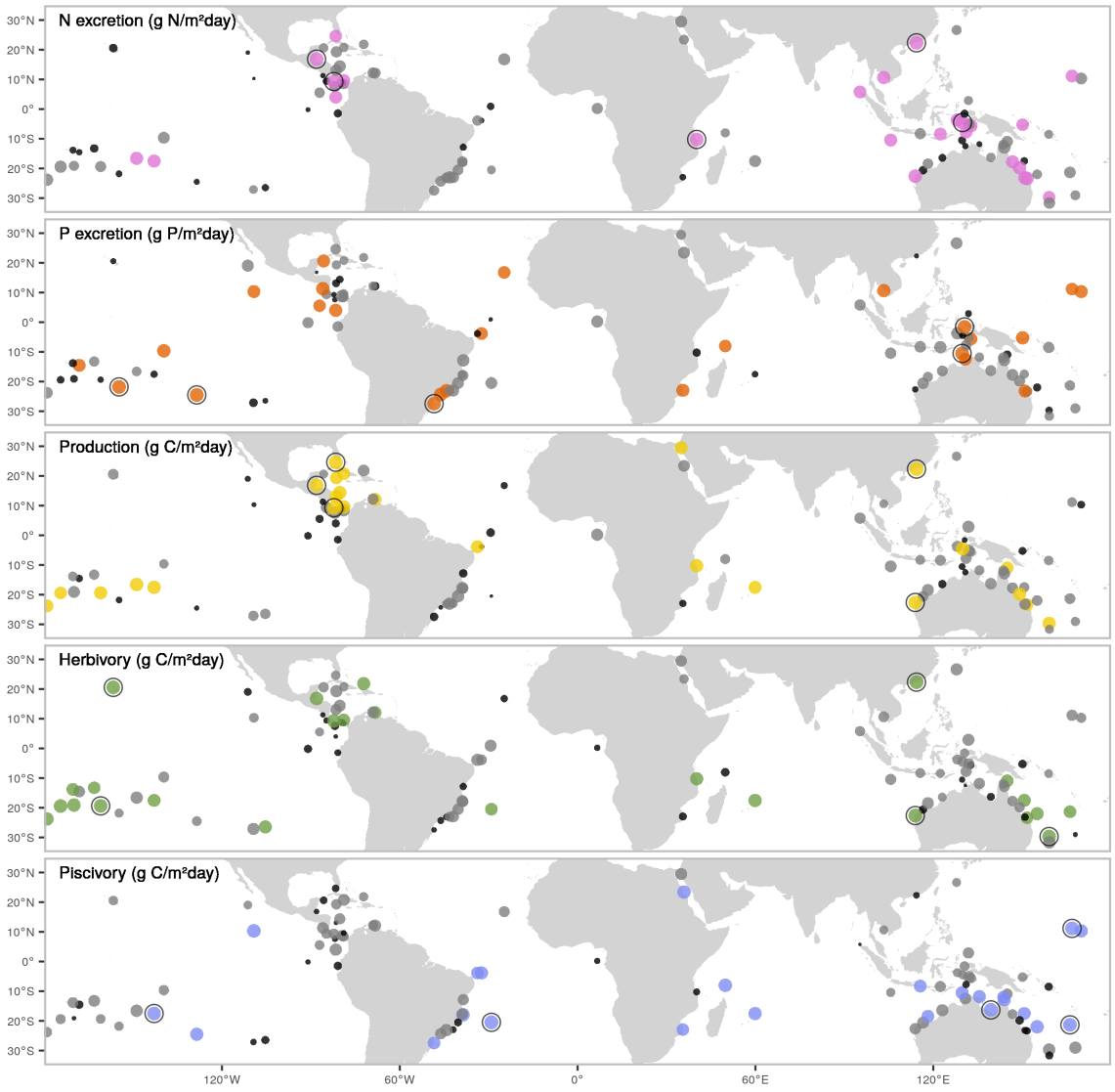

Figure 5.1: Spatial variation in five key, biomass-corrected ecosystem functions. Dots indicate locations of field surveys, with dot sizes representing the ranked values of biomass-corrected function, and color scales showing categorical assignments (black = lower 25%, grey = 25-75%, color = >75%). Black circular outlines highlight the five locations with the highest values of each biomass-corrected function.

Community structure and species-specific traits clearly impact rates of functioning. First, using community-level ecological predictors known to affect elemental fluxes (body size, trophic level, species richness, biomass, temperature, and age structure (Schiettekatte *et al.* 2020); figure 5.2), we show that correlations between functions are mediated by contrasting aspects of community structure (figure 5.2; figure 5.6). For example, phosphorus excretion and piscivory are higher in communities that include large-bodied fishes or occupy high trophic levels (figure 5.2; Allgeier *et al.* (2014)). In contrast, biomass production is highest in communities dominated by small and immature fishes at low trophic levels, creating a trade-off between biomass production and phosphorus excretion. Metabolic theory predicts that small-bodied individuals have higher mass-specific metabolic rates, leading to elevated consumption rates and disproportionate contributions to functions that rely on rapid energetic turnover (Barneche & Allen 2018; Brandl *et al.* 2019b; Morais *et al.* 2020a). Conversely, fishes in early life stages or with a nutrient-poor diet are often limited by phosphorus (Schiettekatte *et al.* 2020), resulting in low contributions to phosphorus excretion. Thus, due to variations in organismal physiology and life-history traits (Schiettekatte *et al.* 2020), fish community structure significantly impacts ecosystem-wide functioning (Schramski *et al.* 2015).

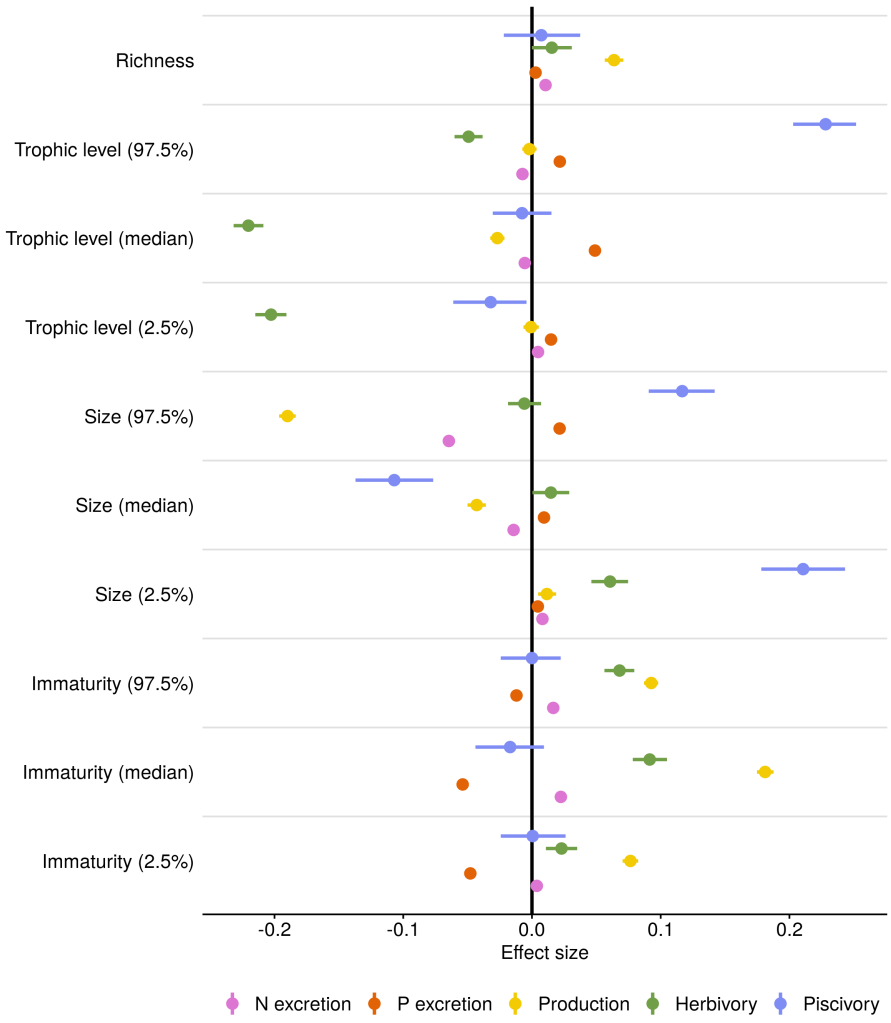

Figure 5.2: Effects of ecological community variables on five functions. Fixed effect values from Bayesian linear regressions that examine effects of species richness, trophic level, size, and immaturity of fishes. To represent both the median and the spread of trophic level, size, and immaturity across individuals inside a community, we included lower and upper 95% quantile values of these three traits as community variables. All data were log-transformed and standardized to compare across functions and variables. Dots represent the average effect size estimate, and horizontal lines indicate the 95% credible interval.

Secondly, alongside community structure, functions may also be influenced by specific high-performing taxa (figure 5.3a; figure 5.7; figure 5.8), which may disproportionately impact rates of functioning at the community level due to high biomass or abundance (Topor *et al.* 2019). At the local scale, we show that functions consistently hinge on a few dominant species (figure 5.3b). Specifically, on average, more than 50% of a given function is upheld by only 12% of the species present within a local community. However, the identity of these species varies dramatically among reefs (figure 5.3c). While few high-performing taxa dominate functioning in each location, there are no species that are dominant across their entire range. In addition, 70% of all species contributed disproportionally to a specific function in at least one community. Despite high species richness on coral reefs, researchers often report the existence of functionally-dominant "key species" (e.g., Bellwood *et al.* 2006). Our results reveal that while functional dominance is indeed prevalent, the identity of local, dominant species varies strongly across locations (Lefcheck *et al.* 2019).

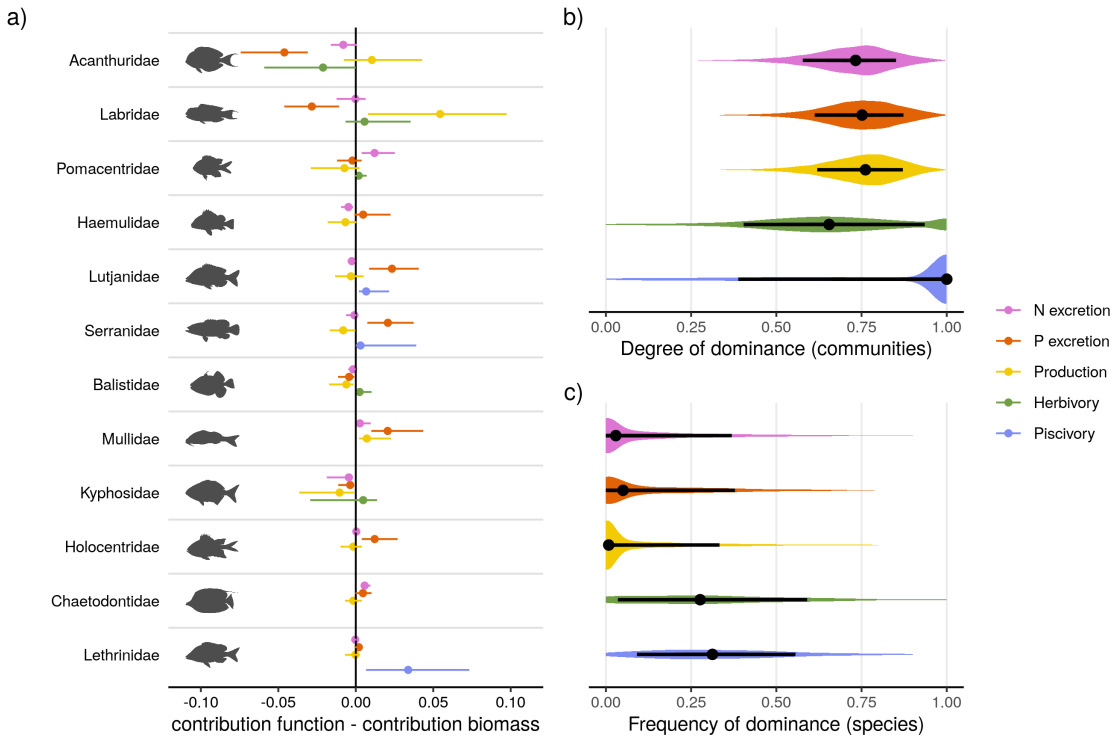

Figure 5.3: Family and species-level contributions to five ecosystem functions on coral reefs. a) The median family-level contributions to each function relative to their contribution to standing stock biomass. The twelve included families are ordered by their median contribution to biomass. b) The distribution of the degree of dominance of communities for each function. Degrees of dominance range between zero (all species contribute equally) and one (a single species is the sole contributor to a given function). c) Species-specific frequencies of dominance in each function across all communities, ranging from zero (species are never dominant) to one (dominant wherever present). A species is categorized as dominant in a community if its contribution to a function is higher than a scenario in which all species are equal (i.e., one divided by the number of species that contribute to the function). Shaded areas show the distribution of the values. Dots represent the median value, and lines indicate the interquartile range.

The critical importance of both reef fish community structure and species-specific contributions shines new light on the vulnerability of coral reef functioning in our changing world. Anthropogenic stressors have caused severe changes in reef fish biomass and community structure (Hughes *et al.* 2017), and our findings suggest that these changes will have strong effects on ecosystem functioning. For example, intensive fishing and associated reductions in biomass of large fishes truncates the size, age, and trophic structure of fish communities (Graham *et al.* 2017). When accounting for the effect of biomass, these effects can enhance nitrogen excretion and production (e.g., Morais *et al.* 2020a) but negatively impact phosphorus excretion, herbivory, and piscivory (figure 5.2). On the other hand, declines in coral cover related to climate change are often associated with a shift toward herbivores, which may deter algal domination (Graham *et al.* 2006). However, herbivores have a minor contribution to phosphorus excretion (Allgeier *et al.* 2014; Schiettekatte *et al.* 2020), so a shift to herbivore dominance and the subsequent decline of community-level phosphorus excretion may change the balance of nutrient cycling on reefs, potentially favoring algal growth (Burkepile *et al.* 2013). Thus, considering multiple functions paints a more nuanced picture of how human-induced shifts in reef fish community structure may impact coral reef ecosystems.

Similarly, the species-specific vulnerability of functionally-dominant species heavily affects the vulnerability of functions. By combining species-level vulnerability scores to fishing and climate change induced coral loss (Graham *et al.* 2011) and the contributions of each species to each function, we illustrate that the loss of individuals most vulnerable to fishing will have greatest impacts on piscivory, followed by phosphorus excretion (figure 5.4). Conversely, the loss of individuals due to climate change and consequent coral mortality may disproportionally reduce phosphorus excretion, nitrogen excretion, and biomass production. Combined, fishing and the loss of live coral impact species important for phosphorus excretion. Surprisingly, although fishing pressure can negatively impact large herbivores such as parrotfishes (Bellwood & Choat 2011), herbivory is the least vulnerable function. This may be due to the high

variability in ecosystem roles within the comparatively large pool of herbivorous fish species. Small herbivores are abundant and not particularly vulnerable to fishing, but larger herbivores are frequently targeted and prone to functional extinction in areas with high fishing pressure (Bellwood *et al.* 2012). While herbivores of all body sizes and functional groups are combined in our assessment, their realized contributions to herbivory are strongly complementary and, thus, potentially more vulnerable.

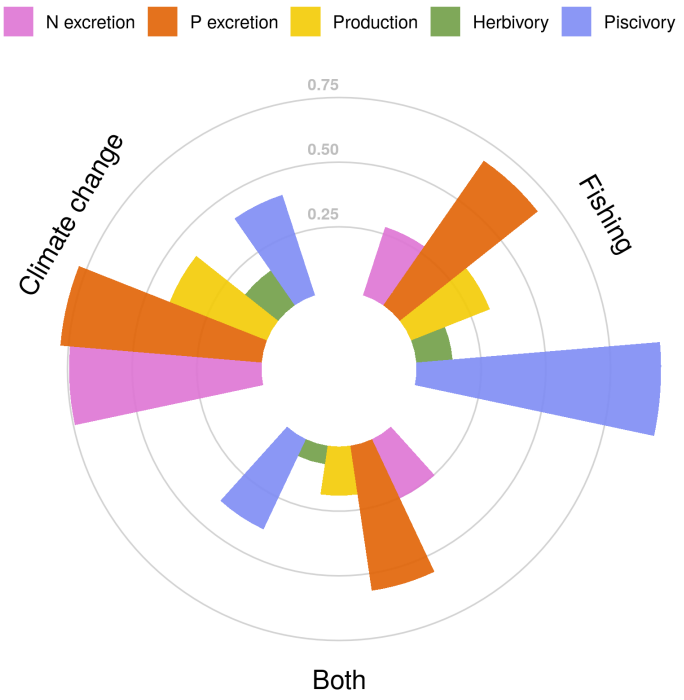

Figure 5.4: Vulnerability of five critical functions to fishing, climate change-induced coral loss, and both stressors combined. Vulnerability is presented as the proportion of communities (filled bars) in which functional vulnerability is higher than vulnerability based on fish biomass (i.e., not accounting for species contributions to each function).

Conserving biomass, diversity, and ecosystem functions are important objectives of most conservation initiatives (Cinner *et al.* 2020). While safeguarding fish biomass enhances functioning, the trade-offs between key functions reveal a critical challenge for coral reef conservation, where actions to enhance one function may negatively impact another. For example, the establishment of marine protected areas, which are one of the primary conservation tactics for coral reefs (Graham *et al.* 2020), may protect herbivorous species and thus provide benefits for herbivory. However, marine protected areas do not protect reefs from the pervasive effects of climate change (Graham *et al.* 2020), and community shifts towards herbivore domination may result in the decline of phosphorus excretion. Thus, measuring conservation success with biomass or solely one function (e.g., herbivory) can mask the collapse of other essential functions. It is necessary to gauge the state of reef ecosystems based on multiple, complementary, process-based functions (Brandl *et al.* 2019a), as well as making informed decisions on local needs and stressors. While there is a general consensus on the role of diversity in enhancing functioning (Zavaleta *et al.* 2010), we highlight the importance of community structure and the identity of dominant species at the local scale. Maintaining the diversity of fishes is critical, yet, at local scales, species richness has a minor impact on individual functions. Importantly, dissimilarity between local communities may be critical to maintain functioning across seascapes since no species consistently provides high contributions for all functions or across its range (Zavaleta *et al.* 2010).

Overall, we demonstrate that the variability in processes that govern the elemental cycling presents an unrecognized challenge for protecting ecosystem functioning. Management strategies that call for the enhancement of coral reef functioning via an economic mindset (i.e., where higher functioning is better) are not feasible. Instead, conserving coral reef ecosystem functioning will require a more nuanced approach that considers processes that vary beyond the effect of standing stock biomass and are subject to variable, local trade-offs, drivers, and anthropogenic threats.

5.3 Materials and methods

5.3.1 Underwater visual census database

We used a published global database of reef fish abundance and sizes collected along belt transects (Barneche *et al.* 2019). This database encompasses 9118 transects across 585 sites (98 localities) in the Central Indo-Pacific, Central Pacific, Eastern Pacific, Western Indian, Eastern Atlantic, Western Atlantic. The database only includes sites at the outer reef slope and with a hard reef bottom. Transects were carried out at a constant depth, parallel to the reef crest. We selected the species inside families for which we have body stoichiometric data, that were at least 7cm to minimize the bias related to the identification of small individuals, and finally we discarded rare species, for which less than 20 individuals were ever recorded across all transects. The dataset then included 1110 species that belong to 25 families (Acanthuridae, Balistidae, Bothidae, Chaetodontidae, Cirrhitidae, Fistulariidae, Haemulidae, Holocentridae, Kyphosidae, Labridae, Lethrinidae, Lutjanidae, Monacanthidae, Mugilidae, Mullidae, Ostraciidae, Pempheridae, Pomacanthidae, Pomacentridae, Sciaenidae, Scorpaenidae, Serranidae, Siganidae, Tetraodontidae, Zanclidae).

5.3.2 Bioenergetic modeling

Here, we focused on 5 key processes mediated by fish: N excretion rate ($gN/day/m^2$), P excretion rate ($gP/day/m^2$), production of body mass through growth ($gC/day/m^2$), herbivory, i.e., ingestion rate of macrophytes ($gC/day/m^2$), and piscivory, i.e., ingestion rate of fishes ($gC/day/m^2$). These 5 processes were estimated in each transect using individual-based bioenergetic models that predicts elemental fluxes, including ingestion rate, excretion rates of N and P, and growth rate. The bioenergetic model framework integrates elements of metabolic theory, stoichiometry, and flexible elemental limitation (Schiettekatte *et al.* 2020). We

quantified the input parameters, including elements of metabolism, growth, and diet and body stoichiometry, for all 1110 species through the integration of empirical data, data synthesis, and Bayesian phylogenetic models (see chapter 4). We ran the model for each combination of species identity, body size, and sea surface temperature (n = 30668) to get the contribution of each individual to each process in each transect and the cumulated estimates for the fish community per surface area. Each process is thus expressed in dry mass per day per square meter. We note that N excretion, P excretion, and biomass production include contributions of all fishes, whereas herbivory and piscivory are carried out by a subset of the community, with respect to their trophic guild (Parravicini *et al.* 2020). To reduce the occurrence of misclassification of herbivores and piscivores, we categorized a species as a herbivore or piscivore if it had both the highest probability to be classified in that trophic group and this probability was more than 0.5, based on the probability scores of trophic guilds for a global fish species database that defines trophic guilds based on empirical data using a quantitative, unbiased, and fully reproducible framework (Parravicini *et al.* 2020). Further, as a comparison, we quantified herbivory and piscivory rates using two alternative trophic guild classifications based on expert opinion (Mouillot *et al.* 2014; Parravicini *et al.* 2020) (figure 5.9). Both the herbivory and piscivory rates are congruent with the expert opinion trophic guild classifications.

5.3.3 Relationship between functions and biomass

The standing stock biomass of communities is inevitably related to all functions because of the additive nature of the quantification and general metabolic theory. Furthermore, because of the known relationship between temperature and parameters related to growth and respiration, all functions are also positively correlated with temperature. To model the effect of biomass and sea surface temperature (sst), we performed a Bayesian regression of each log-transformed function for community-level

(i.e., transect-level) observations (y_j):

$$y_{\mathrm{j}} \sim N(\mu_j, \sigma_j),$$

$$\mu_{\mathrm{j}} = \beta_0 + \beta_1 x_{log(biomass),j} + \beta_2 x_{sst,j}$$

We then assessed the covariation between functions, independent of biomass and sst. To do so, we first extracted the median residuals for each function per transect. In some transects, there were no piscivores or herbivores observed. In those cases, we did not include these transects in the analysis. We then quantified the correlations that exist among the different functions using these median residuals. Finally, for the purpose of visualizing the residual variation of functions per locality on a world map, we ran a supplemental model, similar to the model described above but including random effects both per site and locality. We then extracted and plotted the location effects, which can be interpreted as the average variation per locality.

5.3.4 Effect of community structure on ecosystem functions

To investigate the effect of the community structure while still accounting for the effects of standing biomass and sea surface temperature, we quantified a set of variables that characterize the community. These variables describe the size, age, and trophic distribution of the community, as these may all affect functions (Schiettekatte *et al.* 2020). Specifically, we calculated the 2.5%, 50% and 97.5% quantiles of the total length, immaturity, and trophic level of all individuals per transect. The total length is based on the visual estimation by divers. The immaturity is quantified using the following formula:

$$\mathrm{immaturity}_{\mathrm{i}} = \kappa(\mathrm{l}_\infty - \mathrm{l}_{\mathrm{i}}),$$

where κ is the species-specific growth rate parameter and l_∞ is the species-specific asymptotic adult length, and l_i is the total length of individual i. Essentially, this is the derivative of the Von Bertalanffy growth model for a certain length, and the higher this value is, the younger the individual. Finally, the trophic level was extracted from fishbase (Froese & Pauly 2018). Additionally, we quantified the transect-level species richness. For each log-transformed function we then fitted a Bayesian mixed-effect model with all 12 above-mentioned variables, after verifying that there are no strong correlations between variables (the highest correlation coefficient was 0.5, and 50% of the variable pair correlations varied between -0.1 and 0.2).

$$y_{\mathrm{j}} \sim N(\mu_j, \sigma_j),$$

$$\begin{aligned}\mu_j = \beta_0 + \beta_1 x_{log(biomass),j} + \beta_2 x_{sst,j} + \beta_3 x_{richness,j} + \beta_4 x_{size_m,j} + \\ \beta_5 x_{size_{2.5\%},j} + \beta_6 x_{size_{97.5\%},j} + \beta_7 x_{troph_m,j} + \beta_8 x_{troph_{2.5\%},j} + \\ \beta_9 x_{troph_{97.5\%},j} + \beta_{10} x_{imm_m,j} + \beta_{11} x_{imm_{2.5\%},j} + \beta_{12} x_{imm_{97.5\%},j}\end{aligned}$$

To compare effects across functions and assess the relative importance of each variable, we standardized all variables prior to model fitting. We fitted all 5 models by using 4 cores, that each had 2000 iterations with a warm-up of 1000 iterations, and used weakly-informative priors (Burkner PC 2017).

5.3.5 Species dominance and contributions to functions

We quantified the relative contribution of each species to each function for each transects as followed:

$$\text{contribution}_{f,i,j} = \frac{F_{f,i,j}}{\sum F_{f,j}},$$

where i is a certain species, j is a transect, F is the value of function f.

Then, we quantified the degree of species dominance per function for each transect. We did this by first ranking species according to their contribution to function,

followed by quantifying the cumulative contributions of species to functions. Then, we used the area under the species accumulation curve as a measure for the degree of dominance. Specifically, the degree of dominance (DD) was calculated as followed:

$$\mathrm{DD} = \frac{A - A_{min}}{A_{max} - A_{min}},$$

where A is the area under the curve, A_{min} is the theoretical area under the curve where each species has an equal contribution to a certain function, A_{max} is the theoretical area under the curve where one species performs the entire function. They are quantified as:

$$\mathrm{A}_{min} = \frac{R^2 - 1}{2R},$$

$$\mathrm{A}_{max} = R - 1,$$

$$\mathrm{A} = \sum_{i=2}^{R} \frac{C_i + C_{i-1}}{2},$$

where C_i is the contribution of a certain species and R is the number of species contributing to a certain function. The degree of dominance thus ranges between 0 and 1, where 0 means that each species contributes equally and 1 means that a single species performs the entire function. In the case of N excretion, P excretion, and production, R equals the species richness, while for herbivory and piscivory R represents the number of herbivores and piscivores, respectively.

Finally, to know how often species are contributing more than average for a certain function, we quantified the frequency of dominance, i.e., the number of times a species is dominant divided by the total number of transects in which that species is observed. A species is considered dominant for a certain function in a given transect if their contribution is higher than 1/R, i.e., they contribute more than the situation in which each species contributes equally to a certain function.

5.3.6 Vulnerability to fishing and climate change

For each species, we quantified two measures of vulnerability: vulnerability to climate change and vulnerability to fishing pressure (Graham *et al.* 2011). For species' vulnerability to climate change, we solely focus on their vulnerability to the loss of live corals. Vulnerability to climate change induced coral loss is related to diet specialization, habitat specialization for live coral and body size (Graham *et al.* 2011). Graham *et al.* (2011) developed a score for climate change vulnerability for 134 species. We used these scores to fit a Bayesian mixed effect predictive model that relates the vulnerability with the log-transformed maximum size of fish (extracted from Fishbase Froese & Pauly (2018)), the dependence on coral for food (3 categories: not dependent, facultative corallivore, and obligate corallivore), and dependence on coral for habitat (2 categories: dependent vs. not dependent) (Cole *et al.* 2008; Coker *et al.* 2014). We also included a random effect for family. To verify the fit of the model we inspected the posterior predictive plot, which indicated a good fit. Further, the model had a Bayesian R2 of 0.97. We thus used this model to extrapolate the vulnerability measure to all 1110 species in our dataset. For species' vulnerability to fishing, we extracted the index from Cheung *et al.* (2005). Next, we calculated vulnerability scores per function on the community level by averaging the species-level scores weighted by the contributions to function of those species. We also calculated community-level vulnerability scores based on biomass contributions as a comparison. Finally, we calculated the proportions of communities that had a higher vulnerability score of functions, compared to the vulnerability score based on biomass alone. In other words, we quantified the proportions of communities that have an increased functional vulnerability.

5.4 Supplementary information

Acknowledgements: We thank the staff at CRIOBE, Moorea for field support. We would also like to thank Jérémy Carlot, Beverly French, Titouan Roncin, Yann Lacube, Camille Gache, Gabrielle Martineau, Kailey Bissell, Benoit Espiau, Calvin Quigley, Kaitlyn Landfield and Tommy Norin for their help in the field, Sophie Schiettekatte for proof-reading the manuscript, and Guillemette de Sinéty and Jérémy Wicquart for their contribution to otolith analyis.

Funding: This research was funded by the BNP Paribas Foundation (Reef Services Project) and the French National Agency for Scientific Research (ANR; REEFLUX Project; ANR-17-CE32-0006). This research is product of the SCORE-REEF group funded by the Centre de Synthèse et d'Analyse sur la Biodiversité (CESAB) of the Foundation pour la Recherche sur la Biodiversité (FRB) and the Agence Nationale de la Biodiversité (AFB). VP was supported by the Institut Universitaire de France (IUF) and JMC was supported by a Make Our Planet Great Again Postdoctoral Grant (mopga-pdf-0000000144).

Author contributions: NMDS and VP conceived the idea and NMDS, VP, SJB, and JMC designed methodology; NMDS, JMC, SJB, AM, FM, VP, KSM, JEA and DEB collected the data; All authors shared existing data. NMDS analyzed the data and led the writing of the manuscript. All authors contributed significantly to the drafts and approved the final version for publication.

Competing interests: None declared.

Data and materials availability: All data and code to reproduce figures are available online through GitHub (`https://github.com/nschiett/global_proc`) and figshare (`https://figshare.com/s/f789aec2c20492c4f0f9`). All data on individual fish traits are available from the corresponding author on reasonable request.

5.5 Supplementary figures

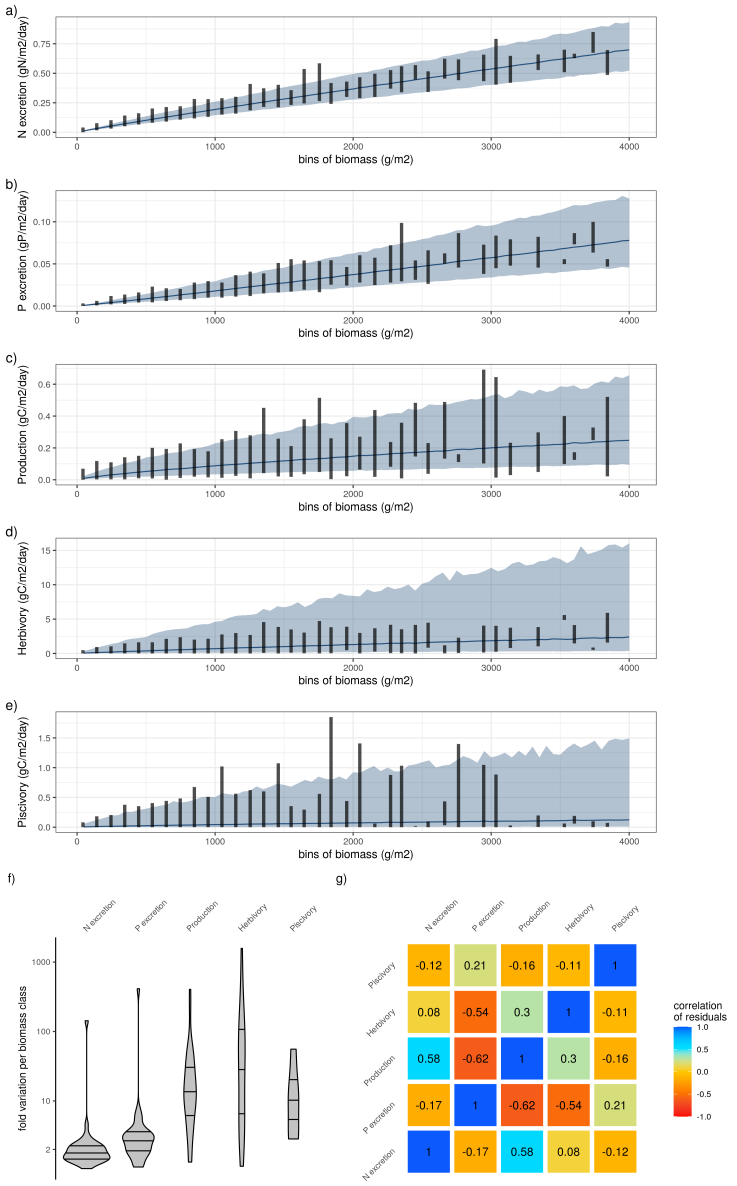

Figure 5.5: a-e) Relationship between biomass and the five functions. Lines and shaded areas show the average and 95% credible interval of the predicted functions respectively, for a constant sea surface temperature of 26 degrees (the average across all sites). Vertical lines show the range of the estimated functions across fish communities per biomass class of 100g/m2. f) Fold variation of each function per biomass class of 100g/m2 across fish communities. g) Correlation matrix of the residuals of the five functions after regression with biomass and sea surface temperature. Standard deviations of correlation coefficients did not exceed 0.01.

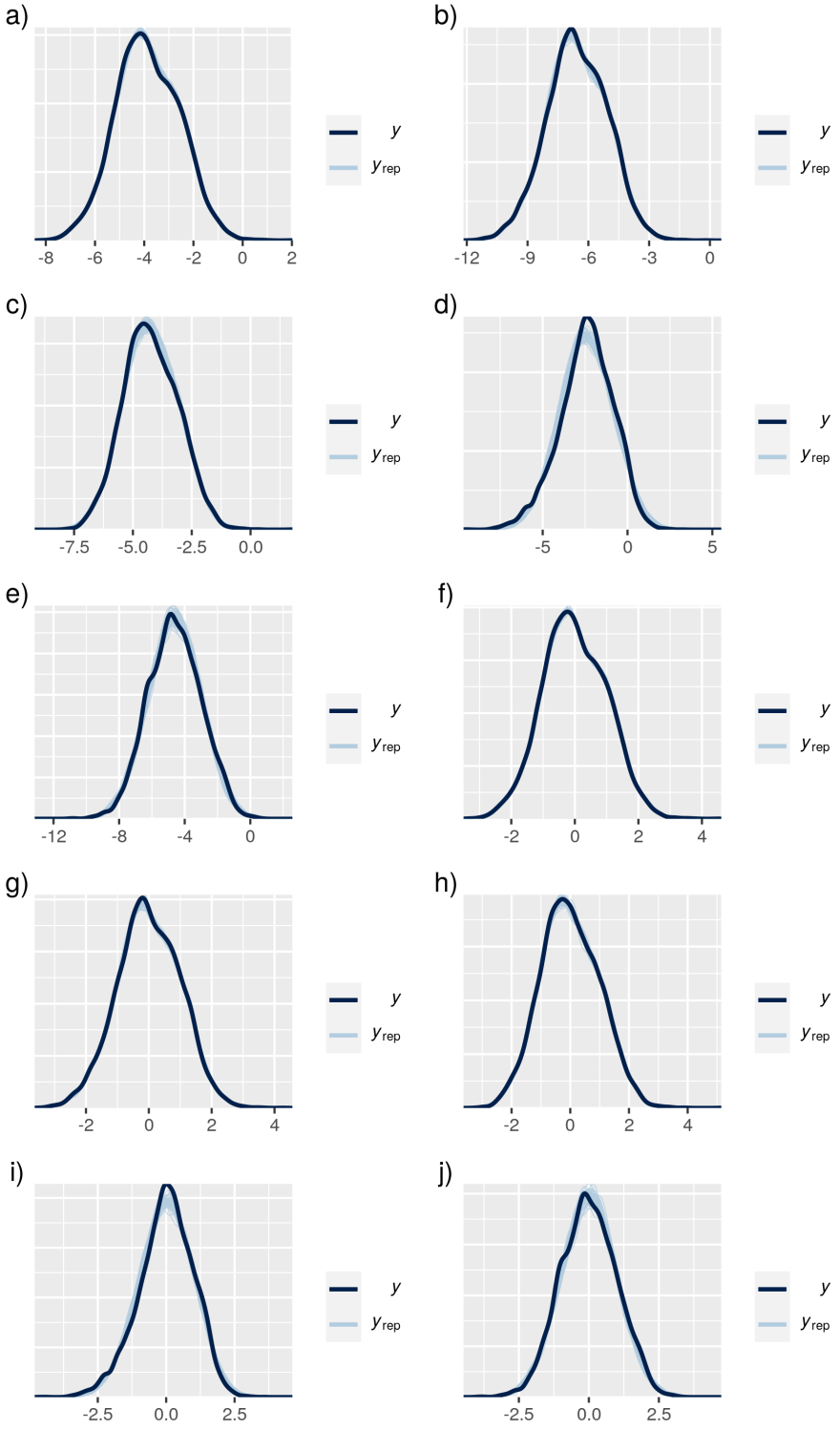

Figure 5.6: Posterior predictive checks of the five models relating functions with biomass and sea surface temperature only (a) N excretion, b) P excretion, c) Production, d) Herbivory, e) Piscivory), and the five models relating functions with community variables (f) N excretion, g) P excretion, h) Production, i) Herbivory, j) Piscivory)

Figure 5.7: Average relative contribution of fish families to all five functions per biogeographical ocean basin. CIP = Central-Indo-Pacific, CP = Central Pacific, EA = Eastern Atlantic, WA = Western Atlantic, WI = Western Indian

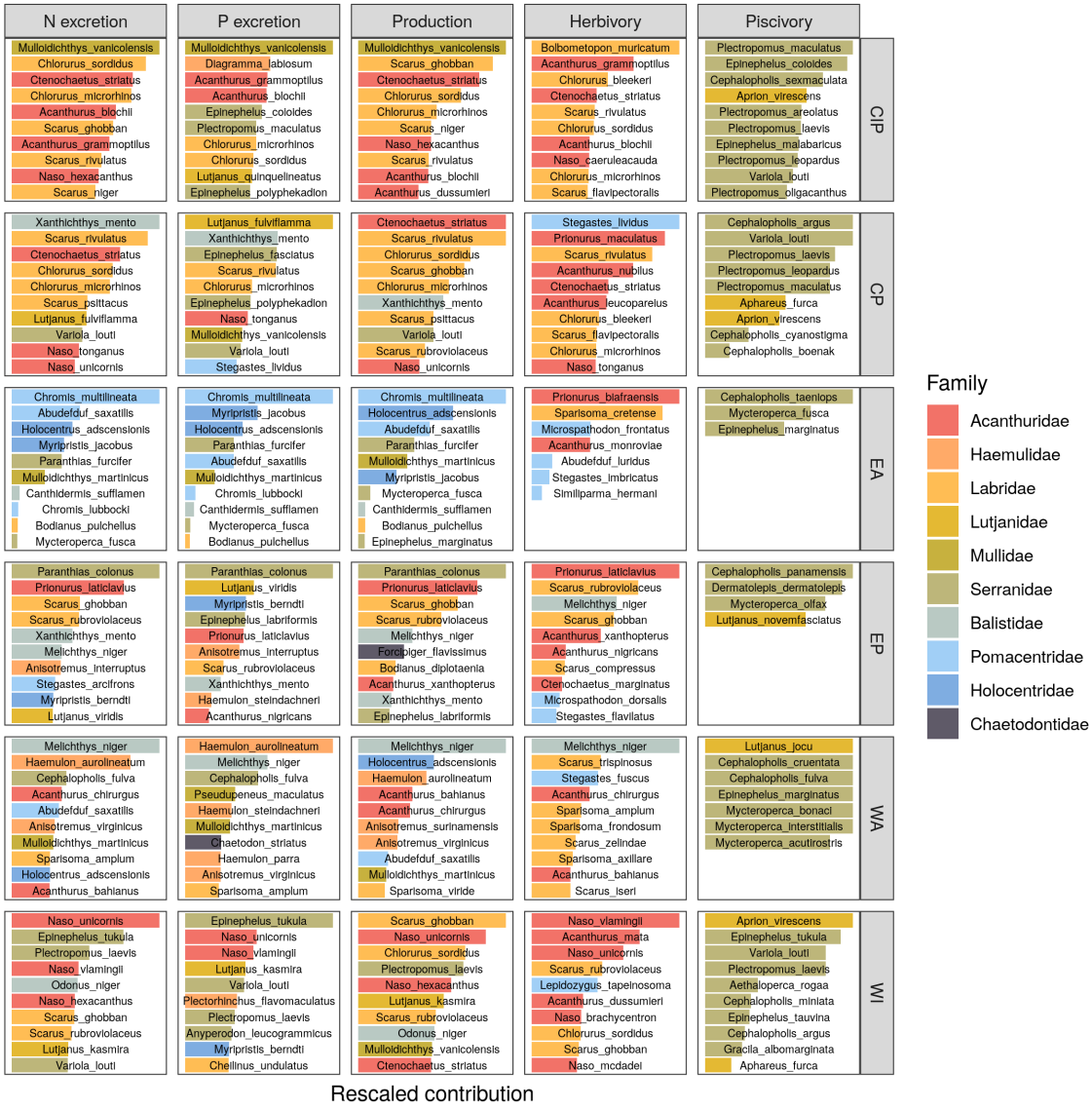

Figure 5.8: Average relative contribution of the top ten most contributing species to all five functions per biogeographical ocean basin. CIP = Central-Indo-Pacific, CP = Central Pacific, EA = Eastern Atlantic, WA = Western Atlantic, WI = Western Indian

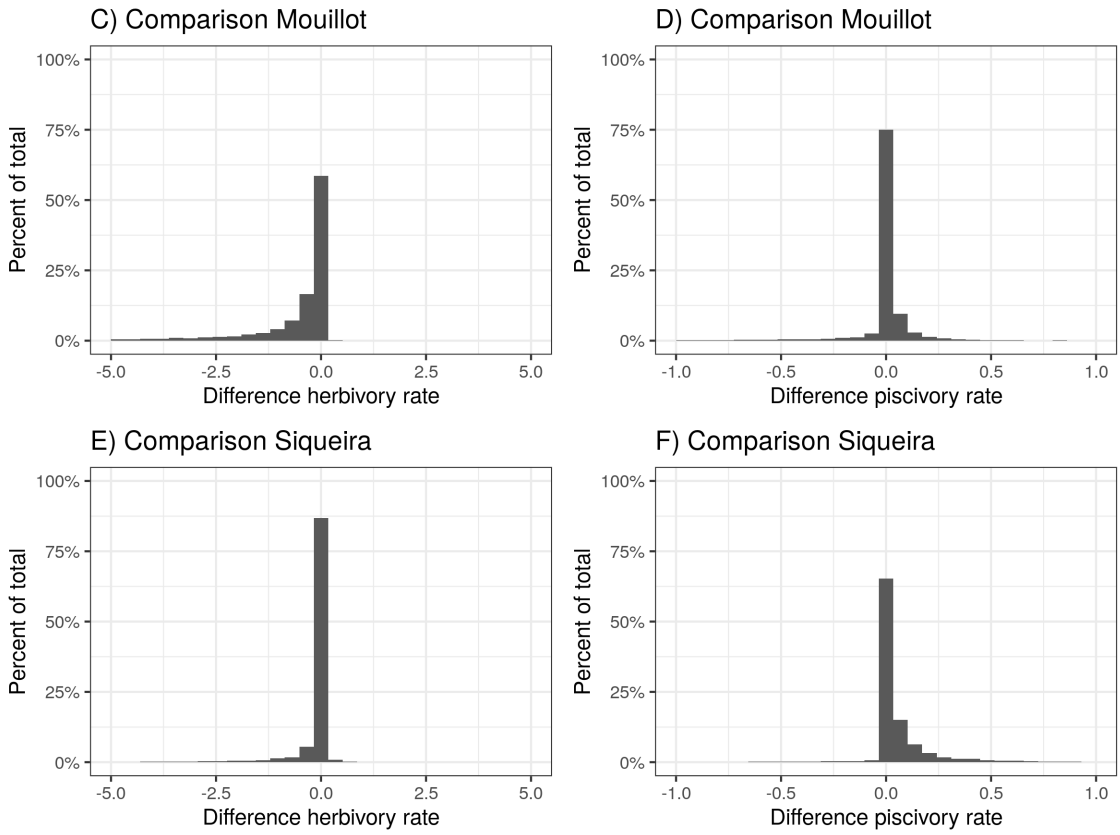

Figure 5.9: Comparison herbivory and piscivory rates when using alternative diet classifications from Mouillot et al. (2014) and Siqueira et al. 2020

Part III: Missing links

Part I and II of my thesis focused on quantifying functions on the individual and community levels. However, there are still many gaps hampering quantification of fish-mediated functions. The third part of my thesis focuses on two elements that have been understudied but heavily impact functioning: fish egestion (chapter 6) and the medabolic rate of fishes in their natural environment (chapter 7).

First, although the importance of fish excretion for coral reefs has increasingly received attention over the past decades, the role of fish egestion is still poorly understood. In chapter 6, I investigate the role of fish egestion by estimating elemental contents of fish feces and quantifying element-specific absorption efficiencies across a wide range of species.

Second, the metabolic rates of fishes have a large influence on the flux of energy and elements. The most commonly studied element of metabolic rate is the standard metabolic rate; i.e., the energy consumption of a fish in rest. However, in the wild, fishes need more energy to perform a suite of activities, and little is known about the field metabolic rate of fishes in their natural environment. In chapter 7, I propose a novel approach to estimate the field metabolic rates of coral reef fishes.

Chapter 6

The role of fish feces in coral reef nutrient-cycling

This chapter is in preparation for *Oikos*.

Authors:

Nina M. D. Schiettekatte, Jordan M. Casey, Simon J. Brandl, Alexandre Mercière, Sam Degregori, Deron Burkepile, Jacey Van Wert, Sébastien Villéger, Valeriano Parravicini

6.1 Abstract

Consumers play an important role in biogeochemical cycles through the consumption and release of essential elements such as carbon (C), nitrogen (N), and phosphorus (P). Indeed, a large proportion of consumed elements are rapidly released back into the environment in inorganic (i.e., excretion) or organic form (i.e., egestion). On coral reefs, fishes represent a large part of the consumer biomass and thus play a key role in the recycling of nutrients. In recent years, excretion rates have been studied intensively, but less is known about the rate and quality of coral reef fish egestion. Nonetheless, fish feces can be an important food source for other animals or fuel the microbial community. In this study, we aim to fill this knowledge gap by quantifying the elemental contents of fish feces, estimating absorption efficiencies, and comparing egestion and excretion rates for 51 coral reef fish species. We show that elemental concentrations decrease remarkably little from food to feces, due to predominantly low absorption efficiencies, resulting in large amounts of energy and nutrients being egested. Moreover, we highlight that the quality of fish feces varies across trophic guilds but remains highly variable even within trophic guilds. Finally, we demonstrate that the N and P release is higher in fish egestion compared to excretion for most species. Overall, our study affirms the need for incorporating animal egestion alongside excretion in assessments of ecosystem functioning and food web structures.

6.2 Introduction

Aquatic consumers play an essential role in biogeochemical cycles through consumption, assimilation, and release of major elements such as carbon (C), nitrogen (N), and phosphorus (P) (Sterner & Elser 2002). A large proportion of consumed elements is not assimilated and released back into the environment in either inorganic or organic form (Kraft 1992; Sterner & Elser 2002). Inorganic nutrient release (i.e., excretion) strongly impacts primary producers, particularly in systems limited by nitrogen or phosphorus (Turner 2002; Doughty *et al.* 2016). In particular, dense aggregations of consumers can create hotspots of N and P and boost primary productivity (e.g., McIntyre *et al.* 2008; Shantz *et al.* 2015). On the other hand, organic release (i.e., egestion) can either serve as a food source for other consumers which in turn release inorganic nutrients (Robertson 1982; Le Mézo & Galbraith 2021) or, if not consumed directly, provide a substrate for decomposing heterotrophic bacterial communities (Turner 2002; Halvorson *et al.* 2017a; Parr *et al.* 2019).

Egestion represents a dominant and dynamic animal-mediated elemental flux (Halvorson & Atkinson 2019). While there is a general assumption that egestion is less important for elemental cycling because of its low bioavailability and nutrient-poor organic form (Atkinson *et al.* 2014; Halvorson & Atkinson 2019), N and P in the form of egestion actually exceed N and P excretion fluxes in many aquatic consumers (Liess 2014; Halvorson & Atkinson 2019). The quality of egesta determines whether it may serve as a direct food source for other animals, which may ingest feces with a nutritional quality that exceeds their diet (Bailey & Robertson 1982). In fact, coprophagy (i.e., the consumption of feces) is a common phenomenon across a variety of ecosystems, and may play an important trophic role by immediately re-integrating valuable elements into the food web (Frankenberg & Smith 1967; Robertson 1982; Sazima *et al.* 2003; Le Mézo & Galbraith 2021).

The rate and quality of egestion depend on the food, the nutritional needs of the consumer, and element-specific absorption efficiencies (i.e., the proportion of the in-

gested material that is absorbed in the intestinal tract) of the consumer. Naturally, the quality of egestion (i.e., concentrations of C, N, and P) directly correlates with the quality of the diet (Sterner & George 2000), while also indirectly affecting the rate of consumption and thus egestion (Schiettekatte *et al.* 2020). Consumers with low diet quality such as herbivores (i.e., animals feeding on primary producers) or detritivores (i.e., animals feeding on detritus), for instance, compensate for the poor nutritional quality by increasing their consumption rates to reach their daily nutritional needs (Cruz-Rivera & Hay 2000). Since N and P are often the limiting element for the growth of aquatic herbivores and detritivores, compensatory feeding helps these consumers to reach their daily requirements (Schindler & Eby 1997; McIntyre *et al.* 2008; Evans-White & Halvorson 2017). Furthermore, compensatory feeding is promoted by the positive correlation between diet quality and absorption efficiency - consumers with low N or P diets also tend to have low absorption efficiencies of these elements (Pandian & Marian 1985; Halvorson *et al.* 2017b; Jochum *et al.* 2017). On the other hand, the digestive tract may act as a nutrient balancing organ by increasing the absorption efficiency of a limiting element, yet this phenomenon appears to be rare (Clissold *et al.* 2010).

On coral reefs, fishes represent a large part of the consumer biomass and play an essential role in the recycling of nutrients. While in recent years, excretion rates have been studied intensively (Allgeier *et al.* (2014); Allgeier *et al.* (2016); Francis & Côté (2018)), less is known about the rate and quality of coral reef fish egestion. Fish feces likely represent an important food source for coral reef fishes (Bailey & Robertson 1982; Robertson 1982) and invertebrates living in crevices where fishes rest at night (Pinnegar & Polunin 2006), little quantitative data exists on the rates of defecation, the uptake of feces, and the nutritional properties of feces. While bioenergetic models can be used to estimate rates of egestion, a lack of information on absorption efficiencies may introduce bias. To date, bioenergetic models applied in coral reef communities use constants for element-specific absorption efficiencies (e.g., Allgeier *et al.* 2014; Schiettekatte *et al.* 2020), which hampers the use of bioenergetic

models to quantify egestion rates.

Here, we aim to quantify the rate and nutritional quality of egestion for a wide range of reef fishes. Specifically, we estimate and compare the C, N, and P concentrations of the food and feces for 51 common coral reef fish species from 15 families in Mo'orea, French Polynesia. With these data we then estimate the element-specific absorption efficiencies and link them to each species' diet. Combining our data with historical observational data on defecation rates and consumption (Robertson 1982), we further establish potential coprophagic links through pairwise comparisons. Finally, we use our data to parametrize bioenergetic models, and compare the N and P flux in excretion and egestion at both species and community level.

6.3 Methods

6.3.1 Data collection and processing

We collected fishes in Mo'orea, French Polynesia across 62 sites distributed across lagoon and outer reef (figure 6.6). We targeted 51 common species from 15 fish families: Cirrhitidae, Zanclidae, Balistidae, Holocentridae, Chaetodontidae, Acanthuridae, Labridae, Aulostomidae, Mullidae, Serranidae, Pomacentridae, Pomacanthidae, Lethrinidae, Tetraodontidae, and Monacanthidae (see supplemental table 6.1). In total, we collected 620 individuals using spear fishing between 10am and 2pm between 2017 and 2019. Fishes were pithed immediately upon capture and transported to the laboratory in a cooler filled with ice. In the laboratory, fishes were measured, weighed, and dissected to expose the full alimentary tract. Samples of ingested material were then taken from the stomach and hindgut. For fishes that do not have a stomach (e.g., Labridae), a sample from the esophagus or foregut was taken instead. When the foregut or hindgut were empty, no sample was collected. The number of replicates per species is shown in table 6.1.

Samples were frozen for at least 24 hours, and then freeze-dried for transport for at least 24h. After lyophilization, samples were ground to a fine powder using a homogenizer. Homogenized samples were then sent to the University of Michigan Biological Station and CNP% concentrations were measured in the lab using standard methods (in g*g-1). Ground samples were analyzed for %C and %N content using a CHN Carlo-Erba elemental analyzer (NA1500), and for %P using dry oxidation-acid hydrolysis extraction followed by a calorimetric analysis (Allen *et al.* 1974). Elemental content was calculated on a dry weight basis.

Ash contents of food and feces samples were determined by combustion at 450 °C in a muffle furnace for at least 6h. The ash content was calculated by dividing the weight of the sample after combustion by the dry weight of the sample before combustion. Since the material was too limited for both nutrient and ash content analysis, we determined the ash content for a subset of samples to calibrate our data. Ash contents for missing species were estimated using information from the literature or based on an average estimate for each trophic guild (see supplemental table 6.2).

We divided the study species into six trophic guilds, mostly based on Parravicini *et al.* (2020) (6.1): detritivores (and heterotrophic microvores): species primarily feeding on detritus or microorganisms); herbivores: species primarily feeding on autotrophs; mixed invertivores: combined group of species (microinvertivores, macroinvertivores, and sessile invertivores) feeding on Asteroidea, Bryozoa, Cirripedia, Porifera, Annelida, Arachnida, Hemichordata, Nematoda, Peracarida, Nemertea, Mollusca and Echinodermata, and Tunicata; corallivores: species primarily feeding on Anthozoa and Hydrozoa; planktivores: species mainly feeding on zooplankton and Harpacticoida; and carnivores: species primarily feeding on Actinopterygii, Cephalopoda, Decapoda, and Stomatopoda.

While detritivores and herbivores are combined in Parravicini *et al.* (2020), we categorized *Acanthurus pyroferus*, *A. olivaceus*, *Ctenochaetus striatus*, and *Chlorurus spilurus* into a separate group of detritivores, according to direct inspection of the

gut in this study, in accordance to previous literature, and due to the considerable nutritional difference between algae and detritus/microbes (Choat *et al.* 2002; Eagle & Jones 2004).

Finally, in order to delineate potential coprophagous behavior, we extracted the data provided by Robertson (1982), which describes the uptake of feces by fishes in a coral reef fish assemblage. For each species, we extracted the number of defecation events as well as the number of feces observed being eaten by another fish species. Further, we compiled a table indicating whether or not a species was classified as a coprophage. We combined this information with our species-level estimates of food and feces nutrient content, resulting in a selection of 14 species. We then predicted the probability of feces being eaten with the nutrient content of feces. Furthermore, we predicted the probability of being a coprophage based on the nutrient composition of the diet.

6.3.2 Data analysis

We predicted the average food and feces content for C, N, and P by fitting a Bayesian regression model for each species with rstan (Carpenter *et al.* 2017). We fitted the data to a student-t distribution to decrease influence of outliers:

$$x_{i,k} \sim student(nu_{i,k}, mu_{i,k}, sigma_{i,k}),$$

where i is either food or feces, k is the element, $x_{food,k}$ and $x_{feces,k}$ are measures of the elemental content of the stomach and the end of the gut respectively, nu is the degrees of freedom, mu is the average elemental content, and $sigma$ is the standard deviation of the distribution.
We used weakly-informative priors:

$$mu_{i,c} \sim normal(30, 30),$$

$$mu_{i,n} \sim normal(5, 5),$$

$$mu_{i,p} \sim normal(1, 1),$$

$$sigma_{i,c} \sim cauchy(0, 5),$$

$$sigma_{i,n} \sim cauchy(0, 1),$$

$$sigma_{i,p} \sim cauchy(0, 0.5),$$

$$nu_{i,k} \sim gamma(2, 0.1)$$

Models were run on 4 chains, for 2000 iterations with 1000 iterations of warm-up for each chain. This resulted in 4000 estimates for each parameter. Using these estimates, we also calculated C:N, C:P, and N:P ratios of food and feces. Finally, we estimated the absorption efficiency. Because food and feces samples were taken at the same time, we could not assume that the food items in the stomach are the same as the digested material in the feces. Therefore, we considered them as independent samples, and we used the iterations of the modeled averages of food and feces contents. We calculated the absorption efficiency for each iteration using the following formula (Montgomery 1980):

$$a_k = 1 - (\frac{ash_{food}}{ash_{feces}} \frac{mu_{feces,k}}{mu_{food,k}})$$

For each parameter described above, we then calculated the mean, standard deviation, 95%, and 50% credible intervals.

To assess the relationship between the probability of being a coprophage and the N and P content, we fitted Bayesian binomial models:

$$y_{cop,k} \sim Bernoulli(eta_k)$$

$$logit(eta) = b0 + b1D_k,$$

where k is the nutrient (N or P), eta is the expected value, b0 is the intercept, b1 is the slope, and y_{cop} is the probability of being a coprophage. We fitted similar models

to relate the probability of feces being eaten with the nutrient content of feces.

Then, we tested the hypothesis if the elemental content of the food can predict the absorption efficiency. We did this by fitting the following Bayesian model using the R package brms with uninformative priors (Burkner PC 2017):

$$a_k \sim beta(mu_k phi, (1 - mu_k) phi),$$

$$logit(mu_k) = b0_k + b_k D_k$$

where k is the element (C, N, or P), b0 is the intercept, b is the slope, mu is the expected value, and phi is the dispersion parameter. mu represents a probability and must therefore be between 0 and 1. We, therefore, used a logit link function to map the linear predictor onto mu.

6.3.3 Bioenergetic models

Finally, we ran bioenergetic models for each species at their median measured body size to predict the N and P fluxes in excretion and egestion using fishflux (see chapter 2; Schiettekatte *et al.* (2020)). These models were parametrized with the elementary concentrations of food and absorption efficiencies estimated in the present study. For all other parameters, we used values quantified in chapter 4. We then calculated the ratios between egestion and excretion for N and P, and for the N:P ratio.

Finally, we estimated the P fluxes on the community level for the outer slope of Mo'orea. We used visual census data from 2009 to 2016 for 13 sites, recorded as a part of the CRIOBE long-term monitoring program. During each census, a single diver swam along a transect of 25 m and counted all fishes within a width of 2 m. All fishes were identified to the species level and their length was estimated to the nearest 1 cm.

Each transect covered an area of 50 m^2, except 2 sites (Tiahura and Haapiti), which covered an area of 100 m2 each. For each individual in the community, we fitted the described bioenergetic model and predicted the P flux in consumption, excretion, and egestion. Then by summing up these values, we estimated the total fluxes per trophic guild per square meter. Furthermore, we estimated the amount of P from egestion that is consumed by coprophagous fishes by multiplying the predicted probability of feces being consumed by half of the daily egestion rates. This calculation rests on the assumption that fishes release half of their daily egestion while resting close to the reef either by day or night. Since the metabolism and digestion of fishes is higher when they are active, such estimates of coprophagy are conservative. Finally, we averaged values across all sites and years and standardized the excretion and egestion rate of each trophic group by the total amount of P consumed by all fishes.

6.4 Results

6.4.1 Elemental stoichiometry of food and feces

The estimates of species-level elemental composition of the food of fishes varied among species to varying degrees for carbon (C), nitrogen (N) and phosphorus (P) (figure 6.1, figure 6.7, table 6.3). The C content of food varied 4.5-fold from 10.0% for *Acanthurus pyroferus* to 45.5 % for *Myripristis berndti*, and the C content of fish feces varied 2.7-fold from 15.5 % for *Acanthurus pyroferus* to 41.5% for *Chromis xanthura*. The N content of food varied 12.9-fold from 0.9% for *Acanthurus pyroferus* to 11.5 % for *Aulostomus chinensis*, and the N content of fish feces varied 8.2-fold from 1.1 % for *Acanthurus olivaceus* to 9.0% for *Forcipiger flavissimus*. The P content of food varied 27-fold from 0.1% for *Ctenochaetus striatus* to 2.7 % for *Cephalopholis urodeta*, and the P content of fish feces varied 10-fold from 0.2 % for *Ctenochaetus striatus* to 2.0% for *Chromis xanthura*. When comparing food and feces compositions, we found a remarkably low difference between them for many species (figure 6.1). For C and P, the percentages in feces were rarely lower than 50% of the food. For N, only 14 species had an N percentage in the feces that was less than half of the food. We found a higher C, N, and P content in feces than in food for 10, 19, and 22 species respectively.

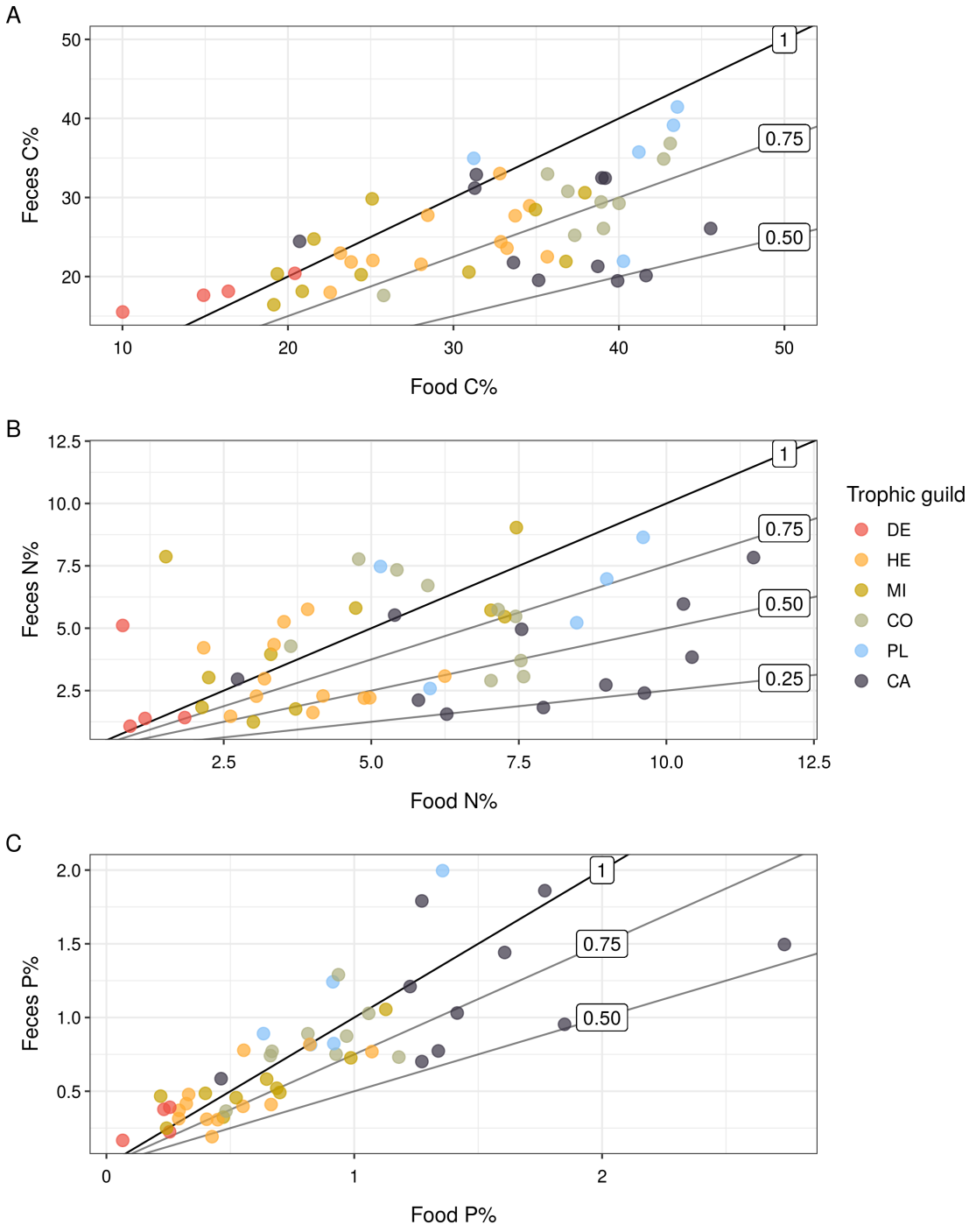

Figure 6.1: The estimated average carbon (A), nitrogen (B), and phosphorus (C) contents of food and feces. Lines indicate the ratio of the elemental content of the feces and the food. DE = detritivores, HE = herbivores, MI = mixed invertivores, CO = corallivores, PL = planktivores, CA = carnivores.

Comparing the percentage of N and P of food and feces among all species, we found that many species have a lower N% or P% value compared to the feces of other fishes (figure 6.2A,B; figure 6.8). In particular, detritivorous and herbivorous fishes had a much lower nutrient concentration in their food compared to the feces of other trophic groups. For N, corallivorous and planktivorous fishes showed a high N content in their feces compared to the food of lower trophic groups. For P, planktivores and carnivores had the most P-rich feces. Specifically, for 677 (27%) of all 2550 potential pairwise comparisons among species, the food N% was lower than the feces N%, and for 915 (36%) pairwise comparisons, the food P% was lower than the feces P% (with no overlap of 75% credible intervals of food and feces N% and P% of comparing species). Further, by coupling our compositional data with observational data found in the literature (Robertson 1982), we reveal that the probability of being a coprophage can be predicted by the N% or P% found in the food, such that the lower the nutrient content in the food, the higher the chance of being coprophagous (figure 6.2C,D; the slopes of the binomial regressions are -5.86 (-15.49 - -1.18 95%CI) and -8.63 (-17.90 - -2.51 95%CI) for N and P respectively). Based on these relationships we predict that 23 out of our 51 study species could exhibit coprophagy to supplement their diets (based on a probability higher than 75%). Furthermore, the probability of feces being eaten by coprophagous fishes can be predicted by the N% or P% content in the feces (figure 6.2E,F; the slopes of the beta regressions are 1.54 (1.29 - 1.78 95%CI) and 2.61 (2.07 - 3.17 95%CI) for N and P respectively. We predict that 31 of our study species have feces that are a desirable source for other fish species (with a higher than 75% probability).

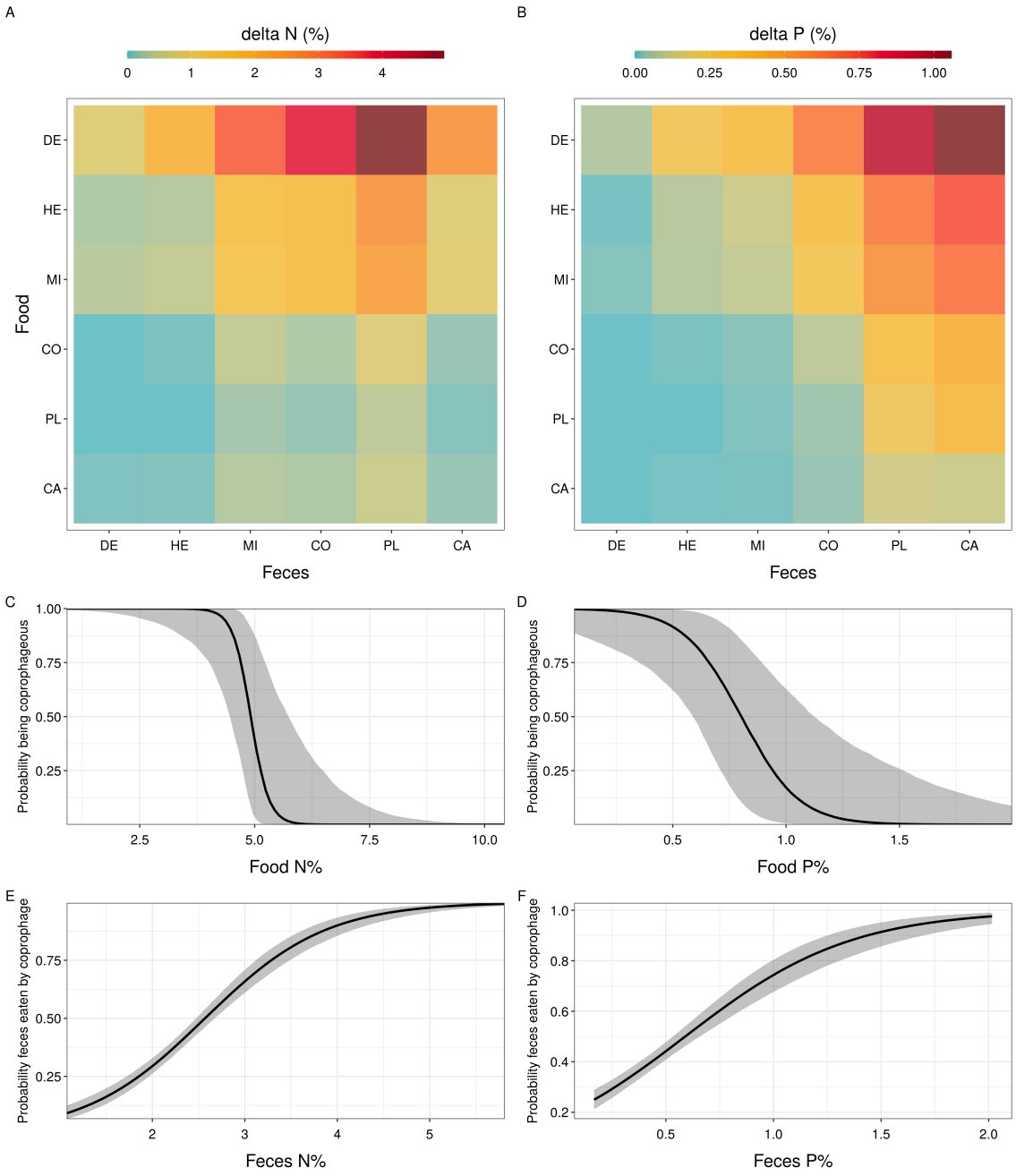

Figure 6.2: Pairwise comparisons of food and feces per trophic guild for N (A) and P (B); fitted probabilities of being coprophagous based on the percentages of N and P in food (C,D); fitted probabilities of feces being eaten based on percentages of N and P in the feces (E,F)

6.4.2 Absorption efficiencies

We estimated element-specific absorption efficiencies for all species by combining our compositional data with ash content data to account for total absorption (table 6.4). Across trophic guilds, carnivorous fishes had the highest absorption efficiencies followed by corallivores. In contrast, detritivorous acanthurids and planktivorous pomacentrids had low, or sometimes even negative absorption efficiencies (figure 6.3A). After excluding species with negative absorption efficiencies, we tested the relationship between food elementary content and absorption efficiencies (figure 6.3B), to show that the N-specific absorption efficiency increases with N concentration in food (average slope: 0.35; 95% CI: 0.09-0.62). This food effect is lower for C (average slope: 0.14 ; 95% CI: -0.12-0.40), and not present for P (average slope: 0.03; 95% CI: -0.24-0.30). Based on the back-transformed intercepts, we estimate that the absorption efficiency of N is generally the highest (average: 0.59; 95%CI: 0.52-0.65), followed by C (average: 0.54; 95%CI: 0.47-0.60), and P (average: 0.43; 95%CI: 0.36-0.49).

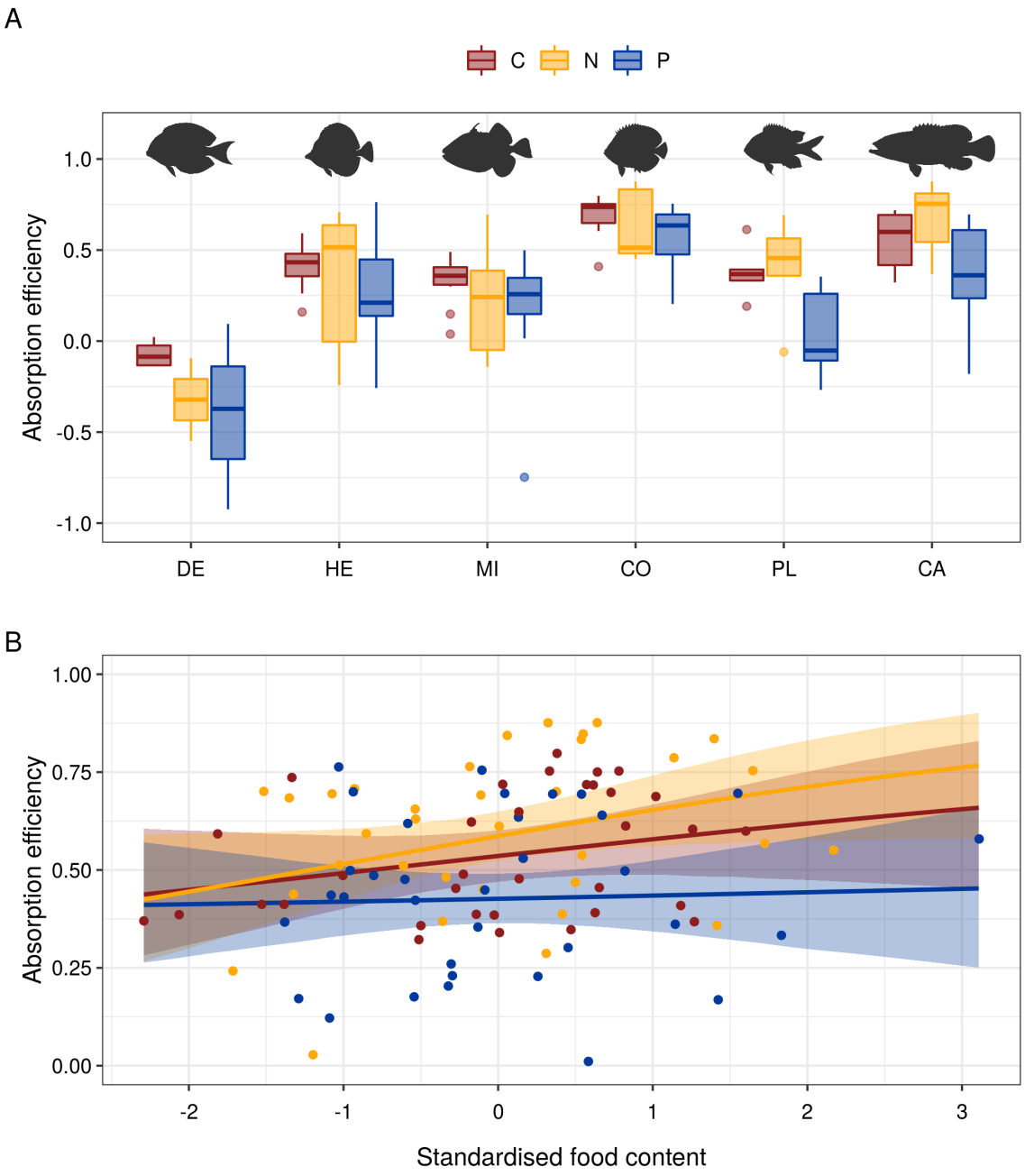

Figure 6.3: Absorption efficiencies across trophic guilds (A) and fitted absorption efficiencies with standardized elemental contents of the stomach content (B). Lines show the average fitted values, and the shaded areas indicate the 95% credible interval. DE = detritivores, HE = herbivores, MI = mixed invertivores, CO = corallivores, PL = planktivores, CA = carnivores.

6.4.3 Egestion rates

Using the estimated food elemental contents and absorption efficiencies (set to 0.1 for species with negative predicted values), we applied bioenergetic models for all 51 species at their median size, and estimated the daily N and P flux in excretion and egestion. We then calculated the log release ratios (egestion/excretion) for N, P, and the N:P ratio. A positive release ratio thus indicates that N, P, or the N:P ratio is higher in egestion compared to excretion. The log release ratio was almost exclusively higher than zero for P, with the exception of *Chaetodon citrinellus*, *Epibulus insidiator*, and *Epinephelus merra*, indicating that there is more P flux through egestion than through excretion. For N, there was more N flux in egestion compared to excretion for 29 species, with mostly carnivorous and corallivorous species excreting more N than they egest (figure 6.4). Consequently, the N:P ratio of excretion tends to be higher than the N:P ratio of egestion for most species (40 species).

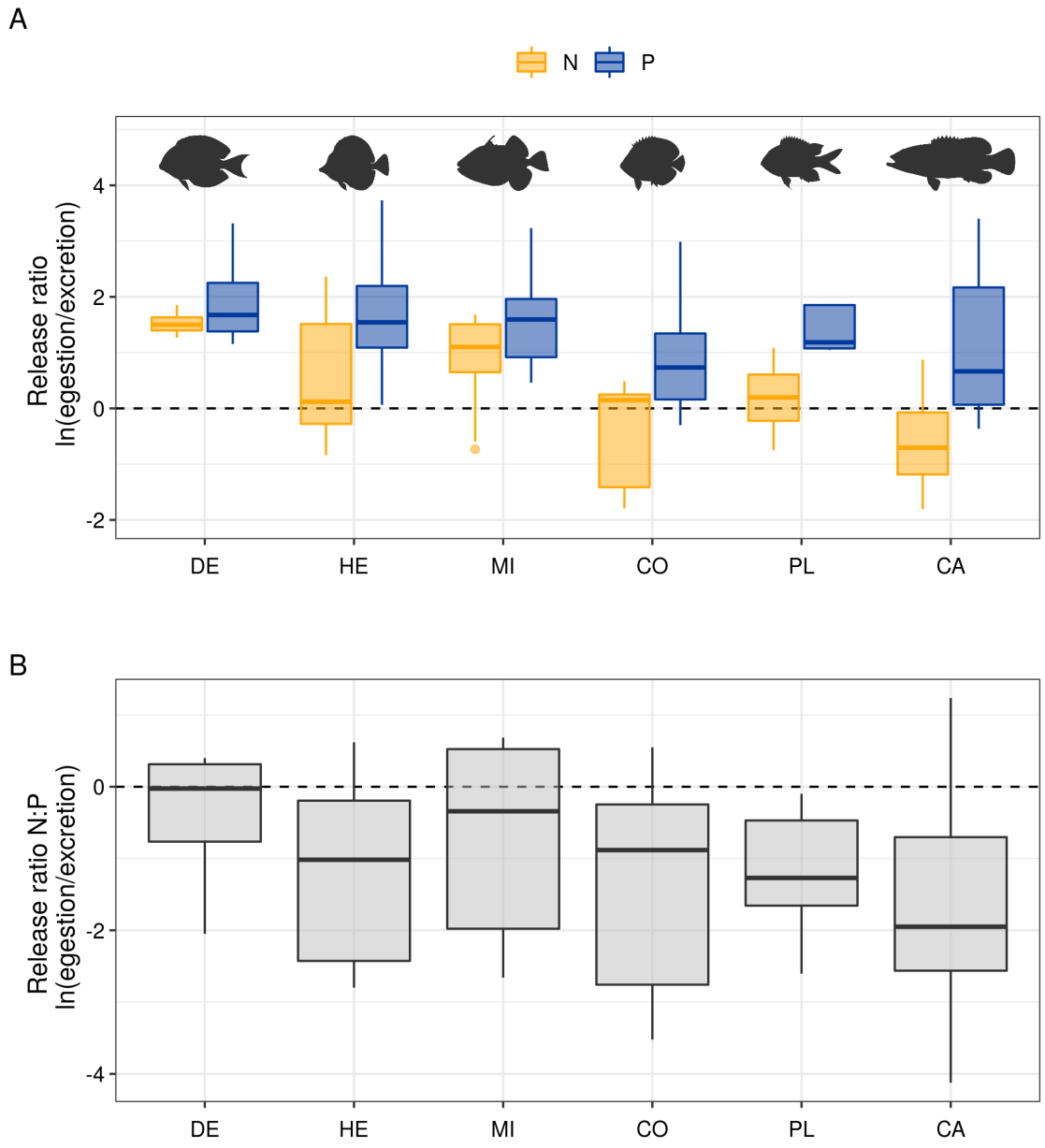

Figure 6.4: Box plots of release ratios (i.e., natural log-transformation of egestion divided by excretion) for N and P (A), and the N:P ratio (B) per trophic guild. DE = detritivores, HE = herbivores, MI = mixed invertivores, CO = corallivores, PL = planktivores, CA = carnivores.

Finally, for our case study on P fluxes at the community level for outer reefs in Mo'orea, French Polynesia (figure 6.5), we found that 82.4% of the total consumed P is released in egestion compared to 8.7% that is released in excretion. This can be explained by the high abundance of detritivores and herbivores present on the reefs of Mo'orea, which egest 71.1% of the total consumed P, although their feces have a low concentration of P.

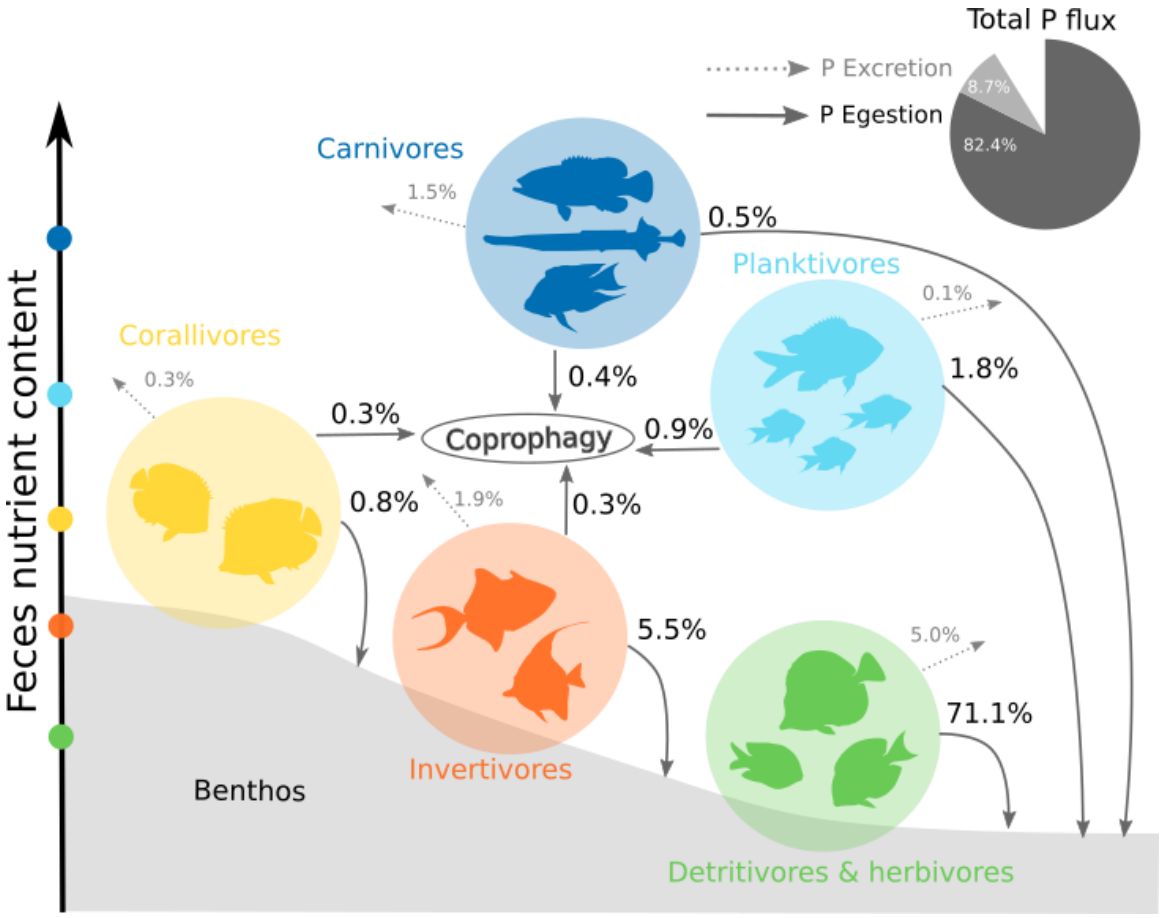

Figure 6.5: P fluxes in egestion and excretion across trophic groups in Mo'orea, French Polynesia. Egestion flows either to the benthos or to coprophages. The amount of feces being eaten by coprophages was determined by multiplying egestion rates of individual fishes in the community by the predicted probability of feces being eaten (see methods). All P fluxes are standardized by dividing by the total amount of P consumed by the fish community on a daily basis.

6.5 Discussion

Understanding how consumers contribute to fluxes of energy and nutrients in ecosystems is an important challenge in ecology. The absorption efficiency of major elements defines how much food is released into a particulate form (i.e., feces). We show that, across a wide range of coral reef fishes, elemental concentrations decrease remarkably little from food to feces, due to predominantly low absorption efficiencies, resulting in considerable amounts of energy and nutrients being egested. While it is commonly assumed that excretion is the primary vector of animal-mediated nutrient flux, our results suggest that most coral reef fishes egest more N and P than they excrete, shedding light on the important role of egestion for nutrient cycling on coral reefs. Further, the quality and quantity of fish egesta varies greatly depending on the trophic guild. As a consequence, the community structure of reef fishes highly influences organic nutrient flow at a given location. Overall, our study affirms the need for incorporating animal egestion alongside excretion in assessments of ecosystem functioning and food web structures (Atkinson *et al.* 2017; Halvorson *et al.* 2017a; Halvorson & Atkinson 2019).

We provide estimates of carbon, nitrogen, and phosphorus concentrations of fish feces for 51 coral reef fish species. Only two previous studies have analyzed the composition of coral reef fish across a small number of species. For example, in Palau, Bailey & Robertson (1982) found an average N concentration of 1.52% for *Zebrasoma scopas*, which is slightly lower than but within the credible range of our average (2.21 %). *Z. scopas* feed primarily on red algae, which can vary 4-fold in N concentration, which may explain this variation (Montgomery 1980). Similarly, Crossman *et al.* (2005) reported relatively low N concentrations in the feces of *A. lineatus* (1.44%) and *A. olivaceus* (0.34%) on reefs in the Northern Great Barrier Reef, compared to our present study (2.97% and 2.98%, respectively). The values reported in both studies are based on proteins or amino acids only (Bailey & Robertson 1982; Crossman *et al.* 2005), and we converted these protein concentrations to total N using

the standard conversion factor of 1:6.25 (N:protein). However, algae can have high and variable concentrations of non-protein nitrogen substances, so the conversion we made from protein estimates by Bailey & Robertson (1982) and Montgomery (1980) are likely to underestimate the total N concentration (Lourenco *et al.* 2002). We thus provide the first estimates for total C, N, and P concentrations of food and feces across 51 study species, and it appears that our values align roughly with the limited data available from previous studies.

We found remarkably low and variable reductions in elemental concentration between food and feces and low absorption efficiencies across species. As expected, N absorption efficiencies are higher than C and P, since N-rich protein is more digestible than other C-rich compounds such as carbohydrates and lipids (Montgomery 1980; Pandian & Marian 1985; Crossman *et al.* 2005). Further, N absorption efficiency increases with the N concentration of the food. This positive relationship exists in other animals (e.g., Jochum *et al.* 2017), and has been suggested for total absorption efficiencies in fishes (Pandian & Marian 1985). This means that fishes with a high-N diet assimilate N more efficiently than those with an N-poor diet, and consequently, the maintenance of fish homeostasis must be occurring through release of already assimilated nutrients (i.e., excretion). A similar, but weaker, pattern is visible for C absorption efficiencies, while P absorption efficiencies were weakly predicted by P content in diet, and were generally low and highly variable across species (Czamanski *et al.* 2011).

Across trophic guilds, carnivorous fishes have the highest absorption efficiencies, which is likely because animal material is easier to digest than plant material (Kozlovsky 1968; Pandian & Marian 1985). For corallivores, which had the second highest absorption efficiency, the high efficiency could be driven by their N-rich diet and their long intestines (Berumen *et al.* 2011). In addition, the highly specialized feeding niche of many coral-feeding chaetodontids (Berumen & Pratchett 2008) may have helped to boost nutrient absorption efficiencies, since the digestive organs and gut microbiomes of specialized feeders are well adapted to a specific range of prey items.

In contrast to corallivores, planktivorous fishes exhibited fairly low absorption efficiencies despite having N-rich diets. Their feeding behaviour, which capitalizes on abundant zooplankton at incoming tides and their high intake rate may satisfy their daily needs even with low absorption efficiencies (Hamner *et al.* 1988). As expected, detritivorous and herbivorous fishes had generally low absorption efficiencies, but within herbivores, absorption efficiencies were remarkably variable. This is in line with previous reported absorption efficiencies for herbivorous coral reef fishes that range between 17.4% and 97.2% for protein and between 5.3% and 80.2% for lipids and carbohydrates (Crossman *et al.* 2005). Herbivorous fishes have specialized digestive strategies linked with differences in diet, even though they are often designated as a single trophic category (Crossman *et al.* 2005). For example, Acanthuridae, which are predominantly classified as herbivorous fishes, exhibit fine-scale dietary, morphological, and behavioral specialization (Brandl *et al.* 2015). Our results suggest that these differences are reflected in their digestive dynamics as well. For instance, *Z. scopas* and *A. pyroferus*, which are both considered to be croppers of small algae but exhibit different morphologies and behaviors, were fundamentally different in terms of their absorption efficiencies. *Z. scopas* appears to feed almost exclusively on fine filamentous red algae, so, an interesting hypothesis to test would be whether herbivores with specialized diets have a higher absorption efficiency. Additionally, especially for herbivores, the fish gut microbiome may play a large role in digestion and resulting absorption efficiencies (Miyake *et al.* 2015). Overall, our results emphasize the high variability of absorption efficiencies among but also within trophic groups. This variation is important to consider when inferring species' roles in system-wide energy and nutrient fluxes (Brandl *et al.* 2019a).

Notably, we found several negative absorption efficiencies, mostly for N and P. For some detritivorous acanthurids (e.g., *Ctenochaetus striatus*), the negative absorption efficiencies can be explained by their gizzard-like stomach in which they retain inorganic material to grind down dietary food particles (Horn 1989; Crossman *et al.* 2005). The presence of inorganic material probably caused an underestimation of

food quality, and thus yielding negative assimilation efficiencies. For these species, it may be better to sample putative food sources from the environment or ingested food from the mouth or esophagus, rather than the stomach. For other taxa, explanations are less straightforward. The higher P in the feces of some planktivores compared to their stomach contents could be caused by a high density of bacteria with low C:N:P stoichiometry, a high proportion of indigestible invertebrate exoskeleton (chitin) in their planktonic prey, or selective absorption of C- and N-containing compounds (Geesey *et al.* 1984). Another possibility would be that planktivores occasionally supplement their diet with P-rich food items such as fish feces, but this peculiarity remains unresolved (Pinnegar & Polunin 2006). Finally, although we sampled to the best of our abilities, some negative absorption efficiencies may result from low sample sizes. N and P in the food are much more variable than carbon, and the more variability in food elemental stoichiometry, the higher the potential bias when sample sizes are low. Most species for which we found negative absorption efficiencies had a sample size lower than 10. On the other hand, the three species for which we have the highest sample size (n>20) also yielded the most robust species-level estimates. Overall, species consistently feeding on a single taxonomic group (e.g., piscivorous groupers) have a less variable food stoichiometry and may thus need less replicates (e.g., *Cephalopholis argus*), while especially species that ingest a conglomerate of taxa (e.g., some herbivorous fishes, planktivores, and omnivores) may require a substantial number of replicates to obtain reliable estimate of assimilation efficiencies.

The low absorption efficiencies of fishes with nutrient-poor diets necessitate compensatory feeding to obtain sufficient N and P for growth and homeostasis. For example, herbivores feed on nutrient-poor algae, thus displaying a large mismatch between the food elemental concentrations and the ideal elemental composition needed for maintenance and growth (Schiettekatte *et al.* 2020). While it may seem intuitive that these fishes increase the absorption efficiency of limiting elements to ameliorate the existing nutrient imbalance (Sterner & George 2000), the opposite appears to be the case, as low absorption efficiencies are common in these species. Except for a

single study on herbivorous terrestrial invertebrates, which compensated for a limiting element by altering absorption efficiency (Clissold *et al.* 2010), compensatory feeding on nutrient-rich resources appears to be the most common approach to make up for low-nutrient diets across many taxa. Indeed, this feeding strategy has been demonstrated for freshwater invertebrates (Evans-White & Halvorson 2017), insects (Jochum *et al.* 2017), snail grazers (Liess 2014), and marine amphipods (Cruz-Rivera & Hay 2000).

Our results highlight the role of fish egestion for system-wide nutrient cycling. A logical consequence of the low absorption efficiencies we discovered is that nutrients may be released more abundantly through egestion instead of excretion, especially for P, resulting in feces with low N:P ratios. Similar findings have been reported for marine invertebrates (Halvorson & Atkinson 2019) and terrestrial vertebrates, in which urine contains little P but a high concentration of N, while feces contain most of the P (Sitters *et al.* 2017). Consumption of such P-rich feces is common among coral reef fishes, and some prey like plankton may pass through three fish stomachs before reaching the bottom (Robertson 1982). Similarly, feces that are not consumed in the water column and reach the bottom are likely consumed by invertebrates in reef crevices (Pinnegar & Polunin 2006), thus fueling a different compartment of the coral reef food web. In contrast, nutrient poor feces from herbivores or detritivores are rarely consumed directly, but are decomposed by microbial communities. Depending on the N:P ratio, these feces may exhibit an uptake of dissolved N or P, suggesting that decomposing feces may serve as a nutrient sink (Halvorson *et al.* 2017a). Further, fish feces may be important vectors of bacteria to coral surfaces and even transform coral microbiomes (Ezzat *et al.* 2019). Our study calls for further research on the diverse fates of fish feces in coral reef ecosystems, to better understand the various pathways in which fish feces affect nutrient cycling and ecosystem functioning.

Our results have several implications for models aiming to estimate fluxes through the food web and nutrient cycling. First, a central goal in ecology is to characterize trophic interactions and some studies have attempted to recreate complex food webs

for coral reef fishes (e.g., Bascompte *et al.* 2005; Casey *et al.* 2019). To understand the interaction strength of food web links, we need to estimate the amount of elements and energy flowing through these interaction which necessitates a quantification of consumption rates. To date, food web models do not take variation of absorption efficiencies into account, which may introduce substantial bias. Further, coprophagic links have not been included in food web models, even though they may represent an important food source. For example, *Naso vlamingii* consumes up to 200 planktivore feces (12% of its own body weight) per hour during periods of high feeding activity (Robertson 1982), suggesting that coprophageous links are a substantial part of energy and nutrient transfer. Finally, bioenergetic models represent a useful tool to estimate multiple individual-level pathways of elements and absorption efficiencies represent important parameters (Schiettekatte *et al.* 2020). Due to a general lack of data it is common practice to use constants from the literature (e.g., 0.8 for N and C absorption efficiency, and 0.7 for P absorption efficiency), rather than values measured in the field for the particular population being modeled (Kraft 1992; Schindler & Eby 1997; Allgeier *et al.* 2015; Schiettekatte *et al.* 2020). Our results illustrate that these values are not an adequate approximation for coral reef fishes, which exhibit remarkable variability in their absorption efficiency, potentially introducing significant bias in the outcomes. Collecting and curating physiological data as presented in the present study across species and locations will greatly enhance the parameterization of ecosystem models and thus increase our understanding of complex systems.

Finally, data on feces quality and quantity can be used to investigate additional pathways in which human impact may disrupt coral reef ecosystem functioning. Fishing selectively targets fishes with high trophic levels and large sizes (Graham *et al.* 2017). The local depletion of large predators or planktivores not only affects prey populations and decreases excretion (Allgeier *et al.* 2016), but also potentially removes an important food source for coprophagous fishes. Likewise, communities that have shifted towards dominance by detritivores and herbivores, which is observed on reefs around as Mo'orea, have a high incidence of nutrient-poor egestion. Further,

coral loss and reduced structural complexity cause declines of planktivores, large carnivores, and corallivores (Graham & McClanahan 2013; Brandl *et al.* 2016; Darling & D'agata 2017), and thus can lead to a decreased nutritional quality of feces in fish communities. As such, system wide elemental fluxes stand to be significantly different on reefs with shifting fish assemblages, with thus far unknown consequences for ecosystem services that reefs can provide to humanity. Overall, our results highlight the important role of fish feces as a nutrient vector. More research quantifying the quality and fate of these feces is necessary to understand how changes in community structure affect ecosystem functioning through trophic interactions, nutrient translocation, and microbial activity.

6.6 Supplementary materials

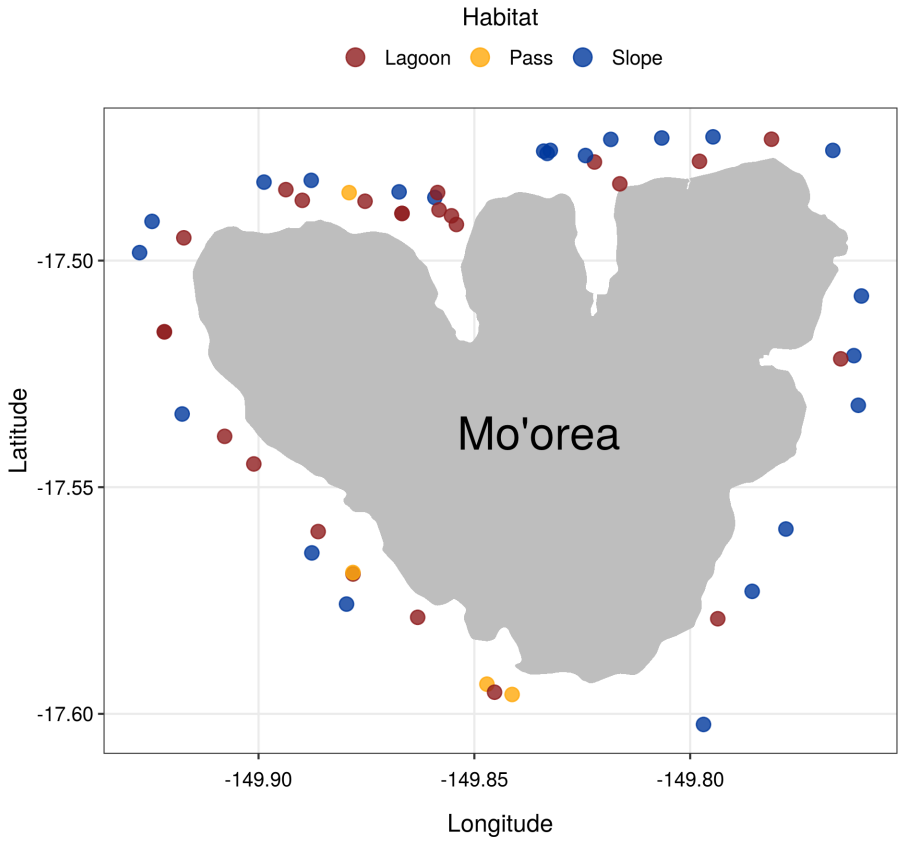

Figure 6.6: Map of sampling stations in Mo'orea.

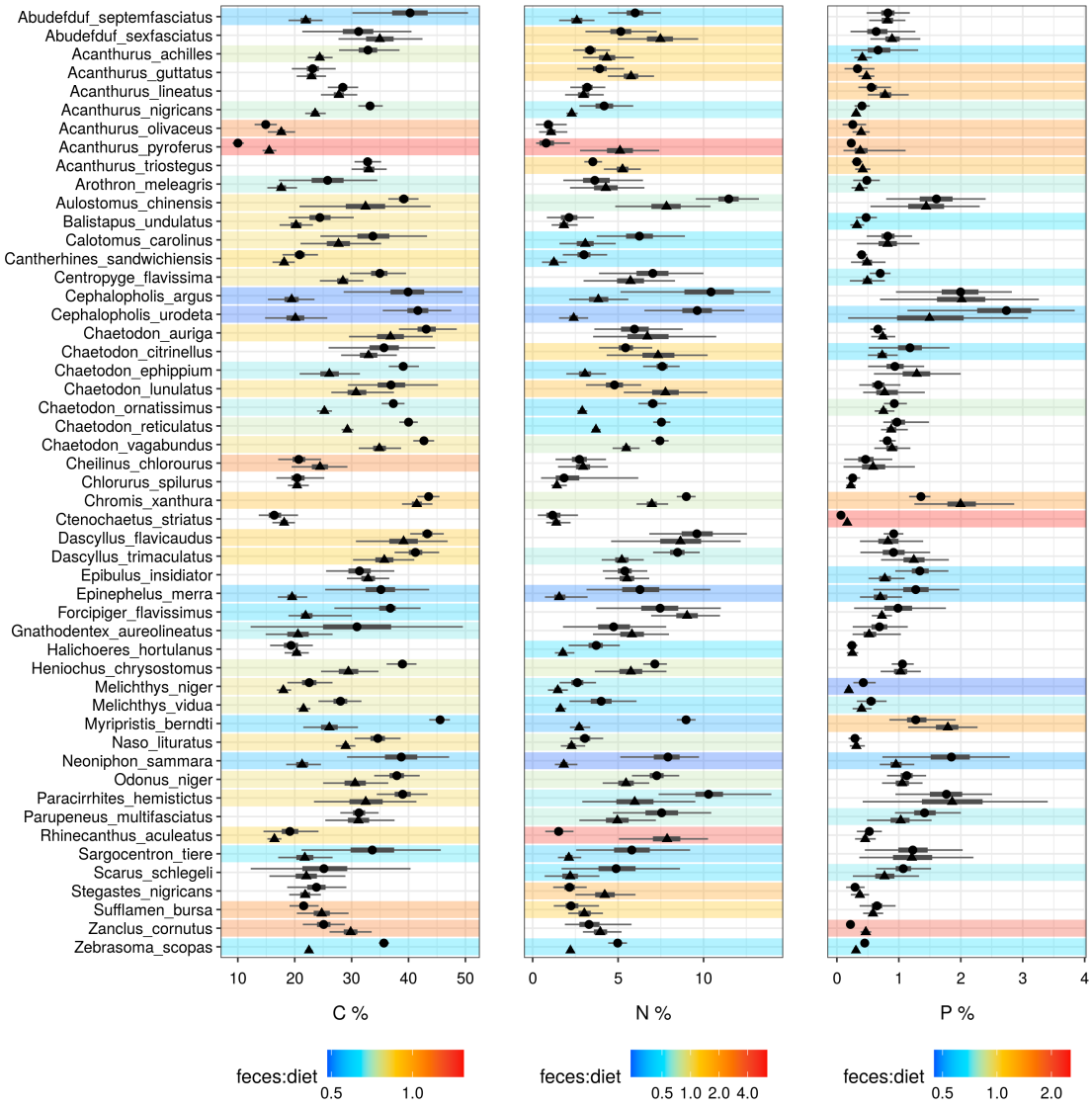

Figure 6.7: Species-level estimates of the C, N, and P content of the food (circles) and the feces (triangles). The thin lines indicate the 95% CI, and the thicker lines show the 50% CI. The color scale indicates the ratio between feces and food elemental content. The color scale is only shown if there is no overlap of the 50% CI's of both.

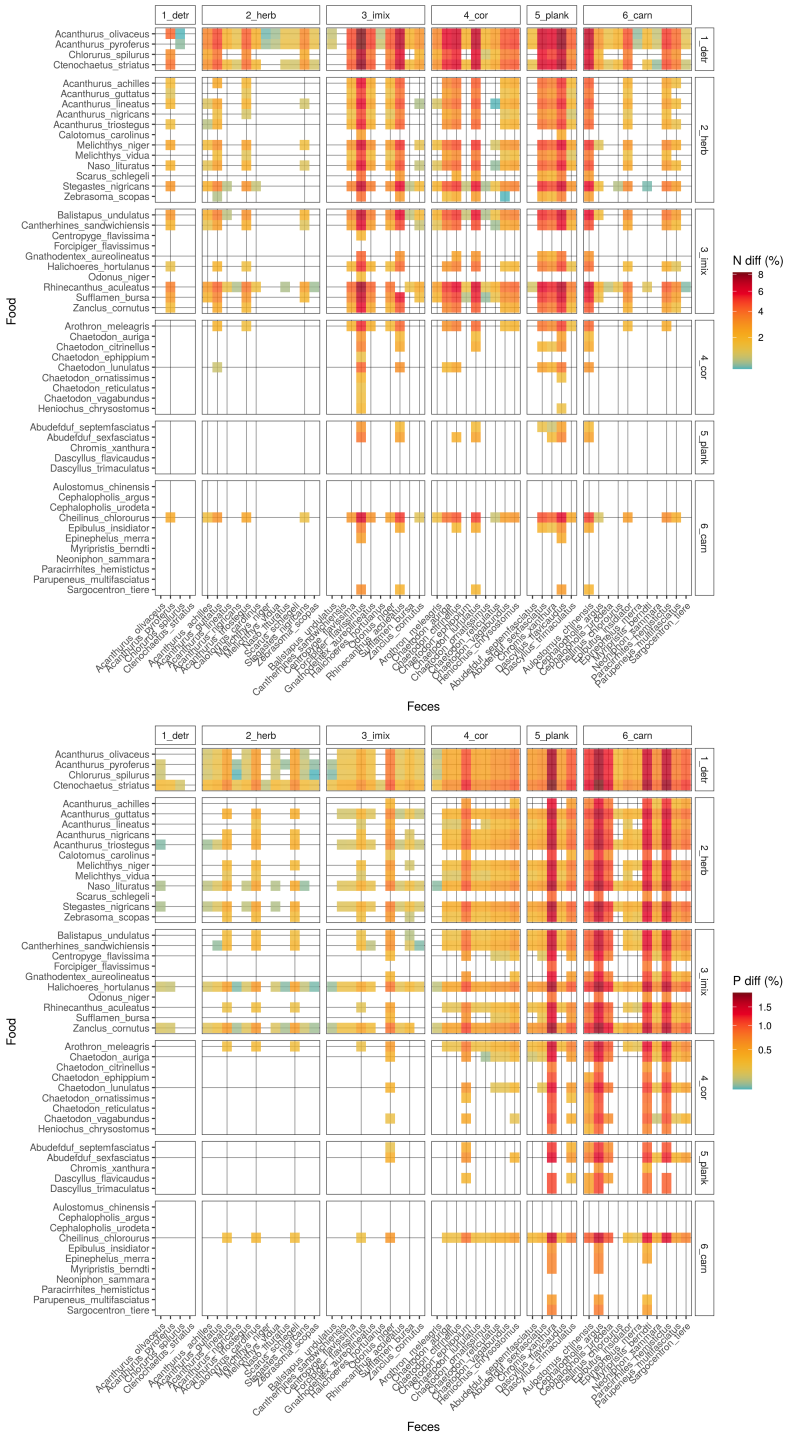

Figure 6.8: Species-level pairwise comparisons between the proportion of N and P of food and feces. Vertical lines indicate the species for which the feces have a predicted probability of being eaten that is higher than 50%. Horizontal lines indicate the species that have a higher than 50% probability of being coprophagous.

Table 6.1: Overview of study species' length and weight range, trophic category, family, and number of replicates

Species	Family	Diet	Range TL (cm)	Range weight (g)	Replicates
Acanthurus achilles	Acanthuridae	herbivore	12.2-22.2	36-241.5	9
Acanthurus guttatus	Acanthuridae	herbivore	16.3-19.8	114.7-206.9	9
Acanthurus lineatus	Acanthuridae	herbivore	22.2-25.1	161.2-216.1	6
Acanthurus nigricans	Acanthuridae	herbivore	8.2-27	11.1-176	17
Acanthurus olivaceus	Acanthuridae	detritivore	23-29	174.7-299.3	5
Acanthurus pyroferus	Acanthuridae	detritivore	13-40.1	36.3-137.3	9
Acanthurus triostegus	Acanthuridae	herbivore	14-16.6	61.4-121.2	14
Ctenochaetus striatus	Acanthuridae	detritivore	12-23.2	45.2-201.5	13
Naso lituratus	Acanthuridae	herbivore	18.1-35.6	106.3-292	15
Zebrasoma scopas	Acanthuridae	herbivore	2.9-18.5	0.6-142.3	51
Aulostomus chinensis	Aulostomidae	carnivore	36.5-62.3	76.5-389	10
Balistapus undulatus	Balistidae	mixed invertivore	12.5-26.7	46-385.5	15
Melichthys niger	Balistidae	herbivore	12.5-26.4	48-368.1	14

Species	Family	Diet	Range TL (cm)	Range weight (g)	Replicates
Melichthys vidua	Balistidae	herbivore	17.6-23.5	158.9-330.8	16
Odonus niger	Balistidae	mixed invertivore	15.8-27.7	61.8-187	15
Rhinecanthus aculeatus	Balistidae	mixed invertivore	14.5-22.2	66.9-201.5	10
Sufflamen bursa	Balistidae	mixed invertivore	11.8-18.2	36.6-117	12
Chaetodon auriga	Chaetodontidae	corallivore	14.5-21.4	62.5-134.6	10
Chaetodon citrinellus	Chaetodontidae	corallivore	10.1-11.3	18.3-299.5	8
Chaetodon ephippium	Chaetodontidae	corallivore	15.7-19.1	81.9-116.2	7
Chaetodon lunulatus	Chaetodontidae	corallivore	9.1-13.5	20.1-57.7	10
Chaetodon ornatissimus	Chaetodontidae	corallivore	7-15	0.1-103.9	31
Chaetodon reticulatus	Chaetodontidae	corallivore	8.6-13	17.7-69.6	32
Chaetodon vagabundus	Chaetodontidae	corallivore	12.5-15.1	59.2-95.3	13
Forcipiger flavissimus	Chaetodontidae	mixed invertivore	14.2-40.9	33.1-55.1	7
Heniochus chrysostomus	Chaetodontidae	corallivore	11-14.2	35.8-97	10
Paracirrhites hemistictus	Cirrhitidae	carnivore	16.2-22.1	92.9-175.9	16

Species	Family	Diet	Range TL (cm)	Range weight (g)	Replicates
Myripristis berndti	Holocentridae	carnivore	12-22.4	50.6-230.1	10
Neoniphon sammara	Holocentridae	carnivore	14.1-22.2	35.2-132.2	16
Sargocentron tiere	Holocentridae	carnivore	19-31.2	76.5-328.2	8
Calotomus carolinus	Labridae	herbivore	26.1-38.6	284.1-558	5
Cheilinus chlorourus	Labridae	carnivore	16.5-20.7	70.3-169.3	6
Chlorurus spilurus	Labridae	detritivore	17.5-47.5	100.4-418.2	11
Epibulus insidiator	Labridae	carnivore	17-27.5	88.7-281.4	14
Halichoeres hortulanus	Labridae	mixed invertivore	15.2-26.1	49.9-249.8	11
Scarus schlegeli	Labridae	herbivore	27.1-30.1	490-490	4
Gnathodentex aureolineatus	Lethrinidae	mixed invertivore	21.4-31.1	121.3-196.8	9
Cantherhines sandwichiensis	Monacanthidae	mixed invertivore	15-17.2	65.1-102	5
Parupeneus multifasciatus	Mullidae	carnivore	13.9-29.8	33.6-370	10
Centropyge flavissima	Pomacanthidae	mixed invertivore	5.5-10.1	7.3-26.8	7

Species	Family	Diet	Range TL (cm)	Range weight (g)	Replicates
Abudefduf septemfasciatus	Pomacentridae	planktivore	16.4-19.4	97.7-162.3	7
Abudefduf sexfasciatus	Pomacentridae	planktivore	12.9-17.4	40.8-117.6	10
Chromis xanthura	Pomacentridae	planktivore	11.1-15.8	24.2-47	20
Dascyllus flavicaudus	Pomacentridae	planktivore	7.5-11	10.1-33.9	13
Dascyllus trimaculatus	Pomacentridae	planktivore	12-13.5	43.6-60.3	8
Stegastes nigricans	Pomacentridae	herbivore	12-14.1	49.1-69.3	9
Cephalopholis argus	Serranidae	carnivore	21-31.5	126.3-470.2	11
Cephalopholis urodeta	Serranidae	carnivore	15.9-18.9	67.6-130.1	7
Epinephelus merra	Serranidae	carnivore	16.5-23	80.9-166.3	10
Arothron meleagris	Tetraodontidae	corallivore	13.6-26.9	80.9-571	9
Zanclus cornutus	Zanclidae	mixed invertivore	13.1-18.1	65.2-135.8	16

Table 6.2: Overview of species-specific estimated ratio's between ash of food and feces from this study and literature.

species	diet	ash_ratio	source_ash
Paracirrhites hemistictus	6_carn	0.7284672	This study, species-level estimate
Zanclus cornutus	3_imix	0.8052683	This study, diet-level estimate
Melichthys niger	2_herb	0.5065069	This study, species-level estimate
Melichthys vidua	2_herb	0.6653408	This study, species-level estimate
Sargocentron tiere	6_carn	0.5585211	This study, species-level estimate
Chaetodon vagabundus	4_cor	0.7223433	This study, species-level estimate
Naso lituratus	2_herb	0.7325541	This study, diet-level estimate
Chlorurus spilurus	1_detr	0.9738648	This study, species-level estimate
Balistapus undulatus	3_imix	0.7007812	This study, species-level estimate
Aulostomus chinensis	6_carn	0.6571061	This study, species-level estimate
Epibulus insidiator	6_carn	0.6072596	This study, species-level estimate
Parupeneus multifasciatus	6_carn	0.6771488	This study, species-level estimate
Cephalopholis urodeta	6_carn	0.6414562	This study, species-level estimate
Halichoeres hortulanus	3_imix	0.5936238	This study, species-level estimate
Acanthurus triostegus	2_herb	0.7325541	This study, diet-level estimate
Cheilinus chlorourus	6_carn	0.4678381	This study, species-level estimate
Sufflamen bursa	3_imix	0.7395958	This study, species-level estimate

species	diet	ash_ratio	source_ash
Stegastes nigricans	2_herb	0.5849620	This study, species-level estimate
Abudefduf sexfasciatus	5_plank	0.7000000	Bailey & Robertson (1982)
Chaetodon reticulatus	4_cor	0.3379186	This study, species-level estimate
Odonus niger	3_imix	0.8052683	This study, diet-level estimate
Neoniphon sammara	6_carn	0.5020749	This study, species-level estimate
Ctenochaetus striatus	1_detr	0.9425958	This study, species-level estimate
Chaetodon ornatissimus	4_cor	0.2988577	This study, species-level estimate
Cephalopholis argus	6_carn	0.6036160	This study, species-level estimate
Zebrasoma scopas	2_herb	0.8278710	This study, species-level estimate
Acanthurus nigricans	2_herb	0.7190284	This study, species-level estimate
Epinephelus merra	6_carn	0.4927403	This study, species-level estimate
Myripristis berndti	6_carn	0.6972230	This study, species-level estimate
Chaetodon auriga	4_cor	0.4626197	This study, species-level estimate
Centropyge flavissima	3_imix	0.8052683	This study, diet-level estimate
Dascyllus flavicaudus	5_plank	0.7000000	Bailey & Robertson (1982)
Gnathodentex aureolineatus	3_imix	0.6664872	This study, species-level estimate
Acanthurus achilles	2_herb	0.7325541	This study, diet-level estimate
Heniochus chrysostomus	4_cor	0.3728032	This study, diet-level estimate
Chaetodon lunulatus	4_cor	0.2907317	This study, species-level estimate

species	diet	ash_ratio	source_ash
Arothron meleagris	4_cor	0.3728032	This study, diet-level estimate
Forcipiger flavissimus	3_imix	0.8052683	This study, diet-level estimate
Acanthurus pyroferus	2_herb	0.7325541	This study, diet-level estimate
Rhinecanthus aculeatus	3_imix	0.8052683	This study, diet-level estimate
Chaetodon citrinellus	4_cor	0.3728032	This study, diet-level estimate
Dascyllus trimaculatus	5_plank	0.7000000	Bailey & Robertson (1982)
Acanthurus guttatus	2_herb	0.7325541	This study, diet-level estimate
Chromis xanthura	5_plank	0.7000000	Bailey & Robertson (1982)
Acanthurus olivaceus	1_detr	0.9513447	This study, diet-level estimate
Chaetodon ephippium	4_cor	0.3728032	This study, diet-level estimate
Cantherhines sandwichiensis	3_imix	0.7041257	This study, species-level estimate
Abudefduf septemfasciatus	5_plank	0.7000000	Bailey & Robertson (1982)
Calotomus carolinus	2_herb	0.7325541	This study, diet-level estimate
Scarus schlegeli	2_herb	0.6200000	Crossman et al. (2005)
Acanthurus lineatus	2_herb	0.8600000	Crossman et al. (2005)

Table 6.3: Overview average elemental composition of food and feces per species. C = carbon, N = nitrogen, P = phosphorus. Values between brackets represent the 95% credible interval.

Species	Diet C (%)	Diet N (%)	Diet P (%)	Feces C (%)	Feces N (%)	Feces P (%)
Naso lituratus	34.6 (30.5-38.6)	3.1 (2.2-4.1)	0.3 (0.2-0.4)	28.9 (27.2-30.7)	2.3 (1.6-3.1)	0.3 (0.2-0.5)
Acanthurus triostegus	32.8 (30.5-35.2)	3.5 (3-4.1)	0.3 (0.2-0.4)	33 (30-36.2)	5.3 (4.2-6.3)	0.4 (0.3-0.5)
Ctenochaetus striatus	16.6 (13.7-20.6)	1.3 (0.3-2.7)	0.1 (0-0.1)	18.1 (16.1-20.1)	1.4 (0.8-2.2)	0.2 (0.1-0.2)
Zebrasoma scopas	35.7 (34.8-36.6)	5 (4.4-5.5)	0.4 (0.4-0.5)	22.5 (21.9-23.2)	2.2 (2.1-2.4)	0.3 (0.3-0.3)
Acanthurus nigricans	33.2 (31.2-35.5)	4.2 (2.7-5.9)	0.4 (0.3-0.5)	23.6 (21.8-25.5)	2.3 (2-2.6)	0.3 (0.3-0.4)
Acanthurus achilles	32.9 (27.8-38.4)	3.4 (2.4-4.5)	0.7 (0.2-1.3)	24.4 (22.3-26.7)	4.4 (2.9-5.9)	0.4 (0.3-0.6)
Acanthurus pyroferus	10 (9.1-11.1)	0.9 (0.2-2.2)	0.2 (0.2-0.3)	15.5 (14.3-16.8)	5.1 (2.8-7.4)	0.4 (0.1-1.1)
Acanthurus guttatus	23.2 (19.5-27.2)	3.9 (2.6-5.4)	0.3 (0.1-0.6)	23 (20.3-25.5)	5.8 (4.4-7.1)	0.5 (0.3-0.6)
Acanthurus olivaceus	14.9 (12.9-16.9)	1 (0.2-2)	0.3 (0.1-0.5)	17.7 (15.3-20.1)	1.1 (0.4-2)	0.4 (0.3-0.5)
Acanthurus lineatus	28.5 (25.8-31.1)	3.2 (2.2-4.3)	0.6 (0.3-0.9)	27.8 (24.6-31)	3 (1.9-4.2)	0.8 (0.5-1.2)
Aulostomus chinensis	39.2 (36.4-41.8)	11.5 (9.5-13.2)	1.6 (0.8-2.4)	32.4 (20.8-43.9)	7.8 (4.8-10.4)	1.4 (0.5-2.3)
Melichthys niger	22.6 (18.7-26.6)	2.6 (1.6-3.7)	0.4 (0.3-0.6)	18 (16.9-19.4)	1.5 (0.9-2.1)	0.2 (0.1-0.3)
Melichthys vidua	28 (24.2-31.7)	4 (2.2-6.1)	0.6 (0.3-0.8)	21.5 (20.4-22.7)	1.6 (1.3-2)	0.4 (0.3-0.6)

Species	Diet C (%)	Diet N (%)	Diet P (%)	Feces C (%)	Feces N (%)	Feces P (%)
Balistapus undulatus	24.5 (18.9-30.4)	2.1 (0.8-3.6)	0.5 (0.3-0.6)	20.3 (17.3-23.2)	1.8 (1.1-2.6)	0.3 (0.2-0.4)
Sufflamen bursa	21.6 (19.1-24.2)	2.3 (1.2-3.9)	0.6 (0.4-0.9)	24.8 (20.4-29.5)	3 (2.1-4.1)	0.6 (0.4-0.7)
Odonus niger	37.9 (34-42)	7.2 (5.8-8.6)	1.1 (0.8-1.4)	30.6 (25-36.4)	5.5 (4.1-6.8)	1.1 (0.7-1.4)
Rhinecanthus aculeatus	19.2 (14.5-24.2)	1.5 (0.7-2.4)	0.5 (0.3-0.7)	16.4 (15.2-17.7)	7.8 (5-10.3)	0.5 (0.3-0.6)
Chaetodon vagabundus	42.7 (40.8-44.5)	7.4 (7-8)	0.8 (0.7-1)	34.9 (31.2-38.7)	5.5 (4.7-6.3)	0.9 (0.6-1.2)
Chaetodon reticulatus	40 (38.4-41.6)	7.5 (7.1-8.1)	1 (0.7-1.5)	29.3 (28.2-30.3)	3.7 (3.5-4)	0.9 (0.7-1.1)
Chaetodon ornatissimus	37.3 (35.3-39.3)	7 (6.2-7.8)	0.9 (0.8-1.1)	25.2 (23.9-26.5)	2.9 (2.6-3.2)	0.8 (0.6-0.9)
Chaetodon auriga	43.2 (38.3-48.5)	6 (3.6-8.8)	0.7 (0.5-0.8)	36.9 (29.5-44.2)	6.8 (3.5-10.7)	0.7 (0.6-0.9)
Heniochus chrysostomus	38.9 (36.1-41.4)	7.2 (6.5-7.9)	1.1 (0.9-1.2)	29.5 (24.6-34.7)	5.7 (3.6-7.8)	1 (0.7-1.4)
Chaetodon lunulatus	37 (29.3-45.2)	4.8 (3.1-6.4)	0.7 (0.4-1)	31.1 (26.4-37.4)	7.8 (5.3-10.2)	0.8 (0.4-1.4)
Forcipiger flavissimus	36 (27-42.1)	7.4 (3.7-11)	1 (0.3-1.8)	22.5 (18.9-30)	9 (6.9-11)	0.7 (0.6-0.9)
Chaetodon citrinellus	35.7 (25.9-44.7)	5.4 (3.9-7)	1.2 (0.5-1.8)	33 (28.1-37.9)	7.3 (4.3-10.2)	0.7 (0.5-1)
Chaetodon ephippium	39.1 (36.5-41.8)	7.6 (6.5-8.6)	0.9 (0.5-1.4)	26.1 (20.9-31.5)	3.1 (2-4.3)	1.3 (0.6-2)
Paracirrhites hemistictus	39 (34.4-43.3)	10.4 (7.4-14)	1.8 (0.9-2.5)	32.5 (23.4-41.4)	6 (2.9-9.5)	1.9 (0.4-3.4)

Species	Diet C (%)	Diet N (%)	Diet P (%)	Feces C (%)	Feces N (%)	Feces P (%)
Sargocentron tiere	33.6 (21.2-45.7)	5.8 (2.5-9.2)	1.2 (0.5-2)	21.8 (17.1-26.7)	2.1 (1.5-2.8)	1.2 (0.4-2.2)
Neoniphon sammara	38.6 (29.2-47.1)	7.8 (5.1-9.7)	1.8 (0.7-2.8)	21.3 (18.5-24.6)	1.9 (1.3-2.6)	1 (0.7-1.2)
Myripristis berndti	45.5 (43.6-47.3)	9 (8.4-9.5)	1.3 (0.8-1.9)	26.1 (21.5-31.1)	2.7 (2.2-3.4)	1.8 (1.1-2.3)
Chlorurus spilurus	20.6 (16.8-25.2)	2.2 (0.5-6.2)	0.3 (0.1-0.4)	20.5 (18.8-22.5)	1.5 (1.1-2)	0.2 (0.2-0.3)
Epibulus insidiator	31.4 (25.5-37.5)	5.4 (4.1-6.7)	1.3 (0.9-1.8)	32.9 (29.2-36.6)	5.5 (4.2-6.8)	0.8 (0.5-1.1)
Halichoeres hortulanus	19.4 (15.7-23.2)	3.7 (2.1-5.1)	0.2 (0.2-0.3)	20.3 (18.2-22.5)	1.8 (1.3-2.4)	0.3 (0.2-0.3)
Cheilinus chlorourus	20.7 (17.1-24.6)	2.8 (1.3-4.3)	0.5 (0.1-0.9)	24.4 (19.5-29.3)	3 (1.5-4.4)	0.6 (0.1-1.3)
Calotomus carolinus	33.8 (24.5-43.3)	6.3 (3.7-8.9)	0.8 (0.5-1.2)	27.7 (21-35.2)	3.1 (1.6-4.9)	0.8 (0.3-1.3)
Scarus schlegeli	25.5 (12.3-40.4)	5 (1.7-8.6)	1.1 (0.6-1.5)	22.1 (15.5-28.9)	2.2 (0.7-3.9)	0.8 (0.3-1.3)
Gnathodentex aureolineatus	31 (12.2-49.5)	4.8 (1.8-7.8)	0.7 (0.3-1.1)	20.6 (14.9-26.7)	5.8 (3.5-8)	0.5 (0.3-1)
Cantherhines sandwichiensis	20.9 (17.8-24.1)	3 (1.8-4.4)	0.4 (0.3-0.5)	18.1 (16.1-20)	1.3 (0.5-2)	0.5 (0.2-0.8)
Parupeneus multifasciatus	31.3 (28-34.7)	7.6 (4.7-10.4)	1.4 (0.9-2)	31.3 (25.4-37.5)	4.9 (2.7-7.2)	1 (0.5-1.5)
Centropyge flavissima	34.8 (29.7-39.6)	7 (3.9-10)	0.7 (0.5-0.9)	28.4 (24.4-32.1)	5.7 (3-8.3)	0.5 (0.2-0.8)
Stegastes nigricans	23.8 (18.7-29.1)	2.2 (1.2-3.2)	0.3 (0.1-0.4)	21.8 (19-24.6)	4.2 (2.5-6)	0.4 (0.2-0.5)

Species	Diet C (%)	Diet N (%)	Diet P (%)	Feces C (%)	Feces N (%)	Feces P (%)
Abudefduf sexfasciatus	31.1 (21.3-40.5)	5.2 (3.1-7.3)	0.7 (0.2-1.3)	35 (27.7-42.5)	7.4 (5-9.7)	0.9 (0.5-1.3)
Dascyllus flavicaudus	43.3 (40.3-46.2)	9.6 (6.8-12.5)	0.9 (0.8-1.1)	39 (30.7-46.9)	8.6 (4.6-12.2)	0.8 (0.4-1.4)
Dascyllus trimaculatus	41.3 (37.5-45.4)	8.5 (7-9.8)	0.9 (0.4-1.5)	35.7 (30.2-41)	5.2 (4-6.5)	1.2 (0.7-1.8)
Chromis xanthura	43.5 (41.6-45.4)	9 (8.4-9.5)	1.4 (1.2-1.5)	41.5 (38.9-44.2)	7 (6.1-7.9)	2 (1.3-2.9)
Abudefduf septemfasciatus	40.3 (30.1-50.4)	6 (4.4-7.5)	0.8 (0.5-1.2)	21.9 (18.9-24.9)	2.6 (1.5-3.6)	0.8 (0.5-1.1)
Cephalopholis urodeta	41.6 (35.5-47.5)	9.6 (6.5-12.4)	2.7 (1.1-3.8)	20.1 (14.8-25.7)	2.4 (1.5-3.2)	1.5 (0.2-3.1)
Cephalopholis argus	39.7 (28.6-49.5)	10.2 (5.1-13.9)	2 (1-2.8)	19.4 (15.3-23.5)	3.9 (2.1-5.6)	2 (0.7-3.3)
Epinephelus merra	35 (25.4-43.6)	6.4 (3.2-10.4)	1.3 (0.6-2)	19.5 (17-22.2)	1.7 (0.7-3.2)	0.7 (0.4-1.1)
Arothron meleagris	25.8 (17.2-34.5)	3.8 (1.8-6.5)	0.5 (0.3-0.7)	17.7 (15.2-20.4)	4.3 (2.2-6.5)	0.4 (0.2-0.5)
Zanclus cornutus	25.1 (21.4-28.8)	3.4 (1.9-5.8)	0.2 (0.2-0.3)	29.8 (26.1-33.5)	4 (2.9-5.2)	0.5 (0.4-0.6)

Table 6.4: Overview average absorption efficiency per species. AE = absorption efficiency, C = carbon, N = nitrogen, P = phosphorus. Values between brackets represent the 95% credible interval.

Species	Family	Diet	AE C	AE N	AE P
Naso lituratus	Acanthuridae	herbivore	0.38 (0.3-0.46)	0.44 (0.15-0.64)	0.17 (-0.37-0.53)
Acanthurus triostegus	Acanthuridae	herbivore	0.26 (0.17-0.35)	-0.1 (-0.39-0.16)	0.04 (-0.41-0.37)
Ctenochaetus striatus	Acanthuridae	detritivore	-0.04 (-0.28-0.2)	-0.55 (-3.6-0.56)	-1.57 (-3.45–0.45)
Zebrasoma scopas	Acanthuridae	herbivore	0.48 (0.46-0.5)	0.63 (0.58-0.68)	0.43 (0.33-0.51)
Acanthurus nigricans	Acanthuridae	herbivore	0.49 (0.44-0.54)	0.59 (0.39-0.72)	0.44 (0.19-0.61)
Acanthurus achilles	Acanthuridae	herbivore	0.45 (0.35-0.55)	0.03 (-0.49-0.42)	0.18 (-0.31-0.79)
Acanthurus pyroferus	Acanthuridae	detritivore	-0.14 (-0.29-0)	-7.18 (-18.7–0.39)	-0.37 (-2.65-0.68)
Acanthurus guttatus	Acanthuridae	herbivore	0.27 (0.11-0.41)	-0.11 (-0.68-0.29)	-0.26 (-1.86-0.47)
Acanthurus olivaceus	Acanthuridae	detritivore	-0.13 (-0.36-0.07)	-2.06 (-4.9-0.7)	-0.92 (-3.26-0.34)
Acanthurus lineatus	Acanthuridae	herbivore	0.16 (0.03-0.28)	0.17 (-0.29-0.53)	-0.25 (-1.26-0.35)
Aulostomus chinensis	Aulostomidae	carnivore	0.46 (0.25-0.65)	0.55 (0.37-0.73)	0.36 (-0.34-0.79)
Melichthys niger	Balistidae	herbivore	0.59 (0.51-0.66)	0.7 (0.49-0.84)	0.76 (0.6-0.86)

Species	Family	Diet	AE C	AE N	AE P
Melichthys vidua	Balistidae	herbivore	0.49 (0.4-0.55)	0.71 (0.48-0.83)	0.49 (0.11-0.73)
Balistapus undulatus	Balistidae	mixed invertivore	0.41 (0.23-0.56)	0.24 (-0.58-0.7)	0.5 (0.19-0.71)
Sufflamen bursa	Balistidae	mixed invertivore	0.15 (-0.05-0.32)	-0.05 (-0.95-0.47)	0.29 (-0.23-0.59)
Odonus niger	Balistidae	mixed invertivore	0.35 (0.2-0.48)	0.39 (0.17-0.56)	0.23 (-0.15-0.51)
Rhinecanthus aculeatus	Balistidae	mixed invertivore	0.3 (0.08-0.46)	-3.55 (-8.05–1.2)	0.27 (-0.25-0.59)
Chaetodon vagabundus	Chaetodontidae	corallivore	0.41 (0.34-0.47)	0.47 (0.39-0.55)	0.2 (-0.1-0.48)
Chaetodon reticulatus	Chaetodontidae	corallivore	0.75 (0.74-0.77)	0.83 (0.82-0.85)	0.7 (0.59-0.79)
Chaetodon ornatissimus	Chaetodontidae	corallivore	0.8 (0.78-0.81)	0.88 (0.86-0.89)	0.75 (0.68-0.81)
Chaetodon auriga	Chaetodontidae	corallivore	0.6 (0.51-0.69)	0.45 (-0.03-0.75)	0.48 (0.29-0.63)
Heniochus chrysostomus	Chaetodontidae	corallivore	0.72 (0.66-0.77)	0.7 (0.59-0.81)	0.63 (0.5-0.76)
Chaetodon lunulatus	Chaetodontidae	corallivore	0.75 (0.68-0.81)	0.51 (0.22-0.7)	0.62 (0.21-0.84)
Forcipiger flavissimus	Chaetodontidae	mixed invertivore	0.49 (0.22-0.6)	-0.12 (-1.01-0.4)	0.01 (-1.08-0.68)
Chaetodon citrinellus	Chaetodontidae	corallivore	0.65 (0.52-0.74)	0.48 (0.2-0.72)	0.69 (0.44-0.87)
Chaetodon ephippium	Chaetodontidae	corallivore	0.75 (0.7-0.8)	0.85 (0.78-0.91)	0.45 (-0.11-0.78)

Species	Family	Diet	AE C	AE N	AE P
Paracirrhites hemistictus	Cirrhitidae	carnivore	0.39 (0.2-0.57)	0.57 (0.26-0.8)	0.17 (-0.78-0.83)
Sargocentron tiere	Holocentridae	carnivore	0.62 (0.4-0.76)	0.76 (0.5-0.88)	0.3 (-0.68-0.85)
Neoniphon sammara	Holocentridae	carnivore	0.72 (0.62-0.78)	0.88 (0.79-0.92)	0.7 (0.32-0.85)
Myripristis berndti	Holocentridae	carnivore	0.6 (0.52-0.67)	0.79 (0.74-0.83)	0.01 (-0.55-0.47)
Chlorurus spilurus	Labridae	detritivore	0.02 (-0.21-0.22)	-0.09 (-1.93-0.77)	0.09 (-0.59-0.51)
Epibulus insidiator	Labridae	carnivore	0.36 (0.2-0.49)	0.37 (0.12-0.55)	0.64 (0.44-0.78)
Halichoeres hortulanus	Labridae	mixed invertivore	0.37 (0.21-0.5)	0.69 (0.45-0.82)	0.37 (-0.05-0.65)
Cheilinus chlorourus	Labridae	carnivore	0.44 (0.27-0.58)	0.45 (-0.13-0.77)	-0.18 (-1.7-0.9)
Calotomus carolinus	Labridae	herbivore	0.39 (0.11-0.58)	0.61 (0.29-0.83)	0.23 (-0.47-0.73)
Scarus schlegeli	Labridae	herbivore	0.41 (-0.15-0.7)	0.66 (0.07-0.92)	0.53 (0.09-0.86)
Gnathodentex aureolineatus	Lethrinidae	mixed invertivore	0.47 (-0.15-0.75)	-0.14 (-1.21-0.59)	0.25 (-0.6-0.79)
Cantherhines sandwichiensis	Monacanthidae	mixed invertivore	0.39 (0.27-0.49)	0.68 (0.41-0.88)	0.12 (-0.49-0.6)
Parupeneus multifasciatus	Mullidae	carnivore	0.32 (0.16-0.46)	0.54 (0.2-0.77)	0.5 (0.14-0.78)
Centropyge flavissima	Pomacanthidae	mixed invertivore	0.34 (0.19-0.46)	0.29 (-0.32-0.68)	0.42 (0.02-0.76)

Species	Family	Diet	AE C	AE N	AE P
Stegastes nigricans	Pomacentridae	herbivore	0.46 (0.3-0.58)	-0.24 (-1.3-0.39)	0.19 (-0.55-0.61)
Abudefduf sexfasciatus	Pomacentridae	planktivore	0.19 (-0.19-0.45)	-0.06 (-0.75-0.39)	-0.27 (-2.02-0.58)
Dascyllus flavicaudus	Pomacentridae	planktivore	0.37 (0.23-0.51)	0.36 (-0.02-0.68)	0.35 (-0.1-0.72)
Dascyllus trimaculatus	Pomacentridae	planktivore	0.39 (0.28-0.5)	0.56 (0.43-0.68)	-0.11 (-1.44-0.55)
Chromis xanthura	Pomacentridae	planktivore	0.33 (0.28-0.38)	0.46 (0.37-0.53)	-0.05 (-0.53-0.35)
Abudefduf septemfasciatus	Pomacentridae	planktivore	0.61 (0.48-0.71)	0.69 (0.52-0.83)	0.26 (-0.29-0.6)
Cephalopholis urodeta	Serranidae	carnivore	0.69 (0.58-0.78)	0.84 (0.74-0.9)	0.58 (-0.1-0.96)
Cephalopholis argus	Serranidae	carnivore	0.7 (0.57-0.79)	0.75 (0.52-0.89)	0.33 (-0.45-0.79)
Epinephelus merra	Serranidae	carnivore	0.72 (0.61-0.79)	0.84 (0.67-0.95)	0.69 (0.35-0.87)
Arothron meleagris	Tetraodontidae	corallivore	0.74 (0.61-0.82)	0.51 (0.02-0.82)	0.7 (0.46-0.84)
Zanclus cornutus	Zanclidae	mixed invertivore	0.04 (-0.16-0.21)	-0.02 (-0.78-0.47)	-0.75 (-1.42–0.26)

Chapter 7

Stereo-video monitoring and physiological trials reveal metabolic demands of reef fishes in the wild

This chapter is in revision for *Journal of Animal Ecology*.

Authors: Nina M. D. Schiettekatte*, Francesca Conte*, Beverly French, Simon J. Brandl, Christopher J. Fulton, Alexandre Mercière, Tommy Norin, Sébastien Villéger, Valeriano Parravicini

* These authors contributed equally

7.1 Abstract

Organismal metabolic rates are the basis of energy and nutrient fluxes through ecosystems. In the marine realm, fishes are the most prominent consumer species. However, their metabolic demand in the wild (field metabolic rate, FMR) is poorly documented, because it is very challenging to measure directly. Here, we introduce a novel approach to estimating the component of FMR associated with voluntary activity in nature (i.e., the field active metabolic rate, AMR_{field}). We do this by combining laboratory-based respirometry and field-based stereo-video systems to estimate the activity of individuals. We exemplify our approach by focusing on seven coral reef fish species, for which we quantified standard and maximum metabolic rates (SMR and MMR, respectively) in the laboratory, and body sizes and swimming speeds in the field. Based on the relationships between metabolic rate, body size, and swimming speeds, we show that the activity scope (i.e., the ratio between AMR_{field} and SMR) varies from 1.2 to 3.2 across species and body sizes. Furthermore, we demonstrate that the scaling exponent for AMR_{field} varies across species and can substantially exceed the widely assumed value of 0.75 for standard metabolic rates. Finally, by scaling organismal AMR_{field} estimates to the assemblage level, we show the potential effect of this variability on community metabolic demand. As a non-destructive, widely applicable technique, our approach can improve our ability to estimate elemental fluxes mediated by a critically important group of aquatic animals.

7.2 Introduction

Anthropogenic stressors, such as climate change, over-harvesting, and pollution, are affecting biological communities at an unprecedented rate (Halpern *et al.* 2008; Venter *et al.* 2016). Scientists and policy-makers are becoming increasingly concerned that these community impacts will irreversibly alter key ecosystem functions, preventing these natural systems from maintaining indispensable services to humans (Cardinale *et al.* 2012). In this context, tools to quantify and monitor ecosystem processes are valuable (Tilman *et al.* 2014). However, while there is a long-standing tradition in measuring ecological processes in mesocosms and controlled *in situ* experiments, the assessment of rates of ecological processes in natural conditions is still in its infancy (Reich *et al.* 2012), especially for marine ecosystems (Brandl *et al.* 2019a).

In coastal marine ecosystems, fishes represent one of the most thoroughly studied, ecologically important, and economically valuable group of consumers (Bozec *et al.* 2004; Tamayo *et al.* 2018). Despite the complexity of measuring the contribution of mobile species to ecosystem fluxes (Wilson *et al.* 2010), several attempts have been made to quantify contributions of fishes to nutrient and carbon cycling (Villéger *et al.* 2017; Brandl *et al.* 2019a). These functions are usually quantified at the individual level, that can then be scaled up to community levels through an additive framework (Allgeier *et al.* 2014; Barneche *et al.* 2014; Brandl *et al.* 2019b; Morais & Bellwood 2019b). While there are inherent limitations to this approach, individual-based modeling currently represents our best means to quantify ecological processes across communities of mobile, aquatic organisms. Nevertheless, the accuracy of these approaches inevitably depends on our capacity to precisely estimate physiological requirements and expenditures of individuals in their natural environment.

The metabolic rate of living organisms is an essential determinant of their physiological requirements and therefore represents a crucial parameter to estimate the flow of energy and nutrients in any ecosystem (Brown *et al.* 2004; Allen *et al.* 2005). Theory predicts that individual metabolic rate increases sub-linearly with body mass

according to a power function with a scaling exponent of approximately 0.75 (West *et al.* 1997; Gillooly *et al.* 2001; Brown *et al.* 2004). This value has been widely accepted and appears to hold roughly true for standard metabolic rates of marine fishes (Barneche *et al.* 2014). Therefore, this metabolic scaling exponent has been used to estimate community-level metabolic rates as well (Cheung *et al.* 2013; e.g., Deutsch *et al.* 2015; Holt & Jørgensen 2015). However, the verification of this scaling exponent is based on laboratory experiments, and whether the metabolic scaling of fishes in the wild follows this general rule remains to be explored.

Metabolic rates of fishes are generally evaluated through two metrics: i) standard metabolic rate (SMR) (FRY 1957; Vinberg 1960), which corresponds to the metabolic rate of an inactive and fasting individual (Clark *et al.* 2013); and ii) maximum metabolic rate (MMR), which corresponds to the aerobic metabolic rate of an animal that is exercising at full capacity (Norin & Clark 2016). Knowledge of these two metrics allows for the calculation of a fish's aerobic scope, which is the difference between MMR and SMR and represents the capacity to elevate metabolic rate above maintenance to support energetically demanding tasks such as physical activity and digestion (Clark *et al.* 2013). Within species, aerobic scope tends to increase with body mass regardless of being expressed in absolute (MMR minus SMR) or factorial (MMR divided by SMR) values (Halsey *et al.* 2018), as the scaling exponent of MMR is often observed to be higher than that of SMR (Glazier 2005; Killen *et al.* 2007). Both SMR and MMR can be estimated relatively accurately in the laboratory through measurements of oxygen uptake rates (Clark *et al.* 2013; Chabot *et al.* 2016; Norin & Clark 2016; Svendsen *et al.* 2016). However, animals in the wild rarely reside at SMR or exercise maximally. Thus, calculations of energy expenditures in wild fishes are hamstrung by our inability to accurately estimate metabolic rates in fishes that pursue their normal, daily activities in their natural environment.

The field metabolic rate (FMR) represents the average metabolic rate of an individual in the wild (Nagy 2005; Chung *et al.* 2019) and lies somewhere between SMR and MMR (Nagy 2005). On average, free-living fishes in their natural habi-

tats will only exploit a given proportion of their aerobic scope and, in non-sedentary fishes, physical activity will be a major component of FMR (Chung *et al.* 2019). Thus, the factorial scope for activity (FSA), which corresponds to the ratio between the component of FMR related to physical activity (the field active metabolic rate, AMR_{field}) and the SMR, is a better reflection of energy expenditure in the wild (Chung *et al.* 2019), bearing in mind that internal homeostatic processes such as digestion and reproduction also incur an energetic cost as part of the full FMR. In terrestrial vertebrates, where the doubly-labeled water technique has allowed for widespread quantification of FMR (Webster & Weathers 1989), the metabolic scaling exponent of FMR tends to be higher than that of SMR (~0.8; Nagy (2005)). While the metabolic scaling exponent of MMR in fishes ranges approximate or exceed 0.8 as well, the scaling of FMR or AMR_{field} remains poorly documented (Norin & Clark 2016). Understanding how metabolic rate scales with body mass in the wild is fundamentally important for fisheries (e.g., stock assessments) and predictions of the effects of climate change, as the metabolic scaling exponent is an integral part of growth models used to forecast the size of fishes at both current and future temperatures (Von Bertalanffy 1957; Cheung *et al.* 2013; Deutsch *et al.* 2015; Marshall & White 2019).

Since FMR is challenging to measure for water-breathing animals in the aquatic environment (Treberg *et al.* 2016), it has only been estimated for a small number of fishes (e.g., Lucas *et al.* 2011; Murchie *et al.* 2011; Cruz-Font *et al.* 2016; Chung *et al.* 2019). These estimates are largely derived from biotelemetry approaches that rely on accelerometry tags and heart rate measurements calibrated with rates of oxygen uptake in the laboratory (Gräns *et al.* 2009; Treberg *et al.* 2016). A major limitation of biotelemetry is that their application is limited to large individuals as it requires surgical attachment or implantation of tags (Gräns *et al.* 2009). More recently, FMR has been estimated from the isotopic composition of carbon in fish otoliths (Chung *et al.* 2019). However, this approach relies on destructive sampling and the generality of the undoubtedly promising results are yet to be applied across a broad range of

species. Thus, non-invasive methods to estimate FMR on many co-occurring fish species in the field are needed to better understand the contributions of fishes to ecosystem functioning.

Here, we propose a new approach to estimate a major component of the FMR, the AMR_{field}. Specifically, we estimated SMR and MMR of seven reef fish species using traditional respirometry techniques in the laboratory, and then quantified *in situ* swimming speeds of the same species using underwater stereo-video systems. This permitted us to derive AMR_{field} and the factorial scope for activity (FSA) on the basis of the theoretical relationship between metabolic rate and swimming speed, and to assess the mass-scaling exponents of AMR_{field} for each species. By combining our results with underwater visual census data of fish size and abundance on reefs around Mo'orea, French Polynesia, we also quantified assemblage-level SMR and AMR_{field}. In doing so, we demonstrate the viability and applicability of our approach to tackle questions across fields of organismal, community, and ecosystem ecology in the marine biome.

7.3 Methods

7.3.1 Summary

Our approach is based on the relationship between swimming speed and metabolic rate (Torres & Childress 1983; Binning *et al.* 2013; Norin & Clark 2016). Specifically, we rely on the notion that the standard metabolic rate (SMR) represents the metabolic rate of an individual when its swimming speed is zero (U_0), while the maximum metabolic rate (MMR) represents the oxygen uptake rate of individuals at their maximum – or critical – swimming speed (U_{crit})(figure 7.1). Further, we assume that metabolic rates vary predictably with swimming speed following a traditional power function (Brett 1964; Korsmeyer *et al.* 2002). Therefore, on the basis of knowledge of SMR and MMR along with the U_0 and U_{crit} of individuals, the active field active metabolic rate (AMR_{field}) of a species can be estimated if the average swimming speed (U) of individuals for a specific body size is known. We estimated SMR and MMR using respirometry in the laboratory, obtained U_{crit} through empirical data available in the literature, and estimated U using stereo-camera video recordings in the field. We then used these estimates of AMR_{field} to quantify the factorial scope for activity (FSA), and the metabolic scaling exponent for AMR_{field}. Finally, to evaluate the impact of assessing assemblage-level metabolic rates on the basis of a realistic proxy of field metabolic rate, AMR_{field} (instead of using the more commonly measured SMR as an estimate of minimum energetic requirements), we scaled up our estimates at assemblage level according to visual census data of fish sizes and abundances on a coral reef in Mo'orea, French Polynesia.

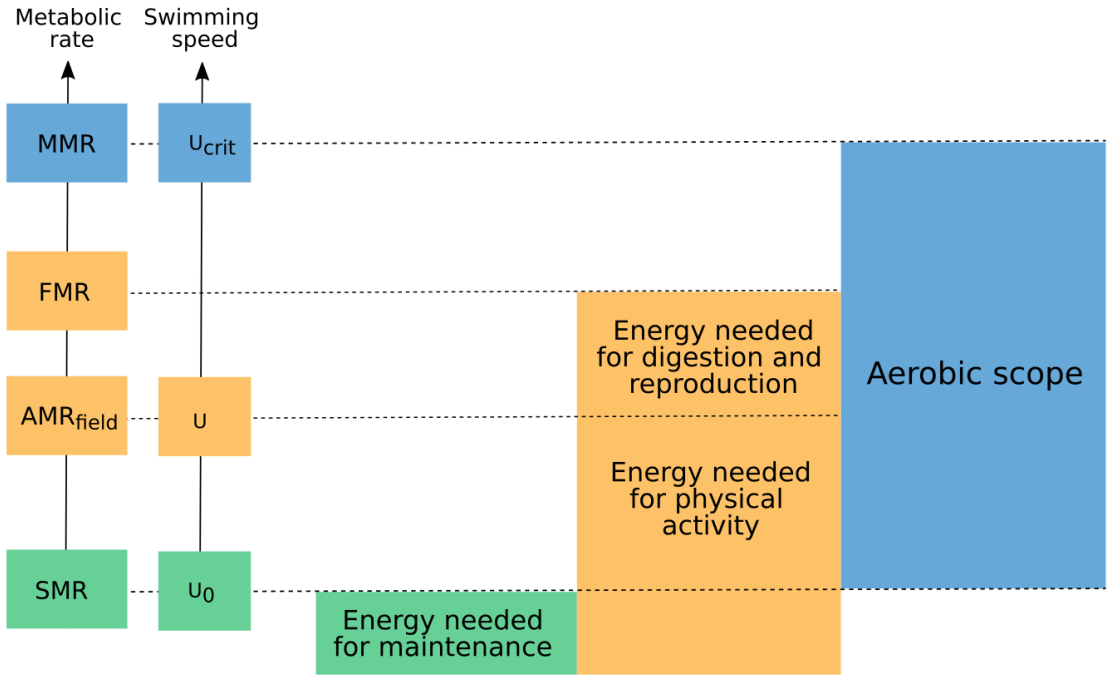

Figure 7.1: Definition of terms used to describe aspects of fish metabolism and their inter-relationships. SMR is standard metabolic rate calculated as the oxygen uptake rate ($\dot{M}O_2$ at swimming speed 0 (U_0). AMR_{field} is field active metabolic rate measured as $\dot{M}O_2$ at spontaneous swimming speed (U). FMR is field metabolic rate including AMR_{field} and the energy needed for digestion and reproduction. MMR is maximum metabolic rate, which can be measured as the $\dot{M}O_2$ at maximum (critical) swimming speed (U_{crit}).

7.3.2 Model species

We focused on seven common reef fish species with varying body sizes and shapes, trophic strategies, and behavioral patterns: *Cephalopholis argus* (family Serranidae), a large, fusiform, sedentary piscivore; *Chaetodon ornatissimus* (family Chaetodontidae), a small-bodied, laterally compressed, obligate coral feeder; *Chromis iomelas* (family Pomacentridae), a small, schooling planktivore; *Ctenochaetus striatus* (family Acanthuridae), a medium-sized, grazing detritivore; *Naso lituratus* (family Acanthuridae), a large-bodied, grazing herbivore feeding on macroalgae; *Odonus niger* (family Ballistidae), a large-bodied schooling planktivore; and *Zebrasoma scopas* (family Acanthuridae), a compressed, small-bodied, grazing herbivore feeding on filamentous algae. All data were collected in Mo'orea, French Polynesia, between March 2018 and February 2019. For respirometry experiments, individuals were collected in the lagoon (depth range 1-6m) next to Opunohu Bay (17.4928°S, 149.8555°W) with hand nets and clove oil.

7.3.3 Standard and maximum metabolic rate

To quantify SMR and MMR, we conducted intermittent-closed respirometry experiments (Steffensen 1989; Clark *et al.* 2013) at 28+-0.5 °C on a total of 68 individuals across the seven study species with the sample size per species ranging between four and 23 individuals. After an acclimation and fasting period of 48 h in aquaria, the fish were individually transferred to a water-filled tub at 28°C and sequentially chased by the experimenter until visibly exhausted to elicit MMR (Clark *et al.* 2012; S. Butail *et al.* 2013). Once the chasing was concluded, each individual was immediately placed in a respirometry chamber submersed in an ambient and temperature-controlled tank, where they were left for approximately 24 h to reach SMR. The intermittent respirometry cycles consisted of a measurement (closed) period followed by an open period during which the respirometry chambers were flushed with fully aerated water from the ambient tank. Based on previous work (Norin & Clark 2016), we considered the

oxygen uptake rate ($\dot{M}O_2$) during the first closed cycle (directly after transferring the fish) to be reflective of the individual's MMR. Depending on fish size, respirometry chambers ranged in volume (including tubes and pumps) from 0.38 to 4.4 L, and measurement and flush periods lasted between 2 to 9 min and 3 to 5 min, respectively. SMR was calculated as the average of the 10 % lowest $\dot{M}O_2$ values measured during the entire respirometry trial, after the removal of outliers, while MMR was calculated from the slope of the first measurement period (Chabot *et al.* 2016).

7.3.4 Swimming speed

We used two underwater stereo-video systems that were placed on the seafloor to record fish movements. Each video system consisted of two small action cameras (GoPro Hero5 Black), mounted 90 cm from each other at an angle of approximately 6°. This method allows three-dimensional (3D) measurements (Hughes & Kelly 1996; S. Butail & Paley 2012). To analyze the recorded videos, we used VidSync, an open-source Mac application providing accurate 3D measurements (Neuswanger *et al.* 2016), which allow for the synchronization, calibration, and analysis of videos. We recorded calibration videos to correct for the nonlinear optical distortion of the images due to camera lenses and underwater housings, and to define the 3D coordinate system (x, y, z) used throughout the analyses. Errors in length measurements through video analysis increase with distance from the cameras (Neuswanger *et al.* 2016). Thus, for each underwater stereo-video system, we fitted a linear regression model describing the error in measurements as a function of their distance from the nearest camera, which we used to adjust all measurements of distances and fish lengths (figure 7.6). We recorded twenty stationary stereo-videos between November 19th 2018 and December 12th 2018. Videos were recorded at 12 to 14 m depth on the reef slope at the Tiahura long-term monitoring site in Mo'orea (17° 29' 00.6" S, 149° 54' 20.9" W) and at five different time-periods: 5:00–7:00, 8:00–10:00, 11:00–13:00, 14:00–16:00, and 17:00–18:00. Each recording lasted for ~1-1.5 h. We then took measurements

during three 10 min sequences with intervals of 10 min that excluded the first 2 min to account for the presence of divers. We took measurements for all fishes visible in both cameras for 3 to 5 s during the three 10 min sequences. For each individual, fork length was measured three times from the videos as the straight-line distance between the fish's head and its tail fork, and three to five consecutive swimming speeds were measured as the distance the fish moved over 3 to 5 s. Final fish lengths and swimming speeds were then calculated as the mean of the repeated measurements. In total, we recorded lengths and speeds for 634 individuals, with sample sizes per species ranging between 64 and 264 individuals.

7.3.5 Maximum swimming speed

We extracted maximum swimming speeds (U_{crit}) from previous work (Fulton 2007). U_{crit} is defined as the swimming speed at which a fish becomes exhausted and stops swimming when it is exposed to regular incremental changes in speed in an experimental flume (Brett 1964). In these experimental conditions, $\dot{M}O_2$ measured at U_{crit} corresponds to MMR (Norin & Clark 2016). In the original work of Fulton (2007), U_{crit} of 192 individuals of five families and their corresponding lengths were measured, and these measurements were then used in the present study to relate maximum swimming speed with body size and aspect ratio of the tail, as a proxy for variations in swimming ability. The aspect ratio of the tail of all species were retrieved from Fishbase (Froese *et al.* 2014).

7.3.6 Data analysis

We quantified AMR_{field} and factorial scope for activity (FSA) by combining multiple regression models, that describe the relationships between SMR and MMR with body mass, swimming speed (U), and maximum swimming speed (U_{crit}; from Fulton 2007) with body size. First, we used the respirometry data to fit a relationship between

either SMR or MMR and body mass using a Bayesian hierarchical model, while accounting for the co-variation between MMR and SMR. We define the log_{10} of SMR and MMR to be normally distributed with a mean (μ) and a standard deviation (σ) as follows:

$$\log_{10}(\text{MR}_i) \sim \text{Normal}(\mu_i, \sigma),$$

$$\mu_i = (a + a_{j,k}) + (b + b_{j,k})\log_{10}(\text{weight}_i),$$

where i is the individual, j is the species, k is the type of metabolic rate (SMR or MMR), a is the global intercept of the regression; $a_{j,k}$ is the effect on the intercept for each species and type of metabolic rate, b is the global slope of $log_{10}(weight)$, $b_{j,k}$ is the effect on the slope for each species and type of metabolic rate. We obtained the mean intercept and slope per species by summing global- and species-level parameters. We used an informative normal prior for the global slope exponent (i.e., metabolic scaling exponent) with average 0.75 and 0.1 as the standard deviation (West *et al.* 1997). For all other parameters, we used weakly informative priors (Burkner PC 2017).

Second, using the data retrieved from the video analyses, we fitted a hierarchical Bayesian regression model for estimating fish swimming speed as a function of body length. We defined the log_{10} transformation of swimming speed to be student-t distributed with degrees of freedom (ν), mean (μ), and a standard deviation (σ).The student's t-distribution was applied to build a robust regression, as our data includes outliers (Motulsky & Brown 2006).

$$\log_{10}(\text{speed}_i) \sim \text{Student}(\nu, \mu_i, \sigma),$$

$$\mu_i = (a + a_j) + (b + b_j)\log_{10}(\text{length}_i),$$

where i is the individual, j is the species, a is the global intercept of the regression,

a_j is the effect on the intercept for each species, b is the global slope , b_j is the effect on the slope of for each species. For each species, regression exponents were estimated by summing two effects of the model: the global parameter and the species-specific effect on the global parameter.

Thirdly, we fitted a similar model to predict maximum swimming speed in function of body length and aspect ratio using data extracted from Fulton (2007), including random effects of the interaction between family and body shape on the intercept and slope of body size.:

$$log_{10}(maxspeed_i) \sim Student(\nu, \mu_i, \sigma),$$

$$\mu_i = (a + a_j) + (b + b_j)log_{10}(length_i) + AR,$$

where i ,j is the interaction of family and body shape, a is the global intercept of the regression, a_j is the effect on the intercept for each family and body shape, b is the global slope , b_j is the effect on the slope for each family and body shape, and AR is the aspect ratio of the tail. Here, we also applied the Student's t-distribution and used general uninformative priors. We then used this model to estimate the maximum swimming speed of the species included in our study. Aspect ratio's were extracted from Fishbase (Froese *et al.* 2014).

7.3.7 Factorial aerobic scope, field active metabolic rate, and factorial scope for activity calculations

We predicted the factorial aerobic scope (FAS), field active metabolic rate (AMR_{field}), and factorial scope for activity (FSA) for the full size range of all model species (per cm). To estimate the fish's FAS at each possible length, we first predicted their SMR and MMR by calculating their weight using published length-weight relationship accessed through FishBase (Froese *et al.* 2014), and making predictions based on

our model parameters. For each iteration of the prediction, FAS was calculated as $FAS = \frac{MMR}{SMR}$ (Fry 1947; Killen *et al.* 2016). Finally, we summarized the FAS for each species at all sizes by taking means, standard deviations, and 95% credible intervals.

FSA is obtained by dividing the fish's AMR_{field} ($\dot{M}O_2$ at average speed U) by their SMR. To describe the relationship between $\dot{M}O_2$ and swimming speed (U), Brett (1964) (Brett 1964) used a traditional power function: $\dot{M}O_2 = a10^{bU}$. Here, we applied the log_{10}-transformed form (Korsmeyer *et al.* 2002). Consequently, the following equation was used in this study to determine individual AMR_{field}:

$$log(AMR_{field}) = log(SMR) + \frac{log(MMR) - log(SMR)}{U_{crit}}U,$$

where we consider the slope $b = \frac{log(MMR)-log(SMR)}{U_{crit}}$. Here, U is predicted through our model relating length and swimming speed, U_{crit} is predicted for each length and species using our model for family-level maximum swimming speeds, and SMR and MMR is predicted as stated above. To include an estimate of uncertainty, we included 1000 iterations of estimates of the swimming speed U. For U_{crit}, SMR and MMR we used the median of the predicted values in this step.

Once we determined AMR_{field}, we calculated FSA with the following equation:

$$FSA = \frac{12AMR_{field} + 12SMR}{24SMR}.$$

We repeated this for each iteration and then summarized FSA per species per size. We assumed that fish rested for 12 h (i.e., sleeping) (Marshall 1972). As such, for all studied species we assumed that they are active during the day and inactive during the night.

7.3.8 Assemblage-level estimates

In 2016, reef fish communities were monitored across 13 sites on the outer reef around Mo'orea using underwater visual censuses. During each census, a single diver swam along a transect of 25 m and counted all fishes within a width of 2 m. All fishes were identified to the species level and their length was estimated to the nearest 1 cm. Each transect covered an area of 50 m^2, except Tiahura and Haapiti, which covered an area of 100 m^2 each. At each site, three transects were performed, except for Tiahura and Haapiti where four and two transects were performed respectively. We extracted data for our model species from this database, which resulted in 802 individuals across the seven species. Then, we quantified the SMR and AMR_{field} for each individual using the above-mentioned methodology. Finally, we calculated the total SMR and AMR_{field} of the fish assemblage composed of the seven species at each site by summing across individual estimates.

7.4 Results

7.4.1 Standard and maximum metabolic rates

The regression model predicting metabolic rates ($\log_{10}$ of SMR and MMR) as a function of $\log_{10}$ of body mass with varying slopes and intercepts per species had a Bayesian R^2 of 0.96 (table 7.1; figure 7.2). The average metabolic scaling exponent across species was 0.73 for SMR and 0.78 for MMR (table 7.1). The median species-specific scaling exponents varied between 0.71 and 0.76 for SMR, and between 0.77 and 0.78 for MMR.

Table 7.1: Overview of species-specific slope coefficients (scaling exponents) of the regression of log_{10}-transformed SMR and MMR on function of log_{10}-transformed body mass. The intercept for each species is expressed as the back-transformed value for an individual of 1g. Values in between brackets represent the 95% CI.

species	SMR slope	SMR (mass = 1g)	MMR slope	MMR (mass = 1g)
Cephalopholis argus	0.7 (0.6;0.79)	0.003 (0.0018;0.0044)	0.78 (0.7;0.88)	0.0119 (0.0071;0.0168)
Chaetodon ornatissimus	0.71 (0.62;0.78)	0.0037 (0.0028;0.0046)	0.78 (0.7;0.86)	0.0089 (0.0068;0.0112)
Chromis iomelas	0.73 (0.6;0.89)	0.0028 (0.0023;0.0035)	0.78 (0.67;0.89)	0.0083 (0.0066;0.0105)
Ctenochaetus striatus	0.76 (0.69;0.84)	0.0041 (0.0031;0.0055)	0.78 (0.71;0.84)	0.0099 (0.0075;0.0128)
Naso lituratus	0.74 (0.6;0.91)	0.0039 (0.0028;0.0053)	0.79 (0.67;0.94)	0.0142 (0.0089;0.0191)
Odonus niger	0.72 (0.63;0.83)	0.0025 (0.0015;0.0037)	0.78 (0.7;0.88)	0.0123 (0.0079;0.017)
Zebrasoma scopas	0.71 (0.65;0.77)	0.0037 (0.0029;0.0045)	0.77 (0.72;0.83)	0.0078 (0.0062;0.0097)

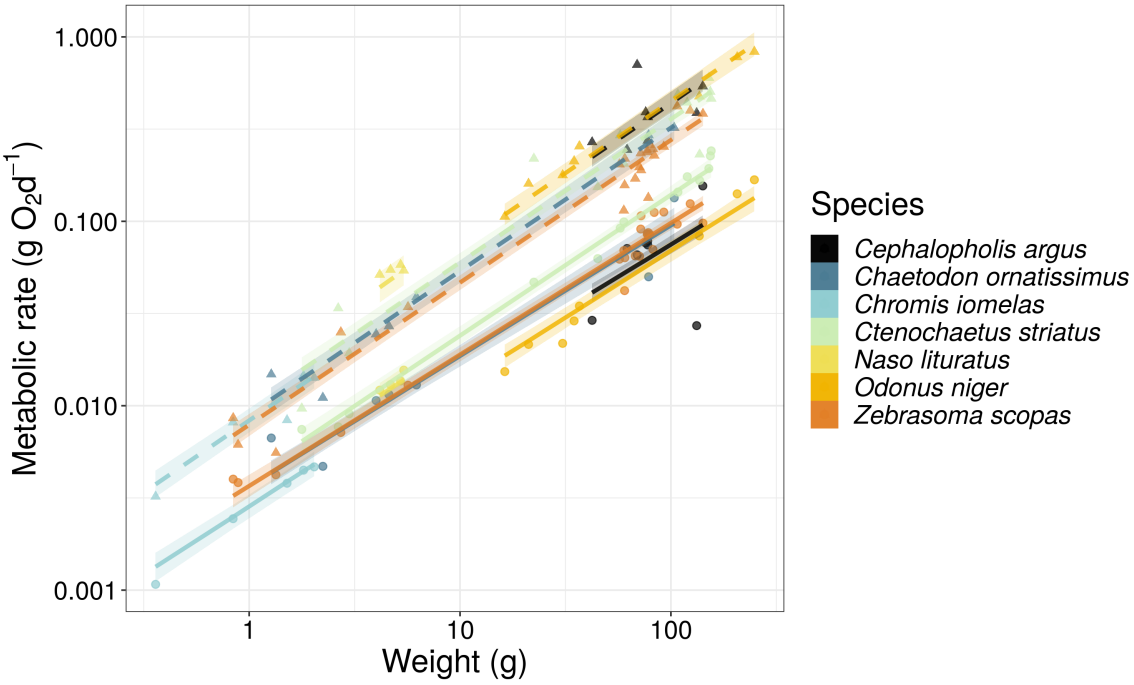

Figure 7.2: Linear regressions between log_{10}-transformed metabolic rate (gO_2d^{-1}) and weight (g) for the study species, predicted by model 1. Symbols represent empirical measurements. Solid and dashed lines represent predicted mean standard metabolic rate (SMR) and maximum metabolic rate (MMR) values, respectively. Transparent areas are the 95% credible intervals of the fitted values of the regression.

7.4.2 Swimming speed

The regression model predicting species-specific swimming speed as a function of body size had a median Bayesian R^2 of 0.57 and its residual variance (σ) was 0.37. The average species-specific slope values varied between 0.18 and 0.97 (figure 7.3, table 7.2). At the individual scale, the 95% credible interval of swimming speed predictions varied between 28.5 and 32.4 cm s^{-1} across all species and size classes. For maximum swimming speed, our model showed an increase with body size and aspect ratio (table 7.3), with a median Bayesian R^2 of 0.46. We then used this model to estimate maximum swimming speeds (figure 7.3).

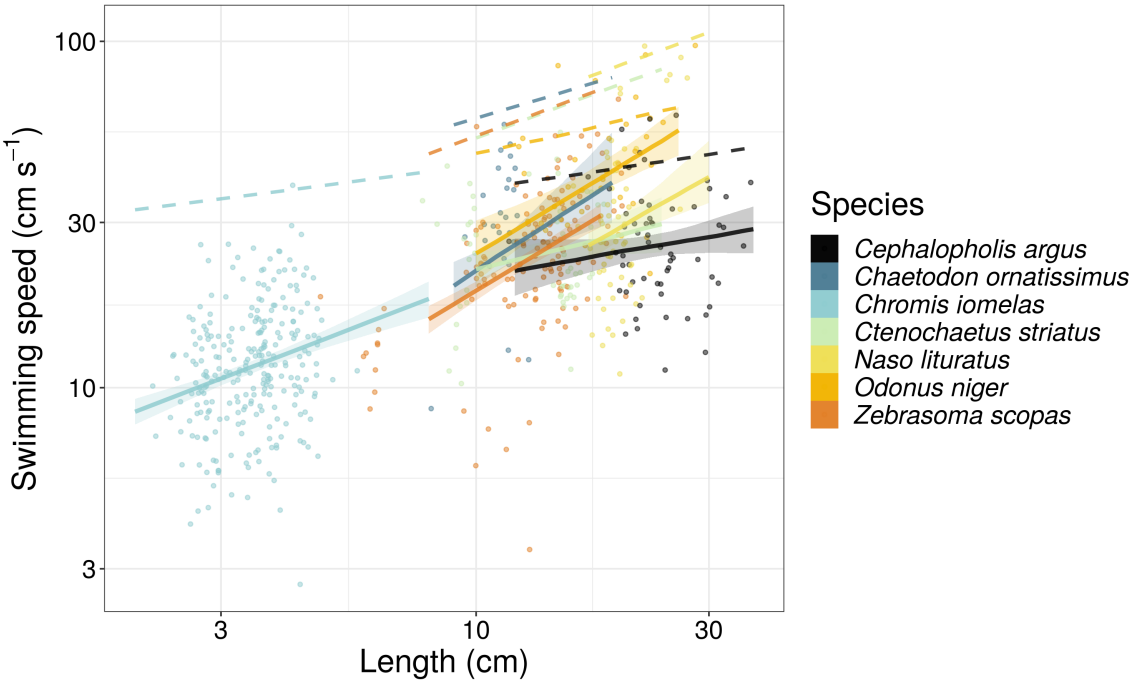

Figure 7.3: Linear regressions between log_{10}-transformed speed (cms^{-1}) and length (cm) for the seven studied fish species. Symbols represent the raw data of individuals measured through stereo-video analysis. Solid lines and shaded areas represent the predicted mean values, and associated 95% credible interval of swimming speeds. The dashed lines represent the predicted maximum swimming speeds.

7.4.3 Field metabolic rate, factorial aerobic scope and factorial scope for activity estimations

We estimated AMR_{field}, FAS, and FSA across the size range of our study species as observed in the monitoring dataset from Mo'orea in 2016. Across all species and size classes, average AMR_{field} estimates ranged between 0.001 and 1.013 g O_2 d^{-1} at the individual level (table 7.4). FAS and FSA estimates range between 2.4 and 7.0, and between 1.2 and 3.2, respectively, across species and sizes. The scaling exponent of AMR_{field} was higher than the SMR exponent for all species, except for *C. striatus* (figure 7.4a), hence, FSA increased with size for all those species (figure 7.4b). The scaling exponent of AMR_{field} was considerably higher than the MMR exponents for *N. lituratus* and *O. niger*.

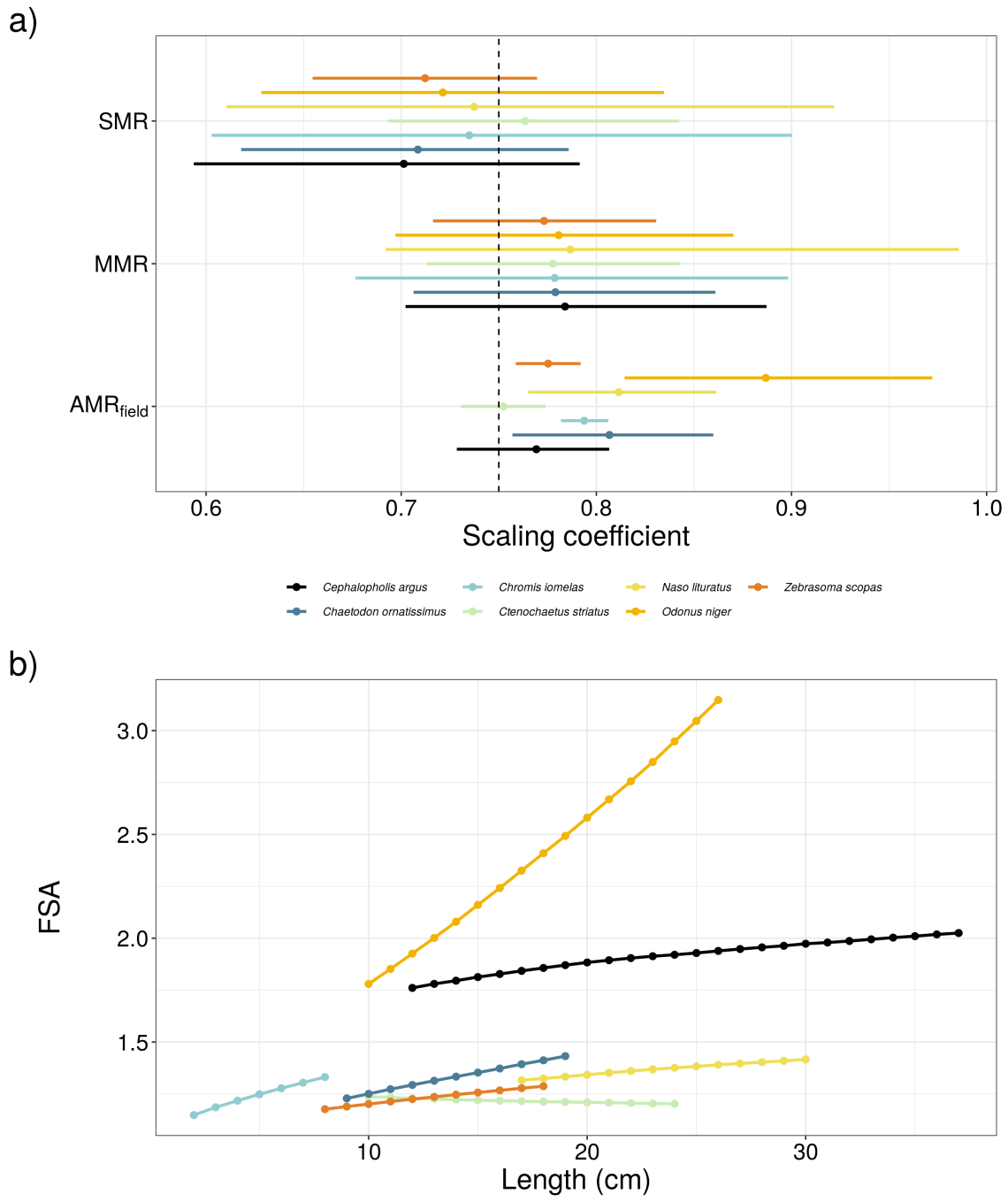

Figure 7.4: a) Fitted scaling exponents for standard metabolic rate (SMR), maximum metabolic rate (MMR), and field metabolic rate (AMR_{field}) based on slopes of the log_{10}-log_{10} relationships between the metabolic rates (gO_2d^{-1}) and body mass (g). Lines represent the 95% credible interval and dots indicate the average values. b) Predicted average factorial scope for activity (FSA) for the seven reef fish species across their body size range.

7.4.4 Assemblage-level predictions

Scaling up SMR and AMR_{field} to the assemblage level revealed major variation in the two estimates of metabolism, with average SMR (± SD) for this assemblage of seven fish species across sites (ranging between 0.026 ± 0.009 and 0.325 ± 0.021 g O_2 m^{-2} d^{-1}; figure 7.5) tending to be about half total AMR_{field} (ranging betwen 0.036 ± 0.014 g O_2 m^{-2} d^{-1} and 0.465 ± 0.07 g O_2 m^{-2} d^{-1}). Spatial variation in total SMR and AMR_{field} reflected patterns in the relative abundance of the seven study species across sites (figure 7.5, figure 7.4). Afareaitu, Maatea, Motu Ahi, Taotaha, and Tetaiuo, sites where *C. argus* and *O. niger* dominated the reef fish assemblage, had a total AMR_{field} about twice as high as the total SMR. On the contrary, sites dominated by *C. striatus* (50 to 95% of the total reef fish abundance) had total AMR_{field} 1.27 to 1.41 times higher than total SMR (i.e., Nuarei, Pihaena, Temae, and Tiahura).

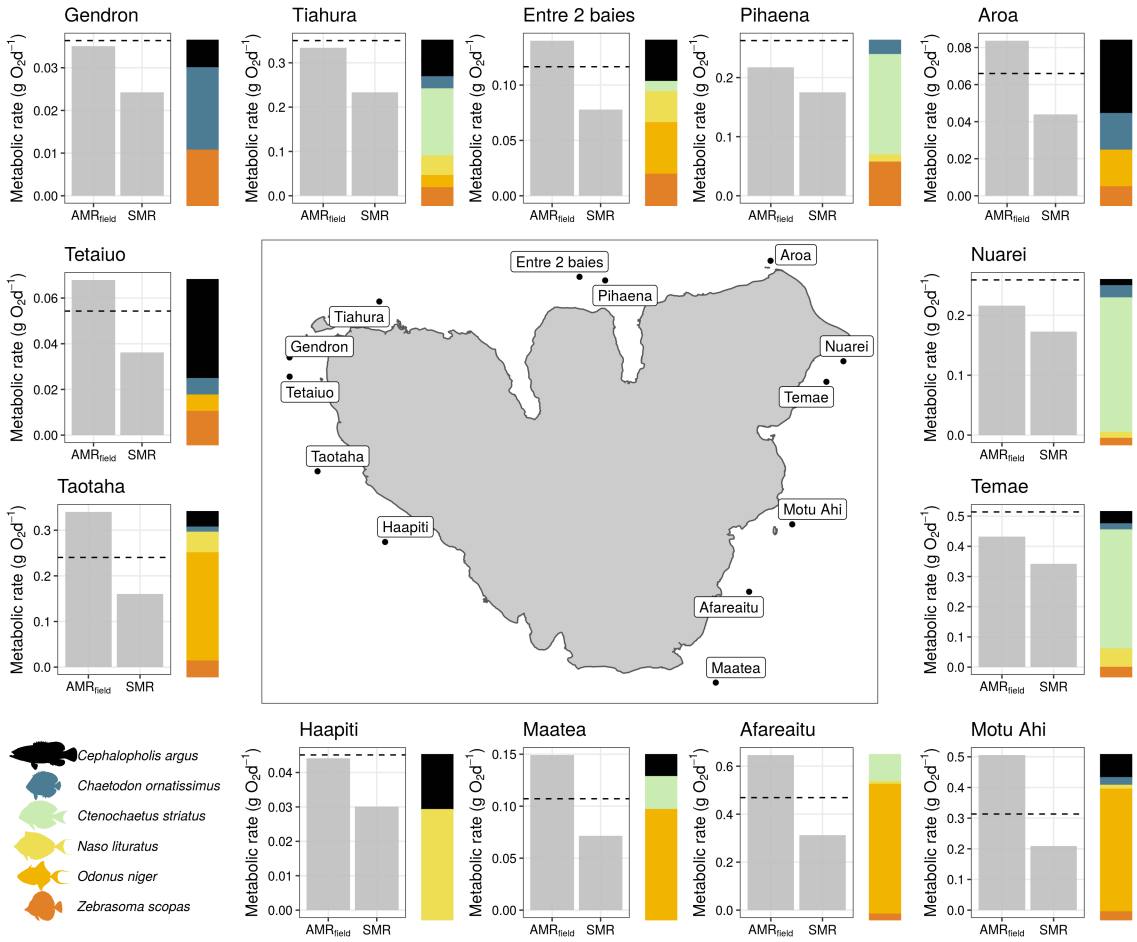

Figure 7.5: Field (AMR_{field}) and standard metabolic rates (SMR) of an assemblage of six reef fish species at 13 sites around Mo'orea, French Polynesia. Dashed lines represent 1.5 times the SMR as a reference. Coloured bars display the relative abundances of the reef fish species at each site.

7.5 Discussion

Field metabolic rate (FMR) is an essential organismal property that mediates elemental fluxes across the food web, thus influencing system-wide movements of energy and nutrients. By coupling laboratory data on metabolic rates with field observations of body size and swimming activity through stereo-video analysis, we estimated the activity component of FMR (the field active metabolic rate, AMR_{field}). Further, we demonstrate that the factorial scope for activity (FSA) of reef fish species varies substantially across species, and that the metabolic scaling exponent of AMR_{field} can substantially exceed the canonical value of 0.75, which also affects community-level estimates of metabolic rate. Therefore, our results highlight the potential pitfalls of estimating the community-level metabolic rate of heterogeneous reef fish assemblages based on scaled-up estimates of SMR instead of AMR_{field}. We suggest that the coupling of physiological traits with stereo-video analyses provides an opportunity to estimate field metabolic rates of fishes in marine environments that allow for visual assessments.

The FSA can be an important parameter to predict the energy consumption of fishes in the wild (e.g., Schiettekatte *et al.* (2020)). Our estimates of FSA were comparable to previous estimates for a small fresh-water fish, in which the FSA was obtained through a combination of bioenergetic modeling and behavioral observations [~1.9; Trudel & Boisclair (1996)]. In contrast, several other fish species may have a much higher AMR_{field} as locomotion has been reported to increase metabolic rate up to five-fold, and up to nine-fold in tuna (*Thunnus albacares*)(Brill & Bushnell 1991; Chabot *et al.* 2016). However, it is still challenging to quantify where AMR_{field} lies for most species.

The varying estimates of FSA may relate to the swimming speed and the aerobic capacity of the studied species (Clark *et al.* 2013). In our case study, the two fishes with the highest FSA were *O. niger* and *C. argus*, which appear to exploit about 45% and 60% of their aerobic scope in their natural environment, respectively. Therefore,

C. argus has a high FSA mostly due to its high aerobic scope, while *O. niger* has the highest FSA in our case study both because of a high aerobic capacity and because it uses a larger proportion of it for swimming. On the other hand, fishes with a lower FSA (i.e., *C. iomelas*, *C. ornatissimus*, *C. striatus*, and *Z. scopas*) were quite active, relative to their maximum swimming capacities, and exploited more than 50% of their aerobic scope. However, because their aerobic scope is low, so is their FSA.

These results corroborate the notion that AMR_{field} in fishes is strongly influenced by ecological traits, such as size, trophic level and habitat use (Brown *et al.* 2004; Nash *et al.* 2015; Killen *et al.* 2016). Larger fishes tend to have a higher aerobic capacity than smaller species (Brown *et al.* 2004), and larger sizes in fishes permit the establishment of larger home ranges (Nash *et al.* 2015). Furthermore, predators often have a higher metabolic capacity, compared to herbivores, and pelagic fishes often have higher metabolic potential than benthic fishes, as they have high locomotory demands because of their mobility in a 3D environment (Nash *et al.* 2015; Killen *et al.* 2016). Pairwise comparisons among our study species (e.g., the herbivorous *Z. scopas* vs. the carnivorous *C. argus* or the benthopelagic *C. striatus* vs. the epipelagic *O. niger*) strongly support an ecological basis for metabolic differentiation.

Beyond interspecific differences, our results suggest that AMR_{field} scales differently with body mass compared to standard metabolic rates (SMR) or maximum metabolic rates (MMR). The SMRs of our study species varied predictably with body mass, in accordance with the metabolic theory of ecology (Brown *et al.* 2004), with the average slope value approximating the allometric scaling exponent of 0.75 predicted by West et al. (West *et al.* 1997). In contrast, except for *C. striatus*, all species had a scaling exponent for AMR_{field}, that considerably exceeded 0.75. Consequently, the FSA was positively correlated with body size for most species, suggesting that large individuals of a species consume more oxygen in their natural environment than previously assumed. For some species, such as *C. argus*, the scaling exponent of AMR_{field} is similar to that of SMR, while for other species such as *N. lituratus* and *O. niger*, the scaling exponent of AMR_{field} is much higher. Importantly, there

is a higher interspecific variability of the scaling exponent of AMR_{field} compared to SMR and MMR. This underlines the importance of both species identity and body size when estimating FMR.

Scaling up, community-level standard metabolic rates should vary predictively with both community composition and intraspecific size structure (Allen *et al.* 2005); Barneche *et al.* 2014). However, failing to account for the increased variation in scaling exponents of field metabolic rates may lead to severe underestimates of the contribution of large mobile fishes to the total respiration of fish communities. Indeed, comparing our assemblage-level estimates based on SMR with assemblage-level estimates based on AMR_{field} reveals the potential pitfalls of using SMR to study community-level metabolic rates (e.g., Cheung *et al.* (2013); Deutsch *et al.* (2015); Holt & Jørgensen (2015)). The ratio between community-level AMR_{field} and SMR is extremely variable, thus suggesting that universal corrections to convert laboratory-estimated SMR into AMR_{field} are likely unreliable. For example, communities with a similar biomass and size structure may be considered as having a similar metabolic rate when using SMR as a proxy. However, if a community includes species that have a much higher metabolic scaling exponent, the role of large individuals, and thus the community-level metabolic rate may be underestimated severely. Thus, it is important to consider a higher variation in metabolic scaling of FMR than previously assumed if we want to estimate energy flow in fish communities.

While our approach offers a novel way to estimate the activity rate and metabolism of fishes, it comes with some limitations. First, we used family-level maximum swimming speeds to reconstruct the relationship between metabolic rate and swimming speed (Fulton 2007). Although we accounted for variation in body shapes, this may introduce some bias into the calculations, as species within a family and body shape can differ substantially. Further, our method relies on the assumption that metabolic rate varies predictively with swimming speed following a traditional power function (Brett 1964; Korsmeyer *et al.* 2002). Ideally, this relationship should be verified empirically by measuring swimming speed and respiration rate simultaneously in

the laboratory. Furthermore, we quantified FSA assuming that fishes' spontaneous swimming activity follows strict circadian cycles, with all activity occurring diurnally. However, activity patterns of reef fishes are often flexible (Zhdanova & Reebs 2006). While, in principle, all our studied families are diurnally active, some species, (e.g., Serranidae) can be nocturnally active (Mourier *et al.* 2016). Thus, our assumption can cause potential underestimates of FSA in *C. argus* and other species with more flexible circadian activity patterns. Currently, stereo-video recordings are unable to quantify fish swimming speeds at night, as measurements are inaccurate and imprecise in darkness and poor visibility (Neuswanger *et al.* 2016). However, infrared lighting in stereo-video recordings could provide a solution to observe nocturnal behavior and movement in fishes (Bassett & Montgomery 2011).

Finally, while AMR_{field} than SMR or routine metabolic rate (the average laboratory-estimated metabolic rate of fish kept in respirometry chambers, which includes spontaneous activity; Norin & Speers-Roesch (2020), it still doesn not include all energy expenditure of fishes in the wild, such as reproduction and digestion. Digestion (often expressed as specific dynamic action; SDA) can be a large component of the energy budget of fishes (e.g., ~17% of SMR; Holt & Jørgensen (2015)). SDA can be measured in the laboratory, where a fish is given a meal and the oxygen consumption is measured for the duration of the digestion of this meal. SDA relates predictively to both meal size and body mass of a fish (Secor 2009), but using this relationship to calculate SDA of species in natural communities is not feasible. It is nearly impossible to track frequency of meals and meal sizes of fishes in the wild, even though some bioenergetic modeling allows for an approximation of consumption rates (e.g., Schiettekatte *et al.* (2020)). Further, these experiments are largely based on predatory fishes, and do not necessarily represent natural feeding behavior as many fishes do not consume and digest a meal before eating the next meal. Notably, herbivores and detritivores, but also planktivores, feed constantly, and their energy expenditure related to digestion is understudied. Therefore, we stress the need for more research on the energy consumption of digestion across a

wide range of fishes to achieve improved FMR approximations for fish communities in the wild.

Despite these limitations, our proposed method increases our awareness of the variation in AMR_{field} among reef fishes, which is necessary to understand ecosystem-level estimates of elemental fluxes. So far, the quantification of AMR_{field} is limited to laboratory techniques that are reliant on destructive sampling [analysis of trace elements in otoliths; Chung *et al.* (2019)], or restricted to species that are big enough to be tagged with biotelemetry equipment (Brodie *et al.* 2016; Treberg *et al.* 2016). When combined with respirometry trials, stereo-video offers a nondestructive alternative to these techniques that can be applied to all species that can be reliably observed using *in situ* cameras. While the post-hoc treatment of the stereo-video outputs demands significant time and effort, the development of open source software to automate data collection from video will greatly strengthen our ability and non-destructive approach to quantifying reef fish AMR_{field} (Guénard *et al.* 2008; Bassett & Montgomery 2011).

7.6 Supporting information

Acknowledgements: We thank the staff at CRIOBE, Moorea for field support. Further we would like to express gratitude to Camille Gache and Yann Lacube for their help in the field. Finally, we thank CRIOBE for sharing UVC data from their long-term monitoring program.

Funding: This work was supported by the BNP Paribas Foundation as a part of the ReefServices project and the Agence National de la Recherche (REEFLUX, ANR-17-CE32-0006). TN was supported by funding from the Danish Council for Independent Research (DFF-4181-00297) and the European Union's Horizon 2020 research and innovation program under the Marie Skłodowska-Curie grant agreement No. 713683.

Author contributions: NMDS conceived the idea and FC, NMDS, and VP designed methodology; BF and NMDS recorded *in situ* stereo-videos; FC performed video analysis; AM and NMDS collected fishes and AM performed respirometry experiments; CJF collected data on maximum swimming speed; FC and NMDS analysed the data and led the writing of the manuscript. All authors contributed significantly to the drafts and approved the final version for publication.

7.7 Supplementary materials

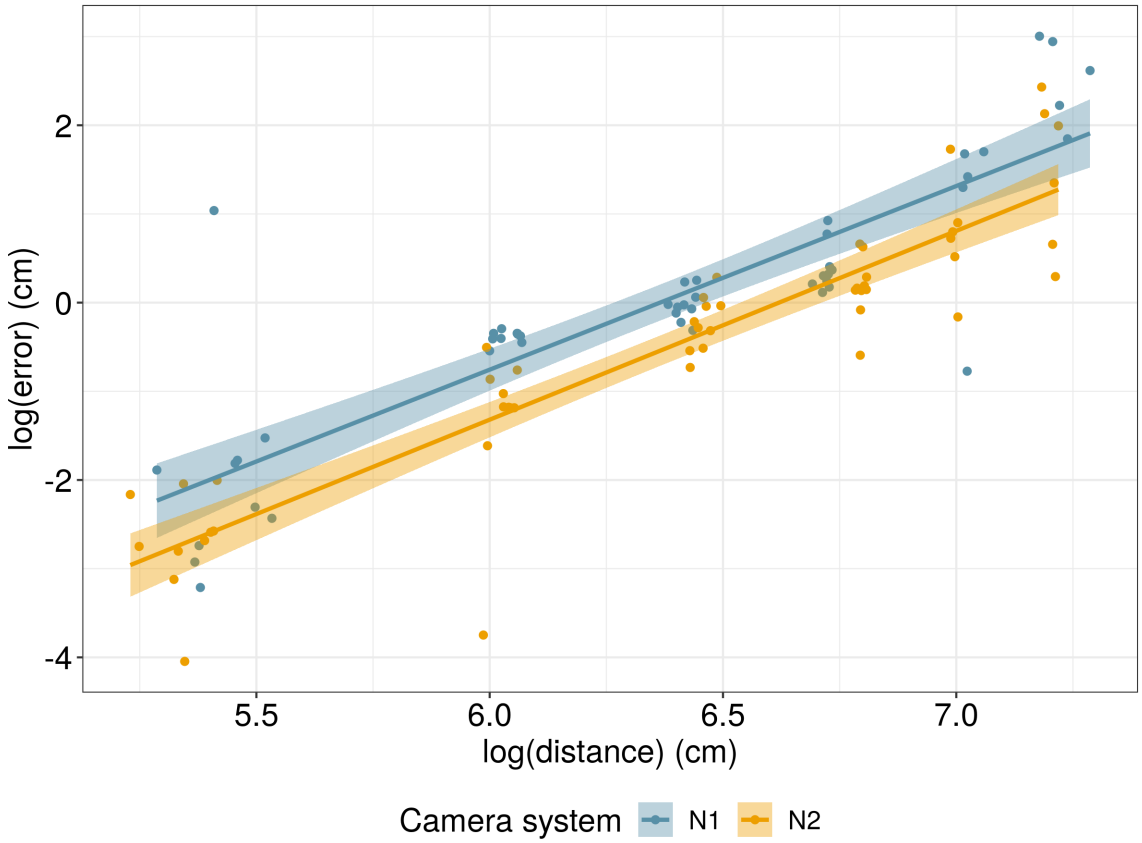

Figure 7.6: Linear regressions between the error (cm) in measurements collected by video analysis and the distance (cm) from the nearest camera for both underwater stereo-video systems. Each color represents an underwater stereo-camera system used in this study. Shaded areas show the linear regression standard errors.

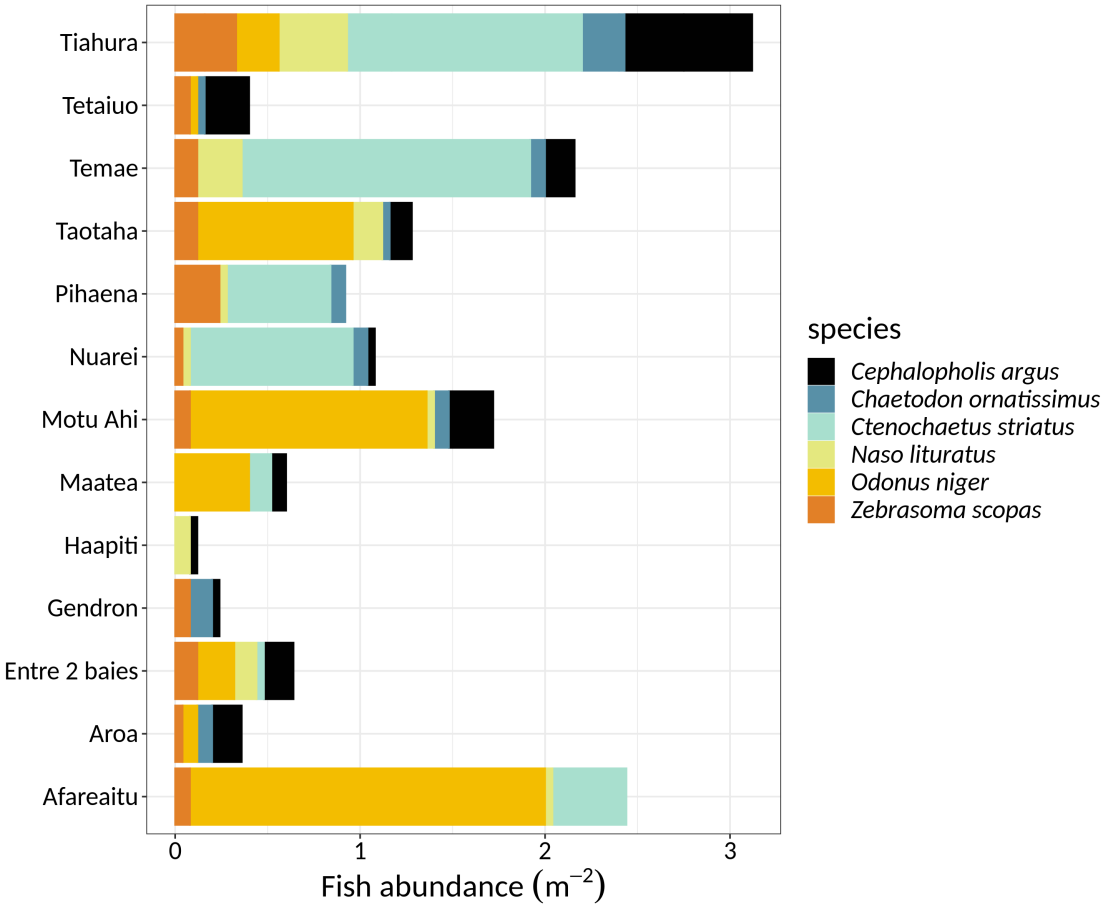

Figure 7.7: Fish abundance (m^{-2}) of the studied sites. Each colour represents the abundance of a specific studied reef fish species.

Table 7.2: Overview of species-specific slope and intercept coefficients for the regression of natural log-transformed swimming speed on natural log-transformed body length (in cm). The 95% credible interval is displayed in the parentheses.

species	slope	intercept
Cephalopholis argus	0.24 (-0.24;0.65)	1.09 (0.57;1.79)
Chaetodon ornatissimus	0.91 (0.15;1.83)	0.43 (-0.54;1.23)
Chaetodon pelewensis	1.17 (0.59;1.87)	0.13 (-0.46;0.65)
Chlorurus spilurus	0.98 (0.66;1.32)	0.32 (-0.13;0.74)
Chromis iomelas	0.54 (0.33;0.76)	0.77 (0.64;0.88)
Ctenochaetus striatus	0.35 (-0.1;0.75)	0.99 (0.54;1.51)
Naso lituratus	0.79 (0.28;1.76)	0.44 (-0.74;1.17)
Odonus niger	0.84 (0.27;1.33)	0.55 (-0.04;1.27)
Zebrasoma scopas	0.85 (0.61;1.12)	0.43 (0.14;0.71)

Table 7.3: Overview of regression parameters of log10-transformed maximum swimming speed as function of log10-transformed body length (in cm), aspect ratio.

term	estimate	std.error	conf.low	conf.high
(Intercept)	1.130	0.162	0.793	1.432
log10Length_cm	0.386	0.149	0.090	0.688
aspect_ratio	0.093	0.022	0.050	0.135

Table 7.4: Overview of average species- and size-specific estimates of standard metabolic rate (SMR, in g $O_2 d^{-1}$), maximum metabolic rate (MMR, in $gO_2 d^{-1}$), field active metabolic rate (AMR_{field}, in $gO_2 d^{-1}$), factorial aerobic scope (FAS), and factorial scope for activity (FSA). Length is expressed in cm.

Family	Species	length	SMR	MMR	FMR	FAS	FSA
Acanthuridae	*Ctenochaetus striatus*	10	0.044	0.112	0.065	2.518	1.237
Acanthuridae	*Ctenochaetus striatus*	11	0.055	0.140	0.081	2.523	1.233
Acanthuridae	*Ctenochaetus striatus*	12	0.067	0.171	0.098	2.532	1.229
Acanthuridae	*Ctenochaetus striatus*	13	0.081	0.206	0.117	2.542	1.225
Acanthuridae	*Ctenochaetus striatus*	14	0.096	0.244	0.138	2.552	1.223
Acanthuridae	*Ctenochaetus striatus*	15	0.112	0.287	0.161	2.560	1.219
Acanthuridae	*Ctenochaetus striatus*	16	0.130	0.333	0.186	2.565	1.217
Acanthuridae	*Ctenochaetus striatus*	17	0.149	0.384	0.213	2.575	1.215
Acanthuridae	*Ctenochaetus striatus*	18	0.169	0.438	0.242	2.583	1.213
Acanthuridae	*Ctenochaetus striatus*	19	0.192	0.497	0.272	2.589	1.211
Acanthuridae	*Ctenochaetus striatus*	20	0.215	0.560	0.306	2.593	1.210

Family	Species	length	SMR	MMR	FMR	FAS	FSA
Acanthuridae	*Ctenochaetus striatus*	21	0.241	0.627	0.340	2.599	1.208
Acanthuridae	*Ctenochaetus striatus*	22	0.267	0.698	0.378	2.604	1.206
Acanthuridae	*Ctenochaetus striatus*	23	0.296	0.773	0.417	2.609	1.204
Acanthuridae	*Ctenochaetus striatus*	24	0.327	0.854	0.459	2.613	1.203
Acanthuridae	*Naso lituratus*	17	0.131	0.596	0.215	4.532	1.316
Acanthuridae	*Naso lituratus*	18	0.149	0.681	0.246	4.567	1.324
Acanthuridae	*Naso lituratus*	19	0.168	0.773	0.279	4.589	1.333
Acanthuridae	*Naso lituratus*	20	0.188	0.871	0.316	4.626	1.342
Acanthuridae	*Naso lituratus*	21	0.209	0.976	0.356	4.660	1.352
Acanthuridae	*Naso lituratus*	22	0.231	1.088	0.398	4.693	1.360
Acanthuridae	*Naso lituratus*	23	0.255	1.208	0.442	4.727	1.368
Acanthuridae	*Naso lituratus*	24	0.280	1.333	0.490	4.762	1.376
Acanthuridae	*Naso lituratus*	25	0.306	1.465	0.540	4.791	1.383
Acanthuridae	*Naso lituratus*	26	0.333	1.607	0.593	4.814	1.390
Acanthuridae	*Naso lituratus*	27	0.362	1.753	0.649	4.841	1.397
Acanthuridae	*Naso lituratus*	28	0.392	1.909	0.708	4.866	1.403
Acanthuridae	*Naso lituratus*	29	0.424	2.071	0.770	4.897	1.409

Family	Species	length	SMR	MMR	FMR	FAS	FSA
Acanthuridae	*Naso lituratus*	30	0.456	2.241	0.836	4.924	1.416
Acanthuridae	*Zebrasoma scopas*	8	0.022	0.054	0.029	2.483	1.176
Acanthuridae	*Zebrasoma scopas*	9	0.028	0.070	0.038	2.535	1.189
Acanthuridae	*Zebrasoma scopas*	10	0.035	0.090	0.049	2.580	1.201
Acanthuridae	*Zebrasoma scopas*	11	0.043	0.112	0.061	2.627	1.213
Acanthuridae	*Zebrasoma scopas*	12	0.051	0.137	0.074	2.667	1.225
Acanthuridae	*Zebrasoma scopas*	13	0.061	0.164	0.089	2.707	1.236
Acanthuridae	*Zebrasoma scopas*	14	0.071	0.195	0.106	2.744	1.246
Acanthuridae	*Zebrasoma scopas*	15	0.082	0.228	0.125	2.780	1.257
Acanthuridae	*Zebrasoma scopas*	16	0.094	0.265	0.145	2.812	1.267
Acanthuridae	*Zebrasoma scopas*	17	0.107	0.305	0.167	2.843	1.278
Acanthuridae	*Zebrasoma scopas*	18	0.121	0.348	0.191	2.872	1.287
Balistidae	*Odonus niger*	10	0.028	0.170	0.072	5.987	1.780
Balistidae	*Odonus niger*	11	0.035	0.212	0.094	6.091	1.852
Balistidae	*Odonus niger*	12	0.042	0.259	0.119	6.188	1.926

Family	Species	length	SMR	MMR	FMR	FAS	FSA
Balistidae	*Odonus niger*	13	0.050	0.311	0.149	6.267	2.002
Balistidae	*Odonus niger*	14	0.058	0.369	0.184	6.346	2.079
Balistidae	*Odonus niger*	15	0.067	0.433	0.224	6.424	2.161
Balistidae	*Odonus niger*	16	0.077	0.502	0.269	6.498	2.242
Balistidae	*Odonus niger*	17	0.088	0.577	0.321	6.554	2.326
Balistidae	*Odonus niger*	18	0.099	0.658	0.380	6.619	2.410
Balistidae	*Odonus niger*	19	0.112	0.745	0.445	6.686	2.493
Balistidae	*Odonus niger*	20	0.124	0.838	0.518	6.748	2.581
Balistidae	*Odonus niger*	21	0.138	0.937	0.598	6.814	2.669
Balistidae	*Odonus niger*	22	0.152	1.043	0.687	6.863	2.756
Balistidae	*Odonus niger*	23	0.167	1.155	0.787	6.916	2.849
Balistidae	*Odonus niger*	24	0.183	1.275	0.898	6.963	2.948
Balistidae	*Odonus niger*	25	0.200	1.401	1.018	7.018	3.047
Balistidae	*Odonus niger*	26	0.217	1.534	1.150	7.078	3.148
Chaetodontidae	*Chaetodon ornatissimus*	9	0.027	0.081	0.040	2.982	1.228
Chaetodontidae	*Chaetodon ornatissimus*	10	0.034	0.104	0.051	3.055	1.250
Chaetodontidae	*Chaetodon ornatissimus*	11	0.042	0.131	0.065	3.123	1.273

Family	Species	length	SMR	MMR	FMR	FAS	FSA
Chaetodontidae	*Chaetodon ornatissimus*	12	0.050	0.160	0.080	3.181	1.293
Chaetodontidae	*Chaetodon ornatissimus*	13	0.060	0.193	0.097	3.238	1.313
Chaetodontidae	*Chaetodon ornatissimus*	14	0.070	0.230	0.116	3.292	1.333
Chaetodontidae	*Chaetodon ornatissimus*	15	0.081	0.270	0.138	3.343	1.353
Chaetodontidae	*Chaetodon ornatissimus*	16	0.093	0.314	0.162	3.394	1.372
Chaetodontidae	*Chaetodon ornatissimus*	17	0.106	0.363	0.189	3.435	1.393
Chaetodontidae	*Chaetodon ornatissimus*	18	0.119	0.415	0.218	3.479	1.412
Chaetodontidae	*Chaetodon ornatissimus*	19	0.134	0.471	0.250	3.524	1.432
Pomacentridae	*Chromis iomelas*	2	0.001	0.002	0.001	2.724	1.148
Pomacentridae	*Chromis iomelas*	3	0.002	0.006	0.003	2.864	1.186
Pomacentridae	*Chromis iomelas*	4	0.004	0.011	0.005	2.963	1.217
Pomacentridae	*Chromis iomelas*	5	0.006	0.019	0.009	3.053	1.248
Pomacentridae	*Chromis iomelas*	6	0.009	0.029	0.014	3.120	1.277

Family	Species	length	SMR	MMR	FMR	FAS	FSA
Pomacentridae	*Chromis iomelas*	7	0.013	0.042	0.021	3.180	1.304
Pomacentridae	*Chromis iomelas*	8	0.018	0.057	0.029	3.247	1.331
Serranidae	*Cephalopholis argus*	12	0.027	0.139	0.068	5.165	1.761
Serranidae	*Cephalopholis argus*	13	0.032	0.168	0.082	5.278	1.780
Serranidae	*Cephalopholis argus*	14	0.037	0.201	0.097	5.386	1.796
Serranidae	*Cephalopholis argus*	15	0.043	0.237	0.114	5.474	1.813
Serranidae	*Cephalopholis argus*	16	0.050	0.276	0.132	5.560	1.828
Serranidae	*Cephalopholis argus*	17	0.056	0.319	0.152	5.649	1.843
Serranidae	*Cephalopholis argus*	18	0.064	0.366	0.173	5.750	1.857
Serranidae	*Cephalopholis argus*	19	0.072	0.417	0.197	5.833	1.870
Serranidae	*Cephalopholis argus*	20	0.080	0.471	0.221	5.912	1.883
Serranidae	*Cephalopholis argus*	21	0.089	0.530	0.248	5.992	1.894
Serranidae	*Cephalopholis argus*	22	0.098	0.593	0.275	6.070	1.904

Family	Species	length	SMR	MMR	FMR	FAS	FSA
Serranidae	*Cephalopholis argus*	23	0.108	0.659	0.305	6.135	1.913
Serranidae	*Cephalopholis argus*	24	0.118	0.729	0.336	6.206	1.920
Serranidae	*Cephalopholis argus*	25	0.129	0.804	0.369	6.276	1.929
Serranidae	*Cephalopholis argus*	26	0.140	0.883	0.404	6.340	1.939
Serranidae	*Cephalopholis argus*	27	0.152	0.967	0.441	6.398	1.948
Serranidae	*Cephalopholis argus*	28	0.165	1.054	0.479	6.462	1.956
Serranidae	*Cephalopholis argus*	29	0.177	1.147	0.519	6.517	1.964
Serranidae	*Cephalopholis argus*	30	0.191	1.244	0.562	6.578	1.974
Serranidae	*Cephalopholis argus*	31	0.204	1.345	0.605	6.631	1.979
Serranidae	*Cephalopholis argus*	32	0.219	1.450	0.651	6.684	1.987
Serranidae	*Cephalopholis argus*	33	0.234	1.561	0.699	6.733	1.995
Serranidae	*Cephalopholis argus*	34	0.249	1.677	0.749	6.778	2.003
Serranidae	*Cephalopholis argus*	35	0.265	1.796	0.800	6.826	2.010

Family	Species	length	SMR	MMR	FMR	FAS	FSA
Serranidae	*Cephalopholis argus*	36	0.281	1.922	0.854	6.870	2.018
Serranidae	*Cephalopholis argus*	37	0.298	2.052	0.910	6.917	2.025

Chapter 8

General discussion and future directions

8.1 Main advances

Through their functioning, coral reefs provide a plethora of ecosystem services that support the livelihood of more than 500 million people worldwide. However, this system is threatened by climate change and human pressures at an unprecedented level and concerns are emerging about the capacity of reefs to deliver services in the near future. In light of the ongoing human-induced degradation of coral reef ecosystems and the important role of coral reef fishes, it is crucial to increase our knowledge concerning fish-mediated functions on coral reefs (i.e., their contribution to fluxes of carbon, nitrogen, and phosphorus through consumption, growth, excretion, and egestion) (Bellwood *et al.* 2019). Indeed these fluxes are tightly related to the overall productivity of the ecosystem and its capacity to provide food of high nutritional value for people. However, methodological challenges have thus far impeded the precise quantification of functions, and most studies in the past relied on proxies (such as standing stock biomass) to infer functioning (Brandl *et al.* 2019a). In this thesis,

I sought to advance our understanding of fish-mediated functions through a variety of new methods and their use to quantify elemental fluxes at the organismal and community level.

My thesis work produced several methodological advances that can help estimate ecosystem functions mediated by fishes. First, on the basis of existing ecological theory, I developed and validated a novel model that can estimate fluxes of carbon, nitrogen, and phosphorus through consumption, growth, respiration, excretion, and egestion (chapter 2). To ensure applicability, I also developed the R package 'fishflux' (appendix A). Second, I introduced an approach to infer biological traits (e.g., trophic guilds, growth rates, body stoichiometry) to a global species list in a Bayesian framework using phylogeny and ancestral state reconstruction (chapter 3, 4). Third, I developed a back-calculation model as well as a Bayesian hierarchical regression model to retrieve growth parameters from otolith measurements, accompanied by the R package 'fishgrowbot' (chapter 4, appendix B). Finally, in chapter 7, I introduced a new framework that integrates stereo-video recording in the field and *ex situ* metabolic rate estimates to approximate field metabolic rates.

Beyond methodological advances, my quantification of multiple functions (which is to my knowledge one of the first efforts to estimate a spectrum of fish-mediated functions) has underlined the undeniable role of the biological characteristics that come with the species identity of an individual for governing community-level functioning. Intuitively, biomass alone is an important predictor of any function, but beyond biomass, there is important variability that is explained by community composition as well as their size and age structure. For example, a fish community consisting of abundant young fast growing damselfishes will inevitably have a high biomass production, while a community dominated by large groupers will excrete a lot of phosphorus. Furthermore, the activity rate of coral reef fishes can vary up to about 3-fold across species (chapter 7). Highly active fishes can contribute disproportionally to energy and nutrient fluxes, but this has never been included in functional studies due to the methodological challenge of estimating activity rates of fishes in

their natural environment. Finally, species identity has a large effect on absorption efficiencies and thus consumption and egestion rates (chapter 6). Indeed, even within the same fish family and trophic guild (e.g., Acanthuridae), there is much variation in absorption efficiency which may be related to fine-scale niche partitioning (Brandl & Bellwood 2014), but the precise mechanisms driving this variation are yet to be understood. In the context of the uneven effects of anthropogenic stressors such as climate change or overexploitation on reef fish community structures (e.g., Pauly *et al.* 1998; Wilson *et al.* 2009; Graham *et al.* 2011), the findings presented in this thesis could help to foster a better understanding of how these impacts will shape reef-wide functioning.

In addition, the work presented in this thesis highlights the existing trade-offs among fish-mediated functions resulting from organismal processes and community structure. On the individual level, there are obvious physiological trade-offs (chapter 2). For example, in an early life stage, fishes are likely to be phosphorus-limited, which entails that they will excrete little phosphorus, while contributing substantially to biomass production. Such individual-level physiological trade-offs, combined with variation among species within communities, result in critical trade-offs among multiple functions at the community-level (chapter 5). Additionally, while not analyzed explicitly, egestion rates also correlate positively or negatively with other functions. For example, herbivory rates are positively correlated with egestion rates, and there can be a trade-off between egestion rate and piscivory or excretion rates. Importantly, there is also a trade-off between egestion quality and quantity. This is important since a community of fishes collectively releasing a high amount of low-nutrient organic matter has an entirely different effect on the environment compared to a community releasing fewer but high-quality egestion.

Finally, the existing trade-offs among functions introduce a new paradigm in coral reef conservation: no particular community can possibly maximize all functions. Currently, maximizing "ecosystem functioning" is seen as the overarching conservation goal to ensure the health of coral reef ecosystems (Hughes *et al.* 2017). However,

efforts to maximize one function may actually simultaneously cause a decline of another function and since most species play a dominant role for one or more functions at a given location, it is impossible to produce a curated list of key species to conserve to ensure functioning. While my thesis work has produced methods and results that permit us to scrutinize coral reef functioning in greater detail, it is clear that more research is needed to aid in the comprehension and protection of coral reef ecosystems in times of unparalleled environmental change.

8.2 Future directions

The work presented in this thesis generated a range of questions and potential research directions related to fish-mediated functions on coral reefs.

In recent decades, trait-based ecology has gained much traction in coral reef fish research (Villéger *et al.* 2017; Brandl *et al.* 2019a; Hadj-Hammou *et al.* 2021; Quimbayo *et al.* 2021). Traits are sometimes used to infer functioning assuming there is a certain relationship between traits and functions. However direct quantifications of the trait-function relationship are scarce and trait-based approaches have been recently questioned in their capacity to describe ecosystem functioning (Bellwood *et al.* 2019) The model presented in chapter 2 provides a way to mechanistically link functions with commonly-used traits including life history traits (e.g., age, growth rate), morphological traits (e.g., size), dietary traits (e.g., diet, trophic level), and physiological traits (e.g., metabolic rate) (Hadj-Hammou *et al.* 2021). Similarly, although the distribution of coarse traits (size, age, and trophic level) at the community level may help predict several functions (chapter 5), physiological and behavioral traits such as the absorption efficiency (chapter 6) and activity rate (chapter 7) stand to be extremely important, but are difficult to quantify for a large number of species. Creating and collating information on species' traits through both empirical data collection and organismal modeling efforts (cf. chapter 2) will greatly advance the power

of trait-based approaches in the future.

Beyond broad trait categories, an important step towards understanding the functioning of coral reef fish communities across trophic levels is to couple fluxes of elements with detailed food web structures. Most food-web analyses in the marine environment are based on either presence-absence of trophic interactions or on interaction strengths derived from biomass. However, according to the mechanisms that structure the food web (e.g., top-down or bottom-up processes) biomass does not equal consumption. Chapter 3 provides a global matrix of potential predator-prey interactions based on machine learning inference. Using the methods and data provided in this thesis, there is a potential to analyze the food web structure based on actual fluxes of energy and elements (i.e., modeled consumption rates). However, this is made difficult by the apparent prevalence of fine-scale niche partitioning within trophic categories (e.g., Brandl & Bellwood 2014; Leray *et al.* 2019; Brandl *et al.* 2020b). Novel techniques such as gut metabarcoding can provide unprecedented detail on the many trophic linkages that exist in coral reef food webs (Leray & Knowlton 2015; Casey *et al.* 2019), although some aspects of trophic interactions (e.g., coprophagy) will remain challenging to detect if not for detailed in situ observations.

In this context, another promising avenue for future research is the effect of behavior and activity on fish-mediated functions and nutrient translocation. Active fishes have a higher metabolic rate and consequently, consume, excrete, and egest more elements. This thesis provided a first quantification of the activity rate of seven reef fishes (chapter 7), but these estimates need to be improved and expanded to other species. For example, linking stereo-video observation with biotelemetry and internal physiological data loggers may increase accuracy of active metabolic rate estimates (Metcalfe *et al.* 2016), while other promising techniques based on otolith isotopes may help elucidate lifetime metabolic demands (Chung *et al.* 2019). Further, space use of fishes will determine the areas that are most influenced by nutrient release. For example, a planktivorous fish spending most of its time in the water column will excrete

nutrients that may be used by phytoplankton for primary production, while egesting organic material that is likely to serve as food for other fishes (Robertson 1982). On the other hand, cryptic fishes that spend most of their time hiding in the reef matrix will have a larger effect on benthic primary production and cryptic detritivores. Yet, horizontal and vertical migration can represent important vectors of nutrients between different habitats. Continuous improvements of biotelemetry, stereo-video observation techniques, and isotope profiles may help elucidate behaviourally mediated transfer of elements across the coral reef seascape (Matley *et al.* 2016; Meese & Lowe 2020).

Perhaps the most widely overlooked aspect of nutrient recycling by fish is the fate of fish feces. In contrast to the excretion of inorganic nutrients, fish egestion contains complex organic molecules and although a part of these nutrients will leach into the water column (Stewart *et al.* 2006), a large proportion of the nutrients found in feces will not directly be available to primary production. However, this does not mean that those nutrients are not recycled in an efficient way. Egested organic material can be consumed by other animals including coprophagous fishes (Robertson 1982), invertebrates inhabiting crevices (Rothans & Miller 1991; Pinnegar & Polunin 2006), and corals (Mills & Sebens 2004). However, we have little knowledge on the precise importance of fecal matter for different animals. More studies using techniques such as behavioral observations (cf. Robertson 1982), fecal traps (cf. Pinnegar & Polunin 2006), and markers (cf. Rothans & Miller 1991) may collectively help clarify how fish feces are integrated in food webs. Given the large proportion of nutrients being released through feces (chapter 6), further studies investigating the fate of fish feces will be crucial to better understand nutrient cycles on coral reefs.

Furthermore, a closer examination of the intra-specific variability of functions provided by fishes is needed. Beyond known effects of body size, age, and temperature, I did not incorporate intra-specific variability in this thesis. It would be useful to investigate pathways in which environmental, geographical or anthropogenic variables or individual-level behavior impact intra-specific variability of functions (Des

Roches *et al.* 2018). For example, the algae on which herbivorous fishes feed can vary greatly in their nutrient content depending on the local conditions. Varying elemental content of the diet can affect nutrient limitation, the consumption rate and consequently excretion and egestion. Such dietary variation is difficult to capture, but a compilation of dietary data from empirical data (cf. Parravicini *et al.* (2020)) could greatly facilitate our understanding of the effect of intraspecific variation across space and time. Similar efforts for other taxa (cf. the Coral Trait Database, Madin *et al.* (2016)) highlight the feasibility and utility of this approach. Finally, while I included temperature related variation for growth rate and metabolic rate using relationships that are well studied, there may be other ways in which temperature affects functioning. For example, evidence from other animals shows that absorption efficiency can increase with temperature (Lang *et al.* 2017), but this has not been broadly established. Given that various physiological parameters and biochemical reactions are highly reactive to temperature, it appears necessary to increase our knowledge of organismal responses to temperature in reef fishes beyond typically studied parameters like whole-organism metabolism or growth (Barneche *et al.* 2014; Barneche & Allen 2018; Morais & Bellwood 2018).

Finally, the majority of my thesis work has focused on large, conspicuous fishes by virtue of their easy detectability in visual censuses. However, the cryptobenthic fish community represents a widely overlooked side of coral reef fish diversity (Brandl *et al.* 2018). Despite their small size, they are an extremely diverse and abundant group of fishes, and a critical component of coral reef food webs (Brandl *et al.* 2018). Indeed, due to their high abundance, rapid growth and high mortality rate, cryptobenthic fishes produce more than half of consumed reef fish biomass (Brandl *et al.* 2019b). Despite their trophic importance, we know very little about their body nutrient stoichiometry, which impedes a more precise understanding of their role in fueling elements to higher trophic levels. Therefore, an investigation of elemental stoichiometry of this diverse group of fishes would be relevant.

8.3 Concluding remarks

Understanding the processes that underpin ecosystem functioning is paramount to preserving healthy ecosystems for future generations (Bellwood *et al.* 2019). While this thesis has contributed to our ability to quantify and understand drivers of fish-mediated functions on coral reefs, it also highlights the vast pool of knowledge that is yet to be gained on the topic. Anthropogenic impacts on coral reefs, however, are intensifying rapidly, and despite a large number of excellent research results geared towards augmenting our understanding of reef functioning, our comprehension of process-based functioning of coral reefs or what a "functional" coral reef really means is still in its infancy (Brandl *et al.* 2019a). In order to keep pace with the human-induced transformation of coral reef ecosystems, we need to accelerate our research efforts through collaborations between specialists via open and reproducible research. In other words, it is necessary to integrate across the fields of macro-ecology, organismal physiology, ecosystem biogeochemistry, and community ecology to advance our knowledge on functions, understand the varying pathways in which humans impact them, and learn how we can improve guidance to conservation management in the future. In my thesis, I have contributed to this cause, by developing and applying a series of tools that can help eliminate perceived boundaries between the aforementioned fields to create a more holistic understanding of the role of fishes for coral reef functioning.

Appendix A

Documentation fishflux

This appendix includes:

- Introduction vignette

- Reference manual

For more documentation see: `https://nschiett.github.io/fishflux/index.html`

Figure A.1: Logo fishflux

Introduction to fishflux

Vignette

Nina M. D. Schiettekatte

Introduction

The `fishflux` package provides a tool to model fluxes of C (carbon), N (nitrogen) and P (phosphorus) in fishes. It combines basic principles from elemental stoichiometry and metabolic theory. The package offers a user-friendly interface to apply the model. `fishflux` is ideal for fish ecologists wishing to predict ingestion, egestion and excretion to study fluxes of nutrients and energy.

Main assets:

- Provides function to model fluxes of Carbon, Nitrogen and Phosphorus for fishes
- Allows for the estimation of uncertainty, dpending on the uncertainy of the input parameters
- Provides some functions to help find parameters as inputs for the model
- Provides functions to extract and illustrate results

Installing and loading fishflux

`fishflux` uses Markov Chain Monte Carlo simulations provided by stan. Therefore, the first step is to install rstan. It's important to closely follow all the steps described on the page depending on your operating system.

GitHub

The best way to install the latest development version of `fishflux` is to install it from GitHub.

```
install.packages("devtools")
devtools::install_github("nschiett/fishflux", dependencies = TRUE)
# if errors are returned, try adding `args = "--preclean"` to `install_github`
library(fishflux)
```

CRAN

`fishflux` will be available on CRAN in the future:

```
install.packages("fishflux")
library(fishflux)
```

Downloaded package file

Another option is to download the source file available on GitHub here.

```
install.packages(path_to_fishflux_file, repos = NULL, type = "source")
library(fishflux)
```

How to use fishflux?

`fishflux` is designed to follow three simple steps:

- Find the right input parameters
- Run the model simulation with those input parameters
- Plot the model results and check sensitivity

Input parameters

Before running the model, the parameters have to be specified. Below, there is a table showing all parameters needed to run the model simulation. `fishflux` provides several functions to find some of these parameters, but note that others have to be provided by the user at this stage. Ideally, all parameters should also have a standard deviation, so that their uncertainty can be reflected in the model predictions

Table 1: . Overview of inputs, including input parameters, to be specified by the user of the model. k indicates c, n or p. VBGC = von Bertalanffy growth curve.

Symbol	Description	Unit
a_{k}	Element-specific assimilation efficiency	—
l_{t}	Total length of individual	cm
$linf$	Asymptotic adult length (VBGC)	cm
κ	Growth rate parameter (VBGC)	yr^{-1}
t_0	Age at settlement (VBGC)	yr
lw_a	Parameter length-weight relationship	g cm^{-1}
lw_b	Parameter length-weight relationship	—
Q_{k}	Element-specific body content percentage	%
f_0	Metabolic normalisation constant independent of body mass	g $\mathrm{Cg}^{-\alpha}\mathrm{d}^{-1}$
$alpha$	Mass-scaling exponent	—
$theta$	Activity scope	—
v	Environmental temperature	°C
h	trophic level	—
r	Aspect ratio of caudal fin	—
$F0nz$	Mass-specific turnover rate of N	g $\mathrm{Ng}^{-1}\mathrm{d}^{-1}$
$F0pz$	Mass-specific turnover rate of P	g $\mathrm{Pg}^{-1}\mathrm{d}^{-1}$
mdw	Ratio of dry mass and wet mass of fish	—
D_{k}	Elemental stoichiometry of diet	%

A good place to start is checking if you are using the correct scientific name of your species of interest. The function `name_errors` will tell you if the species name is correct. This function can be useful, especially when working with larger databases.

```
# example
fishflux::name_errors("Zebrazoma scopas")
#> Inaccurate species names found:
#> [1] "Zebrazoma scopas"
```

Once the species names are verified and/or corrected we can continue with specifying some parameters.

The `find_lw` function searches FishBase to find length-weight relationship parameters `lw_a` and `lw_b` extracted from Froese and Pauly (2018).

```
# example
fishflux::find_lw("Zebrasoma scopas", mirror = "se")
#>            species   lwa_m     lwa_sd lwb_m    lwb_sd
#> 1 Zebrasoma scopas 0.02455 0.00269898  2.98 0.0255102
```

The model uses parameters von Bertalanffy's growth model (VBGM) to estimate growth rates. A quick way to get available information from FishBase is the function `growth_params()`. This can be a good indication, but users should interpret these estimates with a critical eye, as they come from disparate sources of varying accuracy. Alternatively, it is advised to use growth curves derived from otolith readings. In the absence of otolith data, one might consider extracting standardised estimations from Morais and Bellwood (2018).

```
# example
# The option otolith=TRUE filters out sources that used otoliths for
# the estimation of growth parameters
fishflux::growth_params("Sargocentron microstoma", otolith = FALSE)
#> # A tibble: 1 x 7
#>   species           Locality               k  Linf    t0 method        comments
#>   <chr>             <chr>              <dbl> <dbl> <dbl> <chr>         <chr>
#> 1 Sargocentron mic~ Tiahura reef, Moor~     1  18.6    NA length-frequ~ <NA>
```

Further, there are a couple more basic functions to get an indication of parameters that are available on FishBase such as `trophic_level()` and `aspect_ratio()`.

Note that it is always better to get the approximations through analysis, measurements and otolith analysis over parameters extracted from functions, such as `growth_params()`, `trophic_level()` and `aspect_ratio()`.

To get an overview of all parameters available, `fishflux` provides a wrapper function `model_parameters()`.

```
# example
zebsco <- fishflux::model_parameters("Zebrasoma scopas",
                                     family = "Acanthuridae",
                                     temp = 27, mirror = "se")
## Here we set the temperature at 27 degrees as an example,
# this the average sea temperature in Moorea, French Polynesia
```

```
print(zebsco)
#>            species    t0 Linf     k     asp troph   lwa_m     lwa_sd lwb_m
#> 1 Zebrasoma scopas -0.49 13.3 0.425 2.02091     2 0.02455 0.00269898  2.98
#>      lwb_sd     mdw_m        f0_m        f0_sd alpha_m   alpha_sd
#> 1 0.0255102 0.2504833 0.001517989 3.216843e-10    0.77 0.05286288
```

All other parameters have to be provided by the user. For more information on how to acquire these parameters, take a look at ("this paper" add reference to methods paper).

Run model

Once all the parameters are collected, we can run the model through `cnp_model_mcmc()`. Note that this model can be run with or without specifying the standard deviation (sd) of each parameter. If the sd of

a certain parameter is not provided, it will be automatically set to a very low value (1^{-10}). As mentioned before, it is advisable to include uncertainty of parameters. `fishflux` is designed to use the MCMC sampler in order to include uncertainty of predictions.

```
## load the example parameters for Zebrasoma scopas, a list
param_zebsco <- fishflux::param_zebsco
## Run the model, specifying the target length(s) and the parameter list
model <- fishflux::cnp_model_mcmc(TL = 5:20, param = param_zebsco)
```

The object `model` now contains all the samples generated from the MCMC simulation and a summary of all parameters generated. To extract certain variables of interest, use the `extract()` function. Predictions for fluxes of C, N and P are all in g / day.

```
fishflux::extract(model, c("Fn","Fp"))
#>    TL     Fn_mean    Fn_median        Fn_sd      Fn_2.5%    Fn_97.5%
#> 1   5 0.000865498 0.0007901645 0.0004266623 0.0002155917 0.001812691
#> 2   6 0.001333738 0.0012539452 0.0006303633 0.0002819543 0.002754214
#> 3   7 0.00184613 4 0.0017292042 0.0008899991 0.0005445658 0.003836937
#> 4   8 0.002592355 0.0023477024 0.0012557299 0.0007512989 0.005477138
#> 5   9 0.003318977 0.0030607178 0.0016491348 0.0008493116 0.007170141
#> 6  10 0.004390001 0.0039235793 0.0023092157 0.0011736460 0.009644176
#> 7  11 0.005525681 0.0048234215 0.0030990467 0.0013346544 0.013321759
#> 8  12 0.007539917 0.0068580477 0.0044704207 0.0016651136 0.018222282
#> 9  13 0.009177191 0.0080703628 0.0057522474 0.0019206302 0.021619458
#> 10 14 0.010919997 0.0092782040 0.0068858709 0.0022665845 0.029379394
#> 11 15 0.012869289 0.0107010859 0.0085420755 0.0025458709 0.033360973
#> 12 16 0.016458252 0.0136074163 0.0113036946 0.0027319628 0.044906302
#> 13 17 0.019156353 0.0160746543 0.0122038615 0.0034154029 0.046101275
#> 14 18 0.022876566 0.0207892023 0.0135752658 0.0044786612 0.055299709
#> 15 19 0.028012971 0.0240443056 0.0177663918 0.0067133258 0.069334819
#> 16 20 0.032448202 0.0273945060 0.0214161093 0.0076412018 0.082989382
#>          Fn_25%      Fn_75%      Fp_mean    Fp_median        Fp_sd      Fp_2.5%
#> 1  0.0005552009 0.001129592 8.789311e-05 4.449121e-05 0.0001125600 3.301037e-06
#> 2  0.0008998135 0.001651145 1.781781e-04 9.500016e-05 0.0002153971 6.616564e-06
#> 3  0.0011834241 0.002362822 2.953122e-04 1.590450e-04 0.0003277987 1.428904e-05
#> 4  0.0017473826 0.003253593 4.905793e-04 3.124831e-04 0.0004804584 1.284658e-05
#> 5  0.0021216986 0.004193126 6.958065e-04 4.460830e-04 0.0006794054 4.212010e-05
#> 6  0.0026807324 0.005577780 1.042410e-03 7.088466e-04 0.0009378030 4.655138e-05
#> 7  0.0031859019 0.007146965 1.455610e-03 1.087246e-03 0.0012641161 4.332575e-05
#> 8  0.0040216783 0.009915377 2.261623e-03 1.891576e-03 0.0018507826 1.316528e-04
#> 9  0.0046404443 0.012617999 2.862007e-03 2.301698e-03 0.0022754505 1.916098e-04
#> 10 0.0059196673 0.014718882 3.561121e-03 2.883088e-03 0.0027417200 3.021666e-04
#> 11 0.0061902776 0.017605843 4.442872e-03 3.526811e-03 0.0034037676 3.467576e-04
#> 12 0.0082769066 0.022441522 5.985127e-03 4.818493e-03 0.0045754589 6.070533e-04
#> 13 0.0098750296 0.025785902 7.220791e-03 6.085179e-03 0.0049733430 9.664505e-04
#> 14 0.0116742157 0.030460129 8.881020e-03 8.183923e-03 0.0054208041 1.684638e-03
#> 15 0.0144049560 0.035799454 1.111528e-02 9.524836e-03 0.0070308549 2.645643e-03
#> 16 0.0164672672 0.042456662 1.291410e-02 1.092339e-02 0.0085531675 2.976388e-03
#>        Fp_97.5%       Fp_25%       Fp_75%
#> 1  0.0004283892 2.146972e-05 0.0001000052
#> 2  0.0008438546 4.583481e-05 0.0002345847
#> 3  0.0011996053 8.623281e-05 0.0004017513
#> 4  0.0017129359 1.259164e-04 0.0007464626
#> 5  0.0024683824 2.227476e-04 0.0010240593
```

```
#> 6  0.0032489061 3.218557e-04 0.0015496854
#> 7  0.0048796473 4.362123e-04 0.0021512517
#> 8  0.0067100194 7.924988e-04 0.0032731685
#> 9  0.0078996349 1.001101e-03 0.0041666177
#> 10 0.0104437672 1.527580e-03 0.0050958191
#> 11 0.0124709307 1.740371e-03 0.0064001442
#> 12 0.0169826192 2.595457e-03 0.0084189787
#> 13 0.0185083172 3.418455e-03 0.0099387615
#> 14 0.0220496764 4.338024e-03 0.0121141962
#> 15 0.0274448029 5.830521e-03 0.0142951671
#> 16 0.0342496443 6.548229e-03 0.0167089993
```

Plot results

To visualize main outputs of the model, `fishflux` contains a plotting function. The function `limitation()` returns the proportion of iterations of the model simulation that had limitation of C, N and P respectively. The function `plot_cnp()` plots the predicted output of the model.

```
## limitation
fishflux::limitation(model)
```

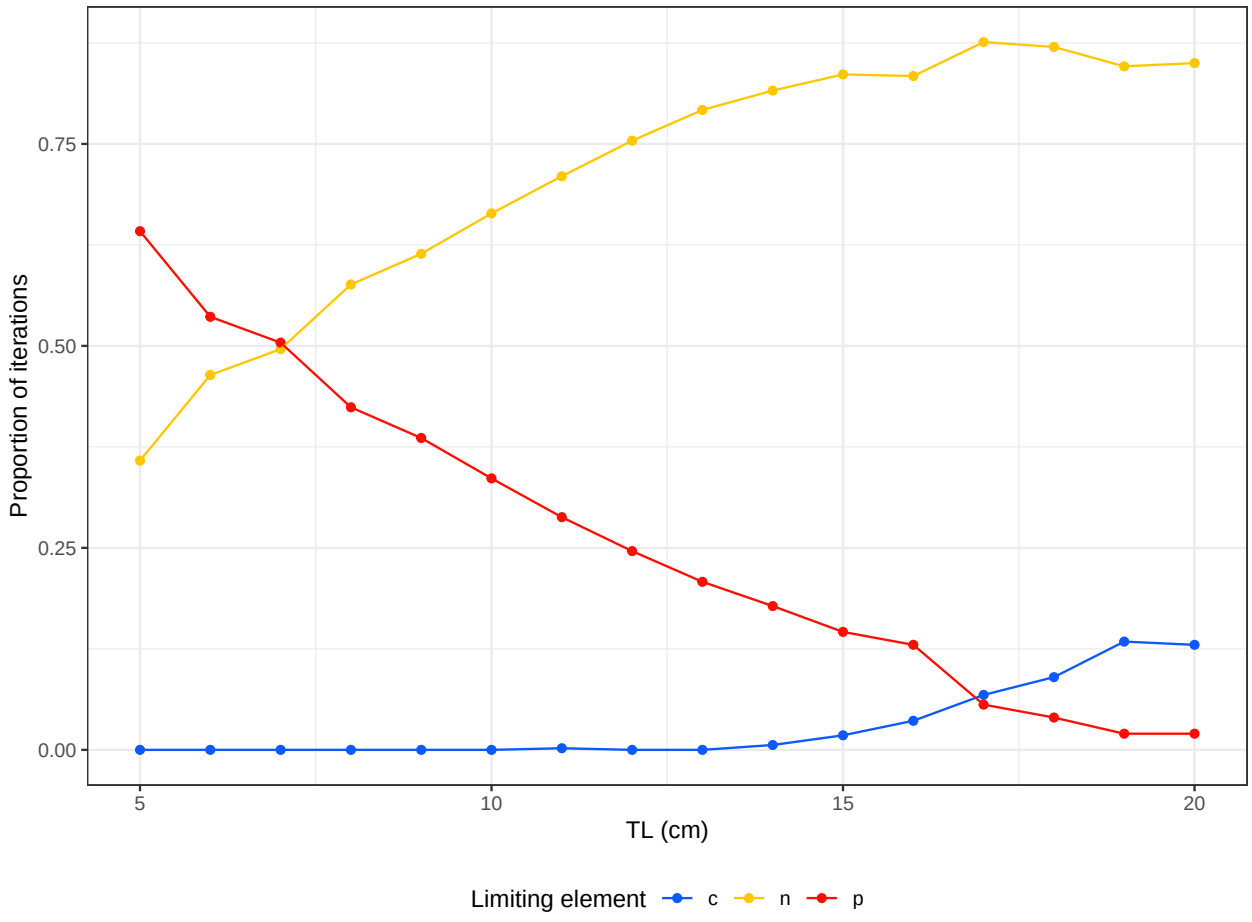


```
#>    tl nutrient prop_lim
#> 1   5        c    0.000
```

```
#> 2   6        c    0.000
#> 3   7        c    0.000
#> 4   8        c    0.000
#> 5   9        c    0.000
#> 6  10        c    0.000
#> 7  11        c    0.002
#> 8  12        c    0.000
#> 9  13        c    0.000
#> 10 14        c    0.006
#> 11 15        c    0.018
#> 12 16        c    0.036
#> 13 17        c    0.068
#> 14 18        c    0.090
#> 15 19        c    0.134
#> 16 20        c    0.130
#> 17  5        n    0.358
#> 18  6        n    0.464
#> 19  7        n    0.496
#> 20  8        n    0.576
#> 21  9        n    0.614
#> 22 10        n    0.664
#> 23 11        n    0.710
#> 24 12        n    0.754
#> 25 13        n    0.792
#> 26 14        n    0.816
#> 27 15        n    0.836
#> 28 16        n    0.834
#> 29 17        n    0.876
#> 30 18        n    0.870
#> 31 19        n    0.846
#> 32 20        n    0.850
#> 33  5        p    0.642
#> 34  6        p    0.536
#> 35  7        p    0.504
#> 36  8        p    0.424
#> 37  9        p    0.386
#> 38 10        p    0.336
#> 39 11        p    0.288
#> 40 12        p    0.246
#> 41 13        p    0.208
#> 42 14        p    0.178
#> 43 15        p    0.146
#> 44 16        p    0.130
#> 45 17        p    0.056
#> 46 18        p    0.040
#> 47 19        p    0.020
#> 48 20        p    0.020
## Plot one variable:
fishflux::plot_cnp(model,  y = "Fp",
                   x = "tl", probs = c(0.5, 0.8, 0.95))
```

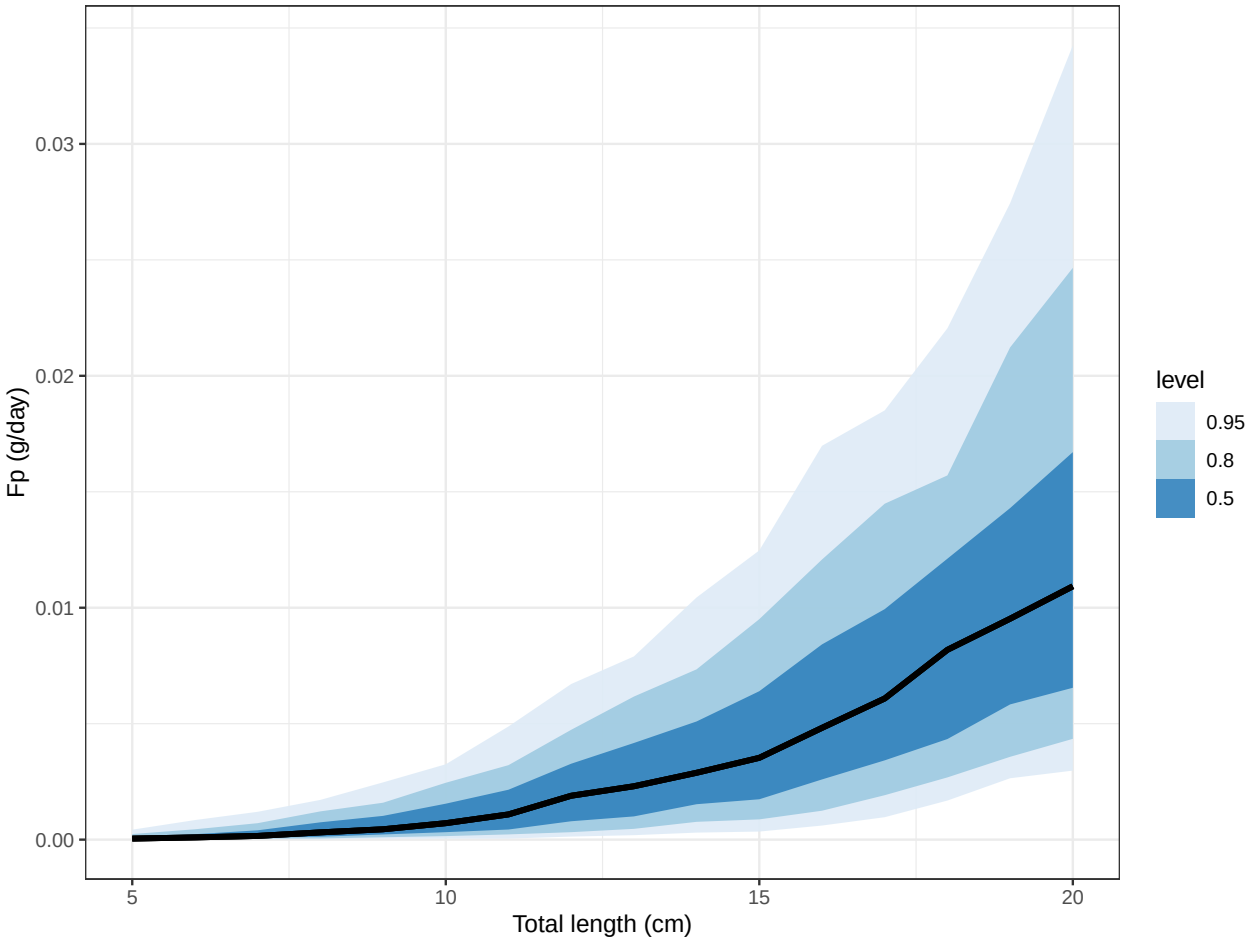


```
## Plot multiple variables:
fishflux::plot_cnp(model,  y = c("Fp", "Gp", "Ip", "Wp"),
                   x = "tl", probs = 0.5)
```

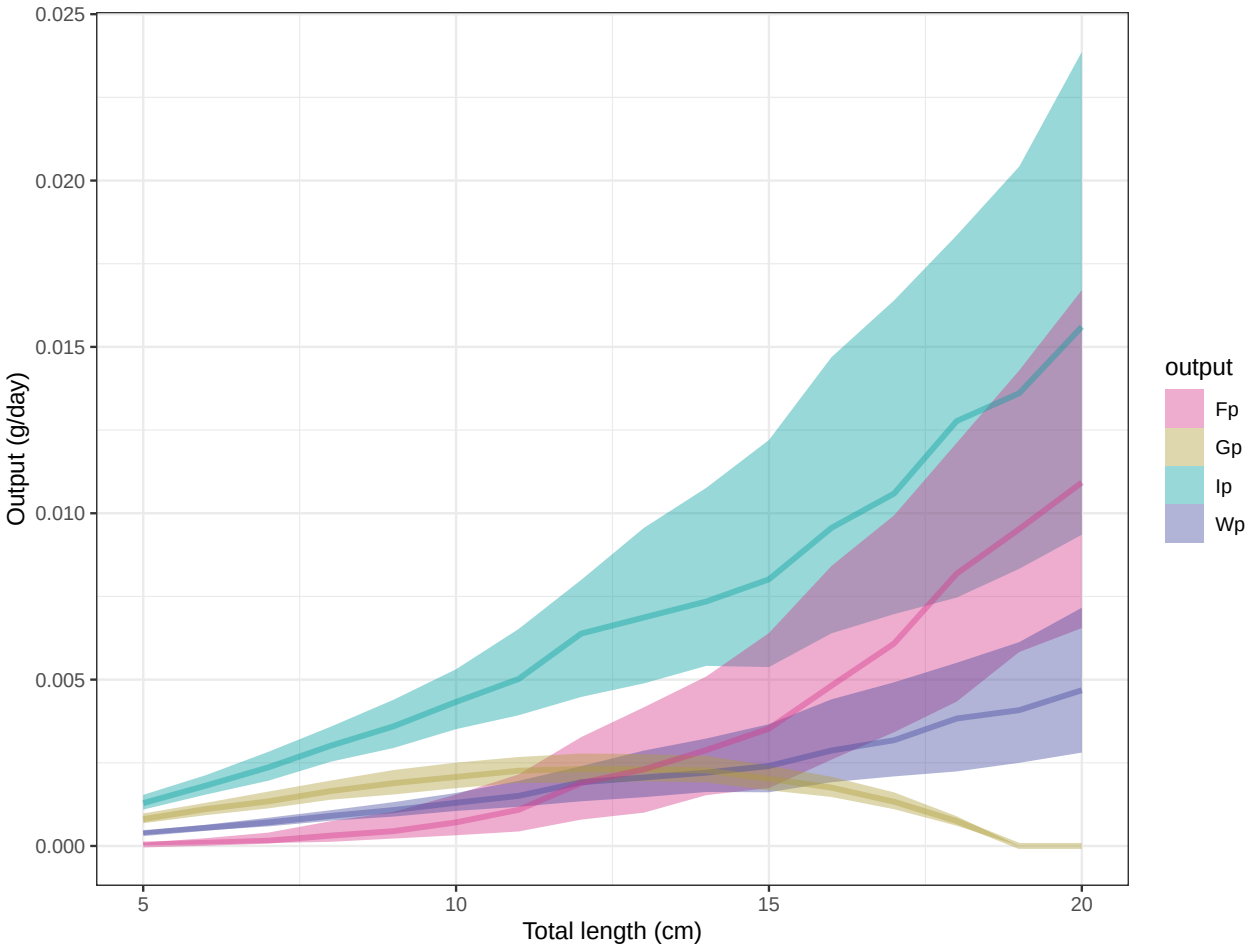

Sensitivity

The function `sensitivity()` looks at how the distribution of the input variables affects the uncertainty of the model predictions. Basically, the model is run for each input parameter, while keeping all the others fixed. The output of the function gives a matrix of the width of the 95% CI for all model predictions (columns), depending on the input variables (rows). The input parameters and output variables of interest can be specified by arguments "par" and "out" respectively.

```
fishflux::sensitivity(TL = 10,
                      param = list(k_sd = 0.2, Dn_sd = 0.2, Dc_sd = 0.1),
                      par = c("k_sd","Dn_sd","Dc_sd"),
                      out = c("Ic", "In", "Ip", "Gc"))
```

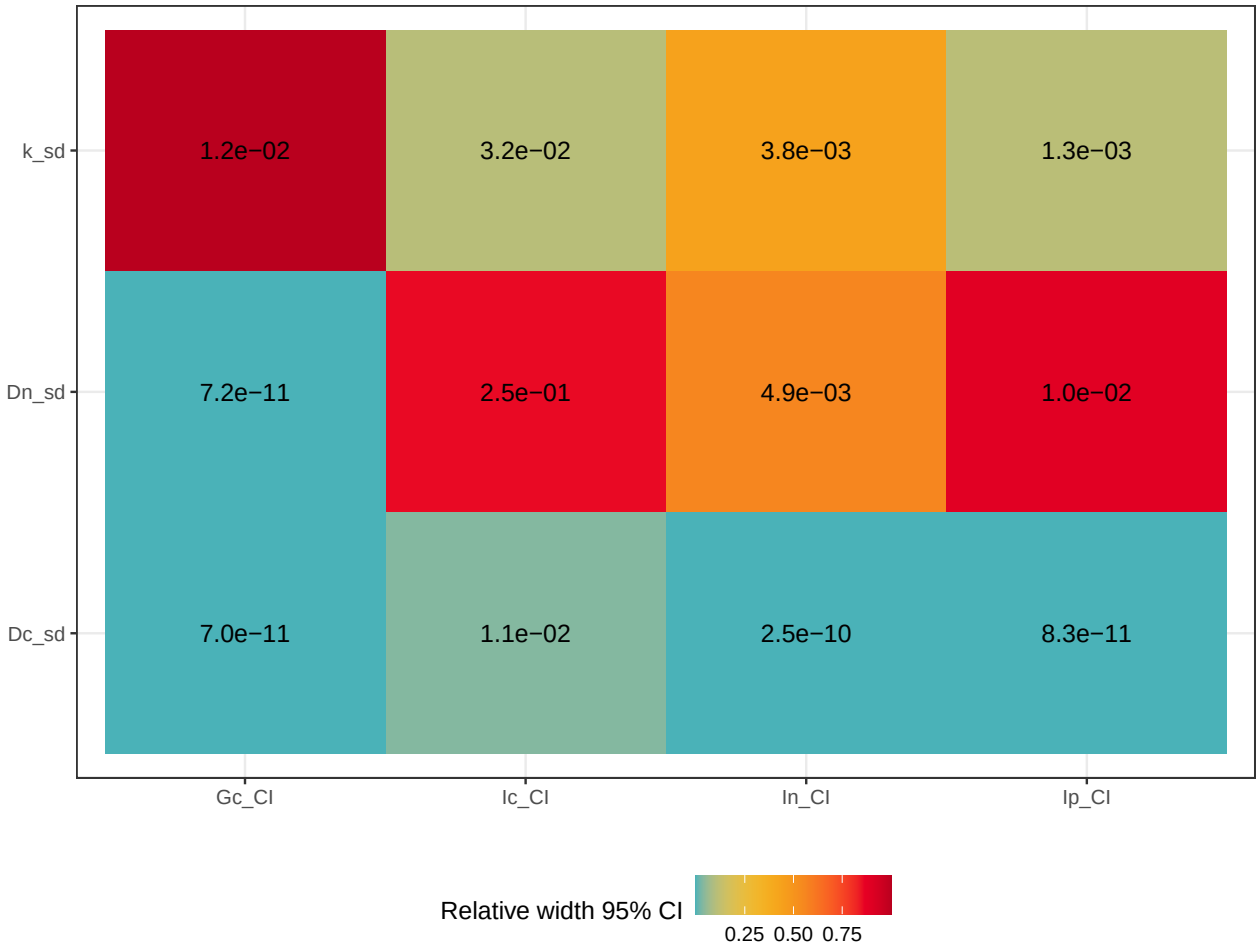


```
#>            Ic_CI        In_CI        Ip_CI        Gc_CI
#> k_sd  0.03169895 3.803873e-03 1.267958e-03 1.217240e-02
#> Dn_sd 0.25328393 4.886941e-03 1.013136e-02 7.222673e-11
#> Dc_sd 0.01129948 2.492667e-10 8.304807e-11 6.961907e-11
```

More information

For more information on the theoretical framework of the model, see (Schiettekatte et al. 2020)(https://doi.org/10.1111/1365-2435.13618) . Every function of `fishflux` has a help page with more documentation. In the case of errors, bugs or discomfort, you are invited to raise an issue on GitHub. `fishflux` is always in development and we are happy to take your comments or suggestions into consideration.

References

Froese, R., and D. Pauly. 2018. "FishBase." *World Wide Web Electronic Publication.*

Morais, Renato A, and David R Bellwood. 2018. "Global Drivers of Reef Fish Growth." *Fish and Fisheries* 19 (5): 874–89.

Schiettekatte, N. M. D., D. R. Barneche, S. Villéger, J. E. Allgeier, D. E. Burkepile, S. J. Brandl, J. M. Casey, et al. 2020. "Nutrient Limitation, Bioenergetics, and Stoichiometry: A New Model to Predict Elemental Fluxes Mediated by Fishes." *Functional Ecology*, no. Accepted Author Manuscript. https://doi.org/10.1111/1365-2435.13618.

Package 'fishflux'

April 27, 2021

Title Model Elemental Fluxes in Fishes

Version 0.0.1.4

Description Model fluxes of carbon, nitrogen, and phosphorus with the use of a coupled bioenergetics and stoichiometric model that incorporates flexible elemental limitation. Additional functions to help the user to find parameters are included. Finally, functions to extract and visualize results are available as well. For an introduction, see vignette. For more information on the theoretical background of this model, see Schiettekatte et al. (2020) <doi:10.1111/1365-2435.13618>.

URL https://nschiett.github.io/fishflux/

BugReports https://github.com/nschiett/fishflux/issues

License MIT + file LICENSE

Encoding UTF-8

Imports methods, Rcpp (>= 0.12.0), RcppParallel (>= 5.0.1), rstan (>= 2.18.1), rstantools (>= 2.0.0), parallel, dplyr, fishualize, ggplot2, plyr, rfishbase, tidybayes, tidyr, httr, curl

Depends R (>= 3.6.0)

Suggests knitr, rmarkdown, testthat, covr

LinkingTo BH (>= 1.66.0), Rcpp (>= 0.12.0), RcppEigen (>= 0.3.3.4.0), RcppParallel (>= 5.0.1), rstan (>= 2.18.1), StanHeaders (>= 2.18.0)

SystemRequirements GNU make

LazyData true

RoxygenNote 7.1.1

VignetteBuilder knitr

Biarch true

NeedsCompilation yes

Author Nina M. D. Schiettekatte [aut, cre], Diego Barneche [aut]

Maintainer Nina M. D. Schiettekatte <nina.schiettekatte@gmail.com>

Repository CRAN

Date/Publication 2021-04-27 07:40:02 UTC

R topics documented:

`fishflux-package` *The 'fishflux' package.*

Description

The 'r fishflux' package provides a tool to model fluxes of C (carbon), N (nitrogen) and P (phosphorus) in fish. It combines basic priciples from elemental stoichiometry and metabolic theory. The package offers a userfriendly interface to make nutrient dynamic modelling available for anyone. 'r fishflux' is mostly targeted towards fish ecologists, wishing to predict nutrient ingestion, egestion and excretion to study fluxes of nutrients and energy. Main assets:

- Provides functions to model fluxes of Carbon, Nitrogen and Phosphorus for fish with or without the MCMC sampler provided by stan.
- Provides some tools to find the right parameters as inputs into the model
- Provides a plotting function to illustrate results

References

Stan Development Team (2020). RStan: the R interface to Stan. R package version 2.19.3. https://mc-stan.org

aspect_ratio *A function to find aspect ratio*

Description

A function to find aspect ratio of a species on either species or genus level using rfishbase. It returns a data frame containing the aspect ratio and the level at which the aspect ratio was found (species or genus).

Usage

```
aspect_ratio(sp)
```

Arguments

sp	A character value containing the species name

Value

dataframe with species, aspect ratio and taxonomy level.

Examples

```
## Not run:
library(fishflux)
library(plyr)
aspect_ratio("Lutjanus griseus")
ldply(lapply(c("Chlorurus spilurus","Zebrasoma scopas"), aspect_ratio))

## End(Not run)
```

check_name_fishbase *Returns error if name is incorrect*

Description

This is a wrapper function to which will return an error (via name_errors) if the provided species name is wrong.

Usage

```
check_name_fishbase(sp)
```

Arguments

sp	A character value containing the species name

Value

returns an error if the species name is wrong.

Examples

```
## Not run:
library(fishflux)
check_name_fishbase("Lutjanus griseus")

## End(Not run)
```

---

cnp_mcmc *cnp_mcmc*

Description

cnp_mcmc

Usage

```
cnp_mcmc(TL, param, iter, params_st, cor, ...)
```

Arguments

TL	Total length(s) in cm
param	List of all parameter means (add "_m") and standard deviations (add "_sd") Default parameters are set with very low sd's. parameters:

- Qc_m, Qc_sd: percentage C of dry mass fish
- Qn_m, Qn_sd: percentage N of dry mass fish
- Qp_m, Qp_sd: percentage P of dry mass fish
- Dc_m, Dc_sd: percentage C of dry mass food
- Dn_m, Dn_sd: percentage N of dry mass food
- Dp_m, Dp_sd: percentage P of dry mass food
- ac_m, ac_sd: C-specific assimilation efficiency
- an_m, an_sd: N-specific assimilation efficiency
- ap_m, ap_sd: P-specific assimilation efficiency
- linf_m, linf_sd: Von Bertalanffy Growth parameter, theoretical maximum size in TL (cm)
- k_m, k_sd: Von Bertalanffy Growth parameter, growth rate (yr^-1)
- t0_m, tO_sd: Von Bertalanffy Growth parameter (yr)
- lwa_m, lwa_sd: Parameter length-weight relationship (g cm^-1)
- lwb_m, lwb_sd: Parameter length-weight relationship
- mdw_m, wprop_sd: Ratio between dry weight and wet weight of fish
- F0nz_m, F0nz_sd: N-specific turnover rate

- F0pz_m, F0pz_sd: P-specific turnover rate
- f0_m, f0_sd: Metabolic normalisation constant independent of body mass (g C g^-alpha d^-1)
- alpha_m, alpha_sd: Metabolic rate mass-scaling exponent
- theta_m, theta_sd: Activity scope
- r_m, r_sd: Aspect ratio of caudal fin
- h_m, h_sd: Trophic level
- v_m, v_sd: Environmental temperature (degrees celcius)

`iter`	A positive integer specifying the number of iterations. The default is 2000.
`params_st`	Standard parameters.
`cor`	A list of correlations between certain parameters: ro_Qc_Qn, ro_Qc_Qp, ro_Qn_Qp, ro_Dc_Dn, ro_Dc_Dp, ro_Dn_Dp, ro_lwa_lwb, ro_alpha_f0
`...`	Additional arguments rstan::sampling, see ?rstan:sampling

---

`cnp_model_mcmc` *A function to predict N and P excretion, CNP egestion, CNP ingestion rate, using MCMC and stan*

Description

This function combines MTE and stoichiometric theory in order to predict nescessary ingestion and excretion processes. A probability distribution is obtained by including uncertainty of parameters and using MCMC sampling with stan.

Usage

```
cnp_model_mcmc(
  TL,
  param,
  iter = 1000,
 cor = list(ro_Qc_Qn = 0.5, ro_Qc_Qp = -0.3, ro_Qn_Qp = -0.2, ro_Dc_Dn = 0.2, ro_Dc_Dp
    = -0.1, ro_Dn_Dp = -0.1, ro_lwa_lwb = 0.9, ro_alpha_f0 = 0.9),
  ...
)
```

Arguments

`TL`	Total length(s) in cm
`param`	List of all parameter means (add "_m") and standard deviations (add "_sd") Default parameters are set with very low sd's. parameters:

- Qc_m, Qc_sd: percentage C of dry mass fish
- Qn_m, Qn_sd: percentage N of dry mass fish
- Qp_m, Qp_sd: percentage P of dry mass fish
- Dc_m, Dc_sd: percentage C of dry mass food

- Dn_m, Dn_sd: percentage N of dry mass food
- Dp_m, Dp_sd: percentage P of dry mass food
- ac_m, ac_sd: C-specific assimilation efficiency
- an_m, an_sd: N-specific assimilation efficiency
- ap_m, ap_sd: P-specific assimilation efficiency
- linf_m, linf_sd: Von Bertalanffy Growth parameter, theoretical maximum size in TL (cm)
- k_m, k_sd: Von Bertalanffy Growth parameter, growth rate (yr^-1)
- t0_m, tO_sd: Von Bertalanffy Growth parameter (yr)
- lwa_m, lwa_sd: Parameter length-weight relationship (g cm^-1)
- lwb_m, lwb_sd: Parameter length-weight relationship
- mdw_m, wprop_sd: Ratio between dry weight and wet weight of fish
- F0nz_m, F0nz_sd: N-specific turnover rate
- F0pz_m, F0pz_sd: P-specific turnover rate
- f0_m, f0_sd: Metabolic normalisation constant independent of body mass (g C g^-alpha d^-1)
- alpha_m, alpha_sd: Metabolic rate mass-scaling exponent
- theta_m, theta_sd: Activity scope
- r_m, r_sd: Aspect ratio of caudal fin
- h_m, h_sd: Trophic level
- v_m, v_sd: Environmental temperature (degrees celcius)

`iter` A positive integer specifying the number of iterations. The default is 2000.

`cor` A list of correlations between certain parameters: ro_Qc_Qn, ro_Qc_Qp, ro_Qn_Qp, ro_Dc_Dn, ro_Dc_Dp, ro_Dn_Dp, ro_lwa_lwb, ro_alpha_f0

`...` Additional arguments rstan::sampling, see ?rstan:sampling

Value

Returns a list with two objects: A stanfit object and a data.frame with a summary of all model components. See `extract` to extract a summary of predicted variables and `limitation` to get information on the limiting element.

Examples

```
library(fishflux)
model <- cnp_model_mcmc(TL = 10, param = list(
Qc_m = 40, Qn_m = 10, Qp_m = 4, theta_m = 3))
```

`extract` *A function to extract specific model output parameters from result*

Description

A function to extract specific model output parameters from result

Usage

```
extract(mod, par)
```

Arguments

`mod`	Output from cnp_mod_mcmc()
`par`	Character vector specifying which output parameter that should be returned.

Value

Main model output parameters:

- F0c: C-specific minimal inorganic flux (g/day)
- F0n: N-specific minimal inorganic flux (g/day)
- F0p: P-specific minimal inorganic flux (g/day)
- Gc: Carbon-specific growth rate (g/day)
- Gn: Nitrogen-specific growth rate (g/day)
- Gp: Phosphorus-specific growth rate (g/day)
- Sc: C-specific minimal supply rate (g/day)
- Sn: N-specific minimal supply rate (g/day)
- Sp: P-specific minimal supply rate (g/day)
- Ic: Ingestion rate of C (g/day)
- In: Ingestion rate of N (g/day)
- Ip: Ingestion rate of P (g/day)
- Wc: Egestion rate of C (g/day)
- Wn: Egestion rate of N (g/day)
- Wp: Egestion rate of P (g/day)
- Fc: Total inorganic flux of C (respiration) (g/day)
- Fn: Total inorganic flux of N (excretion) (g/day)
- Fp: Total inorganic flux of P (excretion) (g/day)

Returns a data.frame with a summary of the selected output parameters

Examples

```
model <- cnp_model_mcmc(TL = 5:10, param = list(Qc_m = 40, Qn_m = 10, Qp_m = 4))
extract(model, c("Fn","Fp"))
```

`find_lw` *A function to find length-weight relationship parameters a and b*

Description

A function to find estimates length-weight relationship parameters available on fishbase. It returns a list of means and standard deviations of a and b obtained from: *Froese, R., J. Thorson and R.B. Reyes Jr., 2013. A Bayesian approach for estimating length-weight relationships in fishes. J. Appl. Ichthyol. (2013):1-7.* Please cite Froese et al. (2013), when using these values. The default mirror for fishbase is set to "de", please change this if needed for your location

Usage

```
find_lw(sp, mirror = "us")
```

Arguments

`sp`	A charachter value containing the species name
`mirror`	Mirror for fishbase (eg. "de", "org", "us", etc.) Default is "us".

Value

A dataframe with means and standard deviations of length-weight parameters

Examples

```
library(fishflux)
library(plyr)
# find length-weight relationship parameters for one species
find_lw("Lutjanus griseus")

# find length-weight relationship parameters for multiple species and return in dataframe
ldply(lapply(c("Chlorurus spilurus","Zebrasoma scopas"), find_lw))
```

`growth_params` *A function to find growth parameters on fishbase*

Description

A function to find growth parameters of a species using rfishbase. It returns a data frame containing K, t0 and Linf, the source. This function is useful to see what is available on fishbase. Nevertheless, we strongly recommend to check the source and only use otolith based studies.

Usage

```
growth_params(sp, otolith = TRUE)
```

Arguments

sp	A charachter value containing the species name
otolith	A logical value. If TRUE, only results from otolith analysis are returned. If false, all growth studies will be returned.

Value

dataframe with available growth rate parameters from fishbase.

Examples

```
## Not run:
library(fishflux)
growth_params("Lutjanus griseus")

## End(Not run)
```

---

limitation *A function to evaluate element limitation of the model*

Description

This function allows you extract the proportions of the iterations for which c, n and p are the limiting element in the model.

Usage

```
limitation(mod, plot = TRUE)
```

Arguments

mod	Model output from cnp_model_mcmc().
plot	Argument to specify if results should be shown in a plot.

Value

Returns a data frame with:

tl Total length, in cm

nutrient c, n or p

prop_lim the proportion of iterations for which there is limitation by the element

Examples

```
library(fishflux)
mod <- cnp_model_mcmc(TL = 5, param = list(Qc_m = 40, Qn_m = 10, Qp_m = 4,
                                           Dc_sd = 0.1, Dn_sd = 0.05, Dp_sd = 0.05))
limitation(mod)
```

metabolic_parameters *Data with metabolic parameters on family level*

Description

Data frame containing means and sd for b0 and a for several fish families, extracted from Barneche & Allen (2018) These paramaters can be used in calculations of metabolic rate in case respirometry data is not available.

Usage

```
data(metabolic_parameters)
```

Format

An object of class `data.frame` with 20 rows and 5 columns.

Examples

```
data(metabolic_parameters)
```

metabolic_rate *A function to calculate metabolic rates*

Description

All model parameters below were estimated by Barneche & Allen 2018 Ecology Letters doi: 10.1111/ele.12947. These parameters are for the best model (Model 2 in the paper online supplementary material) of fish resting metabolic rates reported in the paper, which also includes trophic level as a covariate.

Usage

```
metabolic_rate(temp, troph, asp, B0, m_max, m, a, growth_g_day, f)
```

Arguments

`temp`	Temperature in degrees Celsius
`troph`	Trophic level (from 1 to 5)
`asp`	The caudal fin aspect ratio , a proxy for activity level
`B0`	Constant for resting metabolic rate. If NA, function will calculate an average.
`m_max`	Maximum biomass fish (in g)
`m`	Wet weight fish (in g)
`a`	Resting metabolic rate mass-scaling exponent
`growth_g_day`	Daily growth in grams of wet weight
`f`	Activity scope (from 1 to 4)

Details

All model parameters below were estimated by Barneche & Allen 2018 Ecology Letters doi: 10.1111/ele.12947. These parameters are for the best model (Model 2 in the paper online supplementary material) of fish resting metabolic rates reported in the paper, which also includes trophic level as a covariate.

Value

A dataframe with metabolic rates.

Examples

```
library(fishflux)
fishflux::metabolic_rate(temp = 27, m_max = 600, m = 300, asp = 3,
troph = 2, f = 2, growth_g_day = 0.05, B0 = 0.2, a = 0.6 )
```

---

metabolism *A function to estimate f0 and alpha*

Description

All model parameters below were estimated by Barneche & Allen 2018 Ecology Letters doi: 10.1111/ele.12947. These parameters are for the best model (Model 2 in the paper online supplementary material) of fish resting metabolic rates reported in the paper, which also includes trophic level as a covariate.

Usage

```
metabolism(family, temp, troph_m, troph_sd = 1e-10)
```

Arguments

`family`	family fish
`temp`	Temperature in degrees Celsius
`troph_m`	Trophic level mean (from 1 to 5)
`troph_sd`	Trophic level sd (optional)

Details

All model parameters below were estimated by Barneche & Allen 2018 Ecology Letters doi: 10.1111/ele.12947. These parameters are for the best model (Model 2 in the paper online supplementary material) of fish resting metabolic rates reported in the paper, which also includes trophic level as a covariate.

Value

dataframe with predicted metabolic parameters.

Examples

```
library(fishflux)
metabolism(family = "Pomacentridae", temp = 27, troph_m = 2)
```

`model_parameters` *A function to find a set of parameters*

Description

A function to find a set of parameters

Usage

```
model_parameters(sp, family, otolith = TRUE, temp, ...)
```

Arguments

`sp`	Species name
`family`	family
`otolith`	TRUE or FALSE, if TRUE, function will only search fishbase for growth parameters that are based upon otolith analysis
`temp`	temperature
`...`	Additional arguments to `find_lw`.

Value

Returns a dataframe with all parameters that can be estimated

Examples

```
## Not run:
library(fishflux)
model_parameters(sp = "Scarus psittacus", family = "Scaridae", temp = 27)
## End(Not run)
```

name_errors *A function to find errors in fish species names*

Description

This function allows you to check if there are errors in your fish species list and returns inaccurate scientific names

Usage

```
name_errors(sp)
```

Arguments

sp	A vector containing all your scientific species names.

Value

A vector with the incorrect species names.

Examples

```
## Not run:
library(fishflux)
name_errors(c("Chlorurus spilurus", "Zebrasoma scopas"))
name_errors(c("Chlorurus spilurus", "Zebrasoma copas"))
## End(Not run)
```

param_zebsco *List of all parameters needed to run cnp_model for *Zebrasoma scopas**

Description

List of all parameters needed to run cnp_model for *Zebrasoma scopas*

Usage

```
data(param_zebsco)
```

Format

An object of class `list` of length 37.

Examples

```
data(param_zebsco)
```

`plot_cnp` *A function to plot results model*

Description

This function allows you to plot an overview of the model results in function of the total length of fish

Usage

```
plot_cnp(mod, y, x = "tl", probs = c(0.8, 0.95))
```

Arguments

`mod`	Model output from cnp_model_mcmc()
`y`	Output variable(s) to be plotted. Can be a character or a character vector.
`x`	Variable to be put on x-axis, "biomass" or "tl"
`probs`	Width of the confidence

Value

a ggplot object

Examples

```
library(fishflux)
mod <- cnp_model_mcmc(TL = 5:15, param = list(
          Qc_m = 40, Qn_m = 10, Qp_m = 4, Dn_sd = 0.05))
plot_cnp(mod = mod, y = c("Fp", "Gp", "Wp", "Ip"),
         x = "tl", probs = c(0.5, 0.8))
plot_cnp(mod = mod, y = "Fp", x = "tl",
         probs = c(0.5, 0.8, 0.95))
```

`sensitivity` *A function to check the sensitivity of cnp_model predictions based on the variation of input parameters*

Description

This function runs the cnp_model fixing all parameters SD's but one to test for sensitivity

Usage

```
sensitivity(
  TL,
  param,
  iter = 1000,
  par,
  out = c("Ic", "In", "Ip", "Gc", "Gn", "Gp", "Fc", "Fn", "Fp", "Wc", "Wn", "Wp"),
  ...
)
```

Arguments

TL	total length of a fish in cm
param	list of all parameter means ("_m") and standard deviations ("_sd") Default parameters are set with very low sd's. See cnp_model_mcmc for a list of all requested parameters
iter	A positive integer specifying the number of iterations. The default is 1000
par	Charachter vector specifying which input parameter sd's should be used for sensitivity.
out	Charachter vector specifying which output parameter sd's should be returned.
...	Other arguments that can be used from cnp_model_mcmc

Value

Returns a dataframe with sd's of model predictions. Row names indicate the variable, who's sd was used for the model run. Plots a heatplot with width of the 95

Examples

```
library(fishflux)
sensitivity(TL = 10, param = list(k_sd = 0.2, Dn_sd = 0.2, Dc_sd = 0.1),
            par = c("k_sd","Dn_sd","Dc_sd"), out = c("Ic", "In", "Ip", "Gc"))
```

---

trophic_level *A function to find trophic level*

Description

A function to find trophic level of a species on either species or genus level using rfishbase. It returns a data frame containing the trophic level and the level at which the trophic level was found (species or genus).

Usage

```
trophic_level(sp)
```

Arguments

sp	A character value containing the species name

Value

Returns a dataframe with species, trophic level, and taxonomy level.

Examples

```
## Not run:
library(fishflux)
library(plyr)
trophic_level("Lutjanus griseus")
ldply(lapply(c("Chlorurus spilurus","Zebrasoma scopas"), trophic_level))
## End(Not run)
```

---

weight_prop *Data frame with dry weight/ wet weight proportions for multiple reef fish families.*

Description

Data frame with dry weight/ wet weight proportions for multiple reef fish families.

Usage

```
data(weight_prop)
```

Format

An object of class `data.frame` with 15 rows and 4 columns.

Examples

```
data(weight_prop)
```

wprop *A function to find the ratio of dry weight and wet weight of fish in local database*

Description

This function searches the ratio of dry weight and wet weight of fish on the family level. If the family is not available, an average is returned.

Usage

```
wprop(family)
```

Arguments

family	family

Value

Returns a dataframe with the weight ratio (mdw) and it's sd (mdw_sd).

Examples

```
library(fishflux)
wprop(family="Scaridae")
```

Index

Appendix B

Documentation fishgrowbot

This appendix includes a short note on the R package fishgrowbot. For more documentation see: `https://nschiett.github.io/fishgrowbot/index.html`

Figure B.1: Logo fishgrowbot

fishgrowbot: Fish growth curves through back-calculation of otoliths rings in a Bayesian framework

(In preparation as a short communication for Journal of Fish Biology)

2021-04-22

Authors:

Nina M. D. Schiettekatte[1,2*], Jérémy Wicquart[1,2], Diego R. Barneche[3,4], Valeriano Parravicini[1,2]

[1] PSL Université Paris: EPHE-UPVD-CNRS, USR 3278 CRIOBE, Université de Perpignan, 66860 Perpignan, France

[2] Laboratoire d'Excellence "CORAIL," Perpignan, France

[3] Australian Institute of Marine Science, Indian Ocean Marine Research Centre, Crawley, WA 6009, Australia

[4] Oceans Institute, The University of Western Australia, Crawley, WA 6009, Australia

Correspondence to: N.M.D.S.; Email: nina.schiettekatte@gmail.com

Summary

Somatic growth of fishes is a fundamental trait that determines essential ecosystem services such as food provision and nutrient cycling. Growth rate information can be derived through age estimation based on the analysis of sagittal otoliths. While fitting growth models on size-at-age data is the most frequently employed approach to deriving growth parameters, this method requires a high number of individuals. An alternative approach based on back-calculation can provide approximations to individual-level growth trajectories. We present `fishgrowbot`, an R package that provides functions to perform the back-calculation in a Bayesian framework. Further, the package provides a Bayesian framework to fit the von Bertalanffy growth model to the back-calculated lengths in a hierarchical structure. Finally, `fishgrowbot` provides functions to visualize the results. These models have been verified and applied to estimate growth parameters of 45 coral reef species (Morat et al. 2020). `fishgrowbot` will greatly help researchers to estimate growth parameters, even when a limited amount of otoliths are available.

Description

Somatic growth of fishes is a critical trait to estimate biological processes that range from individuals to communities (Brandl et al. 2019). In the context of fisheries, parameters describing fish growth can be used directly to estimate an important ecosystem service, i.e. food production. Further, somatic growth rate is an important part of an individual's energy budget and thus underlies bioenergetic models that estimate fluxes of energy and elements mediated by fishes (Schiettekatte et al. 2020). Many ecosystems are under major anthropogenic pressure, and fish populations are in decline across the globe (Jackson et al. 2001). As billions of people depend on fishes for food security and fishes can play an important role in nutrient cycling, it is critical to increase our ability to estimate growth parameters.

Fish growth can be estimated by relating fish length with the age. The most common method for aging fish is the analysis of growth rings found on otoliths (i.e. calcified structures of the inner ear that grow with the deposition of successive calcium carbonate layers, which respond to circadian or seasonal rhythms) (Campana 2001). Then, fish growth parameters can be estimated by fitting growth curves on the size-at-age data (Katsanevakis 2006). While there are many types of growth models, the Von Bertalanffy growth curve is by far the most commonly used for fishes. Fitting growth curves calls for a large sample size of individuals with varying sizes. Alternatively, we can estimate individual growth trajectories by measuring the distances between growth rings, and transforming these to fish lengths, a process called back-calculation (Vigliola and Meekan 2009; Vigliola, Harmelin-Vivien, and Meekan 2000). This approach facilitates fitting growth curves with less individuals and is thus less destructive. However, back-calculated lengths are rough estimates that include a level of uncertainty, that is not accounted for in currently described methods and existing tools (Vigliola and Meekan 2009). Moreover, the nature of back-calculated lengths demands a hierarchical modeling approach to account for autocorrelation within individuals growth trajectories. Developing such a model can be challenging and discouraging for the average R user, and there are currently no tools to aid fitting a Von Bertalanffy growth model to back-calculated lengths.

Here, we present the R package `fishgrowbot` to facilitate the application of back-calculation and fitting of von Bertalanffy growth curves on back-calculated size-at-age data. Even though there are R packages for back-calculation and fitting growth models, `fishgowbot` brings a number of new features to the table. First, back-calculation in a Bayesian framework allows for a measure of uncertainty (Stan Development Team 2018), which to date has never been incorporated. Second, to the best of our knowledge, there are no existing R packages that aid fitting growth models, specifically for back-calculated lengths. Due to the individual-level autocorrelation in the data, it is necessary to incorporate a hierarchical structure. Further, aside from the hierarchical structure, the Bayesian framework allows for the incorporation of prior biological knowledge on maximum lengths and growth rate parameters. Third, the back-calculation approach can handle missing data on the otolith radius at hatching (Carpenter et al. 2017), a handy feature as for some individuals this parameter is impossible to measure. The approach is validated through application on a dataset of 45 coral reef fish species (Morat et al. 2020). Finally, as a case study, the package provide the raw dataset of measured otoliths from 710 individuals belonging to 45 coral reef fish species from French Polynesia, that can be used to run examples or to easily include in ecological studies.

Specifically, we used the Modified Fry back-calcuation method that depends on the relationship between the length at capture and the measurements of the radius of the otolith (Vigliola et al. 2000), and adapted it into a Bayesian framework:

$$L_{cpt} = L_{0p} - bR^c_{0p} + bR^c_{cpt}$$

,

where L_{0p} and R_{0p} are the fish size and radius of the otolith at hatching.

If for some individuals, the R_{0p} value is missing, they can still be included in the back-calculation model. To do so, missing R_{0p} values as parameters in the model that are estimated in the posterior (Carpenter et al. 2017). Then, for each iteration of the Bayesian model, the lengths at all ages are calculated are calculated as followed:

$$a_i = L_{0p} - bR^c_{0pi}$$

$$Li = a + exp(log(L_{0p} - a) + \frac{(log(L_{cpt} - a) - log(L_{0p} - a))(log(R_i) - log(R_{0p}))}{(log(R_{cpt}) - log(R_{0p}))})$$

where L_i and R_i are the fish length and otolith radius at age i, L_{0p} and R_{0p} are the fish size and radius of otolith at hatching. The output of the back-calculation function `bcalc()` returns the averages, standard deviations and credible intervals for each L_i.

As a next step, `fishgrowbot` also provides a Bayesian model to fit growth models to back-calculated size-at-age data. We use the Von Bertalanffy growth curve, the most frequently used model to describe fish growth:

$$Lt = L_{\text{inf}}(1 - e^{-K(t-t_0)})$$

, where L_t is the average length at age i, L_{inf} is the asymptotic average length, K is the growth rate coefficient, and t_0 is the age when the average length was zero.

Use

To introduce the functionalities of `fishgrowbot`, we look at an example for *Epinephelus merra*. The function `bcalc()` returns both a dataframe with the back-calculated lengths and their uncertainty and the model object for more details on the fit of the `bc` stan model.

The input data should contain:
+ id: Unique fish id per individual.
+ radi: Measurements of otolith growth rings (in mm).
+ agei: Age estimation of fish.
+ lencap: Length at capture (in mm).
+ radcap: Radius of otolith at capture (in mm).
+ l0p: Length of fish at hatching (in mm).

```
# get data
em <- filter(coral_reef_fishes_data, species == "Epinephelus merra",
             location == "Moorea")
# back-calculation
bc <- bcalc(data = em)
```

```
head(bc$lengths)
```

```
##                   id age      l_m         l_sd     l_lb     l_ub
## 1 CH_SO_MO_03_16_001   0   1.6500 3.570679e-14   1.6500   1.6500
## 2 CH_SO_MO_03_16_001   1 192.8638 9.667175e+00 171.8699 209.7544
## 3 CH_SO_MO_03_16_001   2 242.5329 5.234313e+00 230.9617 251.4320
## 4 CH_SO_MO_03_16_001   3 260.9157 3.058368e+00 254.1158 266.0663
## 5 CH_SO_MO_03_16_001   4 273.6994 1.385600e+00 270.6071 276.0180
## 6 CH_SO_MO_03_16_002   0   1.6500 3.581811e-14   1.6500   1.6500
```

```
library(ggplot2)
library(fishgrowbot)
ggplot(aes(x = agecap, y = lencap), data = em) +
  geom_point()
```

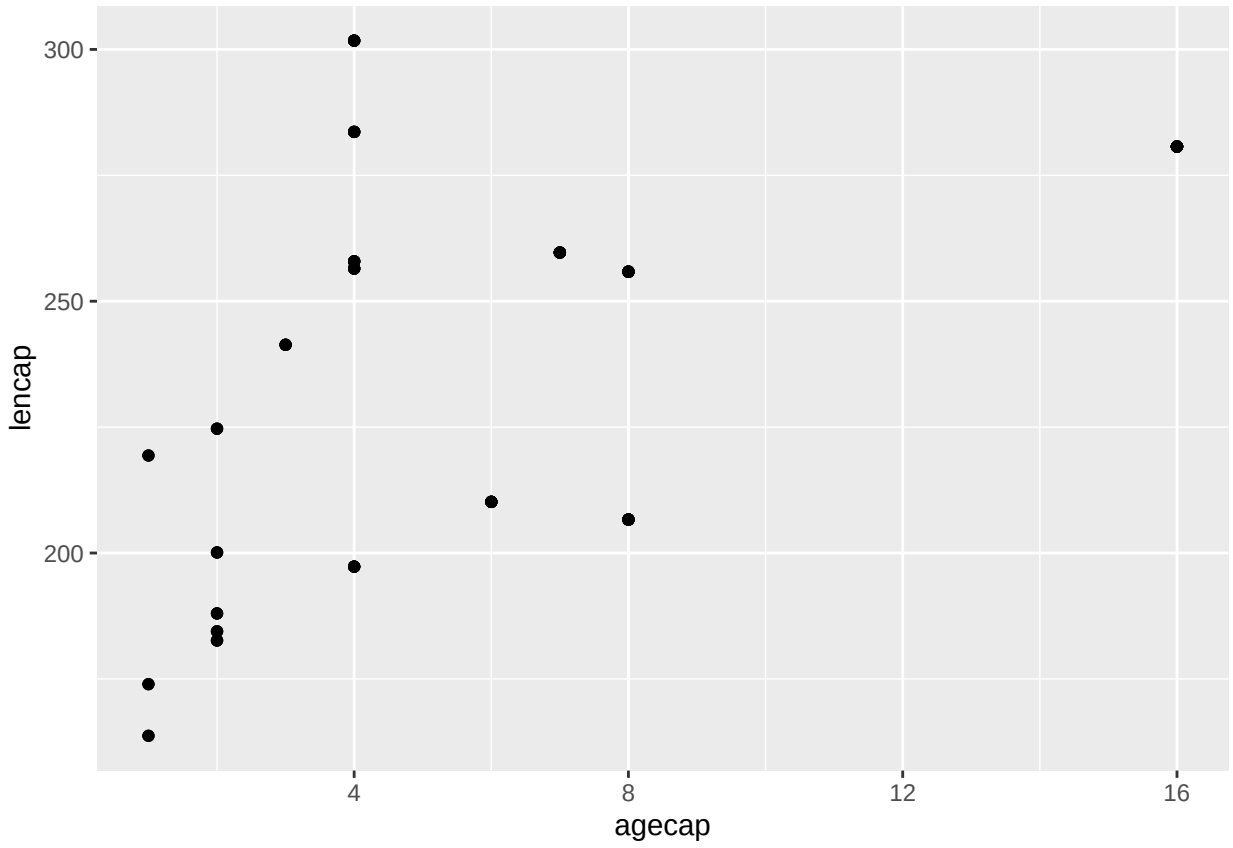


```
gmplot(growthmodel) +
  geom_point(aes(x = agecap, y = lencap/10, color = id), data = em)
```

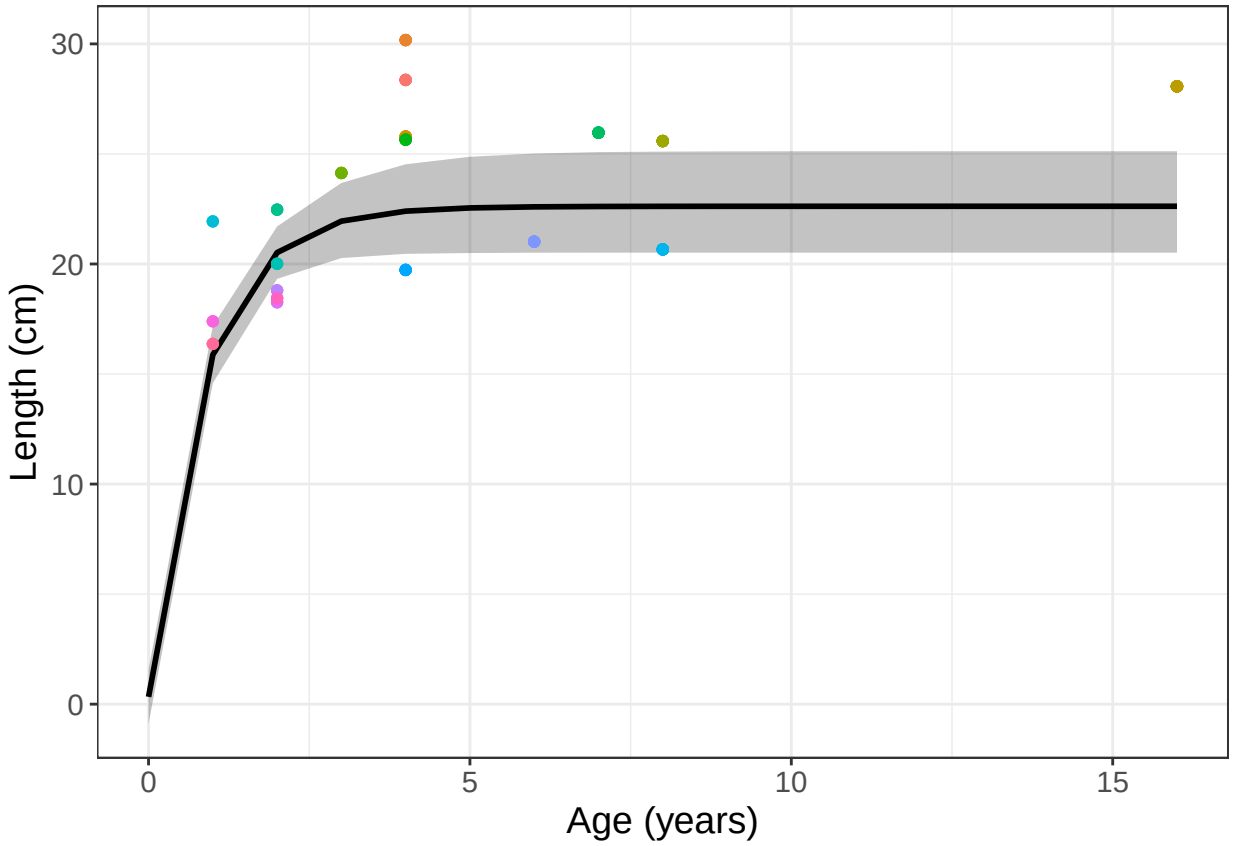

The function `bcplot` helps visualize the back calculation. Setting error to TRUE adds the 95% credible intervals of the length estimates.

```
bcplot(bc$lengths, error = TRUE, facet = TRUE)
```

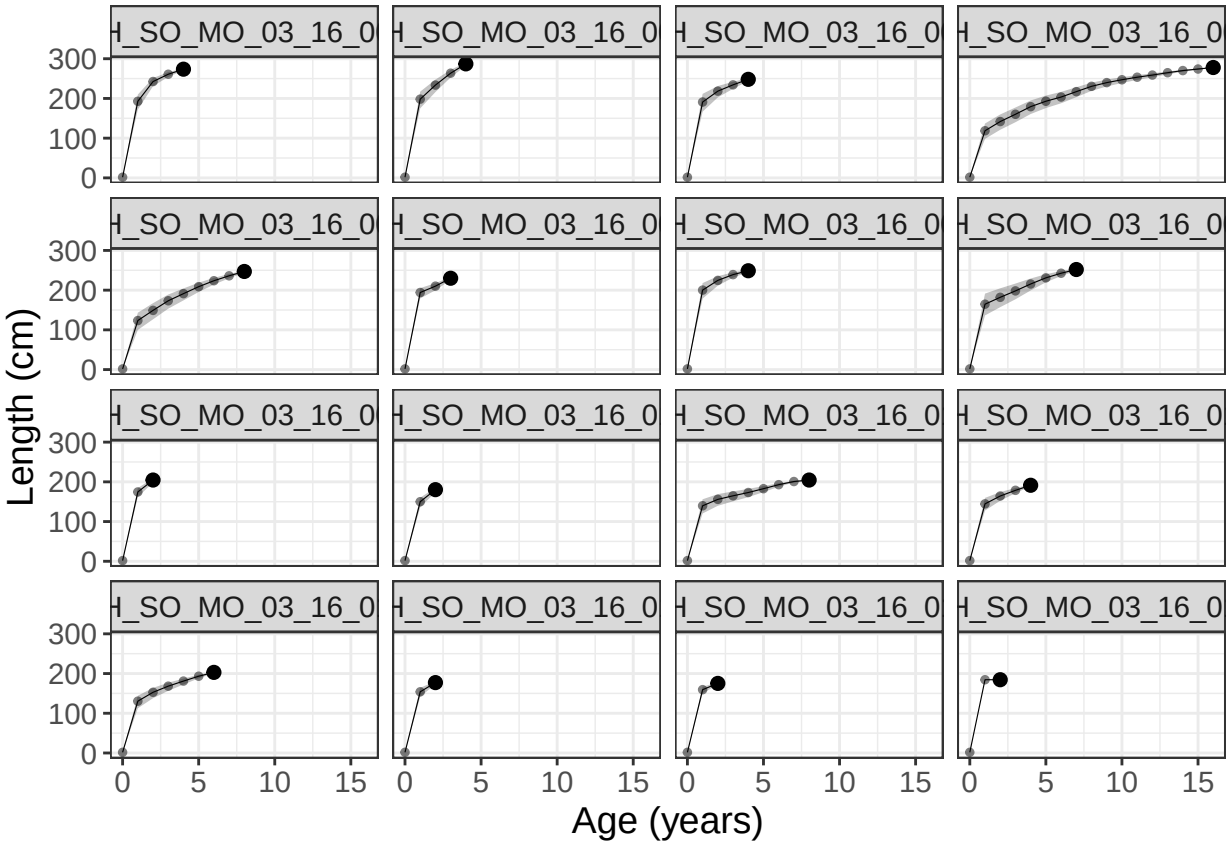

Then, we can fit the hierarchical von Bertalanffy growth model that allows for the estimation of multiple parameters. Importantly, length measures should be given in cm. Priors for Linf (i.e. asymptotic length) and l0 (length at hatching) s hould be specified by the user.

```
# fit growth model
growthmodel <- growthreg(length = bc$lengths$l_m / 10, age =  bc$lengths$age,
                         id =  bc$lengths$id, lmax = 32, linf_m = 28,
                         linf_sd = 5, l0_m = 0.15, l0_sd = 0.015, iter = 4000,
                         open_progress = FALSE, plot = FALSE)
```

```
# summary growth parameters
growthmodel$summary
```

```
##              mean      se_mean         sd        2.5%         25%         50%
## k     1.21759396 0.0032353328 0.18116826  0.90147864  1.09074960  1.20705146
## linf 22.62232772 0.0234612229 1.15696683 20.51601047 21.84600773 22.55817660
## l0    0.33207979 0.0057334577 0.62044794 -0.89492024 -0.07489291  0.33498481
## t0   -0.01332498 0.0002244964 0.02397879 -0.06449012 -0.02803510 -0.01216818
## kmax  0.61612395 0.0007725673 0.06177841  0.50281216  0.57444993  0.61267084
##                75%       97.5%
## k     1.327397754  1.60922888
## linf 23.318151649 25.12215501
## l0    0.734124677  1.57094987
## t0    0.002693189  0.03072865
## kmax  0.654570031  0.74532319
```

Now we can visualize the fit with the function `gmplot()`.

```
gmplot(growthmodel, id = TRUE, facet = FALSE)
```

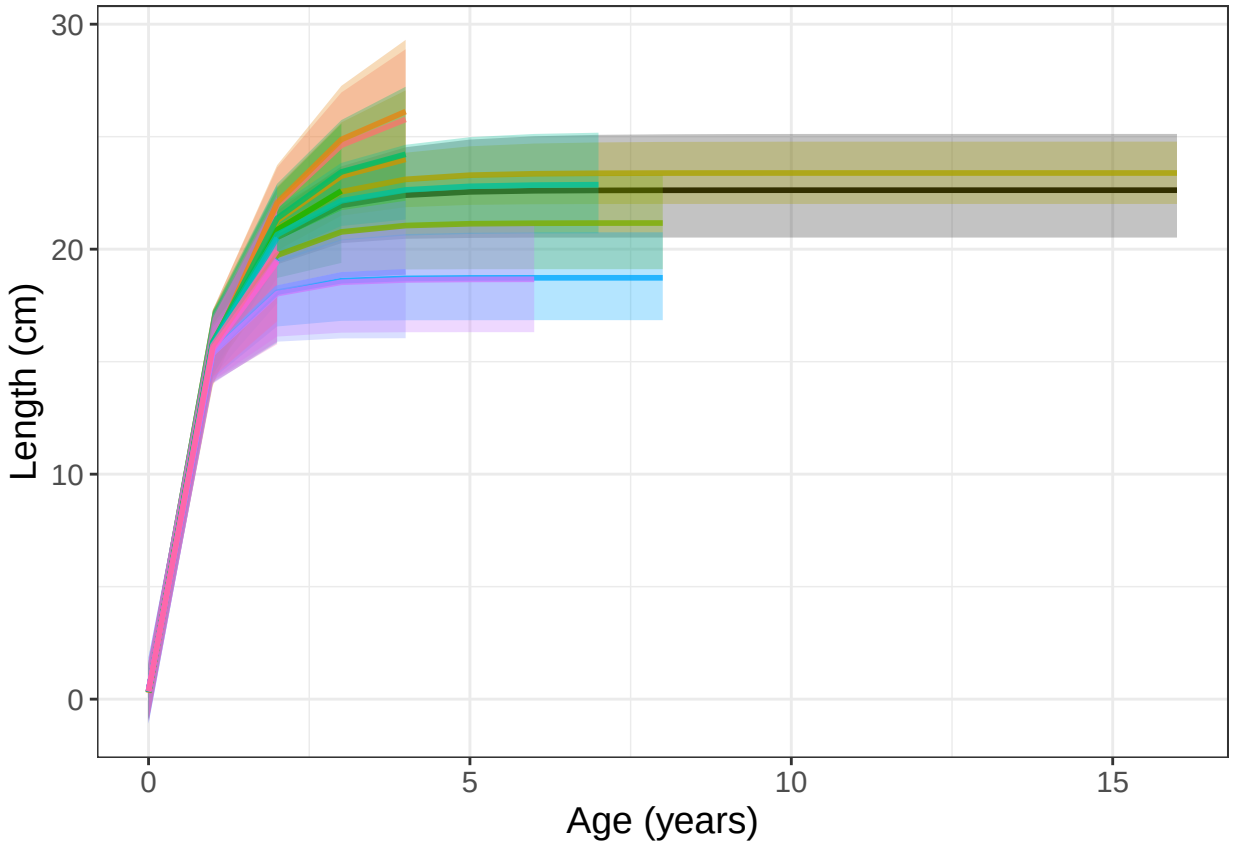

More plotting options are exemplified in the package documentation and introduction vignette.

Acknowledgements

We thank Jordan M. Casey for designing the logo for fishgrowbot.

References

Brandl, Simon J, Douglas B Rasher, Isabelle M Côté, Jordan M Casey, Emily S Darling, Jonathan S Lefcheck, and J Emmett Duffy. 2019. "Coral reef ecosystem functioning: eight core processes and the role of biodiversity." *Frontiers in Ecology and the Environment, Advance Online Publication.* 17 (8): 445–54. https://doi.org/10.1002/fee.2088.

Campana, S. E. 2001. "Accuracy, precision and quality control in age determination, including a review of the use and abuse of age validation methods." *Journal of Fish Biology* 59: 197–242. https://doi.org/10.1111/j.1095-8649.2001.tb00127.x.

Carpenter, Bob, Andrew Gelman, Matthew D. Hoffman, Daniel Lee, Ben Goodrich, Michael Betancourt, Marcus Brubaker, Jiqiang Guo, Peter Li, and Allen Riddell. 2017. "Stan : A Probabilistic Programming Language." *Journal of Statistical Software* 76 (1): 1–31. https://doi.org/10.18637/jss.v076.i01.

Jackson, J B, M X Kirby, W H Berger, K A Bjorndal, L W Botsford, B J Bourque, R H Bradbury, et al. 2001. "Historical overfishing and the recent collapse of coastal ecosystems." *Science (New York, N.Y.)* 293 (5530): 629–37. https://doi.org/10.1126/science.1059199.

Katsanevakis, Stelios. 2006. "Modelling fish growth: Model selection, multi-model inference and model selection uncertainty." *Fisheries Research* 81 (2-3): 229–35. https://doi.org/10.1016/j.fishres.2006.07.002.

Morat, Fabien, Jérémy Wicquart, Nina M. D. Schiettekatte, Guillemette de Sinéty, Jean Bienvenu, Jordan M. Casey, Simon J. Brandl, et al. 2020. "Individual back-calculated size-at-age based on otoliths from Pacific coral reef fish species." *Scientific Data* 7 (370). https://doi.org/10.1038/s41597-020-00711-y.

Schiettekatte, Nina M D, Diego R Barneche, Sébastien Villéger, Jacob E Allgeier, Deron E Burkepile, Simon J Brandl, Jordan M Casey, et al. 2020. "Nutrient limitation, bioenergetics, and stoichiometry: a new model to predict elemental fluxes mediated by fishes." *Functional Ecology* 34 (9): 1857–69. https://doi.org/10.1111/1365-2435.13618.

Stan Development Team. 2018. "RStan: the R interface to Stan. R package version 2.17.3." https://doi.org/10.3168/jds.S0022-0302(63)89186-9.

Vigliola, Laurent, Mireille Harmelin-Vivien, and Mark G. Meekan. 2000. "Comparison of techniques of back-calculation of growth and settlement marks from the otoliths of three species of Diplodus from the Mediterranean Sea." *Canadian Journal of Fisheries and Aquatic Sciences* 57 (6): 1291–99. https://doi.org/10.1139/cjfas-57-6-1291.

Vigliola, Laurent, and Mark G. Meekan. 2009. "The Back-Calculation of Fish Growth From Otoliths." In *Tropical Fish Otoliths: Information for Assessment, Management and Ecology*, 174–211. https://doi.org/10.1007/978-1-4020-5775-5_6.

Appendix C

Documentation fishualize

This appendix includes the reference manual of `fishualize`.

For more documentation see: `https://nschiett.github.io/fishualize/index.html`

Figure C.1: Logo fishualize

Package 'fishualize'

April 9, 2021

Type Package

Title Color Palettes Based on Fish Species

Version 0.2.2

Maintainer Nina M. D. Schiettekatte <nina.schiettekatte@gmail.com>

Description Implementation of color palettes based on fish species.

License GPL-2

Encoding UTF-8

LazyData true

Depends R (>= 2.10)

Suggests testthat, knitr, rmarkdown, rfishbase, rnaturalearth, pkgdown

URL https://github.com/nschiett/fishualize

BugReports https://github.com/nschiett/fishualize/issues

Imports ggplot2 (>= 1.0.1), gridExtra, grid, png, downloader, utils, httr, magrittr, stringr, dplyr, tidyr, scales, rlang, curl

RoxygenNote 7.1.1

VignetteBuilder knitr

NeedsCompilation no

Author Nina M. D. Schiettekatte [cre, aut],
Simon J. Brandl [aut],
Jordan M. Casey [aut]

Repository CRAN

Date/Publication 2021-04-09 16:50:02 UTC

R topics documented:

`add_fishape` *fish silhouette in ggplot2*

Description

Adds a fish silhouette to your plot

Usage

```
add_fishape(
  family = "Pomacanthidae",
  option = "Centropyge_loricula",
  xmin = -Inf,
  xmax = Inf,
  ymin = -Inf,
  ymax = Inf,
  scaled = FALSE,
  xlim = NULL,
  ylim = NULL,
  fill = "#000000",
  alpha = 1
)
```

Arguments

`family`	character string indicating the fish family.
`option`	character string indicating the fish species. If NA, the first available option within a family will be selected
`xmin`	x location giving minimum horizontal location of silhouette
`xmax`	x location giving maximum horizontal location of silhouette
`ymin`	y location giving minimum vertical location of silhouette
`ymax`	y location giving maximum vertical location of silhouette
`scaled`	logical parameter. If TRUE, location parameters (xmin, xmax, ymin, ymax) should range between 0 and 1. If FALSE, location parameters should be provided according to the values on the plot axes.
`xlim, ylim`	vectors of length = 2, contains the data limits and must be provided if scaled is TRUE.
`fill`	color of fish shape
`alpha`	transparency of fish shape (value between 0 and 1)

Examples

```
library(ggplot2)

ggplot() + add_fishape(fill = fish(n = 5)[4])

ggplot(diamonds)+
  geom_bar(aes(cut, fill = cut)) +
  scale_fill_fish_d(option = "Naso_lituratus") +
  add_fishape(family = "Acanthuridae",
              option = "Naso_unicornis",
              xmin = 1, xmax = 3, ymin = 15000, ymax = 20000,
              fill = fish(option = "Naso_lituratus", n = 5)[3],
              alpha = 0.8) +
  theme_bw()

## example with relative coordinates
ggplot(diamonds)+
  geom_bar(aes(cut, fill = cut)) +
  scale_fill_fish_d(option = "Naso_lituratus") +
  add_fishape(family = "Acanthuridae",
              option = "Naso_unicornis",
              xmin = 0, xmax = 0.3, ymin = 0.8, ymax = 1,
              scaled = TRUE,
              xlim = c(0.5, 5.5), ylim = c(0, 21000) ,
              fill = fish(option = "Naso_lituratus", n = 5)[3],
              alpha = 1) +
  theme_bw()
```

`fish` *fish Colour Map.*

Description

This function creates a vector of n equally spaced colors along the 'fish colour map' of your selection

Usage

```
fish(
  n,
  alpha = 1,
  begin = 0,
  end = 1,
  direction = 1,
  option = "Centropyge_loricula"
)

fish_pal(
```

```
  alpha = 1,
  begin = 0,
  end = 1,
  direction = 1,
  option = "Centropyge_loricula"
)
```

Arguments

n	The number of colors (≥ 1) to be in the palette.
alpha	The alpha transparency, a number in [0,1], see argument alpha in hsv.
begin	The (corrected) hue in [0,1] at which the fish colormap begins.
end	The (corrected) hue in [0,1] at which the fish colormap ends.
direction	Sets the order of colors in the scale. If 1, the default, colors are ordered from darkest to lightest. If -1, the order of colors is reversed.
option	A character string indicating the fish species to use.

Value

fish returns a character vector, cv, of color hex codes. This can be used either to create a user-defined color palette for subsequent graphics by palette(cv), a col = specification in graphics functions or in par.

Semi-transparent colors ($0 < alpha < 1$) are supported only on some devices: see rgb.

Examples

```
library(ggplot2)
library(fishualize)

dat <- data.frame(x = rnorm(1e4), y = rnorm(1e4))
ggplot(dat, aes(x = x, y = y)) +
  stat_density_2d(geom = "raster",
  aes(fill = after_stat(density)), contour = FALSE) +
  scale_fill_gradientn(colors = fish(128, option = 'Ostracion_cubicus'))

pal <- fish(256, option = "Thalassoma_hardwicke", direction = -1)
image(volcano, col = pal)
```

---

fishapes *Available fish silhouettes*

Description

This function returns a dataframe containing the all the available fish silhouettes accessible through the 'fishualize' package.

Usage

```
fishapes()
```

Value

fishapes returns a dataframe containing the all the available fish silhouettes available to use.

Examples

```
fishapes()
```

---

fishcolors *Original fish color database*

Description

A dataset containing some colour palettes inspired by fish species

Usage

```
fishcolors
```

Format

A data frame containing all the colours used in the palette:

- option: It is intended to be a general option for choosing the specific colour palette.
- hex: hex color code

---

fishualize *Visualization of fish color palette*

Description

This function creates an image of the specified fish color palette.

Usage

```
fishualize(option = "Centropyge_loricula", n = 5, ...)
```

Arguments

option	A character string indicating the fish species to use.
n	The number of colors (≥ 1) to be in the palette.
...	Other arguments as can be specified in the function fish. See ?fishualize::fish for details.

Value

fishualize returns a visualisation of the specified color palette.

Examples

```
fishualize::fishualize()
fishualize::fishualize(option = "Zanclus_cornutus", n = 8)
```

---

fish_palettes *Available Palettes.*

Description

This function returns a vector containing the names of all the available palettes in the 'fishualize' package.

Usage

```
fish_palettes()
```

Value

fish_palettes returns a character vector with the names of the fish palettes available to use.

Examples

```
fish_palettes()
```

---

scale_color_fish *fish colour scales*

Description

Uses the fish color scale.

Usage

```
scale_color_fish(
  option = "Centropyge_loricula",
  ...,
  alpha = 1,
  begin = 0,
  end = 1,
  direction = 1,
  discrete = FALSE
)

scale_colour_fish(
  option = "Centropyge_loricula",
  ...,
  alpha = 1,
  begin = 0,
  end = 1,
  direction = 1,
  discrete = FALSE
)

scale_colour_fish_d(
  option = "Centropyge_loricula",
  ...,
  alpha = 1,
  begin = 0,
  end = 1,
  direction = 1
)

scale_color_fish_d(
  option = "Centropyge_loricula",
  ...,
  alpha = 1,
  begin = 0,
  end = 1,
  direction = 1
)

scale_fill_fish_d(
  option = "Centropyge_loricula",
  ...,
  alpha = 1,
  begin = 0,
  end = 1,
  direction = 1
)
```

```
scale_fill_fish(
  option = "Centropyge_loricula",
  ...,
  alpha = 1,
  begin = 0,
  end = 1,
  direction = 1,
  discrete = FALSE
)
```

Arguments

option	A character string indicating the fish species to use.
...	parameters to discrete_scale or scale_fill_gradientn
alpha	pass through parameter to fish
begin	The (corrected) hue in [0,1] at which the fish colormap begins.
end	The (corrected) hue in [0,1] at which the fish colormap ends.
direction	Sets the order of colors in the scale. If 1, the default, colors are as output by fish_pal. If -1, the order of colors is reversed.
discrete	generate a discrete palette? (default: FALSE - generate continuous palette)

Details

For discrete == FALSE (the default) all other arguments are as to scale_fill_gradientn or scale_color_gradientn. Otherwise the function will return a discrete_scale with the plot-computed number of colors.

Examples

```
library(ggplot2)
library(fishualize)


ggplot(diamonds, aes(factor(cut), fill=factor(cut))) +
geom_bar() +
scale_fill_fish(discrete = TRUE, option = "Centropyge_loricula")

ggplot(mtcars, aes(factor(gear), fill=factor(carb))) +
geom_bar() +
scale_fill_fish(discrete = TRUE, option = "Trimma_lantana")

ggplot(mtcars, aes(x = mpg, y = disp, colour = drat)) +
geom_point(size = 4) +
scale_colour_fish(option = "Ostracion_cubicus", direction = -1)
```

Index

References

Albouy, C., Archambault, P., Appeltans, W., Araújo, M.B., Beauchesne, D., Cazelles, K., *et al.* (2019). The marine fish food web is globally connected. *Nature Ecology & Evolution*, 3, 1153–1161.

Allen, A.P., Gillooly, J.F. & Brown, J.H. (2005). Linking the global carbon cycle to individual metabolism. *Functional Ecology*, 19, 202–213.

Allen, S.E., Grimshaw, H.M., Parkinson, J.A. & Quarmby, C. (1974). *Chemical analysis of ecological materials,*. Blackwell Scientific Publications.

Allgeier, J.E., Burkepile, D.E. & Layman, C.A. (2017). Animal pee in the sea: consumer-mediated nutrient dynamics in the world's changing oceans.

Allgeier, J.E., Layman, C.A., Mumby, P.J. & Rosemond, A.D. (2014). Consistent nutrient storage and supply mediated by diverse fish communities in coral reef ecosystems. *Global Change Biology*, 20, 2459–2472.

Allgeier, J.E., Valdivia, A., Cox, C. & Layman, C.A. (2016). Fishing down nutrients on coral reefs. *Nature Communications*, 7.

Allgeier, J.E., Wenger, S.J., Rosemond, A.D., Schindler, D.E. & Layman, C.A. (2015). Metabolic theory and taxonomic identity predict nutrient recycling in a diverse food web. *Proceedings of the National Academy of Sciences*, 112, E2640–E2647.

Allgeier, J.E., Wenger, S. & Layman, C.A. (2020). Taxonomic identity best explains variation in body nutrient stoichiometry in a diverse marine animal community.

Scientific Reports, 10, 1–10.

Allgeier, J.E., Yeager, L.A. & Layman, C.A. (2013). Consumers regulate nutrient limitation regimes and primary production in seagrass ecosystems. *Ecology*, 94, 521–529.

Allouche, O., Tsoar, A. & Kadmon, R. (2006). Assessing the accuracy of species distribution models: prevalence, kappa and the true skill statistic (TSS): Assessing the accuracy of distribution models. *Journal of Applied Ecology*, 43, 1223–1232.

Alvarez-Filip, L., Dulvy, N.K., Gill, J.A., Côté, I.M. & Watkinson, A.R. (2009). Flattening of Caribbean coral reefs: Region-wide declines in architectural complexity. *Proceedings of the Royal Society B: Biological Sciences*, 276, 3019–3025.

Aminot, A. & Kérouel, R. (2007). *Dosage automatique des nutriments dans les eaux marines : méthodes en flux continu.*

Anderson, T.R., Hessen, D.O., Elser, J.J. & Urabe, J. (2005). Metabolic stoichiometry and the fate of excess Carbon and Nutrients in Consumers. *The American Naturalist*, 165, 1–15.

Angermeier, P.L. & Karr, J.R. (1994). Biological integrity versus biological diversity as policy directives. Protecting biotic resources. *BioScience*, 44, 690–697.

Atkinson, C.L., Capps, K.A., Rugenski, A.T. & Vanni, M.J. (2017). Consumer-driven nutrient dynamics in freshwater ecosystems: from individuals to ecosystems. *Biological Reviews*, 92, 2003–2023.

Atkinson, C.L., Kelly, J.F. & Vaughn, C.C. (2014). Tracing Consumer-Derived Nitrogen in Riverine Food Webs. *Ecosystems*, 17, 485–496.

Atkinson, M.J., Carlson, B. & Crow, G.L. (1995). Coral growth in high-nutrient, low-pH seawater: a case study of corals cultured at the Waikiki Aquarium, Honolulu, Hawaii. *Coral Reefs*, 14, 215–223.

Aubin, I., Venier, L., Pearce, J. & Moretti, M. (2013). Can a trait-based multi-taxa

approach improve our assessment of forest management impact on biodiversity? *Biodiversity and Conservation*, 22, 2957–2975.

Bailey, T.G. & Robertson, D.R. (1982). Organic and caloric levels of fish feces relative to its consumption by coprophagous reef fishes. *Marine Biology*, 69, 45–50.

Barneche, D.R. & Allen, A.P. (2018). The energetics of fish growth and how it constrains food-web trophic structure. *Ecology Letters*, 21, 836–844.

Barneche, D.R., Kulbicki, M., Floeter, S.R., Friedlander, A.M., Maina, J. & Allen, A.P. (2014). Scaling metabolism from individuals to reef-fish communities at broad spatial scales. *Ecology Letters*, 17, 1067–1076.

Barneche, D.R., Rezende, E.L., Parravicini, V., Maire, E., Edgar, G.J., Stuart-Smith, R.D., *et al.* (2019). Body size, reef area and temperature predict global reef-fish species richness across spatial scales. *Global Ecology and Biogeography*, 28, 315–327.

Barrat, A., Barthelemy, M., Pastor-Satorras, R. & Vespignani, A. (2004). The architecture of complex weighted networks. *Proceedings of the National Academy of Sciences*, 101, 3747–3752.

Barton, A.D., Pershing, A.J., Litchman, E., Record, N.R., Edwards, K.F., Finkel, Z.V., *et al.* (2013). The biogeography of marine plankton traits.

Bascompte, J., Melian, C.J. & Sala, E. (2005). Interaction strength combinations and the overfishing of a marine food web. *Proceedings of the National Academy of Sciences*, 102, 5443–5447.

Bassett, D.K. & Montgomery, J.C. (2011). Investigating nocturnal fish populations in situ using baited underwater video: With special reference to their olfactory capabilities. *Journal of Experimental Marine Biology and Ecology*, 409, 194–199.

Beckett, S.J. (2016). Improved community detection in weighted bipartite networks. *Royal Society Open Science*, 3, 140536.

Bejarano, S., Pardede, S., Campbell, S.J., Hoey, A.S. & Ferse, S.C.A. (2019). Herbivorous fish rise as a destructive fishing practice falls in an Indonesian marine national park. *Ecological Applications*, 29.

Bellwood, D.R. & Choat, J.H. (2011). Dangerous demographics: The lack of juvenile humphead parrotfishes Bolbometopon muricatum on the Great Barrier Reef. *Coral Reefs*, 30, 549–554.

Bellwood, D.R., Hoey, A.S. & Choat, J.H. (2003). Limited functional redundancy in high diversity systems: Resilience and ecosystem function on coral reefs. *Ecology Letters*, 6, 281–285.

Bellwood, D.R., Hoey, A.S. & Hughes, T.P. (2012). Human activity selectively impacts the ecosystem roles of parrotfishes on coral reefs. *Proceedings of the Royal Society B: Biological Sciences*, 279, 1621–1629.

Bellwood, D.R., Hughes, T.P., Folke, C. & Nyström, M. (2004). Confronting the coral reef crisis. *Nature*, 429, 827–833.

Bellwood, D.R., Hughes, T.P. & Hoey, A.S. (2006). Sleeping Functional Group Drives Coral-Reef Recovery. *Current Biology*, 16, 2434–2439.

Bellwood, D.R., Streit, R.P., Brandl, S.J. & Tebbett, S.B. (2019). The meaning of the term 'function' in ecology: A coral reef perspective.

Belmaker, J., Parravicini, V. & Kulbicki, M. (2013). Ecological traits and environmental affinity explain Red Sea fish introduction into the Mediterranean. *Global Change Biology*, 19, 1373–1382.

Benstead, J.P., Hood, J.M., Whelan, N.V., Kendrick, M.R., Nelson, D., Hanninen, A.F., *et al.* (2014). Coupling of dietary phosphorus and growth across diverse fish taxa: A meta-analysis of experimental aquaculture studies. *Ecology*, 95, 2768–2777.

Bertalanffy, L. von. (1957). Quantitative laws in metabolism and growth. *The Quarterly review of biology*, 32, 217–231.

Berumen, M.L. & Pratchett, M.S. (2008). Trade-offs associated with dietary specialization in corallivorous butterflyfishes (Chaetodontidae: Chaetodon). *Behavioral Ecology and Sociobiology*, 62, 989–994.

Berumen, M.L., Pratchett, M.S. & Goodman, B.A. (2011). Relative gut lengths of coral reef butterflyfishes (Pisces: Chaetodontidae). *Coral Reefs*, 30, 1005–1010.

Binning, S.a., Roche, D.G. & Layton, C. (2013). Ectoparasites increase swimming costs in a coral reef fish. *Biology letters*, 9, 20120927–20120927.

Boettiger, C., Lang, D.T. & Wainwright, P.C. (2012). rfishbase: exploring, manipulating and visualizing FishBase data from R. *Journal of Fish Biology*, 81, 2030–2039.

Bozec, Y.-M., Gascuel, D. & Kulbicki, M. (2004). Trophic model of lagoonal communities in a large open atoll (Uvea, Loyalty islands, New Caledonia). *Aquatic Living Resources*, 17, 151–162.

Brandl, S.J. (2019). Demographic dynamics of the smallest marine vertebrates fuel coral-reef ecosystem functioning. *Nature*, 402, 799–802.

Brandl, S.J. & Bellwood, D.R. (2014). Individual-based analyses reveal limited functional overlap in a coral reef fish community. *Journal of Animal Ecology*, 83, 661–670.

Brandl, S.J., Casey, J.M. & Meyer, C.P. (2020b). Dietary and habitat niche partitioning in congeneric cryptobenthic reef fish species. *Coral Reefs*.

Brandl, S.J., Casey, J.M. & Meyer, C.P. (2020a). Dietary and habitat niche partitioning in congeneric cryptobenthic reef fish species. *Coral Reefs*, 39, 305–317.

Brandl, S.J., Emslie, M.J., Ceccarelli, D.M. & T. Richards, Z. (2016). Habitat degradation increases functional originality in highly diverse coral reef fish assemblages. *Ecosphere*, 7, e01557.

Brandl, S.J., Goatley, C.H.R., Bellwood, D.R. & Tornabene, L. (2018). The hid-

den half: ecology and evolution of cryptobenthic fishes on coral reefs. *Biological Reviews*, 93, 1846–1873.

Brandl, S.J., Rasher, D.B., Côté, I.M., Casey, J.M., Darling, E.S., Lefcheck, J.S., *et al.* (2019a). Coral reef ecosystem functioning: eight core processes and the role of biodiversity. *Frontiers in Ecology and the Environment*, 17, 445–454.

Brandl, S.J., Robbins, W.D. & Bellwood, D.R. (2015). Exploring the nature of ecological specialization in a coral reef fish community: Morphology, diet and foraging microhabitat use. *Proceedings of the Royal Society B: Biological Sciences*, 282.

Brandl, S.J., Tornabene, L., Goatley, C.H.R., Casey, J.M., Morais, R.A., Côté, I.M., *et al.* (2019b). Demographic dynamics of the smallest marine vertebrates fuel coral reef ecosystem functioning. *Science*, 364, 1189–1192.

Breiman, L. (2001). Random forests. *Machine Learning*, 45, 5–32.

Brett, J.R. (1964). The Respiratory Metabolism and Swimming Performance of Young Sockeye Salmon. *Journal of the Fisheries Research Board of Canada*, 21, 1183–1226.

Bridgewater, P., Kim, R.E. & Bosselmann, K. (2014). Ecological Integrity: A Relevant Concept for International Environmental Law in the Anthropocene? *Yearbook of International Environmental Law*, 25, 61–78.

Brill, R.W. & Bushnell, P.G. (1991). Metabolic and cardiac scope of high energy demand teleosts, the tunas. *Canadian Journal of Zoology*, 69, 2002–2009.

Brodie, S., Taylor, M.D., Smith, J.A., Suthers, I.M., Gray, C.A. & Payne, N.L. (2016). Improving consumption rate estimates by incorporating wild activity into a bioenergetics model. *Ecology and Evolution*, 6, 2262–2274.

Brown, J.H., Gillooly, J.F., Allen, A.P., Savage, V.M. & West, G.B. (2004). Toward a metabolic theory of ecology. *Ecology*, 85, 1771–1789.

Bruggeman, J., Heringa, J. & Brandt, B.W. (2009). PhyloPars: Estimation of missing parameter values using phylogeny. *Nucleic Acids Research*, 37, W179–W184.

Bruno, J.F., Côté, I.M. & Toth, L.T. (2019). Climate Change, Coral Loss, and the Curious Case of the Parrotfish Paradigm: Why Don't Marine Protected Areas Improve Reef Resilience? *Annual Review of Marine Science*, 11, 307–334.

Burkepile, D.E., Allgeier, J.E., Shantz, A.A., Pritchard, C.E., Lemoine, N.P., Bhatti, L.H., *et al.* (2013). Nutrient supply from fishes facilitates macroalgae and suppresses corals in a Caribbean coral reef ecosystem. *Scientific Reports*, 3, 1493.

Burkepile, D.E. & Hay, M.E. (2008). Herbivore species richness and feeding complementarity affect community structure and function on a coral reef. *Proceedings of the National Academy of Sciences of the United States of America*, 105, 16201–16206.

Burkner PC. (2017). brms : An R Package for Bayesian Multilevel Models using Stan. *Journal of Statistical Software*, 80, 1–28.

Calow, P. (1987). Towards a Definition of Functional Ecology. *Functional Ecology*, 1, 57.

Cano-Barbacil, C., Radinger, J. & García-Berthou, E. (2020). Reliability analysis of fish traits reveals discrepancies among databases. *Freshwater Biology*, 65, 863–877.

Capps, K.A. & Flecker, A.S. (2013). Invasive Fishes Generate Biogeochemical Hotspots in a Nutrient-Limited System. *PLoS ONE*, 8, e54093.

Cardinale, B.J., Duffy, J.E., Gonzalez, A., Hooper, D.U., Perrings, C., Venail, P., *et al.* (2012). Biodiversity loss and its impact on humanity.

Carpenter, B., Gelman, A., Hoffman, M.D., Lee, D., Goodrich, B., Betancourt, M., *et al.* (2017). Stan : A Probabilistic Programming Language. *Journal of Statistical Software*, 76, 1–31.

Casey, J.M., Meyer, C.P., Morat, F., Brandl, S.J., Planes, S. & Parravicini, V. (2019).

Reconstructing hyperdiverse food webs: Gut content metabarcoding as a tool to disentangle trophic interactions on coral reefs. *Methods in Ecology and Evolution*, 10, 1157–1170.

Cashion, T., Al-Abdulrazzak, D., Belhabib, D., Derrick, B., Divovich, E., Moutopoulos, D.K., *et al.* (2018). Reconstructing global marine fishing gear use: Catches and landed values by gear type and sector. *Fisheries Research*, 206, 57–64.

Ceballos, G., Ehrlich, P.R., Barnosky, A.D., García, A., Pringle, R.M. & Palmer, T.M. (2015). Accelerated modern human-induced species losses: Entering the sixth mass extinction. *Science Advances*, 1, 1–5.

Chabot, D., Steffensen, J.F. & Farrell, A.P. (2016). The determination of standard metabolic rate in fishes. *Journal of Fish Biology*, 88, 81–121.

Chang, J., Rabosky, D.L., Smith, S.A. & Alfaro, M.E. (2019). An R package and online resource for macroevolutionary studies using the ray-finned fish tree of life. *Methods in Ecology and Evolution*.

Chen, T. & Guestrin, C. (2016). XGBoost: A Scalable Tree Boosting System. *Proceedings of the 22nd ACM SIGKDD International Conference on Knowledge Discovery and Data Mining*, 785–794.

Cheung, W.W.L., Pitcher, T.J. & Pauly, D. (2005). A fuzzy logic expert system to estimate intrinsic extinction vulnerabilities of marine fishes to fishing. *Biological Conservation*, 124, 97–111.

Cheung, W.W.L., Sarmiento, J.L., Dunne, J., Frölicher, T.L., Lam, V.W.Y., Palomares, M.L.D., *et al.* (2013). Shrinking of fishes exacerbates impacts of global ocean changes on marine ecosystems. *Nature Climate Change*, 3, 254–258.

Choat, J.H., Clements, K.D. & Robbins, W.D. (2002). The trophic status of herbivorous fishes on coral reefs 1: Dietary analyses. *Marine Biology*, 140, 613–623.

Chung, M.-T., Trueman, C.N., Godiksen, J.A., Holmstrup, M.E. & Grønkjær, P. (2019). Field metabolic rates of teleost fishes are recorded in otolith carbonate.

Communications Biology, 2, 24.

Cinner, J.E., Zamborain-Mason, J., Gurney, G.G., Graham, N.A.J., MacNeil, M.A., Hoey, A.S., *et al.* (2020). Meeting fisheries, ecosystem function, and biodiversity goals in a human-dominated world. *Science*, 368, 307–311.

Clark, T.D., Donaldson, M.R., Pieperhoff, S., Drenner, S.M., Lotto, A., Cooke, S.J., *et al.* (2012). Physiological benefits of being small in a changing world: Responses of coho salmon (Oncorhynchus kisutch) to an acute thermal challenge and a simulated capture event. *PLoS ONE*, 7, 1–8.

Clark, T.D., Sandblom, E. & Jutfelt, F. (2013). Aerobic scope measurements of fishes in an era of climate change: Respirometry, relevance and recommendations.

Clements, K.D., German, D.P., Piché, J., Tribollet, A. & Choat, J.H. (2016). Integrating ecological roles and trophic diversification on coral reefs: multiple lines of evidence identify parrotfishes as microphages. *Biological Journal of the Linnean Society*.

Clissold, F.J., Tedder, B.J., Conigrave, A.D. & Simpson, S.J. (2010). The gastrointestinal tract as a nutrient-balancing organ. In: *Proceedings of the royal society b: Biological sciences*. pp. 1751–1759.

Coker, D.J., Wilson, S.K. & Pratchett, M.S. (2014). Importance of live coral habitat for reef fishes.

Cole, A.J., Pratchett, M.S. & Jones, G.P. (2008). Diversity and functional importance of coral-feeding fishes on tropical coral reefs.

Côté, I.M. & Darling, E.S. (2010). Rethinking ecosystem resilience in the face of climate change. *PLoS biology*, 8, e1000438.

Crossman, D.J., Choat, J.H. & Clements, K.D. (2005). Nutritional ecology of nominally herbivorous fishes on coral reefs. *Marine Ecology Progress Series*, 296, 129–142.

Crutzen, P. & Stoermer, E. (2000). The Anthropocene. *Global Change, IGBP Newsletter*, 17–18.

Cruz-Font, L., Shuter, B.J. & Blanchfield, P.J. (2016). Energetic costs of activity in wild lake trout: a calibration study using acceleration transmitters and positional telemetry. *Canadian Journal of Fisheries and Aquatic Sciences*, 73, 1237–1250.

Cruz-Rivera, E. & Hay, M.E. (2000). Can quantity replace quality? Food choice, compensatory feeding, and fitness of marine mesograzers. *Ecology*, 81, 201–219.

Czamanski, M., Nugraha, A., Pondaven, P., Lasbleiz, M., Masson, A., Caroff, N., *et al.* (2011). Carbon, nitrogen and phosphorus elemental stoichiometry in aquacultured and wild-caught fish and consequences for pelagic nutrient dynamics. *Marine Biology*, 158, 2847–2862.

D'agata, S., Mouillot, D., Kulbicki, M., Andréfouët, S., Bellwood, D.R., Cinner, J.E., *et al.* (2014). Human-Mediated Loss of Phylogenetic and Functional Diversity in Coral Reef Fishes.

D'Angelo, C. & Wiedenmann, J. (2014). Impacts of nutrient enrichment on coral reefs: New perspectives and implications for coastal management and reef survival.

Dalla Riva, G.V. & Stouffer, D.B. (2016). Exploring the evolutionary signature of food webs' backbones using functional traits. *Oikos*, 125, 446–456.

Dalton, C.M., El-Sabaawi, R.W., Honeyfield, D.C., Auer, S.K., Reznick, D.N. & Flecker, A.S. (2017). The influence of dietary and whole-body nutrient content on the excretion of a vertebrate consumer. *PLoS ONE*, 12, e0187931.

Dalton, C.M., Tracy, K.E., Hairston, N.G. & Flecker, A.S. (2018). Fasting or fear: disentangling the roles of predation risk and food deprivation in the nitrogen metabolism of consumers. *Ecology*, 99, 681–689.

Darling, E.S. & D'agata, S. (2017). Coral Reefs: Fishing for Sustainability.

Darwin, C. (1839). *Journal and Remarks (The Voyage of the Beagle).*

De Deyn, G.B., Cornelissen, J.H.C. & Bardgett, R.D. (2008). Plant functional traits and soil carbon sequestration in contrasting biomes. *Ecology Letters*, 11, 516–531.

De Goeij, J.M., Van Oevelen, D., Vermeij, M.J.A., Osinga, R., Middelburg, J.J., De Goeij, A.F.P.M., *et al.* (2013). Surviving in a marine desert: The sponge loop retains resources within coral reefs. *Science*, 342, 108–110.

Des Roches, S., Post, D.M., Turley, N.E., Bailey, J.K., Hendry, A.P., Kinnison, M.T., *et al.* (2018). The ecological importance of intraspecific variation. *Nature Ecology and Evolution*, 2, 57–64.

Deslauriers, D., Chipps, S.R., Breck, J.E., Rice, J.A. & Madenjian, C.P. (2017). Fish Bioenergetics 4.0: An R-Based Modeling Application. *Fisheries*, 42, 586–596.

Deutsch, C., Ferrel, A., Seibel, B., Pörtner, H.O. & Huey, R.B. (2015). Climate change tightens a metabolic constraint on marine habitats. *Science*, 348, 1132–1135.

Díaz, S. & Cabido, M. (2001). Vive la différence: Plant functional diversity matters to ecosystem processes.

Doughty, C.E., Roman, J., Faurby, S., Wolf, A., Haque, A., Bakker, E.S., *et al.* (2016). Global nutrient transport in a world of giants. *Proceedings of the National Academy of Sciences*, 113, 868–873.

Duffy, E.J., Godwin, C.M. & Cardinale, B.J. (2017). Biodiversity effects in the wild are common and as strong as key drivers of productivity. *Nature*, 549, 261–264.

Duffy, J.E. (2002). Biodiversity and ecosystem function: the consumer connection. *Oikos*, 99, 201–219.

Eagle, J.V. & Jones, G.P. (2004). Mimicry in coral reef fishes: Ecological and behavioural responses of a mimic to its model. *Journal of Zoology*, 264, 33–43.

Eaton, A.D., Clesceri, L.S., Greenberg, A.E. & Franson, M.A.H. (1995). *Standard Methods for the Examination of Water and Wastewater.* American Public Health

Association.

Edwards, C.B., Friedlander, A.M., Green, A.G., Hardt, M.J., Sala, E., Sweatman, H.P., *et al.* (2013). Global assessment of the status of coral reef herbivorous fishes: evidence for fishing effects. *Proceedings of the Royal Society of London B: Biological Sciences*, 281.

Elith, J., Leathwick, J.R. & Hastie, T. (2008). A working guide to boosted regression trees. *Journal of Animal Ecology*, 77, 802–813.

Elliott, J.M. & Persson, L. (1978). The Estimation of Daily Rates of Food Consumption for Fish. *The Journal of Animal Ecology*, 47, 977–991.

El-Sabaawi, R.W., Warbanski, M.L., Rudman, S.M., Hovel, R. & Matthews, B. (2016). Investment in boney defensive traits alters organismal stoichiometry and excretion in fish. *Oecologia*, 181, 1209–1220.

Eurich, J., McCormick, M. & Jones, G. (2018). Habitat selection and aggression as determinants of fine-scale partitioning of coral reef zones in a guild of territorial damselfishes. *Marine Ecology Progress Series*, 587, 201–215.

Evans-White, M.A. & Halvorson, H.M. (2017). Comparing the ecological stoichiometry in green and brown food webs - A review and meta-analysis of freshwater food webs.

Ezzat, L., Lamy, T., Maher, R.L., Munsterman, K.S., Landfield, K., Schmeltzer, E.R., *et al.* (2019). Surgeonfish feces increase microbial opportunism in reef-building corals. *Marine Ecology Progress Series*, 631, 81–97.

Ferreira, C.E.L., Floeter, S.R., Gasparini, J.L., Ferreira, B.P. & Joyeux, J.C. (2004). Trophic structure patterns of Brazilian reef fishes: a latitudinal comparison. *Journal of Biogeography*, 31, 1093–1106.

Ferrier-Pages, C., Gattuso, J.P., Dallot, S. & Jaubert, J. (2000). Effect of nutrient enrichment on growth and photosynthesis of the zooxanthellate coral Stylophora pistillata. *Coral Reefs*, 19, 103–113.

Finke, D.L. & Snyder, W.E. (2008). Niche partitioning increases resource exploitation by diverse communities. *Science*, 321, 1488–1490.

Floeter, S.R., Bender, M.G., Siqueira, A.C. & Cowman, P.F. (2018). Phylogenetic perspectives on reef fish functional traits: Evolution of functional traits. *Biological Reviews*, 93, 131–151.

Flynn, D.F.B., Mirotchnick, N., Jain, M., Palmer, M.I. & Naeem, S. (2011). Functional and phylogenetic diversity as predictors of biodiversity-ecosystem-function relationships. *Ecology*, 92, 1573–1581.

Folke, C., Carpenter, S., Walker, B., Scheffer, M., Elmqvist, T., Gunderson, L., *et al.* (2004). Regime Shifts, Resilience, and Biodiversity in Ecosystem Management. *Annu. Rev. Ecol. Evol. Syst*, 35, 557–81.

Fox, R.J. & Bellwood, D.R. (2007). Quantifying herbivory across a coral reef depth gradient. *Marine Ecology Progress Series*, 339, 49–59.

Francis, F.T. & Côté, I.M. (2018). Fish movement drives spatial and temporal patterns of nutrient provisioning on coral reef patches. *Ecosphere*, 9, e02225.

Frankenberg, D. & Smith, K.L. (1967). Coprophagy In Marine Animals. *Limnology and Oceanography*, 12, 443–450.

Friederichs, K. (1958). A Definition of Ecology and Some Thoughts About Basic Concepts. *Ecology*, 39, 154.

Friedlander, A.M., Brown, E.K., Jokiel, P.L., Smith, W.R. & Rodgers, K.S. (2003). Effects of habitat, wave exposure, and marine protected area status on coral reef fish assemblages in the Hawaiian archipelago. *Coral Reefs*, 22, 291–305.

Froese, R. & Pauly, D. (2018). FishBase. *World Wide Web electronic publication.*

Froese, R., Thorson, J.T. & Reyes, R.B. (2014). A Bayesian approach for estimating length-weight relationships in fishes. *Journal of Applied Ichthyology*, 30, 78–85.

Frost, P.C., Benstead, J.P., Cross, W.F., Hillebrand, H., Larson, J.H., Xenopoulos,

M.A., *et al.* (2006). Threshold elemental ratios of carbon and phosphorus in aquatic consumers. *Ecology Letters*, 9, 774–779.

Fry, F. (1947). Effects of the environment on animal activity. *Univ. Toronto Stud. Biol. Ser.*, 55, 1–62.

FRY, F.E.J. (1957). The Aquatic Respiration of Fish. In: *The physiology of fishes*. Elsevier, pp. 1–63.

Fulton, C.J. (2007). Swimming speed performance in coral reef fishes: Field validations reveal distinct functional groups. *Coral Reefs*, 26, 217–228.

Gajdzik, L., Aguilar-Medrano, R. & Frédérich, B. (2019). Diversification and functional evolution of reef fish feeding guilds. *Ecology Letters*, 22, 572–582.

Gallagher, R., Falster, D.S., Maitner, B., Salguero-Gomez, R., Vandvik, V., Pearse, W., *et al.* (2020). The Open Traits Network: Using Open Science principles to accelerate trait-based science across the Tree of Life. *Nature Ecology & Evolution*, 4, 294–303.

Gardner, T.A., Côté, I.M., Gill, J.A., Grant, A. & Watkinson, A.R. (2003). Long-term region-wide declines in caribbean corals. *Science*, 301, 958–960.

Garland, T. & Ives, A.R. (2000). Using the Past to Predict the Present: Confidence Intervals for Regression Equations in Phylogenetic Comparative Methods. *The American Naturalist*, 155, 19.

Gaston, K.J. & Fuller, R.A. (2008). Commonness, population depletion and conservation biology. *Trends in Ecology and Evolution*, 23, 14–19.

Geesey, G.G., Alexander, G.V., Bray, R.N. & Miller, A.C. (1984). Fish fecal pellets are a source of minerals for inshore reef communities. *Marine Ecology Progress Series*, 15, 19–25.

Gilarranz, L.J., Mora, C. & Bascompte, J. (2016). Anthropogenic effects are associated with a lower persistence of marine food webs. *Nature Communications*,

7.

Gillooly, J.F., Brown, J.H., West, G.B., Savage, V.M. & Charnov, E.L. (2001). Effects of size and temperature on metabolic rate. *Science*.

Glazier, D.S. (2005). Beyond the '3/4-power law': Variation in the intra- and interspecific scaling of metabolic rate in animals. *Biological Reviews of the Cambridge Philosophical Society*, 80, 611–662.

Glynn, P.W. & Enochs, I.C. (2011). Invertebrates and Their Roles in Coral Reef Ecosystems. In: *Coral reefs: An ecosystem in transition* (eds. Dubinsky, Z. & Stambler, N.). Springer Netherlands, Dordrecht, pp. 273–325.

Goberna, M. & Verdú, M. (2016). Predicting microbial traits with phylogenies. *The ISME Journal*, 10, 959–967.

González-Salazar, C., Martínez-Meyer, E. & López-Santiago, G. (2014). A hierarchical classification of trophic guilds for North American birds and mammals. *Revista Mexicana de Biodiversidad*, 85, 931–941.

Gove, J.M., McManus, M.A., Neuheimer, A.B., Polovina, J.J., Drazen, J.C., Smith, C.R., *et al.* (2016). Near-island biological hotspots in barren ocean basins. *Nature Communications*, 7, 1–8.

Graham, N.A.J., Chabanet, P., Evans, R.D., Jennings, S., Letourneur, Y., Aaron Macneil, M., *et al.* (2011). Extinction vulnerability of coral reef fishes. *Ecology Letters*, 14, 341–348.

Graham, N.A.J., Cinner, J.E., Norström, A.V. & Nyström, M. (2014). Coral reefs as novel ecosystems: EMBRACING new futures.

Graham, N.A.J., Jennings, S., MacNeil, M.A., Mouillot, D. & Wilson, S.K. (2015). Predicting climate-driven regime shifts versus rebound potential in coral reefs. *Nature*, 518, 94–97.

Graham, N.A.J. & McClanahan, T.R. (2013). The last call for carine wilderness?

BioScience, 63, 397–402.

Graham, N.A.J., McClanahan, T.R., MacNeil, M.A., Wilson, S.K., Cinner, J.E., Huchery, C., *et al.* (2017). Human Disruption of Coral Reef Trophic Structure. *Current Biology*, 27, 231–236.

Graham, N.A.J., Robinson, J.P.W., Smith, S.E., Govinden, R., Gendron, G. & Wilson, S.K. (2020). Changing role of coral reef marine reserves in a warming climate. *Nature Communications*, 11, 1–8.

Graham, N.A.J., Wilson, S.K., Jennings, S., Polunin, N.V.C., Bijoux, J.P. & Robinson, J. (2006). Dynamic fragility of oceanic coral reef ecosystems. *Proceedings of the National Academy of Sciences of the United States of America*, 103, 8425–8429.

Gravel, D., Poisot, T., Albouy, C., Velez, L. & Mouillot, D. (2013). Inferring food web structure from predator-prey body size relationships. *Methods in Ecology and Evolution*, 4, 1083–1090.

Gräns, A., Axelsson, M., Pitsillides, K., Olsson, C., Höjesjö, J., Kaufman, R.C., *et al.* (2009). A fully implantable multi-channel biotelemetry system for measurement of blood flow and temperature: A first evaluation in the green sturgeon. *Hydrobiologia*, 619, 11–25.

Guariento, R.D., Luttbeg, B., Carneiro, L.S. & Caliman, A. (2018). Prey adaptive behaviour under predation risk modify stoichiometry predictions of predator-induced stress paradigms. *Functional Ecology*, 32, 1631–1643.

Guénard, G., Boisclair, D., Ugedal, O., Forseth, T. & Jonsson, B. (2008). Comparison between activity estimates obtained using bioenergetic and behavioural analyses. *Canadian Journal of Fisheries and Aquatic Sciences*, 65, 1705–1720.

Guénard, G., Legendre, P. & Peres-Neto, P. (2013). Phylogenetic eigenvector maps: a framework to model and predict species traits. *Methods in Ecology and Evolution*, 4, 1120–1131.

Hadj-Hammou, J., Mouillot, D. & Graham, N.A.J. (2021). Response and Effect

Traits of Coral Reef Fish. *Frontiers in Marine Science*, 8, 640619.

Halpern, B.S., Walbridge, S., Selkoe, K.A., Kappel, C.V., Micheli, F., D'Agrosa, C., *et al.* (2008). A global map of human impact on marine ecosystems. *Science (New York, N.Y.)*, 319, 948–52.

Halsey, L.G., Killen, S.S., Clark, T.D. & Norin, T. (2018). Exploring key issues of aerobic scope interpretation in ectotherms: absolute versus factorial. *Reviews in Fish Biology and Fisheries*, 18, 405–415.

Halvorson, H.M. & Atkinson, C.L. (2019). Egestion Versus Excretion: A Meta-Analysis Examining Nutrient Release Rates and Ratios across Freshwater Fauna. *Diversity*, 11, 189.

Halvorson, H.M., Hall, D.J. & Evans-White, M.A. (2017a). Long-term stoichiometry and fates highlight animal egestion as nutrient repackaging, not recycling, in aquatic ecosystems. *Functional Ecology*, 31, 1802–1812.

Halvorson, H.M., Sperfeld, E. & Evans-White, M.A. (2017b). Quantity and quality limit detritivore growth: mechanisms revealed by ecological stoichiometry and co-limitation theory. *Ecology*, 98, 2995–3002.

Hamner, W.M., Jones, M.S., Carleton, J.H., Hauri, I.R. & Williams, D.McB. (1988). Zooplankton,planktivorous fish, and watwer currents on a windward reef face - Great Barrief Reef, Australia. *Bulletin of Marine Science*, 42, 459–479.

Hanson, P., Johnson, T.B., Schindler, D.E. & Kitchell, J.F. (1997). Fish Bioenergetics 3.0.

Harmelin-Vivien, M. (1979). Ichtyofaune des recifs coralliens de Tulear (Madagascar): ecologie et relations trophiques. PhD thesis. L'Université d'Aix-Marseille II.

Harris, D.L., Rovere, A., Casella, E., Power, H., Canavesio, R., Collin, A., *et al.* (2018). Coral reef structural complexity provides important coastal protection from waves under rising sea levels. *Science Advances*, 4, eaao4350.

Hernández-León, S., Fraga, C. & Ikeda, T. (2008). A global estimation of mesozooplankton ammonium excretion in the open ocean. *Journal of Plankton Research*, 30, 577–585.

Hessen, D.O., Ågren, G.I., Anderson, T.R., Elser, J.J. & De Ruiter, P.C. (2004). Carbon sequestration in ecosystems: The role of stoichiometry. *Ecology*, 85, 1179–1192.

Hiatt, R.W. & Strasburg, D.W. (1960). Ecological relationships of the fish fauna on coral reefs of the Marshall Islands. *Ecological Monographs*, 30, 65–127.

Hobson, E.S. (1974). Feeding relationships of teleostean fishes on coral reefs in Kona, Hawaii. *Fishery Bulletin*, 72, 915–1031.

Holdren, J.P. & Ehrlich, P.R. (1974). Human population and the global environment. *American Scientist*, 62, 282–292.

Holt, R.E. & Jørgensen, C. (2015). Climate change in fish: effects of respiratory constraints on optimal life history and behaviour. *Biology Letters*, 11, 20141032.

Hood, J.M., Vanni, M.J. & Flecker, A.S. (2005). Nutrient recycling by two phosphorus-rich grazing catfish: The potential for phosphorus-limitation of fish growth. *Oecologia*, 146, 247–257.

Hopkins, J.B. & Ferguson, J.M. (2012). Estimating the Diets of Animals Using Stable Isotopes and a Comprehensive Bayesian Mixing Model. *PLoS ONE*, 7, e28478.

Horn, M. (1989). Biology of marine herbivorous fishes. In: *Oceanogr mar biol annu rev.* pp. 167–272.

Hou, C., Zuo, W., Moses, M.E., Woodruff, W.H., Brown, J.H. & West, G.B. (2008). Energy Uptake and Allocation During Ontogeny. *Science*, 322, 736–739.

Hughes, N.F. & Kelly, L.H. (1996). New techniques for 3-D video tracking of fish swimming movements in still or flowing water.

Hughes, T.P., Baird, A.H., Bellwood, D.R., Card, M., Connolly, S.R., Folke, C., *et al.*

(2003). Climate change, human impacts, and the resilience of coral reefs. *Science (New York, N.Y.)*, 301, 929–33.

Hughes, T.P., Bellwood, D.R., Connolly, S.R., Cornell, H.V. & Karlson, R.H. (2014). Report Double Jeopardy and Global Extinction Risk in Corals and Reef Fishes. *Current Biology*, 24.

Hughes, T.P., Bellwood, D.R., Folke, C.S., McCook, L.J. & Pandolfi, J.M. (2007). No-take areas, herbivory and coral reef resilience.

Hughes, T.P., Kerry, J.T., Álvarez-Noriega, M., Álvarez-Romero, J.G., Anderson, K.D., Baird, A.H., *et al.* (2017). Global warming and recurrent mass bleaching of corals. *Nature*, 543, 373–377.

Jax, K. (2005). Function and "functioning" in ecology: What does it mean?

Jeliazkov, A., Mijatovic, D., Chantepie, S., Andrew, N., Arlettaz, R., Barbaro, L., *et al.* (2020). A global database for metacommunity ecology, integrating species, traits, environment and space. *Scientific Data*, 7.

Jochum, M., Barnes, A.D., Weigelt, P., Ott, D., Rembold, K., Farajallah, A., *et al.* (2017). Resource stoichiometry and availability modulate species richness and biomass of tropical litter macro-invertebrates. *Journal of Animal Ecology*, 86, 1114–1123.

Johnson, C.N., Balmford, A., Brook, B.W., Buettel, J.C., Galetti, M., Guangchun, L., *et al.* (2017). Biodiversity losses and conservation responses in the Anthropocene.

Jordano, P. (2016). Chasing Ecological Interactions. *PLOS Biology*, 14, e1002559.

Keddy, P.A. (1992). A Pragmatic Approach to Functional Ecology. *Functional Ecology*, 6, 621.

Kembel, S.W., Cowan, P.D., Helmus, M.R., Cornwell, W.K., Morlon, H., Ackerly, D.D., *et al.* (2010). Picante: R tools for integrating phylogenies and ecology. *Bioinformatics*, 26, 1463–1464.

Kembel, S.W., Wu, M., Eisen, J.A. & Green, J.L. (2012). Incorporating 16S Gene Copy Number Information Improves Estimates of Microbial Diversity and Abundance. *PLoS Computational Biology*, 8, e1002743.

Killen, S.S., Costa, I., Brown, J.A. & Gamperl, A.K. (2007). Little left in the tank: metabolic scaling in marine teleosts and its implications for aerobic scope. *Proceedings of the Royal Society B: Biological Sciences*, 274, 431–438.

Killen, S.S., Glazier, D.S., Rezende, E.L., Clark, T.D., Atkinson, D., Willener, A.S.T., *et al.* (2016). Ecological Influences and Morphological Correlates of Resting and Maximal Metabolic Rates across Teleost Fish Species. *The American Naturalist*, 187, 592–606.

Killen, S.S., Norin, T. & Halsey, L.G. (2017). Do method and species lifestyle affect measures of maximum metabolic rate in fishes? *Journal of Fish Biology*, 90, 1037–1046.

Kitchell, J.F., Koonce, J.F., Magnuson, J.J., O'Neill, R.V., Shugart, H.H. & Booth, R.S. (1974). Model of fish biomass dynamics. *Transactions of the American Fisheries Society*, 103, 786–798.

Knouft, J.H., Losos, J.B., Glor, R.E. & Kolbe, J.J. (2006). Phylogenetic analysis of the evolution of the niche in lizards of the Anolis sagrei group. *Ecology*, 87, 29–38.

Knowlton, N., Brainard, R.E., Fisher, R., Moews, M., Plaisance, L. & Caley, M.J. (2010). Coral Reef Biodiversity. In: *Life in the world's oceans: Diversity, distribution, and abundance*. pp. 65–78.

Kooijman, S.A.L.M. (2010). Dynamic energy budget theory - summary of concepts of the third edition. *Dynamic Energy Budget Theory for metabolilc organization*, 64.

Korsmeyer, K.E., Steffensen, J.F. & Herskin, J. (2002). Energetics of median and paired fin swimming, body and caudal fin swimming, and gait transition in parrotfish (Scarus schlegeli) and triggerfish (Rhinecanthus aculeatus). *The Journal of*

experimental biology, 205, 1253–63.

Kozlovsky, D.G. (1968). A Critical Evaluation of the Trophic Level Concept. I. Ecological Efficiencies. *Ecology*, 49, 48–60.

Kraft, C. (1992). Estimates of phosphorus and nitrogen cycling by fish using a bioenergetics approach. *Canadian Journal of Fisheries and Aquatic Sciences*, 49, 2596–2604.

Kraft, N.J.B., Valencia, R. & Ackerly, D.D. (2008). Functional traits and niche-based tree community assembly in an Amazonian forest. *Science*, 322, 580–582.

Laigle, I., Aubin, I., Digel, C., Brose, U., Boulangeat, I. & Gravel, D. (2018). Species traits as drivers of food web structure. *Oikos*, 127, 316–326.

Lang, B., Ehnes, R.B., Brose, U. & Rall, B.C. (2017). Temperature and consumer type dependencies of energy flows in natural communities. *Oikos*, 126, 1717–1725.

Lavorel, S. & Garnier, E. (2002). Predicting changes in community composition and ecosystem functioning from plant traits: revisiting the Holy Grail. *Functional Ecology*, 16, 545–556.

Le Mézo, P.K. & Galbraith, E.D. (2021). The fecal iron pump: Global impact of animals on the iron stoichiometry of marine sinking particles. *Limnology and Oceanography*, 66, 201–213.

LeDell, E., Gill, N., Aiello, S., Fu, A., Candel, A., Click, C., *et al.* (2020). *h2o: R Interface for the 'H2O' Scalable Machine Learning Platform*.

Lefcheck, J.S., Innes-Gold, A.A., Brandl, S.J., Steneck, R.S., Torres, R.E. & Rasher, D.B. (2019). Tropical fish diversity enhances coral reef functioning across multiple scales. *Science Advances*, 5, eaav6420.

Leray, M., Alldredge, A.L., Yang, J.Y., Meyer, C.P., Holbrook, S.J., Schmitt, R.J., *et al.* (2019). Dietary partitioning promotes the coexistence of planktivorous species on coral reefs. *Molecular Ecology*, 28, 2694–2710.

Leray, M. & Knowlton, N. (2015). DNA barcoding and metabarcoding of standardized samples reveal patterns of marine benthic diversity. *Proceedings of the National Academy of Sciences of the United States of America*, 112, 2076–2081.

Levine, J.M. & HilleRisLambers, J. (2009). The importance of niches for the maintenance of species diversity. *Nature*, 461, 254–257.

Liess, A. (2014). Compensatory feeding and low nutrient assimilation efficiencies lead to high nutrient turnover in nitrogen-limited snails. *Freshwater Science*, 33, 425–434.

Lin, D.T. & Fong, P. (2008). Macroalgal bioindicators (growth, tissue N, δ15N) detect nutrient enrichment from shrimp farm effluent entering Opunohu Bay, Moorea, French Polynesia. *Marine Pollution Bulletin*, 56, 245–249.

Loreau, M., Naeem, S., Inchausti, P., Bengtsson, J., Grime, J.P., Hector, A., *et al.* (2001). Ecology: Biodiversity and ecosystem functioning: Current knowledge and future challenges.

Lotze, H.K., Tittensor, D.P., Bryndum-Buchholz, A., Eddy, T.D., Cheung, W.W.L., Galbraith, E.D., *et al.* (2019). Global ensemble projections reveal trophic amplification of ocean biomass declines with climate change. *Proceedings of the National Academy of Sciences*, 116, 12907–12912.

Lourenco, S.O., Barbarino, E., De-Paula, J.C., da S. Pereira, L.O. & Marquez, U.M.L. (2002). Amino acid composition, protein content and calculation of nitrogen-to-protein conversion factors for 19 tropical seaweeds. *Phycological Research*, 50, 233–241.

Lovette, I.J. & Hochachka, W.M. (2006). *SIMULTANEOUS EFFECTS OF PHYLOGENETIC NICHE CONSERVATISM AND COMPETITION ON AVIAN COMMUNITY STRUCTURE* (No. 7). John Wiley & Sons, Ltd.

Lubchenco, J. & Gaines, S.D. (1981). A Unified Approach to Marine Plant-Herbivore Interactions. I. Populations and Communities. *Annual Review of Ecology and*

Systematics, 12, 405–437.

Lucas, M.C., Johnstone, A.D.F. & Priede, I.G. (2011). Use of Physiological Telemetry as a Method of Estimating Metabolism of Fish in the Natural Environment. *Changed publisher: Wiley.*

Mackenzie, F.T., Ver, L.M., Sabine, C., Lane, M. & Lerman, A. (1993). C, N, P, S Global Biogeochemical Cycles and Modeling of Global Change. In: *Interactions of c, n, p and s biogeochemical cycles and global change.* Springer Berlin Heidelberg, Berlin, Heidelberg, pp. 1–61.

MacNeil, M.A., Graham, N.A.J., Cinner, J.E., Wilson, S.K., Williams, I.D., Maina, J., *et al.* (2015). Recovery potential of the world's coral reef fishes. *Nature*, 520, 341–344.

Madin, J.S., Anderson, K.D., Andreasen, M.H., Bridge, T.C.L., Cairns, S.D., Connolly, S.R., *et al.* (2016). The Coral Trait Database, a curated database of trait information for coral species from the global oceans. *Scientific Data*, 3, 160017.

Manolagas, S.C. (2000). Birth and Death of Bone Cells: Basic Regulatory Mechanisms and Implications for the Pathogenesis and Treatment of Osteoporosis 1. *Endocrine Reviews*, 21, 115–137.

Marshall, D.J. & White, C.R. (2019). Have We Outgrown the Existing Models of Growth?

Marshall, N.B. (1972). Normal Sleep in Animals and Man [Abridged]: Sleep in Fishes [Abstract]. *Journal of the Royal Society of Medicine.*

Mason, N.W.H. & Bello, F. de. (2013). Functional diversity: a tool for answering challenging ecological questions. *Journal of Vegetation Science*, 24, 777–780.

Matley, J.K., Tobin, A.J., Lédée, E.J.I., Heupel, M.R. & Simpfendorfer, C.A. (2016). Contrasting patterns of vertical and horizontal space use of two exploited and sympatric coral reef fish. *Marine Biology*, 163, 1–12.

Mayor, D.J., Cook, K., Thornton, B., Walsham, P., Witte, U.F.M., Zuur, A.F., *et al.* (2011). Absorption efficiencies and basal turnover of C, N and fatty acids in a marine Calanoid copepod. *Functional Ecology*, 144, 381–394.

Mazel, F., Pennell, M.W., Cadotte, M.W., Diaz, S., Dalla Riva, G.V., Grenyer, R., *et al.* (2018). Prioritizing phylogenetic diversity captures functional diversity unreliably. *Nature Communications*, 9.

McCauley, D.J., Desalles, P.A., Young, H.S., Dunbar, R.B., Dirzo, R., Mills, M.M., *et al.* (2012). From wing to wing: The persistence of long ecological interaction chains in less-disturbed ecosystems. *Scientific Reports*, 2, 1–5.

McClanahan, T.R. (1995). A coral reef ecosystem-fisheries model: impacts of fishing intensity and catch selection on reef structure and processes. *Ecological Modelling*, 80, 1–19.

McCue, M.D. (2006). Specific dynamic action: A century of investigation. *Comparative Biochemistry and Physiology - A Molecular and Integrative Physiology*, 144, 381–394.

McGill, B.J., Enquist, B.J., Weiher, E. & Westoby, M. (2006). Rebuilding community ecology from functional traits. *Trends in Ecology and Evolution*, 21, 178–185.

McIntyre, P.B., Flecker, A.S., Vanni, M.J., Hood, J.M., Taylor, B.W. & Thomas, S.A. (2008). Fish distributions and nutrient cycling in streams: can fish create biogeochemical hotspots. *Ecology*, 89, 2335–2346.

McManamay, R.A., Webster, J.R., Valett, H.M. & Dolloff, C.A. (2011). Does diet influence consumer nutrient cycling? Macroinvertebrate and fish excretion in streams. *Journal of the North American Benthological Society*, 30, 84–102.

Mcmanus, J.W., Reyes, R.B. & Nañola, C.L. (1997). Effects of some destructive fishing methods on coral cover and potential rates of recovery.

McWilliam, M., Pratchett, M.S., Hoogenboom, M.O. & Hughes, T.P. (2020). Deficits in functional trait diversity following recovery on coral reefs. *Proceedings of the*

Royal Society B: Biological Sciences, 287.

Meese, E.N. & Lowe, C.G. (2020). Active acoustic telemetry tracking and tri-axial accelerometers reveal fine-scale movement strategies of a non-obligate ram ventilator. *Movement Ecology*, 8.

Meilă, M. (2007). Comparing clusterings-an information based distance. *Journal of Multivariate Analysis*, 98, 873–895.

Metcalfe, J.D., Wright, S., Tudorache, C. & Wilson, R.P. (2016). Recent advances in telemetry for estimating the energy metabolism of wild fishes. *Journal of Fish Biology*, 88, 284–297.

Meyer, J.L., Schultz, E.T. & Helfman, G.S. (1983). Fish Schools: An Asset to Corals. *Science*, 220, 1047–1049.

Micheli, F., Mumby, P.J., Brumbaugh, D.R., Broad, K., Dahlgren, C.P., Harborne, A.R., *et al.* (2014). High vulnerability of ecosystem function and services to diversity loss in Caribbean coral reefs. *Biological Conservation*, 171, 186–194.

Millennium Ecosystem Assessment. (2005). *Ecosystems and Human Well-being: Synthesis*. Island press, Washington, DC.

Mills, M.M. & Sebens, K.P. (2004). Ingestion and assimilation of nitrogen from benthic sediments by three species of coral. *Marine Biology*, 145, 1097–1106.

Miyake, S., Ngugi, D.K. & Stingl, U. (2015). Diet strongly influences the gut microbiota of surgeonfishes. *Molecular Ecology*, 24, 656–672.

Moberg, F. & Folke, C. (1999). Ecological goods and services of coral reef ecosystems. *Ecological Economics*, 29, 215–233.

Montgomery, W.L. (1980). Comparative feeding ecology of two herbivorous damselfishes (Pomacentridae: Teleostei) from the Gulf of California, Mexico. *Journal of Experimental Marine Biology and Ecology*, 47, 9–24.

Moody, E.K., Carson, E.W., Corman, J.R., Espinosa-Pérez, H., Ramos, J., Sabo, J.L.,

et al. (2018). Consumption explains intraspecific variation in nutrient recycling stoichiometry in a desert fish. *Ecology*, 99, 1552–1561.

Moody, E.K., Lujan, N.K., Roach, K.A. & Winemiller, K.O. (2019). Threshold elemental ratios and the temperature dependence of herbivory in fishes. *Functional Ecology*, 33, 913–923.

Mora, C. & Sale, P.F. (2011). Ongoing global biodiversity loss and the need to move beyond protected areas: A review of the technical and practical shortcomings of protected areas on land and sea. *Marine Ecology Progress Series*, 434, 251–266.

Morais, R.A. & Bellwood, D.R. (2018). Global drivers of reef fish growth. *Fish and Fisheries*, 19, 874–889.

Morais, R.A. & Bellwood, D.R. (2019a). Pelagic Subsidies Underpin Fish Productivity on a Degraded Coral Reef. *Current Biology*, 29, 1521–1527.e6.

Morais, R.A. & Bellwood, D.R. (2019b). Pelagic Subsidies Underpin Fish Productivity on a Degraded Coral Reef. *Current Biology*, 29, 1521——1527.e6.

Morais, R.A., Connolly, S.R. & Bellwood, D.R. (2020a). Human exploitation shapes productivity-biomass relationships on coral reefs. *Global Change Biology*, 26, 1295–1305.

Morais, R.A., Depczynski, M., Fulton, C., Marnane, M., Narvaez, P., Huertas, V., *et al.* (2020b). Severe coral loss shifts energetic dynamics on a coral reef. *Functional Ecology*.

Morales-Castilla, I., Matias, M.G., Gravel, D. & Araújo, M.B. (2015). Inferring biotic interactions from proxies. *Trends in Ecology & Evolution*, 30, 347–356.

Morat, F., Wicquart, J., Schiettekatte, N.M.D., Sinéty, G. de, Bienvenu, J., Casey, J.M., *et al.* (2020). Individual back-calculated size-at-age based on otoliths from Pacific coral reef fish species. *Scientific Data*, 7.

Motulsky, H.J. & Brown, R.E. (2006). Detecting outliers when fitting data with

nonlinear regression - A new method based on robust nonlinear regression and the false discovery rate. *BMC Bioinformatics*, 7, 1–20.

Mouillot, D., Graham, N.A.J., Villéger, S., Mason, N.W.H. & Bellwood, D.R. (2013). A functional approach reveals community responses to disturbances.

Mouillot, D., R. Krasnov, B., I. Shenbrot, G., J. Gaston, K. & Poulin, R. (2006). Conservatism of host specificity in parasites. *Ecography*, 29, 596–602.

Mouillot, D., Villeger, S., Parravicini, V., Kulbicki, M., Arias-Gonzalez, J.E., Bender, M., *et al.* (2014). Functional over-redundancy and high functional vulnerability in global fish faunas on tropical reefs. *Proceedings of the National Academy of Sciences*, 111, 13757–13762.

Mourier, J., Maynard, J., Parravicini, V., Ballesta, L., Clua, E., Domeier, M.L., *et al.* (2016). Extreme Inverted Trophic Pyramid of Reef Sharks Supported by Spawning Groupers. *Current Biology*, 26, 2011–2016.

Murchie, K.J., Cooke, S.J., Danylchuk, A.J. & Suski, C.D. (2011). Estimates of field activity and metabolic rates of bonefish (Albula vulpes) in coastal marine habitats using acoustic tri-axial accelerometer transmitters and intermittent-flow respirometry. *Journal of Experimental Marine Biology and Ecology*, 396, 147–155.

Nagy, K.A. (2005). Field metabolic rate and body size.

Nash, K.L., Watson, R.A., Halpern, B.S., Fulton, E.A. & Blanchard, J.L. (2017). Improving understanding of the functional diversity of fisheries by exploring the influence of global catch reconstruction. *Scientific Reports*, 7, 10746.

Nash, K.L., Welsh, J.Q., Graham, N.A.J. & Bellwood, D.R. (2015). Home-range allometry in coral reef fishes: comparison to other vertebrates, methodological issues and management implications. *Oecologia*, 177, 73–83.

Neuswanger, J.R., Wipfli, M.S., Rosenberger, A.E. & Hughes, N.F. (2016). Measuring fish and their physical habitats: versatile 2D and 3D video techniques with user-friendly software. *Canadian Journal of Fisheries and Aquatic Sciences*, 73, 1861–

1873.

Newman, M.J.H., Paredes, G.A., Sala, E. & Jackson, J.B.C. (2006). Structure of Caribbean coral reef communities across a large gradient of fish biomass. *Ecology Letters*, 9, 1216–1227.

Newman, S.P., Meesters, E.H., Dryden, C.S., Williams, S.M., Sanchez, C., Mumby, P.J., *et al.* (2015). Reef flattening effects on total richness and species responses in the Caribbean. *Journal of Animal Ecology*, 84, 1678–1689.

Newton, K., Côté, I.M., Pilling, G.M., Jennings, S. & Dulvy, N.K. (2007). Current and Future Sustainability of Island Coral Reef Fisheries. *Current Biology*, 17, 655–658.

Norin, T. & Clark, T.D. (2016). Measurement and relevance of maximum metabolic rate in fishes. *Journal of Fish Biology*, 88, 122–151.

Norin, T. & Speers-Roesch, B. (2020). Metabolism. In: *The physiology of fishes* (eds. Currie, S. & Evans, D.). CRC Press, Boca Raton, FL, USA., pp. 129–141.

Nugraha, A., Pondaven, P. & Tréguer, P. (2010). Influence of consumer-driven nutrient recycling on primary production and the distribution of N and P in the ocean. *Biogeosciences Discussions*, 7, 111–164.

Odum, H.T. & Odum, E.P. (1955). Trophic Structure and Productivity of a Windward Coral Reef Community on Eniwetok Atoll. *Ecological Monographs*, 25, 291–320.

Pandian, T.J. & Marian, M.P. (1985). *Nitrogen content of food as an index of absorption efficiency in fishes *.*

Parr, T.B., Capps, K.A., Inamdar, S.P. & Metcalf, K.A. (2019). Animal-mediated organic matter transformation: Aquatic insects as a source of microbially bioavailable organic nutrients and energy. *Functional Ecology*, 33, 524–535.

Parravicini, V., Casey, J.M., Schiettekatte, N.M.D. & Brandl, S.J. (2020). Global gut

content data synthesis and phylogeny delineate reef fish trophic guilds. *bioRxiv*, 0–3.

Parravicini, V., Villéger, S., Mcclanahan, T.R., Arias-González, J.E., Bellwood, D.R., Belmaker, J., *et al.* (2014). Global mismatch between species richness and vulnerability of reef fish assemblages. *Ecology Letters*, 17, 1101–1110.

Pauly, D. (1980). On the interrelationships between natural mortality, growth parameters, and mean environmental temperature in 175 fish stocks. *ICES Journal of Marine Science*, 39, 175–192.

Pauly, D., Christensen, V., Dalsgaard, J., Froese, R. & Torres, F. (1998). Fishing down marine food webs. *Science*, 279, 860–3.

Pauly, D., Christensen, V., Guénette, S., Pitcher, T.J., Sumaila, U.R., Walters, C.J., *et al.* (2002). Towards sustainability in world fisheries.

Peres-Neto, P.R. (2004). Patterns in the co-occurrence of fish species in streams: the role of site suitability, morphology and phylogeny versus species interactions. *Oecologia*, 140, 352–360.

Pichler, M., Boreux, V., Klein, A.-M., Schleuning, M. & Hartig, F. (2020). Machine learning algorithms to infer trait-matching and predict species interactions in ecological networks. *Methods in Ecology and Evolution*, 11, 281–293.

Pillans, R.D., Franklin, C.E. & Tibbetts, I.R. (2004). Food choice in Siganus fuscescens: Influence of macrophyte nutrient content and availability. *Journal of Fish Biology*, 64, 297–309.

Pinnegar, J.K. & Polunin, N.V.C. (2006). Planktivorous damselfish support significant nitrogen and phosphorus fluxes to Mediterranean reefsFish fecal pellets are a source of minerals for inshore reef communities*. *Marine Biology*, 148, 1089–1099.

Pinsky, M.L., Eikeset, A.M., McCauley, D.J., Payne, J.L. & Sunday, J.M. (2019). Greater vulnerability to warming of marine versus terrestrial ectotherms. *Nature*, 569, 108–111.

Poisot, T., Mouquet, N. & Gravel, D. (2013). Trophic complementarity drives the biodiversity-ecosystem functioning relationship in food webs. *Ecology Letters*, 16, 853–861.

Polunin, N.V.C., Harmelin-Vivien, M. & Galzin, R. (1995). Contrasts in algal food processing among five herbivorous coral-reef fishes. *Journal of Fish Biology*, 47, 455–465.

Pratchett, M., Munday, P., Wilson, S., Graham, N., Cinner, J., Bellwood, D., *et al.* (2008). Effects Of Climate-Induced Coral Bleaching On Coral-Reef Fishes. *Oceanography and Marine Biology - An Annual Review*, 251–296.

Pratchett, M.S., Hoey, A.S., Wilson, S.K., Messmer, V. & Graham, N.A.J. (2011). Changes in biodiversity and functioning of reef fish assemblages following coral bleaching and coral loss. *Diversity*, 3, 424–452.

Quimbayo, J.P., Silva, F.C. da, Mendes, T.C., Ferrari, D.S., Danielski, S.L., Bender, M.G., *et al.* (2021). Life-history traits, geographical range, and conservation aspects of reef fishes from the Atlantic and Eastern Pacific. *Ecology*, e03298.

R Core Team. (2019). *R: A language and environment for statistical computing*. R Foundation for Statistical Computing, Vienna, Austria.

Rabosky, D.L., Chang, J., Title, P.O., Cowman, P.F., Sallan, L., Friedman, M., *et al.* (2018). An inverse latitudinal gradient in speciation rate for marine fishes. *Nature*, 559, 392–395.

Randall, J.E. & Brock, V.E. (1960). Observations on the Ecology of Epinepheline and Lutjanid Fishes of the Society Islands, with Emphasis on Food Habits. *Transactions of the American Fisheries Society*, 89, 9–16.

Rasher, D.B., Hoey, A.S. & Hay, M.E. (2013). Consumer diversity interacts with prey defenses to drive ecosystem function. *Ecology*, 94, 1347–1358.

RCore Team. (2018). R: A Language and Environment for Statistical Computing. *R Foundation for Statistical Computing, Vienna.*

Reich, P.B., Tilman, D., Isbell, F., Mueller, K., Hobbie, S.E., Flynn, D.F.B., *et al.* (2012). Impacts of biodiversity loss escalate through time as redundancy fades. *Science*, 336, 589–592.

Reiss, J., Bridle, J.R., Montoya, J.M. & Woodward, G. (2009). Emerging horizons in biodiversity and ecosystem functioning research.

Robertson, D. (1982). Fish Feces as Fish Food on a Pacific Coral Reef. *Marine Ecology Progress Series*, 7, 253–265.

Rogers, A., Blanchard, J.L. & Mumby, P.J. (2014). Vulnerability of coral reef fisheries to a loss of structural complexity. *Current Biology*, 24, 1000–1005.

Roman, J. & McCarthy, J.J. (2010). The whale pump: Marine mammals enhance primary productivity in a coastal basin. *PLoS ONE*, 5.

Rosenfeld, J.S. (2002). Functional redundancy in ecology and conservation. *Oikos*, 98, 156–162.

Rothans, T.C. & Miller, A.C. (1991). A link between biologically imported particulate organic nutrients and the detritus food web in reef communities. *Marine Biology*, 110, 145–150.

S. Butail & Paley, D.A. (2012). Three-dimensional reconstruction of the fast-start swimming kinematics of densely schooling fish. *J.\ Royal Society Interface*, 9, 77–88.

S. Butail, Paley, D.A., Shapiro, C.M., Hepburn, H.R., Wieser, W., Forstner, H., *et al.* (2013). Trophic model of lagoonal communities in a large open atoll (Uvea, Loyalty islands, New Caledonia). *Canadian Journal of Fisheries and Aquatic Sciences*, 7, 1–8.

Samoilys, M.A. & Carlos, G. (2000). Determining methods of underwater visual census for estimating the abundance of coral reef fishes. *Environmental Biology of Fishes*, 57, 289–304.

Sander, E.L., Wootton, J.T. & Allesina, S. (2017). Ecological Network Inference from Long-Term Presence-Absence Data. *Scientific Reports*, 7, 1–12.

Sano, M., Shimizu, M. & Nose, Y. (1984). Food habits of teleostean reef fishes in Okinawa Island, southern Japan.

Sazima, I., Sazima, C. & Silva, J.M. (2003). The cetacean offal connection: Feces and vomits of spinner dolphins as a food source for reef fishes. *Bulletin of Marine Science*, 72, 151–160.

Schaus, M.H., Vanni, M.J., Wissing, T.E., Bremigan, M.T., Garvey, J.E. & Stein, R.A. (1997). Nitrogen and phosphorus excretion by detritivorous gizzard shad in a reservoir ecosystem. *Limnology and Oceanography*, 42, 1386–1397.

Schiettekatte, N., Brandl, S. & Casey, J. (2019). *Fishualize: Color palettes based on fish species*.

Schiettekatte, N.M.D., Barneche, D.R., Villéger, S., Allgeier, J.E., Burkepile, D.E., Brandl, S.J., *et al.* (2020). Nutrient limitation, bioenergetics, and stoichiometry: a new model to predict elemental fluxes mediated by fishes. *Functional Ecology*, 34, 1857–1869.

Schindler, D.E. & Eby, L.A. (1997). Stoichiometry of fishes and their prey: Implications for nutrient recycling. *Ecology*, 78, 1816–1831.

Schmera, D., Podani, J., Heino, J., Erős, T. & Poff, N.L. (2015). A proposed unified terminology of species traits in stream ecology. *Freshwater Science*, 34, 823–830.

Schneider, F.D., Fichtmueller, D., Gossner, M.M., Güntsch, A., Jochum, M., König-Ries, B., *et al.* (2019). Towards an ecological trait-data standard. *Methods in Ecology and Evolution*, 10, 2006–2019.

Schramski, J.R., Dell, A.I., Grady, J.M., Sibly, R.M. & Brown, J.H. (2015). Metabolic theory predicts whole-ecosystem properties. *Proceedings of the National Academy of Sciences of the United States of America*, 112, 2617–2622.

Schreck, C.B. & Moyle, P.B. (1990). *Methods for Fish Biology.*

Secor, S.M. (2009). Specific dynamic action: A review of the postprandial metabolic response. *Journal of Comparative Physiology B: Biochemical, Systemic, and Environmental Physiology*, 179, 1–56.

Serafini, P. (1994). Simulated Annealing for Multi Objective Optimization Problems. In: *Multiple criteria decision making* (eds. Tzeng, G.H., Wang, H.F., Wen, U.P. & Yu, P.L.). Springer, New York, pp. 283–292.

Shantz, A.A., Ladd, M.C., Schrack, E. & Burkepile, D.E. (2015). Fish-derived nutrient hotspots shape coral reef benthic communities. *Ecological Applications*, 25, 2142–2152.

Sih, A., Englund, G. & Wooster, D. (1998). Emergent impacts of multiple predators on prey.

Silvertown, J., Dodd, M., Gowing, D., Lawson, C. & McConway, K. (2006). Phylogeny and the hierarchical organization of plant diversity. *Ecology*, 87, S39——S49.

Siqueira, A.C., Bellwood, D.R. & Cowman, P.F. (2019). The evolution of traits and functions in herbivorous coral reef fishes through space and time. *Proceedings of the Royal Society B: Biological Sciences*, 286, 20182672.

Siqueira, A.C., Morais, R.A., Bellwood, D.R. & Cowman, P.F. (2020). Trophic innovations fuel reef fish diversification. *Nature Communications*, 11, 1–11.

Sitters, J., Bakker, E.S., Veldhuis, M.P., Veen, G.F., Olde Venterink, H. & Vanni, M.J. (2017). The Stoichiometry of Nutrient Release by Terrestrial Herbivores and Its Ecosystem Consequences. *Frontiers in Earth Science*, 5.

Soler, G.A., Edgar, G.J., Stuart-Smith, R.D., Smith, A.D.M. & Thomson, R.J. (2016a). Predicting the diet of coastal fishes at a continental scale based on taxonomy and body size. *Journal of Experimental Marine Biology and Ecology*, 480, 1–7.

Soler, G., Thomson, R., Stuart-Smith, R., Smith, A. & Edgar, G. (2016b). Contributions of body size, habitat and taxonomy to predictions of temperate Australian fish diets. *Marine Ecology Progress Series*, 545, 239–249.

Sperfeld, E., Martin-Creuzburg, D. & Wacker, A. (2012). Multiple resource limitation theory applied to herbivorous consumers: Liebig's minimum rule vs. interactive co-limitation. *Ecology Letters*, 15, 142–150.

Stan Development Team. (2018). RStan: the R interface to Stan. R package version 2.17.3.

Steffen, W., Grinevald, J., Crutzen, P. & McNeill, J. (2011). The Anthropocene: conceptual and historical perspectives. *Philosophical Transactions of the Royal Society of London A: Mathematical, Physical and Engineering Sciences*, 369.

Steffensen, J.F. (1989). Some errors in respirometry of aquatic breathers: How to avoid and correct for them. *Fish Physiology and Biochemistry*, 6, 49–59.

Stehman, S.V. (1997). Selecting and interpreting measures of thematic classification accuracy. *Remote Sensing of Environment*, 62, 77–89.

Sterner, R.W. (1990). The ratio of nitrogen to phosphorus resupplied by herbivores: zooplankton and the algal competitive arena. *American Naturalist*, 136, 209–229.

Sterner, R.W. & Elser, J.J. (2002). *Ecological Stoichiometry: The Biology of Elements from Molecules to the Biosphere*. Princeton University Press.

Sterner, R.W. & George, N.B. (2000). Carbon, nitrogen, and phosphorus stoichiometry of cyprinid fishes. *Ecology*, 81, 127–140.

Stewart, N.T., Boardman, G.D. & Helfrich, L.A. (2006). Characterization of nutrient leaching rates from settled rainbow trout (Oncorhynchus mykiss) sludge. *Aquacultural Engineering*, 35, 191–198.

Stuart-Smith, R.D., Bates, A.E., Lefcheck, J.S., Duffy, J.E., Baker, S.C., Thomson, R.J., *et al.* (2013). Integrating abundance and functional traits reveals new global

hotspots of fish diversity. *Nature*, 501, 539–542.

Stuart-Smith, R.D., Brown, C.J., Ceccarelli, D.M. & Edgar, G.J. (2018). Ecosystem restructuring along the Great Barrier Reef following mass coral bleaching. *Nature*, 560, 92–96.

Sun, Z., Xia, S., Feng, S., Zhang, Z., Rahman, M.M., Rajkumar, M., *et al.* (2014). Effects of water temperature on survival, growth, digestive enzyme activities, and body composition of the leopard coral grouper Plectropomus leopardus. *Fisheries Science*, 81, 107–112.

Suzumura, M., Miyajima, T., Hata, H., Umezawa, Y., Kayanne, H. & Koike, I. (2002). Cycling of phosphorus maintains the production of microphytobenthic communities in carbonate sediments of a coral reef. *Limnology and Oceanography*, 47, 771–781.

Svendsen, M.B.S., Bushnell, P.G. & Steffensen, J.F. (2016). Design and setup of intermittent-flow respirometry system for aquatic organisms. *Journal of Fish Biology*, 88, 26–50.

Takeuchi, Y., Ochi, H., Kohda, M., Sinyinza, D. & Hori, M. (2010). A 20-year census of a rocky littoral fish community in Lake Tanganyika. *Ecology of Freshwater Fish*, 19, 239–248.

Tamayo, N.C.A., Anticamara, J.A. & Acosta-Michlik, L. (2018). National Estimates of Values of Philippine Reefs' Ecosystem Services. *Ecological Economics*, 146, 633–644.

Taylor, B.W., Keep, C.F., Hall, R.O., Koch, B.J., Tronstad, L.M., Flecker, A.S., *et al.* (2007). Improving the fluorometric ammonium method: matrix effects, background fluorescence, and standard additions. *Journal of the North American Benthological Society*, 26, 167–177.

Teh, L.S.L., Teh, L.C.L. & Sumaila, U.R. (2013). A Global Estimate of the Number of Coral Reef Fishers. *PLoS ONE*, 8, 65397.

Terborgh, J.W. (2015). Toward a trophic theory of species diversity.

Tilman, D., Isbell, F. & Cowles, J.M. (2014). Biodiversity and Ecosystem Functioning. *Annual Review of Ecology, Evolution, and Systematics*, 45, 471–493.

Topor, Z.M., Rasher, D.B., Duffy, J.E. & Brandl, S.J. (2019). Marine protected areas enhance coral reef functioning by promoting fish biodiversity. *Conservation Letters*, 12, e12638.

Torres, J.J. & Childress, J.J. (1983). Relationship of oxygen consumption to swimming speed in Euphausia pacifica - 1. Effects of temperature and pressure. *Marine Biology*, 74, 79–86.

Treberg, J.R., Killen, S.S., MacCormack, T.J., Lamarre, S.G. & Enders, E.C. (2016). Estimates of metabolic rate and major constituents of metabolic demand in fishes under field conditions: Methods, proxies, and new perspectives. *Comparative Biochemistry and Physiology -Part A : Molecular and Integrative Physiology*, 202, 10–22.

Trudel, M. & Boisclair, D. (1996). Estimation of fish activity costs using underwater video cameras. *Journal of Fish Biology*, 48, 40–53.

Turner, J. (2002). Zooplankton fecal pellets, marine snow and sinking phytoplankton blooms. *Aquatic Microbial Ecology*, 27, 57–102.

Urabe, J. & Watanabe, Y. (1992). Possibility of N or P limitation for planktonic cladocerans: An experimental test. *Limnology and Oceanography*, 37, 244–251.

Vanni, M.J. (2002). Nutrient Cycling by Animals in Freshwater Ecosystems. *Annual Review of Ecology and Systematics*, 33, 341–370.

Vanni, M.J., McIntyre, P.B., Allen, D., Arnott, D.L., Benstead, J.P., Berg, D.J., *et al.* (2017). A global database of nitrogen and phosphorus excretion rates of aquatic animals. *Ecology*, 98, 1475.

Venter, O., Sanderson, E.W., Magrach, A., Allan, J.R., Beher, J., Jones, K.R., *et*

al. (2016). Sixteen years of change in the global terrestrial human footprint and implications for biodiversity conservation. *Nature Communications*, 7, 1–11.

Vigliola, L., Harmelin-Vivien, M. & Meekan, M.G. (2000). Comparison of techniques of back-calculation of growth and settlement marks from the otoliths of three species of Diplodus from the Mediterranean Sea. *Canadian Journal of Fisheries and Aquatic Sciences*, 57, 1291–1299.

Vigliola, L. & Meekan, M.G. (2009). The Back-Calculation of Fish Growth From Otoliths. In: *Tropical fish otoliths: Information for assessment, management and ecology*. pp. 174–211.

Villéger, S., Brosse, S., Mouchet, M., Mouillot, D. & Vanni, M.J. (2017). Functional ecology of fish: current approaches and future challenges. *Aquatic Sciences*, 79, 783–801.

Vinberg, G. (1960). *Rate of metabolism and food requirements of fishes*. Distributed by the Fisheries Research Board of Canada Biological Station, Nanaimo B.C.

Violle, C., Navas, M.-L., Vile, D., Kazakou, E., Fortunel, C., Hummel, I., *et al.* (2007). Let the concept of trait be functional! *Oikos*, 116, 882–892.

Von Bertalanffy, L. (1957). Quantitative laws in metabolism and growth. *The Quarterly review of biology*, 32, 217–231.

Webb, T.J. & Mindel, B.L. (2015). Global patterns of extinction risk in marine and non-marine systems. *Current Biology*, 25, 506–511.

Webster, M.D. & Weathers, W.W. (1989). Validation of single-sample doubly labeled water method. *American Journal of Physiology-Regulatory, Integrative and Comparative Physiology*, 256, R572–R576.

Weiblen, G.D., Webb, C.O., Novotny, V., Basset, Y. & Miller, S.E. (2006). Phylogenetic dispersion of host use in a tropical insect herbivore community. *Ecology*, 87, S62——S75.

Weiss, K.C.B. & Ray, C.A. (2019). Unifying functional trait approaches to understand the assemblage of ecological communities: synthesizing taxonomic divides. *Ecography*, 42, 2012–2020.

Weisser, W.W., Roscher, C., Meyer, S.T., Ebeling, A., Luo, G., Allan, E., *et al.* (2017). Biodiversity effects on ecosystem functioning in a 15-year grassland experiment: Patterns, mechanisms, and open questions. *Basic and Applied Ecology*, 23, 1–73.

West, G.B., Brown, J.H. & Enquist, B.J. (1997). A general model for the origin of allometric scaling laws in biology. *Science*, 276, 122–126.

Western, D. (2001). Human-modified ecosystems and future evolution. *Proceedings of the National Academy of Sciences of the United States of America*, 98, 5458–65.

Westoby, M. (2006). Phylogenetic ecology at world scale, a new fusion between ecology and evolution. *Ecology*, 87, S163——S165.

Whiles, M.R., Huryn, A.D., Taylor, B.W. & Reeve, J.D. (2011). Influence of handling stress and fasting on estimates of ammonium excretion by tadpoles and fish: recommendations for designing excretion experiments. *Limnology and Oceanography: Methods*, 7, 1–7.

Whittaker, R.H., Levin, S.A. & Root, R.B. (1973). Niche, Habitat, and Ecotope. *The American Naturalist*, 107, 321–338.

Wilkinson, C. (2008). Status of Coral Reefs of the World: 2008. *Status of Coral Reefs of the World: 2008*, 5–19.

Williams, D. & Hatcher, A. (1983). Structure of Fish Communities on Outer Slopes of Inshore, Mid-Shelf and Outer Shelf Reefs of the Great Barrier Reef. *Marine Ecology Progress Series*, 10, 239–250.

Williams, G.J., Graham, N.A.J., Jouffray, J.B., Norström, A.V., Nyström, M., Gove, J.M., *et al.* (2019). Coral reef ecology in the Anthropocene. *Functional Ecology*, 33, 1014–1022.

Williams, S.L. & Carpenter R. C. (1988). Nitrogen-limited primary productivity of coral reef algal turfs: potential contribution of ammonium excreted by Diadema antillarum. *Marine ecology progress series*, 47, 145–152.

Wilson, J.B. (1999). Guilds, Functional Types and Ecological Groups. *Oikos*, 86, 507.

Wilson, S.K., Adjeroud, M., Bellwood, D.R., Berumen, M.L., Booth, D., Bozec, Y.-M., *et al.* (2010). Crucial knowledge gaps in current understanding of climate change impacts on coral reef fishes. *Journal of Experimental Biology*, 213, 894–900.

Wilson, S.K., Dolman, A.M., Cheal, A.J., Emslie, M.J., Pratchett, M.S. & Sweatman, H.P.A. (2009). Maintenance of fish diversity on disturbed coral reefs. *Coral Reefs*, 28, 3–14.

Wilson, S.K., Graham, N.A.J., Pratchett, M.S., Jones, G.P. & Polunin, N.V.C. (2006). Multiple disturbances and the global degradation of coral reefs: are reef fishes at risk or resilient? *Global Change Biology*, 12, 2220–2234.

Wohl, D.L., Arora, S. & Gladstone, J.R. (2004). Functional Redundancy Supports Biodiversity and Ecosystem Function in a Closed and Constant Environment. *Ecology*, 85, 1534–1540.

Wolanski, E., Martinez, J.A. & Richmond, R.H. (2009). Quantifying the impact of watershed urbanization on a coral reef: Maunalua Bay, Hawaii. *Estuarine, Coastal and Shelf Science*, 84, 259–268.

Xie, N.B., Feng, L., Liu, Y., Jiang, J., Jiang, W.D., Hu, K., *et al.* (2011). Growth, body composition, intestinal enzyme activities and microflora of juvenile Jian carp (Cyprinus carpio var. Jian) fed graded levels of dietary phosphorus. *Aquaculture Nutrition*, 17, 645–656.

Yeager, L.A., Deith, M.C.M., McPherson, J.M., Williams, I.D. & Baum, J.K. (2017). Scale dependence of environmental controls on the functional diversity of coral reef

fish communities. *Global Ecology and Biogeography*, 26, 1177–1189.

Yu, G., Smith, D.K., Zhu, H., Guan, Y. & Lam, T.T.-Y. (2017). ggtree: an R package for visualization and annotation of phylogenetic trees with their covariates and other associated data. *Methods in Ecology and Evolution*, 8, 28–36.

Zavaleta, E.S., Pasari, J.R., Hulvey, K.B. & Tilman, G.D. (2010). Sustaining multiple ecosystem functions in grassland communities requires higher biodiversity. *Proceedings of the National Academy of Sciences of the United States of America*, 107, 1443–1446.

Zhdanova, I.V. & Reebs, S.G. (2006). Circadian Rhythms in Fish. *Fish Physiology*, 24, 197–238.

RÉSUMÉ

Les récifs coralliens fournissent une multitude de services écosystémiques, assurant la subsistance de millions de personnes dans le monde. Cependant, le changement climatique et les activités anthropiques font peser des menaces sans précédent sur ces écosystèmes, remettant en question la capacité des récifs coralliens à fournir ces services dans un futur proche. Dans ce contexte de dégradation continue des écosystèmes coralliens due à l'homme et en connaissant l'importance du rôle des poissons récifaux dans le fonctionnement des récifs coralliens, il est crucial d'accroître nos connaissances sur les fonctions assurées par les poissons dans les récifs coralliens (c'est-à-dire leur contribution aux flux de carbone, d'azote et de phosphore par la consommation, la croissance, l'excrétion et l'égestion). Cependant, les défis méthodologiques ont jusqu'à présent empêché la quantification précise des fonctions et la plupart des études dans le passé se sont appuyées sur des proxys (tels que la biomasse des stocks sur pied) pour en déduire des informations sur le fonctionnement des récifs. Dans cette thèse, j'ai cherché à faire progresser notre compréhension des fonctions assurées par les poissons à travers un ensemble de nouvelles méthodes et leur utilisation pour quantifier les flux d'éléments au niveau de l'organisme et de la communauté.

MOTS-CLÉS

Recyclage des nutriments, écologie, poissons des récifs coralliens, écologie fonctionnelle, modèles bioénergétiques, fonctions écosystémiques

ABSTRACT

Through their functioning, coral reefs provide a plethora of ecosystem services that support the livelihood of millions of people worldwide. However, this system is threatened by climate change and human pressures at an unprecedented level and concerns are emerging about the capacity of reefs to still deliver services in the near future. In light of this ongoing human-induced degradation of coral reef ecosystems and the important role of coral reef fishes, it is crucial to increase our knowledge concerning fish-mediated functions on coral reefs (i.e. their contribution to fluxes of carbon, nitrogen, and phosphorus through consumption, growth, excretion, and egestion). However, methodological challenges have thus far impeded the precise quantification of functions, and most studies in the past relied on proxies (such as standing stock biomass) to infer functioning. In this thesis, I sought to advance our understanding of fish-mediated functions through a variety of new methods and their use to quantify elemental fluxes at the organismal and community level.

KEYWORDS

Nutrient cycling, ecology, coral reef fishes, functional ecology, bioenergetic models, ecosystem functions